**UNIVERSITA' DEGLI STUDI DI PADOVA**

**UNIVERSITE' DE VERSAILLES SAINT-QUENTIN-EN-YVELINES**

DIPARTIMENTO SCIENZE CHIMICHE

SCUOLA DI DOTTORATO IN SCIENZE MOLECOLARI

*Indirizzo* SCIENZE CHIMICHE

CICLO **XXV**

INSTITUT LAVOISIER DE VERSAILLES

ECOLE DOCTORALE SCIENCES ET TECHNOLOGIES DE VERSAILLES

# Peptide−based foldamers: new photo−controlled devices towards opto−electronic and mechanical applications

**Direttore della Scuola :**

Ch.mo Prof. Antonino Polimeno

**Supervisore :**

Dr. Alessandro Moretto

**Directeur de l'Ecole Doctorale :**

Prof. Chantal Larpent

**Co-Directeur de Thése** :

Prof. François Couty

**Dottorand**o : Edoardo Longo

*A mio padre e mia madre*

**UNIVERSITA' DEGLI STUDI DI PADOVA**

**UNIVERSITE' DE VERSAILLES SAINT-QUENTIN-EN-YVELINES**

DIPARTIMENTO SCIENZE CHIMICHE

SCUOLA DI DOTTORATO IN SCIENZE MOLECOLARI

*Indirizzo* SCIENZE CHIMICHE

CICLO **XXV**

INSTITUT LAVOISIER DE VERSAILLES

ECOLE DOCTORALE SCIENCES ET TECHNOLOGIES DE VERSAILLES

# Peptide−based foldamers: new photo−controlled devices towards opto−electronic and mechanical applications

**Direttore della Scuola :**

Ch.mo Prof. Antonino Polimeno

**Supervisore :**

Dr. Alessandro Moretto

**Directeur de l'Ecole Doctorale :**

Prof. Chantal Larpent

**Co-Directeur de Thése** :

Prof. François Couty

Fondazione Cassa di Risparmio di Padova e Rovigo

**Dottorando** : Edoardo Longo

**AKNOWLEDGEMENT**

I wish to address a particular thank to the research group of prof. François Couty (University of Versailles Saint-Quentin-en-Yvelines, Versailles, France) for the kind support. I desire also to aknowledge prof. Venanzi and his research group in Rome (University of Tor-Vergata) for the electro-chemical measurements on the Adt-containing peptides. Finally, I wish to thank CARIPARO Foundation for the financial support of this Ph.D. project.

## *INDEX*

# *ABSTRACT*

## *I*

An ECD investigation aiming at assessing the critical main-chain length for peptide helix formation in water solution is reported. To this goal, it was synthesized by a solution step-by-step protocol a complete series of N-terminally acetylated, C-terminally methoxylated oligopeptides, characterized only by alternating Aib and Ala residues, from the di- to the nonamer stage. All of these compounds were investigated by ECD in the far-UV region in water solution as a function of chemical structure, the presence/absence of the ester moiety at the C-terminus and temperature. The critical main-chain lengths for $3_{10}$- and α-helices, although still formed to a partial extent, in aqueous solution are six and eight residues, respectively.

## *II*

A whole series of AuNps was synthesized from mercaptopropionic derivatives of alternating Aib/Ala peptide series. Our studies established the occurrence of chiroptical properties in peptide-coated 2 nm diameter gold nanoparticles. The peptides induce a chiral effect onto the plasmon resonance band detectable *via* ECD. Such a behavior appears to be strongly influenced by the secondary structure assumed by the coating peptides.

## *III*

The water solubility displayed by alternating Aib/Ala peptide series was investigated. The evidences of the formation of self-assembled structures in water, likewise responsible for the unexpected solubility properties, are presented. These peptide aggregates are spherical, with diameters up to 100 nm. They can also incorporate other molecular structures of relevant size, such as Au nanoparticles. Such systems may widen the number of applications currently accessible to self-assembled aggregates in the fields of biomedicine and materials science.

## *IV*

Two new $C^{\alpha}$-tetrasubstituted α-amino acids bearing two identical azobenzene-derived side chains have been synthesized. Photo-reversible isomerization process was detected. Intermediate chiral species are generated during the isomerization process driven by

light. Diastereomers where generated when a chiral protein amino acid was inserted. The conjugation of one of the bis(azobenzene)-derived amino acids with different metal nanoparticles allowed the isomerization process to be detected even in solid state. Furthermore, the Au-derived nanoparticles exhibit a magnetic susceptibility dependence on the light-driven isomerization state that can be simply detected by $^{1}$H-NMR spectroscopy. Based on this behavior, these amino acids are of relevant potential for the development of a novel class of materials.

## *V*

A series of Ferrocene and Pyrene labelled helical peptides containing one or more 4-amino-1,2-dithiolane-4-carboxylic acid (Adt) residues have been synthetized. Such peptides have been prepared to be employed in the formation of SAMs over gold surfaces (by means of linkage with the dithiolane Adt side chains) for electrochemical applications. In particular, the peptides have been designed for ensuring: (i) an high-rigidity of the peptide scaffold and (ii) a parallel disposition of the peptide axle respect the metal surface. Conformational characterizations and CV tests on a Ferrocene binding 6-mer are presented. Preliminary experiment on the photo-current generation property has also been performed.

# *RÉSUMÉ*


## *I*

Au fin de déterminer la longueur critique de formation de hélices peptidiques en eau, on a effectué des mensurations de dichroïsme circulaire sur une série complète de peptides acétylés, composés par résidus alternés de L-Ala et Aib et terminant avec l'ester méthylique. Même s'ils n'ont pas fonctionnalités chargées ou polaires, ces peptides sont hydrosolubles. On a effectué les mensurations dans la région entre 250 et 190 nm, où le dichroïsme est sensible à la conformation peptidique. On a testé aussi les effets de la substitution de l'ester méthylique avec la fonctionnalité carboxylique ou carboxylate, ainsi que la variation de la température. On a trouvé que les longueurs critiques pour la transitions de structure *random* à hélice $3_{10}$ et de $3_{10}$ à $\alpha$ sont le esapeptide et le octapeptide.

## *II*

On a synthétisé une série complète de nanoparticules d'Or en départant de les peptides de la série alternée Aib/L-Ala, après fonctionnalisation avec l'acide 3-mercaptan-propionique. L'étude a investigué la présence de effets chiraux sur l'Or causés par la présence des ligands peptidiques. Cet effet a été déterminé par ECD et c'est dépendent de la structure secondaire du peptide et de l'aminoacide dans le ligands le plus proche a l'Or.

## *III*

On a investigué les raisons de la solubilité en eau de les peptides ci-dessus décrives. On a supposé de mécanismes de auto-agrégation en eau. Des mensurations de microscopie électronique TEM ont confirmé cette hypothèse. En le cas de l'undeca-peptide Z-$Ala_3$-$(AibAla)_4$OMe, ces agrégats résultent être sphériques et avec dimensions environs 100 nm très réguliers. Après, c'en a étudié la capacité de encapsuler des nanoparticules d'Or. Ça pourrait étendre les applications des systèmes auto-assemblant dans le champ de recherche biomédicale et de les matériaux.

## *IV*

On a synthétisé deux nouveaux aminoacides $C^{\alpha}$-tetrasubstitués avec deux fonctionnalités azo-benzéniques identiques en chaîne latérale. Donc, on a étudié des

processus de photo-isomérisation réversibles. C'a été aussi déterminé la formation de intermèdies chiraux dans le processus. On a couplé ces aminoacides à un résidu chiral (L-Leu). En ce cas, au cours du processus de isomérisation on a formé des espèces diastereoisomériques intermèdies. Après, des nanoparticules métalliques ont été synthétisé. En particulaire, le processus de photo-isomérisation a été effectué aussi sur le solide directement. Un étude sur le propriétés magnétiques dépendent de la isomérisation a été effectué.

## *V*

On a synthétisé une série de peptides hélicoïdaux rigides avec des Pyrènes ou Ferrocènes à la fin N-terminale. La rigidité a été assuré par l'utilisation de résidus alternés de L-Ala et Aib. Ces peptides ont été préparé pour la formation de SAM sur des superficies d'Or pour applications en électrochimie. Pour faire ça, les peptides contiennent aussi un ou plus résidus de acide 4-amine-1,2-ditiolane-4-carboxylique (Adt), un résidu qui peut lier l'Or par des liaisons disulfures. Ce genre de liaison assure aussi une disposition parallèle des chaînes peptidiques sur la superficie d'Or. Donc, on a synthétisé deux décapeptides avec deux Adt en positions 1 et 8 (deux tours de $\alpha$-hélice) et une séries de esapeptides avec deux Adt en position 1 et 4 (un tour de hélice $3_{10}$). Cette géométrie permit une liaison la plus efficiente à la superficie, parce que le résidus de Adt sont à la même côte du peptide. Le produits finals ont été caractérisé chimiquement. On a conduit des investigations détaillés sur la conformation de deux esapeptides. Pour un esapeptide avec un Fèrrocene, on a conduit des mensurations électrochimiques pour tester les propriétés de oxydoréduction du Fèrrocene lié au peptide et des mensurations aussi de génération de photo-courant.

# *RIASSUNTO*

## *I*

Al fine di determinare la lunghezza critica per la formazione di eliche peptidiche in acqua è stata effettuata un'indagine ECD su una serie completa di oligopeptidi acetilati composti da residui alternati di L-Ala ed Aib e terminante come estere metilico. Tali peptidi, pur non presentando funzionalità cariche o polari, risultano essere idrosolubili. L'indagine è stata effettuata nell'UV da 250 a 190 nm, ovvero nella regione dello spettro dicroico sensibile alla conformazione peptidica. Anche l'assenza dell'estere metilico (residuo C-terminale come carbossile o carbossilato) e la variazione della temperatura sono state studiate per osservare gli effetti sulla confomazione. Le lunghezze critiche per la transizione da struttura *random* ad elica $3_{10}$ e da elica $3_{10}$ ad elica $\alpha$ risultano essere l'esapeptide e l'ottapeptide rispettivamente.

## *II*

Una serie completa di nanoparticelle d'Oro sono state sintetizzate dai peptidi della serie alternata Aib/L-Ala descritta, opportunamente funzionalizzati con acido 3-mercapto propionico. Lo studio ha stabilito la presenza di effetti chirali indotti sull'oro dalla presenza dei leganti peptidici. Tale effetto è stato determinato via indagine ECD ed è dipendente dalla struttura secondaria del peptide e dall'amminoacido più prossimo in catena nei leganti peptidici.

## *III*

Le cause della solubilità in acqua evidenziata dai peptide della serie è stata indagata. Sono stati supposti dei meccanismi di auto aggregazione in acqua. Un' indagine TEM ha confermato tale ipotesi. Nel caso dell'undeca-peptide Z-$Ala_3$-$(AibAla)_4$OMe tali aggregati risultano sferici e di dimensioni dell'ordine dei 100 nm. Ne è stata inoltre studiata la capacità di inglobare nanoaparticelle di Oro. Tali sistemi possono ampliare le applicazioni di sistemi auto assemblanti nei campi della biomedicina e dei materiali.

## *IV*

Due nuovi ammino acidi $C^{\alpha}$ tetrasostituiti recanti due unità azobenzeniche identiche in catena laterale sono stati sintetizzati. Sono stati studiati processi di foto-isomerizzazione reversibili. E' stata inoltre determinata la formazione di speci intermedie chirali durante

tale processo. Tali amminoacidi sono stati accoppiati a residui chirali (L-Leu). In tal caso, durante il processo di isomerizzazione è stata riscontrata la formazione di speci diastereoisomeriche. Tali amminoacidi recanti due unità azobenzeniche sono stati quindi opportunamente derivatizzati per la formazione di nanoaparticelle metalliche. In particolare, il processo di foto-isomerizzazione è stato testato in fase solida su nanoparticelle di Oro con tali ammino acidi come leganti. E' stato quindi svolto uno studio sulle proprietà magnetiche di tali nanoparticelle e la sua dipendenza dal processo di foto-isomerizzazione delle catene laterali dei leganti.

***V***

Sono stati sintetizzati una serie di peptidi elicoidali rigidi funzionalizzati con unità Pireneacetica o Ferrocenica all'estremità N-terminale. La rigidità di tali eliche peptidiche è stata ottenuta utilizzando residui alternati di L-Ala ed Aib. Tali peptidi sono stati sintetizzati per formare SAM su superfici di Oro per applicazioni in elettrochimica. A tale scopo, i peptidi contengono anche uno o più residui di acido 4-ammino-1,2-ditiolano-4-carbossilico (Adt), un residuo in grado di legare l'Oro grazie al legame disolfuro in catena laterale. Tale tipo di legame assicura inoltre una disposizione parallela delle catene peptidiche rispetto la superficie. Sono stati sintetizzati due decapeptidi recanti due Adt in posizione 1 e 8 (due giri esatti in un'$\alpha$-elica) ed una serie di esapeptidi recanti gli Adt in posizione 1 e 4 (un giro di elica $3_{10}$). Tale geometria consente il legame più efficiente possibile alla superficie, in quanto i residui di Adt si trovano dallo stesso lato dell'elica. I prodotti finali sono stati chimicamente caratterizzati. Sono state condotte approfondite indagini conformazionali su due esapeptidi. Su un esapeptide contenente Ferrocene sono stati inoltre condotti degli esperimenti di voltammetria ciclica e di generazione di foto-corrente.

## TABLE OF ABBREVIATIONS

Ac = Acetyl
AcOH = Acetic acid
Adt = 4-amino-1,2-dithiolane-4-carboxylic acid
AgNp = Silver nanoparticle
Aib = 2-amino *iso*butirric acid
Ala = Alanine
AuNp = Gold nanoparticle
Boc = Terbutyloxycarbonyl
CD = Circular dichroism
COSY = Correlation spectroscopy
CV = Circular Voltammetry
DCM = Dichloromethane
DEA = Diethylamine
DIEA = *N*,*N*-diisopropylethylamine
DLS = Dynamic light scattering
DMAP = Dimetylamino pyridine
DMF = Dimethylformamide
DMSO = Dimethyl sulphoxide
ECD = Circular dichroism in UV-Vis range
EDC = *N*-ethyl-*N'*-(3-dimethylamino)propyl-carbodiimide
EtOAc = Ethyl acetate
PE = Petroleum ether
EtOH = Ethanol
$Et_2O$ = Diethyl ether
ESI = Electron spray ionization
Fc = Ferrocene
Fmoc = 9-fluorenylmetoxycarbonyl
FTIR = Fourier transformed infrared spectroscopy
Gly = Glycin
HATU = O-(azabenzotriazol-1-yl)-1,1,3,3-tetramethyluronium esafluoro phosphate
HFIP = Esafluoroisopropanole

HOAt = 1-hydroxy-7-aza-1,2,3-benzotriazole

HOBt = 1-hydroxy -1,2,3-benzotriazole

HPLC = High performance liquid chromatography

IR = Infrared spectroscopy

*m*Dazbg = Di (3-(phenylazo) benzyl) glycine

MeCN = Acetonytrile

MeOH = Methanol

NMM = N-methylmorfoline

NMR = Nuclear magnetic resonance

NOESY = Nuclear Overhauser effect spectroscopy

OMe = Metoxy

OSu = 1-oxy-succinimide

OXYMA = Ethyl-2-cyano-2-(hydroxyimino) acetate

*p*Dazbg = Di (4-(phenylazo) benzyl) glycine

PtNp = Platinum nanoparticle

Pyr = Pyrene

PyrAc = Pyrene acetyl

$R_f$ = Retention factor

ROESY = Rotating-frame nuclear Overhauser Spectroscopy

SAM = Self assembled monolayer

TEA = Triethyl amine

TEM = Transmission electron microscopy

TFA = Trifluoroacetic acid

TGA = Thermogravimetry

THF = Tetrahydrofurane

TIS = Triisopropylsilane

TLC = Thin layer chromatography

TOCSY = Total correlation spectroscopy

TOF = Time of flight

Trt = Triphenylmethyl

UV-Vis = Ultraviolet-Visible Absorption spectroscopy

Z = Benzyloxycarbonyl

## INTRODUCTION

Nucleic acids and protein amino acids are two crucial building blocks of living organisms. These moieties are chiral molecules, involved in biosynthesis as precursors of two of the most important biopolymers, DNA and proteins. Therefore, this points out the important function of handedness in nature. The ability of controlling the folding properties of synthetic molecules has been the aim of several, recently developed, research fields. Foldamers are sequence-specific synthetic oligomers analogue to peptides, proteins and oligonucleotides that fold into well-defined three-dimensional structures. They offer to the chemical biologist a broad pallet of building blocks for the construction of molecules that test and extend our understanding on protein folding and function. Foldamers also provide templates for presenting complex arrays of functional groups in virtually unlimited geometrical patterns, thereby presenting attractive opportunities for the design of molecules that bind in a sequence- and structure-specific manner to oligosaccharides, nucleic acids, membranes and proteins.[1] On the base of the definitions of foldamers,[2] a pool of suitable monomers can be exploited in order to access synthetically those abilities that only natural macromolecules displayed. In fact, foldamers consist in a wide range of oligomers that adopt in solution a well defined structure on the base of intra-molecular interactions (such as hydrogen bonds, constrain, repulsion) among non-consecutive residues. Several classifications of foldamers have been employed. For instance, foldamers could be classified into two main classes, determined by the presence or absence of aromatic units within the monomer unit (**Fig. 1**). "Aliphatic" foldamers have saturated carbon chains separating amide or urea groups.

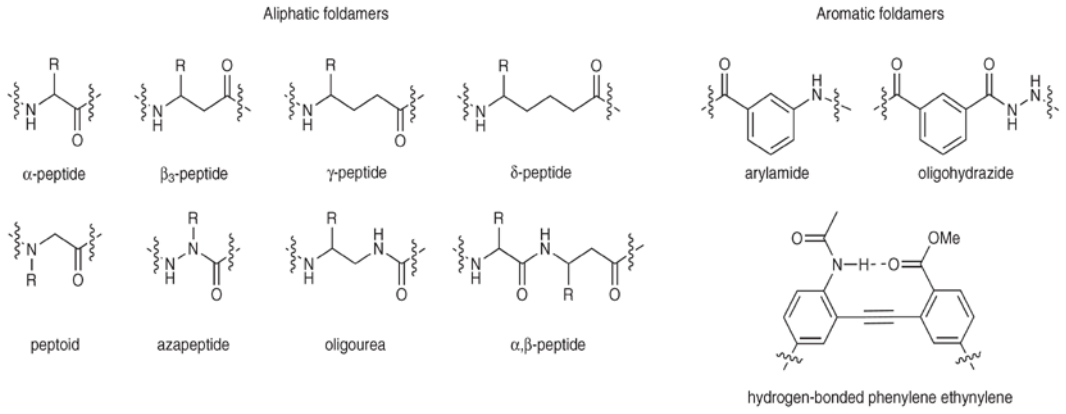


***Fig. 1*** Examples of foldamer frameworks.

Examples of this group include the β-,[2b,3] γ-,[4] and δ-,[5] oligoureas,[6] azapeptides,[7] pyrrolinones,[8] α-aminoxy-peptides,[9] and sugar-based peptides.[10] The second class presents aromatic spacers within the backbone. The poly-pyrrole/imidazole DNA-binding oligomers,[11] provided early examples of heteroaryl oligomers that bind biologically relevant targets. In either case, the initial monomer selection is typically affected by a variety of factors, including the ease of their synthesis and structural characterization. The classes of residues and related oligomers that have been designed to exhibit such folding properties are nowadays many, and are still growing, being the research on foldamers an open field.[12] The secondary structure formed by a given type of amide foldamer depends on the planar amide bonds, the number and substitution patterns of the methylene units within the backbone, and conformational restraints such as the incorporation of cyclic structures within the amino acid. The helices formed by foldamers are characterized by their handedness and the number of atoms within repeating hydrogen bonding rings of their structures. In conventional peptides, the main conformations are $3_{10}$- and α-helices, with 10 atoms and 13 atoms in the hydrogen bonded rings. In **Table 1** examples are reported on the effect of insertion of one or more methylenes in the peptide back-bone.[1,3c,4b,13]

| Backbone structure type | Amino acid substitution pattern[a] | Number of atoms per H-bond ring[b] | Residues involved in hydrogen bonding (*i*) | Helix polarity[c] |
|---|---|---|---|---|
| $\alpha_n$ ($3_{10}$-helix) | Cα | 10 | 3 | N |
| $\alpha_n$ (α-helix) | Cα | 13 | 4 | N |
| αβ (11-helix) | Cα/C3 or Cα/cyclic C2,3 cyclopentane ring | 11 | 3 | N |
| αβ (14,15-helix) | Cα/C3 or Cα/cyclic C2,3 cyclopentane ring | 14, 15 | 4 | N |
| $\alpha_2\beta$ | Cα/C3 or Cα/cyclic C2,3 cyclopentane ring | 10, 11, 11 | 3 | N |
| $\alpha_2\beta$ | Cα/C3 | 14 | 4 | N |
| $\alpha\beta_2$ | Cα/C3 or Cα/cyclic C2,3 cyclopentane ring | 11, 11, 12 | 3 | N |
| $\alpha\beta_2$ | Cα/C3 or Cα/cyclic C2,3 cyclopentane ring | 15 | 4 | N |
| $\beta_n$ (12-helix) | Cyclic C2,3 cyclopentane ring | 12 | 3 | N |
| $\beta_n$ (14-helix) | C2, C3 or C2,3 cyclohexane ring | 14 | 4 | C |
| $\beta_n$ | C2,3[d] | 8 | 1 | N |
| $\beta_n$ (10/12-helix) | Mixed C2/C3 | 10, 12 | 1/2 | Mixed |
| $\beta_n$ | C2,3 (*cis*-oxetane residues) | 10 | 1 | C |
| $\gamma_n$ | C4 | 9 | 2 | N |
| αγ | Cα/C3 | 9 | 1 | N |

***Tab.1*** Conformation available to synthetic foldamers: a) Cα corresponds to $C^{\alpha}$-substituted α-amino acids (normal substitution pattern), or disubstituted amino acids (as in α-amino-isobutyric acid). C2 and C3 correspond to the carbon that bears a substituent in β-amino acids. b) The number of atoms in the hydrogen bonded rings corresponds to the number of atoms, including the hydrogen of the amide. Note that for some mixed α/β-amino acids, there is more than one ring type that repeats throughout the helix. For example, in α2β the hydrogen bonding occurs between each amide carbonyl at position i and an amide at i + 3. If the ring is formed between the carbonyl of a β-amino acid (at i), then the ring includes two subsequent α-amino acids (at i + 1 and i + 2) before coming to the hydrogen bonded amide proton. Hence there are 10 atoms, as in the $3_{10}$-helix for this case. The subsequent two hydrogen bonded rings will include an α-amino acid and a β-amino acid, resulting in 11-atom rings. c) Direction that the carbonyl group points, toward either the C terminus or the N terminus. A 'mixed' entry indicates that the carbonyl group points in both directions, at different points in the helix. d) This hydrogen bonding pattern is observed when the C2 position is substituted with a hydroxyl group, when the C2 position is a part of a cyclopropane ring, or when C2 and C3 are part of an oxo-norbonene ring system.

For instance, β-peptides in which the monomer is a *trans*-2-amino-cyclopentane-carboxylic acid (or cyclized residues in which the β2 and β3 positions are part of a five-member ring) adopt a "12-helix" conformation, with the same hydrogen bonding pattern as the $3_{10}$-helix of α-peptides, but with two additional carbon atoms inserted into the backbone. Park *et al.* examined the impact of incorporating acyclic residues into this structure using a series of peptides, with one to four β2-substituted residues present in a background of cyclized amino acids.[14] Although the helical propensity was lower because of the incorporation of the β2 residues, the 12-helix previously observed to be the predominant form for cyclic residues remained the favored structure. Other substitution patterns of β-peptides (including residues constructed from cyclohexane rings or β3-substituted residues) favor the 14-helix, which bears both similarities and differences to the α-helix. The 14-helix has two intervening amide units within each hydrogen bonded ring (as in the α-helix), butthe amide carbonyl groups are directed toward the N terminus rather than the C terminus as in the α-helix.

Among the non-coded α-amino acids, $C^{\alpha,\alpha}$-tetra substituted amino acids constitute a wide class of molecules with well recognized folding induction abilities.[15] They are naturally wide spread but do not belong to the coded 20 proteinogenic amino acids. Aib (α-amino-*iso*-butirric acid) is the simplest achiral tetra-substituted amino acid. For instance, its omo-peptides have been synthesized up to the undecamer level without ceasing to prefer the $3_{10}$-helical conformation, even though in many analogues with the replacement of tri-substitued coded amino acids the α-helix conformation was demonstrated to be more stable.[16] Conformational energy calculation demonstrated that the presence of the two methyl groups (Aib can be seen as a di-methyl glycine) induces a restriction in the conformational space available for the chain, that results in a propensity to induce an helical folding.[17] Moreover, the ability of Aib to induce β-turn confomation has been demonstrated for very short peptides (tripeptide).[17b] Many analogues of Aib have been exploited in order to build sequence with predictable lengths and shapes and impart novel functionalities. For examples, cyclic analogues of Aib such as $Ac_5c$, TOAC, Api and others exhibited inducing ability for $C_{10}$ (β-turn).[15]

In order to classificate the amino acids on the base of their conformational preference is essential to define their geometric features. In 1963, Ramachandran et al. introduced the ϕ and φ angles (**Figure 2**) as a parameterization of the protein backbone.[18] The plot of these angles, the Ramachandran plot, has become a standard tool used in determining

protein structure and in defining secondary structure. Using an analysis of local hard-sphere repulsions between atoms that are at least third neighbors (1-4 interactions), it was constructed a steric map of the Ramachandran plot that predicted the commonly allowed regions for peptide secondary structure.

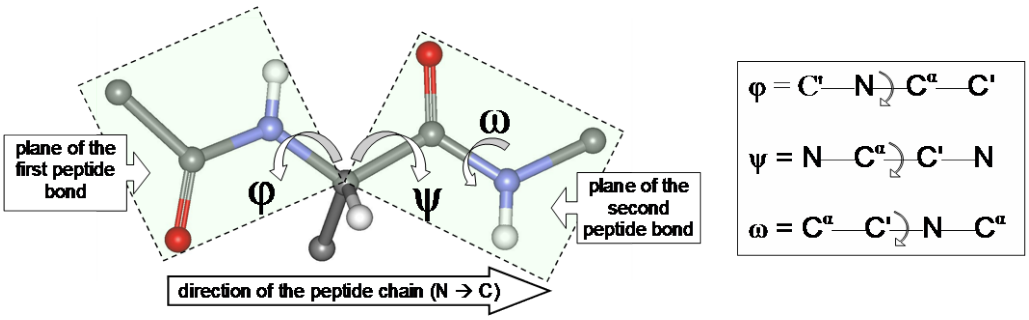


*Peptide torsion angles (dihedral angles; angles between planes).*

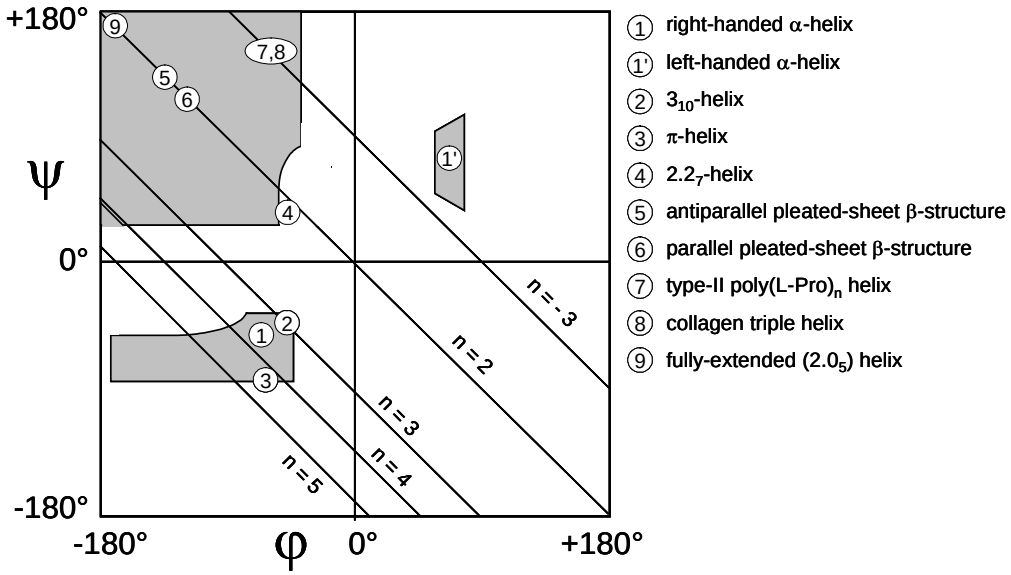


***Fig. 2*** Representation of a short peptide structure. The torsional angles indicated as suggested by the IUPAC-IUB Commission for biochemical nomenclature.[19]

In **Table 2** are reported the fundamental parameters that characterize the α-helix and the $3_{10}$ helix conformations.

| **Parameters** | **Elica $3_{10}$** | **Elica α** |
|---|---|---|
| ϕ | –57° | –63° |
| ψ | -30° | -42° |
| Hydrogen bond angle NH•••O=C | 128° | 156° |
| Rotation per residue | 111° | 99° |
| Axial traslaction per residue | 1.94 Å | 1.56 Å |
| Residues per turn | 3.24 | 3.63 |
| Pitch | 6.29 Å | 5.67Å |

***Tab.2*** Geometric elements for model α- and $3_{10}$-helices.

The α-helix results in a larger coil than the $3_{10}$-helix. In fact, the hydrogen bonding in α-helix involves the CO of residue *i* and the NH of residue *i+4* whereas in $3_{10}$-helix the interaction is between the $CO_i$ and $NH_{i+3}$. In **Figure 3** the description of the hydrogen bonding for the most common turns is reported.

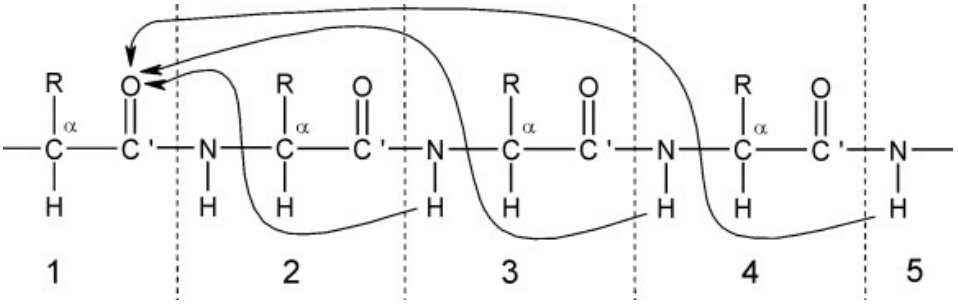


***Fig.3*** Representation of γ- (*i*→*i+2*), β- (*i*→*i+3*) and α-turn (*i*→*i+4*).

Many efforts during the past decades have been accomplished in order to design conformational constrained peptides that would be able to overcome the recognized problems to design peptides as drug for receptors targeting.[20] The contribution of tetra-substituted amino acids in this field relies on the ability of such residue to preserve or to induce a well-defined conformation requirements.

**Aims of the present work**

In this PhD work will be presented and discussed a series of supramolecular applications which involved a well conformational defined short peptides, based on non-coded amino acids. The applications will range from self-assembly, chiro-optical, magneto-optical to electrochemistry.

REFERENCES


1) Goodman C.M., Choi S., Shandler S.,DeGrado W.F., *Nature Chemical Biology*, **2007**, 3 (5), 252-262
2) a) Gellman S.H., *Accounts of Chemical Research*, **1998**, 31, 173-160 ; b) Appella D.H., Christianson L.A., *et al.*, *Journal of American Chemical Society*, **1996**, 118, 13071-13072
3) a) Cheng R.P., Gellman s.H.,DeGrado W.F., *Chemical Reviews*, **2001**, 101, 3219-3232 ; b) Seebach D., Gademann J., *et al.*, *Helvetica Chimica Acta*, **1997**, 80 (7), 2033-2038 ; c) Seebach D., Hook D.F.,Glatti A., *Biopolymers*, **2006**, 84, 23-37 ; d) Pilsl L.K.A.,Reiser O., *Amino Acids*, **2011**, 41, 709-718
4) a) Sharma G.V.M.,*al. e.*, *Angewandte Chemie International Edition*, **2006**, 45, 2944-2947 ; b) Baldauf C., Günther R.,Hofmann H.-J., *Journal of Organic Chemistry*, **2006**, 71, 1200-1208
5) a) Arndt H.D., Ziemer B.,Koert U., *Organic Letters*, **2004**, 6, 3269-3272 ; b) Trabocchi A., Guarna F.,Guarna A., *Current Organic Chemistry*, **2005**, 9, 1127-1153
6) a) Violette A.,*al. e.*, *Journal of American Chemical Society*, **2005**, 127, 2156-2164 ; b) Violette A., Averlant-Petit M.C., *et al.*, *Journal of American Chemical Society*, **2005**, 127, 2156-2164
7) a) Salaun A., Potel M., *et al.*, *Journal of Organic Chemistry*, **2005**, 70, 6499-6502 ; b) Zega A., *Current Medicinal Chemistry*, **2005**, 12, 589-597
8) Smith A.B., Knight S.D., Sprengeler P.A.,Hirschmann R., *Biorganic Medicinal Chemistry*, **1996**, 4, 1021-1034
9) Li X.,Yang D., *Chemical Communications*, **2006**, 3367-3379
10) a) Chakraborty T.K., Srinivasu P., Tapadar S.,Mohan B.K., *Glycoconjugate Journal*, **2005**, 22, 83-93 ; b) Claridge T.D.W.,*al. e.*, *Journal of Organic Chemistry*, **2005**, 70, 2082-2090
11) Dervan P.B., *Science*, **1986**, 232, 464-471
12) a) Hecht S.,Huc I., *Foldamers*, **2007**. Weinheim, Wiley-VCH; b) Guichard G.,Huc I., *Chemical Communications*, **2011**, 47, 5933-5941 ; c) Hill D.J., Mio M.J., *et al.*, *Chemical Review*, **2001**, 101, 3893-4011
13) Chen Y., Mant C.T., *et al.*, *The Journal of Biological Chemistry*, **2005**, 13, 12316-12329
14) Park J.S., Lee H.S., *et al.*, *Journal of American Chemical Society*, **2003**, 125, 8539-8545
15) Toniolo C., Crisma M., Formaggio F.,Peggion C., *Biopolymers (Pept. Sci.)*, **2001**, 60, 396-419
16) Toniolo C., Crisma M., Formaggio F.,Peggion C., *Biopolymers (Pept. Sci.)*, **2001**, 60, 396
17) a) Rose G.D., Gierasch L.M.,Smith J.A., *Advances in Protein Chemistry*, **1985**, 37, 1 ; b) Benedetti E., Bavoso A., *et al.*, *Journal of American Chemical Society*, **1982**, 104, 2437 ; c) Venkataram P.,Sasisekharan V., *Macromolecules*, **1979**, 12, 1107 ; d) Paterson Y., Rumsey S.M., *et al.*, *Journal of American Chemical Society*, **1981**, 103, 2947
18) Ramachandran G.N.,Sasisekharan V., *Journal of Molecular Biology*, **1963**, 7, 95-99
19) Nomenclature I.-I.C.o.B., **1970,** 9**,** 3471,
20) Santagada V.,Caliendo G., *Peptides and Peptidomimetics*, **2003**. Padova, Piccin Nuova Libraria

# I

## ECD characterization in water of the first totally water-soluble peptide series based on –(Aib-Ala)$_n$- and –(Ala-Aib-Ala)$_n$- oligomers

### INTRODUCTION

Constrained peptides and peptidomimetics have emerged as a powerful tool for the design of ligands for proteins, enzymes and receptors targeting.[1] In fact, the peptide conformation plays a central role in the binding activity to biological targets. Many problems are connected with the exploitation of peptides as drugs: *i*) low metabolic stability, in particular at the gastrointestinal stage, *ii*) low absorption after oral assumption due to their high molecular weight or because of lacking of active transport, *iii*) rapid expulsion through liver or kidney, *iv*) not-selective interactions, *v*) not-selective delivering.[1] Therefore, the ability of ensuring folding ability along with stability in biological environment is a central topic in peptides and peptidomimetics research.[2] In this field, non-proteinogenic α-amino-acids, and in particular $C^{\alpha}$-tetra substituted amino acids, represent a powerful tool for designing peptides with controlled length and conformation.[2c,2e,3] Different classes of $C^{\alpha}$-tetra substituted amino acids have been tried as inductor of different turns stabilization. For instance, $C^{\alpha,\alpha}$-dialchyl amino acids possess the ability to induce β-turn structure even in short-length peptides. In the Aib omo-peptides this ability has been recognized even for the shortest oligomer possible for this conformation, the tri-peptide.[4] Nevertheless, the helical conformation preference of Aib containing peptide is dependent on the ratio of proteinogenic and tetra-substituted amino acid.[5] Another factor that influences the conformational preference is the length. Twenty years ago was published the first X-ray diffraction proof for a $3_{10}\rightarrow\alpha$-helix conversion in the crystal state induced by peptide lengthening only.[5] The -(Aib-Ala)$_3$- sequential oligomer was found to be fully $3_{10}$-helical, while the -(Aib-Ala)$_4$- octamer, as well as the higher oligomers -(Aib-Ala)$_{5,6}$-, was essentially α-helical (when discussing the remarkably short peptides found to be helical in these series, one should remind that they are heavily based on the strongly helicogenic, non-coded Aib residue).[3g,6] However, it was subsequently found that the isomeric -(Ala-Aib)$_4$- octapeptide sequence adopts a C-terminally distorted $3_{10}$-helix structure in the crystal state.[7] It is evident that, at a main-chain length near the critical size between

these two types of helices, even subtle differences in the chemical structure, terminal protecting groups, packing motifs, and co-crystallized solvent molecules, may bias significantly the helix preference. In this same paper, it was also reported that the long oligomer -(Ala-Aib)$_8$- is in α-helical conformation under the same experimental conditions. Moreover, according to an ECD study -(Aib-Ala)$_3$- is right-handed helical in the solid state (KBr pellets).[78]

FTIR absorption and NMR investigations support the view that in $CDCl_3$ solutions the penta- and heptamers -Ala-(Aib-Ala)$_n$- (*n* = 2 and 3) are in a $3_{10}$-helical conformation.[9] However, partially conflicting results were reported in this secondary structure-supporting organic solvent for the longer oligomer -(Aib-Ala)$_5$- in the sense that NMR data are consistent with its $3_{10}$-helicity, while FTIR absorption favors the concomitant occurrence of $3_{10}$- and α-helical conformations. This latter conclusion was also proposed for -Ala-(Aib-Ala)$_5$- [in particular, the parameter indicative of the early onset of the α-helical conformation (an intense 1659 $cm^{-1}$ band) is first seen in -(Aib-Ala)$_5$-]. The polar, strong hydrogen-bonding acceptor, DMSO seems to destabilize the $3_{10}$-helial conformation of this series favoring the α-helix.[9b,10] Furthermore, the results of our NMR analysis supported the conclusion the all -(Ala-Aib)$_n$- (*n* = 4, 6, 8) are folded in the α-helix conformation in $CD_3CN$ solution.[7] Using electronic circular dichroism (ECD) spectroscopy it was shown that in the polar hydrogen-bonding donor solvents methanol, ethanol, and 2,2,2-trifluoroethanol (TFE) the characteristic features (double negative maxima near 222 and 205 nm) of a right-handed helical conformation are first seen at the octapeptide -(Aib-Ala)$_4$- or -(Ala-Aib)$_4$-/nonapeptide -Ala-(Aib-Ala)$_4$- levels.[11] ECD patterns indicative of partially developed $3_{10}$- and α-helical conformations first appear at the 7- and 8-mers, respectively. Heating and increase in peptide concentration do not deteriorate dramatically the helix content. However, the ECD of the $N^{\alpha}$-*para*-bromobenzoylated short -(Aib-Ala)$_3$- oligomer in TFE is characterized by a bisignated pattern centered at 238 nm originated from the exciton split transition of the aromatic chromophore interacting with the amido-chromophores of the peptide molecules arranged in a right-handed helical array.[12] Interestingly, according to the authors,when the -(Aib-Ala)$_5$- decapeptide is covalently bound at the C-terminus to a strongly water-solubilizing polymer, the corresponding ECD curve is reminiscent of that typical of the mainly unordered conformation (however, for a comment see below).[13] This is the only conformational study reported in the literature to date of a

sequential Aib/Ala peptide in water solution. From the vast amount of results discussed above, it is quite clear that the conformations preferentially adopted by the sequential Aib/Ala oligomers were extensively investigated in the crystal (solid) state and in a variety of organic solvents, but the corresponding studies in water are almost completely missing. Conversely, the first example of water soluble $3_{10}$ helix was reported just 12 years ago.[14] In that publication, two analogue sequences both containing ATANP [(L)-2-amino-3[1-(1,4,7)-triazacyclononane] residues, respectively based on (L)-Iva (Isovaline) and Aib, were designed in a way that ensured water solubility and helical conformation, leading to $3_{10}$ helix stabilization. By chance, intriguing physic-chemical applications of the -Aib-Ala- series have been performed recently by Kimura and co-workers.[7,11,15] In this work the extent of the ordered secondary structure steadily increases to the 14-mer level in the (Aib-Ala)$_n$ series and to the 64-mer level in the (Ala-Aib)$_n$ series. In particular, these authors reported the scientific stimulating ability of their helical structures to transfer electrons to long distances (up to 120 Å), through a self-assembled monolayer of peptide on a gold surface. Recently, in order to exploit these systems as a molecular-electronics, we decided to re-prepare the -(Aib-Ala)$_n$- and -Ala-(Aib-Ala)$_n$- sequential peptide series up to the nonamer stage. Serendipitously, during the step-by-step synthesis in solution, we discovered that a non-insignificant amount of each peptide went lost during the purification procedures, which *inter alia* involved extraction of the impurities from an ethyl acetate (or a methylene chloride) solution with water. The unexpected water solubility of this family of peptides, even in the absence of a covalently-bound, strong hydrophilic moiety, prompted us to fill the aforementioned gap by exploiting ECD spectroscopy in the far-UV region to assess its critical main-chain length for helix formation in water for the first time.

## RESULT AND DISCUSSION

The physical properties and analytical data for the -(Aib-Ala)$_n$- and -Ala-(Aib-Ala)$_n$- peptides synthesized in this work are listed in **Table 1**. All peptides were prepared by classical solution methodology. 1-(3-dimethylaminopropyl)-3-ethylcarbodiimide (EDCI) was used in combination with the efficient additive 7-aza-1-hydroxy-1,2,3-benzotriazole (HOAt) in $CH_2Cl_2$ in the presence of N,N-diisopropyl-ethylamine (DIEA) for coupling reactions.[16] Removal of the benzyloxycarbonyl (Z) $N^{\alpha}$-protecting group was carried out by catalytic hydrogenation. The $N^{\alpha}$-acetylated (Ac) peptide esters were obtained in 70-98% yield by reacting the $N^{\alpha}$-deprotected synthetic precursor with acetic anhydride in dichloromethane. A 6 mM LiOH solution was used to remove the C-terminal methyl ester (OMe) functionality (quantitative yield). All peptides were chemically characterized by melting point determination, polarimetric measurement, thin-layer chromatography (TLC) in three solvent systems, and solid-state IR absorption in KBr (**Table 1**), and by $^1$H NMR (chemical shift reported in experimental section).

***Tab. 1*** Chemical chracterization data for the synthesized peptides

| Peptide | M.p. (°C)[a] | $R_f$(I)[c] | $R_f$(II)[c] | $R_f$(III)[c] | $[\alpha]_D^{20}$ [d] | IR[e], ν ($cm^{-1}$) |
|---|---|---|---|---|---|---|
| Z–Aib–Ala–OMe | 68–69 | 0.90 | 0.95 | 0.30 | -21.1 | 3311, 1747, 1702, 1691, 1527 |
| Z–Ala–Aib–Ala–OMe | 157–158 | 0.80 | 0.85 | 0.15 | -25.0 | 3377, 1741, 1704, 1680, 1537 |
| Z–(Aib–Ala)$_2$–OMe | 58–60 | 0.50 | 0.85 | 0.10 | -28.8 | 3326, 1740, 1706, 1660, 1529 |
| Z–Ala–(Aib–Ala)$_2$–OMe | 156–158 | 0.50 | 0.80 | 0.10 | -21.3 | 3315, 1741, 1703, 1665, 1531 |
| Z–(Aib–Ala)$_3$–OMe | 151–153 | 0.45 | 0.80 | 0.10 | -3.7 | 3321, 1743, 1704, 1662, 1531 |
| Z–Ala–(Aib–Ala)$_3$–OMe | 96–99 | 0.35 | 0.75 | 0.10 | -10.7 | 3321, 1745, 1705, 1662, 1531 |
| Z–(Aib–Ala)$_4$–OMe | 204–206 | 0.35 | 0.75 | 0.10 | -27.4 | 3321, 1742, 1704, 1660, 1530 |
| Z–Ala–(Aib–Ala)$_4$–OMe | 103–105 | 0.35 | 0.75 | 0.10 | -26.8 | 3321, 1744, 1704, 1662, 1531 |
| Ac–Aib–Ala–OMe | 83–85 | 0.80 | 0.85 | 0.20 | -72.4 | 3329, 1754, 1657, 1534 |
| Ac–Ala–Aib–Ala–OMe | 87–89 | 0.65 | 0.75 | 0.15 | -78.8 | 3310, 1742, 1653, 1535 |
| Ac–(Aib–Ala)$_2$–OMe | 97–99 | 0.40 | 0.75 | 0.10 | -26.7 | 3312, 1743, 1657, 1534 |
| Ac–Ala–(Aib–Ala)$_2$–OMe | 103–105 | 0.40 | 0.70 | 0.10 | -73.1 | 3330, 1741, 1669, 1533 |
| Ac–(Aib–Ala)$_3$–OMe | 107–109 | 0.35 | 0.70 | 0.10 | -58.0 | 3341, 1745, 1657, 1533 |
| Ac–Ala–(Aib–Ala)$_3$–OMe | 110–112 | 0.25 | 0.65 | 0.10 | -84.2 | 3337, 1743, 1660, 1533 |
| Ac–(Aib–Ala)$_4$–OMe | 154–156 | 0.20 | 0.65 | 0.10 | -88.4 | 3317, 1743, 1656, 1534 |
| Ac–Ala–(Aib–Ala)4–OMe | 149–151 | 0.20 | 0.60 | 0.10 | -110.3 | 3353, 1742, 1653, 1538 |

[a]Determined on a Leitz model Laborlux apparatus (Wetzlar, Germany).
[b]$Et_2O$, diethyl ether; EtOAc, ethyl acetate; PE, petroleum ether.
[c]Silica gel plates (60F-254 Merk, Darmstadt, Germany), solvent systems: (I) chloroform/ethanol 9:1, (II) butan-1-ol/water/acetic acid 3:1:1, and (III) toluene/ethanol7:1. The compounds were detected on the plates with an UV lamp (for Z Na-derivatives only) and/or revealed by oxidation with a potassium permanganate solution.
[d]Determined on a Perkin-Elmer 241 polarimeter equipped with a Haake (Karlsruhe, Germany) L thermostat; a 10 cm path length cell was used; c =0.1 mg/mL(methanol).
[e]Determined in KBr pellets on a Perkin-Elmer 1720X FT-IR spectrophotometer

**ECD characterization**

The ECD spectra (**Figure 1**) in the far-UV region of the oligomers with alternating Aib and Ala residues in water solution at neutral pH were recorded.

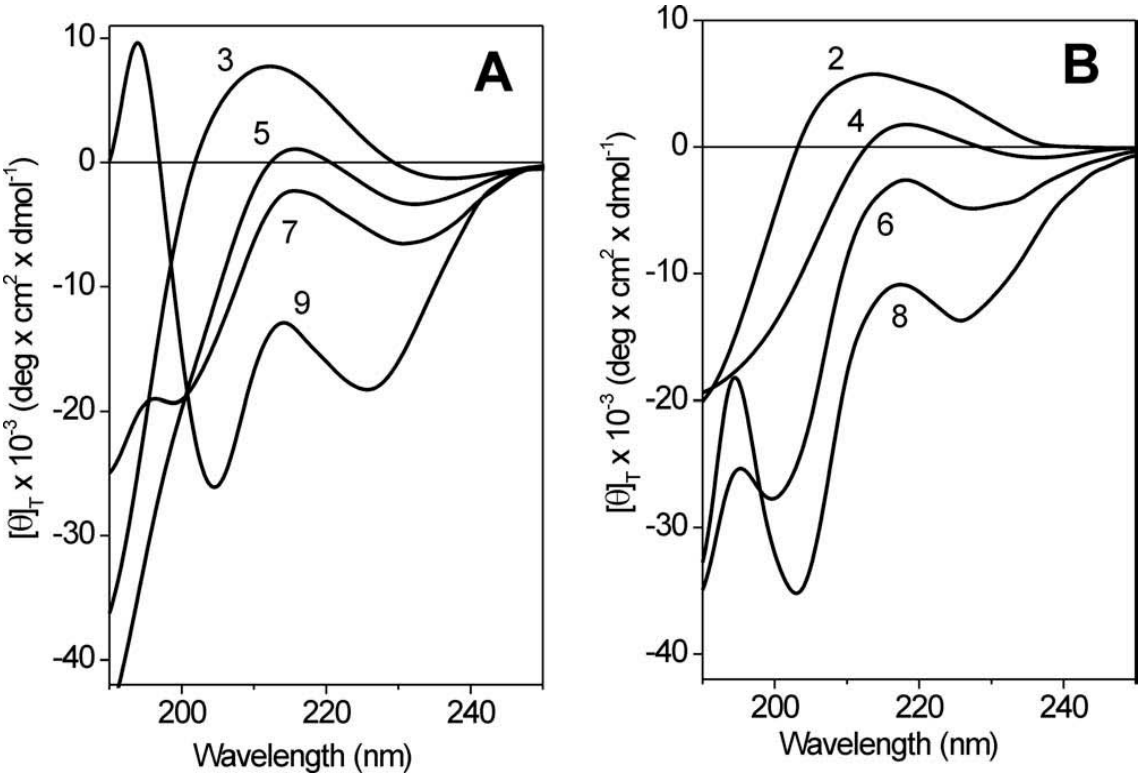


***Fig. 1*** Far-UV ECD spectra of: (A) Ac–Ala–(Aib–Ala)$_n$–OMe (n=1,2,3,4). (B) Ac–(Aib–Ala)$_n$–OMe (n= 1,2,3,4). All measurements were recorded in water at 20°C.

In these peptides, in addition to the peptide chromophores, the other chromophores possibly contributing to this spectral region are the N-terminal acetamido and the C-terminal methyl ester.[17] However, these contributions are not expected to modify significantly the overall patterns. **Figure 1A** shows the ECD spectra of the odd oligomers and **Figure 1B** illustrates those of the even oligomers. In the analysis of the ECD spectra, one should take into account two contrasting types of contributions: (i) our sequential peptides were synthesized beginning from a C-terminal Ala residue. Therefore, it is reasonable to assume that all even-number oligomers will exhibit a significantly higher helicity than that of their immediately lower (odd) oligomers, not only by virtue of their slightly longer main chain but mostly because the newly incorporated residue is the strongly helicogenicAib;[3c,3g] (ii) on the other hand, an added

chiral Ala (from an even to an odd oligomer), although this residue would be remarkably less helicogenic than Aib, is expected to contribute to the peptide ellipticity values much more than the achiral Aib. It is widely recognized that the ECD spectra with a strong negative Cotton effect well below 200 nm (peptide π-π* transition) are indicative of an unordered conformation, often with a substantial contribution from the extended poly-(L-Pro)$_n$ II helix component (especially when the spectra show clear evidence for a positive dichroism at 215–220 nm).[17]On the other hand, when the peptide is folded into a right-handed ($3_{10}$ or α-) helical conformation to a significant extent, the interacting peptide chromophores generate a split π-π* transition, the (parallel) component of which is observed as a negative band red-shifted to 203–208 nm. The discrimination between the $3_{10}$and α-helices (the former is expected to predominate at main-chain lengths lower than those typical of the latter) is feasible by ECD, at least to a first approximation, by calculating the ratio (R) of the ellipticities between the negative 222 nm (peptide *n*-π* transition) Cotton effect and that near 205 nm.[18] More specifically, a value of 0.15–0.35 for R is considered diagnostic for the $3_{10}$-helix, while a value close to the unity is typical of the α-helix. On the basis of the assumptions and considerations discussed above, from the ECD spectra shown in **Figure 1**, we extracted the following conclusions in terms of the preferred conformations of our sequential peptides in water:

1. The spectra of dimer, trimer, tetramer, and pentamer, with their wide range of positive ellipticities between 200 and 235 nm and the absence of any strong negative Cotton effect above 190 nm, can be safely assigned to an ensemble of a predominant poly-(L-Pro)$_n$ II component and a unordered conformation.

2. The curves of hexamer and heptamer, with a clear negative Cotton effect at about 200 nm, but with an increasingly negative ellipticity below 195 nm, are consistent with the onset of a partially helical conformation. We assign the nature of the helix that is formed to be of the$3_{10}$-type, as the calculated R values are 0.15 for the hexamer and 0.30 for the heptamer (however, it is worth mentioning here that the ECD curves appear to contain a significant positive contribution near 220 nm from the poly-(L-Pro)$_n$ II component that might lower the R value).

3. The curves of the octamer and nonamer, both showing negative Cotton effects at 225 and 203 nm, are indicative of well-developed helical structures. The corresponding R values, 0.40 for the octamer and 0.70 for the nonamer, strongly support the view that the

former peptide begins to fold in the α-helix conformation, while the latter peptide is largely α-helical. It is also worth pointing out that the ellipticity of the negative Cotton effect near 200 nm increases significantly from the 7-mer to the 8-mer, but it decreases from either the 6-mer to the 7-mer or from the 8-mer to the 9-mer. This observation seems not only to indicate that the overall peptide helicity is much more influenced by the incorporation of an Aib residue, as expected,[3c,3g] but also that the overall ellipticity is poorly sensitive to the addition of an extra, although chiral, Ala residue. Finally, we checked the influence of a few chemical and environmental parameters on the ECD spectrum of the octapeptide: (i) nature of the C-terminal group, a carboxylic ester (–$COOCH_3$), a carboxylic acid (-COOH), or an ionized (–$COO^-$) moiety (**Figure 2**); and (ii) heating.

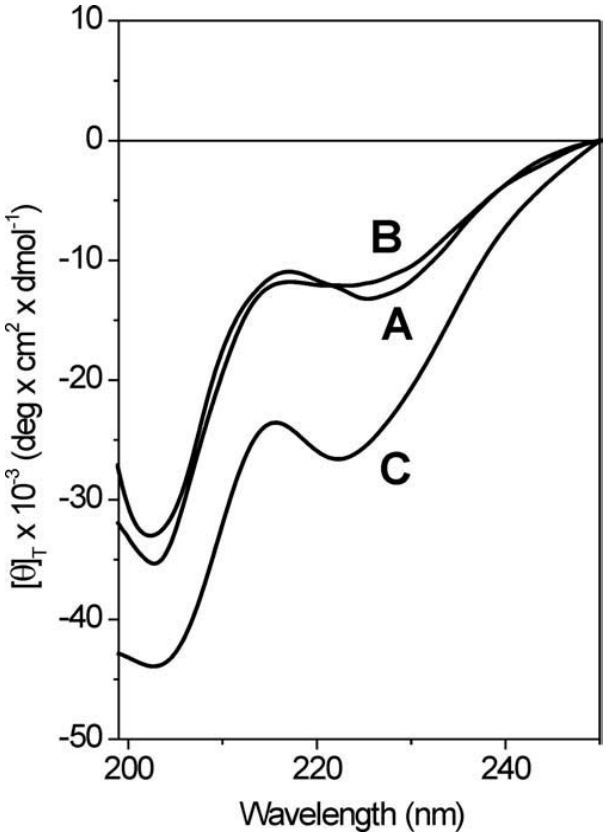


***Fig. 2*** ECD spectra of Ac–(Aib–Ala)$_4$–OMe in water at 20°C before (A) and after (B) alkaline hydrolysis, and after protonation of the C-terminal group to –COOH (C).

The results suggest that temperature (at least in the range 20-50°C, data not shown) as well as alkaline hydrolysis of the ester bond to the -$COO^-$ function have only a negligible effect on the ECD spectrum (**Figure 2**). Conversely, protonation of the

ionized -COO$^-$ moiety to -COOH tends to shift the $3_{10}$-helix↔α-helix equilibrium significantly in favor of the latter secondary structure (R=0.60). Similar results have already been reported and discussed by our group on a related peptide octamer.[19]As stated earlier, more than 30 years ago, Oekonomopulos and Jung reported the ECD spectrum of the terminally protected decapeptide Boc–(Aib–Ala)$_5$–OPOE [*tert*-butoxycarbonyl (Boc), polyethyleneglycol (POE)] in water.[20] The curve shows two negative Cotton effects, at 202 nm (stronger) and 229 nm (weaker). The R value is 0.35. Considering that the ECD spectrum of a $3_{10}$-helix was not known yet, not unexpectedly the authors proposed a "mainly unordered conformation" for that peptide. We tend to mainly ascribe the different R values (0.70 versus 0.35) and the related percentages of $3_{10}$-versus α-helix conformations in our nonapeptide and Oekonomopulos and Jung's decapeptide to the different N- and C-protecting groups in the two peptides. In particular, the role of the highly hydrophilic POE polymer, although known not to alter the global helicity in water of the peptide to the C-terminus of which it is covalently linked, has not been deeply investigated to date as far as this specific conformational transition is concerned.[21]

C$^\alpha$-tetrasubstituted α-amino acids, the prototype of which is Aib, are instrumental in remarkably stabilizing turn and helical structures in short peptides.[3c,3g] Determining the main-chain length for the onset of a given helical structure is essential for the study of how peptides and proteins fold. In this connection, it is widely recognized that folding initially implies formation of intramolecular C=O···H–N hydrogen bonds of the helical, type-III, β-turn conformation. Subsequently, this same H-bonding pattern propagates, affording a $3_{10}$-helix. As the helical stretch elongates further, the less-constrained, but structurally related, α-helix tends to become more stable than the $3_{10}$-helix.[3g,5b,22] Terminally protected Aib homopeptides adopt the type-III (III') β-turn conformation at a stage as low as the trimer in the crystal state. A fully developed $3_{10}$-helix is first seen at the homo-pentamer level.[4,23]These same conformations were observed in the trimer and octamer in solvents of low polarity, e.g. $CDCl_3$.[9a,24] ECD spectroscopy showed that the terminally blocked (αMe)Val (C$^\alpha$-methyl Val) homo-hexamer is $3_{10}$-helical in methanol.[3f,25]A solvent-controlled, reversible $3_{10}$-/α-helix transition does take place for this oligomer on going to highly polar alcohols.[3e] Crystals of an N-acetylated (αMe)Val homo-heptamer alkylamide exhibits $3_{10}$-/α-helix dimorphism depending on the alcohol solution from which they are grown.[26] An N-benzyloxycarbonyl/C$^\alpha$methoxy protected

homo-octamer based on a chiral, $C^{\alpha}\leftrightarrow C^{\alpha}$ cyclized, α-amino acid was found to fold in the α-helix structure in the crystalline state.[27] None of these homo-oligomers is water soluble. As for the extensively investigated, sequential peptides based exclusively on Aib and Ala, the terminally protected –Aib-(Ala-Aib)$_2$- and -(Aib-Ala)$_3$- are the shortest oligomers reported till date to be folded in the $3_{10}$-helix structure in the crystal state (interestingly, the –Ala–Aib–Ala– tripeptide does form a β-turn, but it is not of the helical type).[5a,28] Further main-chain elongation to the octapeptide -(Aib-Ala)$_4$-,but not to the isomeric -(Ala-Aib)$_4$-, generates an α-helix structure. In $CDCl_3$ solution, a nascent $3_{10}$-helix is seen in the -(Aib-Ala)$_2$ tetrapeptide,and a fully developed $3_{10}$-helix in the -Ala-(Aib-Ala)$_2$- pentapeptide.The onset of the α-helix is first observed in the -(Ala-Aib)$_5$- decapeptide. In alcohol solutions, the ECD signatures typical of the $3_{10}$- and α-helices are recognized at the heptamer and octamer levels, respectively.[5a,7,9,11,13,15c,20,29]The present study was intended to fill the gap derived from the absence in the literature of any detailed conformational study in the much more biologically relevant aqueous solution (at physiological pH and temperature) on a complete peptide series rich in helicogenic $C^{\alpha}$-tetrasubstituted α-amino acids aimed at assessing their critical main-chain length for helix formation. We find that, in the sequential series based on Aib and Ala residues only, the "borderline" peptides between different (non-helical versus $3_{10}$-helical, and $3_{10}$-helical versus α-helical) conformations under these experimental conditions are the hexamers and octamers, respectively.

In summary, we reported the synthesis and conformational electronic CD characterization in water of the whole series of alternating -Aib-Ala- and -Ala-Aib-Ala- oligomers up to nonamer. This work represents the first example of a wholly water soluble peptide series whose conformation has been fully characterized *via* ECD spectroscopy in water. This investigation allowed to fill the gap in the knowledge on the conformational behavior for this peptide series in a so relevant biological solvent. It was shown that the conformation is mostly $3_{10}$ even from the tetramer stage, and is fully developed at the hexamer stage. These are the shortest examples ever seen in water for such a conformation. Moreover, it was possible to determinate the turn point for the $3_{10}\leftrightarrow$α-helix transition. It is indeed well known that Aib-containing peptides, relying on the content of the $C^{\alpha}$-tetra substituted amino acid, show a $3_{10}$ preference for shortest peptide even in alcohols, whereas α-helix is preferred for the longest ones. In this case, the values of R (a parameter calculated on the ratio between molar ellipticies of the two

negative maxima in UV-ECD spectra at 203 and 220nm) clearly indicates that the α-form contributes significantly at the eptamer stage, whereas the octamer is quite completely an α-helix. The helix stability has also been confirmed for different ionization form of C-terminus, where nor saponification to carboxylate nor further re-acidification to free carboxyl can induce a destabilization of the structure. The temperature also had only negligible effects on conformation. This property of Aib-containing peptide has also already been demonstrated in DMSO solution for omo-Aib, up to very high temperature.[3d,9b,29e] In conclusion, the reported work permitted to investigate the conformation dependence varying the chain-length only. Further investigation will explain the reasons for the solubility properties in water. In fact, none structure element in these peptides had been inserted in order to induce hydrophylicity as in ATANP-containing peptides, nor the peptide itself presents charge or polar moieties.[14]

## EXPERIMENTAL SECTION

### GENERAL METHODS

**NMR:** $^1$H spectra were recorded at room temperature on a Bruker AV-200 (200 MHz) instrument using deuterated chloroform (98.8% Fluka). The multiplicity of a signal is indicated as: s - singlet, d - doublet, t - triplet, q - quartet, m - multiplet. Chemical shifts (δ) are expressed in ppm .

**TLC**: The products and intermediates have been checked on TLC plate with the following eluant systems:

| | |
|---|---|
| $CHCl_3$/EtOH 9:1 | $Rf_1$ |
| 1-Butanol/AcOH/$H_2O$ 3:1:1 | $Rf_2$ |
| toluene/EtOH 7:1 | $Rf_3$ |

**FT IR:** The KBr spectra were recorded on a Perkin-Elmer 580 B equipped with an IR data station Perkin-Elmer 3600. For spectra in $CDCl_3$ (98.8% Fluka), a Perkin-Elmer 1720X was emploeyd. The instrument operates in FT and is interfaced to a IBM PS/2 50 Z computer. 0.1 and 1cm $CaF_2$ pathway cells have been employed. For each spectrum have been collected 50 scans (4cm$^{-1}$ resolution) under nitrogen.

**Mass Spectrometry:** High-resolution mass spectra were obtained by electrospray ionization (ESI) on a Perseptive Biosystem Mariner ESI-TOF or a Bruker Microtof-Q spectrometer.

**CD:** The ECD spectra were obtained on a Jasco (Tokyo, Japan) model J-715 spectropolarimeter. Cylindrical fused quartz cells (Hellma, Müllheim, Germany) of 0.1and 0.01 cm pathlength were used. The data are expressed in terms of $[\Theta]_T$, total molar ellipticity (degx cm$^2$xdmol$^{-1}$). The solvent used was pH 7 Milli-Q water (Millipore Corporation, Billerica, MA). A Haake (Karlsruhe, Germany) model F3 thermostat was used for the measurements at temperatures >20°C. Values are reported in total molar ellipticy (deg x cm$^2$ x dmol$^{-1}$) :

$$[\Theta]_T = (MW \times \Theta)/(l \times c) = 3300 \times \Delta\varepsilon = 3300 \times (\varepsilon_L - \varepsilon_R)$$

Θ = observed ellipticy

MW = molecular weight

l = pathway length (cm)

c = concentration in gr/l

$\Delta\varepsilon = \varepsilon_L - \varepsilon_R$ = difference between left- and right-handed component of estinction coefficients of polarized light

SYNTHESIS AND CHARACTERIZATION

**HCl·H-L-Ala-OMe**

To 100 mL of anydrous MeOH at -15°C, 25 g ofH-L-Ala-OH [380 mmol] and $SOCl_2$ (32.68 mL, 450 mmol) were added under stirring. The flask was closed with $CaCl_2$ tube and the temperature was left rising up to r.t. Therefore,the system has been refluxed for 20 hours. The solvent has been removed under reduced pressure, taking many times the residue in $Et_2O$. The product precipitated as a white powder from MeOH/$Et_2O$. Yield 92%.**IR** (KBr): 3421, 2987, 1740 $cm^{-1}$. **$^1$H NMR** (200 MHz, $CDCl_3$): δ 8.68 [broad s, 3H, Ala $NH_3$], 4.06-4.31 [q, 1H, Ala α-CH], 3.73 [s, 3H, Ala -OMe], 1.43-1.40 [d, 3H, Ala β-$CH_3$].

**Z-L-Ala-OH**

To 100 mL of $H_2O$/MeCN 1:1 15.6 g of H-L-Ala-OH (170 mmol) were added under stirring. The mixture was cooled down to 0°C and then 43.15g (170 mmol) of Z-OSu, previously solved in 100 mL of MeCN, were added along with 24.2 mL of TEA (170 mmol).The mixture temperature was rised up to r.t. and the reaction followed on TLC plate. After 24 hours mostly of the MeCN was removed under vacuum, and the aqueous solution diluted with 50 mL of 5% $NaHCO_{3(aq.)}$.The solution was washed with 10 mL of $Et_2O$, acidified slowly with solid $KHSO_4$ and the extracted with EtOAc (3x100 mL). The organic layers were put together and washed with water (6x50 mL) and brine. The organic layer was dried on $Na_2SO_4$ and the solvent removed under vacuum. The product precipitated from EtOAc/PE as a white solid. Yield 95%. **IR** (KBr): 3388, 1736$cm^{-1}$.**$^1$H NMR** (200 MHz, $CDCl_3$): δ 10.06 [broad s, 1H, Ala -COOH], 7.36 [s, 5H, Z fenile], 5.35 [d, 1H, Ala NH], 5.14 [s, 2H, Z $CH_2$], 4.47-4.40 [m, 1H, Alaα-CH], 1.49-1.45 [d, 3H, Alaβ-$CH_3$].

**Z-Aib-OH**

To 100 mL of $H_2O$/MeCN 1:1, 20 g of H-Aib-OH [194 mmol] were added under stirring. The mixture was cooled down to 0°C and then 76 g (306 mmol) of Z-OSu, previously solved in 100 mL of MeCN, were added along with 40 mL of TEA (306 mmol). The mixture temperature was rised up to r.t. and the reaction followed on TLC plate. Another equivalent of Z-OSu has been added in six times during 3 days. The basicity of the solution has been corrected by addition of TEA. Then, mostly of the MeCN was removed under vacuum, and the aqueous solution diluted with 50 mL of 5% $NaHCO_{3(aq.)}$. The solution was washed with 10 mL of $Et_2O$, acidified slowly with solid $KHSO_4$and the extracted with EtOAc (3x100 mL). The organic layers were put together and washed with water (6x50 mL) and brine. The organic layer was dried on $Na_2SO_4$ and the solvent removed under vacuum. The product precipitated from EtOAc/PE as a white solid. Yield 95%. **IR** (KBr): 3334, 1714, 1519cm$^{-1}$. **$^1$H NMR** (200 MHz, $CDCl_3$): δ: 7.34 (s, 5H, phenyl ring), 5.45 (s, 1H, NH), 5.10 (s, 2H, $CH_2$), 1.56 (s, 6H, β-$CH_3$).

**Synthesis of Z- series**

**Z-Aib-L-Ala-OMe**

To a solution of 7g of Z-Aib-OH (30 mmol), 4.5bg of HOAt [33 mmol] and 6.3 g of EDC (33 mmol) in dry $CH_2Cl_2$ at 0°C, 12.1g of HCl·H-L-Ala-OMe (41mmol) were added along with 10mL of NMM (41mmol). The reaction has been kept at r.t. and under stirring and closed with $CaCl_2$ tube for 18 hours. The solvent has so been removed at low pressure and taken in EtOAc. The solution has been washed with 5% $KHSO_4$, $H_2O$, 5% $NaHCO_3$and brine.The organic layer was dried on $Na_2SO_4$ and the solvent removed under vacuum. The product precipitated from EtOAc/PE as a white solid. Yield 95%. **M.p.**: 55-59°C. **$Rf_1$:** 0.90; **$Rf_2$:** 0.95; **$Rf_3$:** 0.30. **$[\alpha]_D^{20}$**: -31.5° (c[g·mL$^{-1}$] =1.2, MeOH). **IR** (KBr): 3311, 1747, 1691, 1527 cm$^{-1}$. **IR** (KBr): 3311, 1747, 1691, 1527 cm$^{-1}$. **$^1$H NMR** (200 MHz, $CDCl_3$): δ 7.35 [s, 5H, Z fenile], 6.79-6.77 [d, 1H, Ala NH], 5.29 [s, 1H, AibNH], 5.10 [s, 2H, Z $CH_2$], 4.62-4.51 [m, 1H, Alaα-CH], 3.74 [s, 3H, -OMe $CH_3$], 1.55-1.53 [m, 6H, Aib 2 β-$CH_3$], 1.38-1.35 [d, 3H, Alaβ-$CH_3$].

**Z-L-Ala-Aib-L-Ala-OMe**

7 g of Z-Aib-L-Ala-OMe (22 mmol) were solved into 250 mL of MeOH in a 500 mL round bottom flask. Under stirring, $N_2$ was flushed for 15'. Then, 1.05 g of Pd/C (10%) was added and $H_2$ flushed instead of $N_2$. The reaction was followed for 3 hours at r.t. The catalyzer was filtered off on celite and the MeOH removed under reduced pressure till complete dryness. Then, a freshly prepared 50 mL solution indry $CH_2Cl_2$ at 0°C was added, containing 7.37 g of Z-L-Ala-OH (33 mmol), 4.9 g of HOAt (33 mmol) and 7.59 g of EDC (33 mmol) at 0°C. 4.65 mLof NMM (40 mmol) was added, too. The reaction has been followed on TLC plate for 18 hours. The solvent was removed under vacuum and the residue taken in 200 mL of EtOAc. The organic layer was then washed with 5%$KHSO_{4(aq.)}$, $H_2O$, 5%$NaHCO_{3(aq.)}$and brine.The organic layer was then dried over $Na_2SO_4$and solvent removed under vacuum. The product precipitated from EtOAc/PE as a white solid. Yield 70%.**M.p.**: 159-161°C. **$Rf_1$:** 0.80; **$Rf_2$:** 0.85; **$Rf_3$:** 0.15. **$[\alpha]_D^{20}$**: -51.0° (c[g·mL$^{-1}$] =1.2, MeOH). **IR** (KBr): 3377, 1741, 1680, 1537cm$^{-1}$. **$^1$H NMR** (200 MHz, $CDCl_3$): δ 7.35 [s, 5H, Z fenile], 6.95-6.92 [d, 1H, Ala NH], 6.50 [s, 1H, AibNH], 5.27-5.24 [d, 1H, Ala NH], 5.12 [s, 2H, Z $CH_2$], 4.61-4.46 [m, 1H, Alaα-CH], 4.19-4.05 [m, 1H, Alaα-CH], 3.74 [s, 3H, -OMe $CH_3$], 1.56-1.52 [m, 6H, Aib 2 β-$CH_3$], 1.40-1.37 [m, 6H, 2 Alaβ-$CH_3$].

**Z-Aib-L-Ala-Aib-L-Ala-OMe**

This product was obtained from 3.6 g of Z-Aib-OH (16 mmol) and H-L-Ala-Aib-L-Ala-OMe (15 mmol; obtained *via* catalytic hydrogenation as seen previously). The activation was accomplished with HOAt/EDC coupling reactant in dry DCM. The product precipitated from EtOAc/PE as a white solid. Yield 83%.**M.p.**: 60-63°C. **$Rf_1$:** 0.50; **$Rf_2$:** 0.85; **$Rf_3$:** 0.10. **$[\alpha]_D^{20}$**: -32.8° (c[g·mL$^{-1}$] =2.3, MeOH). **IR** (KBr): 3326, 1740, 1660, 1529cm$^{-1}$. **$^1$H NMR** (200 MHz, $CDCl_3$): δ 7.36 [s, 5H, Z fenile], 7.22-7.18 [d, 1H, Ala NH], 7.03 [s, 1H, Aib NH], 6.50-6.47 [d, 1H, Ala NH], 5.19 [s, 1H, Aib NH], 5.10 [s, 2H, Z $CH_2$], 4.59-4.45 [m, 1H, Alaα-CH], 4.24-4.14 [m, 1H, Alaα-CH], 3.72 [s, 3H, -OMe $CH_3$], 1.54-1.52 [m, 12H, 2 Aib 2 β-$CH_3$], 1.38-1.34 [m, 6H, 2 Alaβ-$CH_3$].

**Z-L-Ala-Aib-L-Ala-Aib-L-Ala-OMe**

This product was obtained from 2.6 g of Z-L-Ala-OH (12 mmol) and H-Aib-L-Ala-Aib-L-Ala-OMe [12 mmol; obtained *via* catalytic hydrogenation as seen previously]. The activation was accomplished with HOAt/EDC coupling reactant in dry DCM. The product was purified on silica gel chromatographic column (95:5 $CHCl_3$:EtOH) and then precipitated from EtOAc/PE as a white solid. Yield 80%.**M.p.**: 62-65°C. **$Rf_1$:** 0.50; **$Rf_2$:** 0.80; **$Rf_3$:** 0.10. **$[\alpha]_D^{20}$**: -25.6° (c[g·mL$^{-1}$] =2.3, MeOH). **IR** (KBr): 3315, 1741, 1665, 1531cm$^{-1}$. **$^1$H NMR** (200 MHz, $CDCl_3$): δ 7.35 [s, 5H, Z fenile], 7.20-7.14 [m, 3H, Ala NH, Aib NH, Ala NH], 6.52 [s, 1H, Aib NH], 5.54-5.52 [d, 1H, Ala NH], 5.13-4.94 [q, 2H, Z $CH_2$], 4.61-4.50 [m, 1H, Alaα-CH], 4.46-4.01 [2m, 2H, Alaα-CH, Alaα-CH], 3.67 [s, 3H, -OMe $CH_3$], 1.55-1.03 [m, 21H, 2 Aib 2 β-$CH_3$, 3 Alaβ-$CH_3$].

**Z-Aib-L-Ala-Aib-L-Ala-Aib-L-Ala-OMe**

This product was obtained from 2.1 g of Z-Aib-OH (9 mmol) and H-L-Ala-Aib-L-Ala-Aib-L-Ala-OMe (9 mmol; obtained *via* catalytic hydrogenation as seen previously). The activation was accomplished with HOAt/EDC coupling reactant in dry DCM. The product was purified on silica gel chromatographic column (90:10 $CHCl_3$:EtOH) and then precipitated from EtOAc/PE as a white solid. Yield 99%.**M.p.**: 65-68°C. **$Rf_1$:** 0.45; **$Rf_2$:** 0.80; **$Rf_3$:** 0.10. **$[\alpha]_D^{20}$**: -13.3° (c[g·mL$^{-1}$] =1.7, MeOH). **IR** (KBr): 3321, 1743, 1662, 1531cm$^{-1}$. **$^1$H NMR** (200 MHz, $CDCl_3$): δ 7.45-7.15 [5m, 5H, 2 Aib NH, 3 Ala NH], 7.35 [s, 5H, Z fenile], 6.56 [s, 1H, Aib NH], 5.19-5.01 [q, 2H, Z $CH_2$], 4.63-4.52 [m, 1H, Alaα-CH], 4.48-4.30 [m, 1H, Alaα-CH], 4.02-3.97 [m, 1H, Alaα-CH], 3.64 [s, 3H, -OMe $CH_3$], 1.55-1.32 [m, 27H, 3 Aib 2 β-$CH_3$, 3 Alaβ-$CH_3$].

**Z-L-Ala-Aib-L-Ala-Aib-L-Ala-Aib-L-Ala-OMe**

This product was obtained from 1.8 g of Z-L-Ala-OH (8 mmol) and H-Aib-L-Ala-Aib-L-Ala-Aib-L-Ala-OMe (8 mmol; obtained *via* catalytic hydrogenation as seen previously). The activation was accomplished with HOAt/EDC coupling reactant in dry DCM. The product was purified on silica gel chromatographic column (90:10 $CHCl_3$:EtOH) and then precipitated from EtOAc/PE as a white solid. Yield 50%. **M.p.**: 70-73°C. **$Rf_1$:** 0.35; **$Rf_2$:** 0.75; **$Rf_3$:** 0.10. **$[\alpha]_D^{20}$**: -17.7° (c[g·mL$^{-1}$] =1.1, MeOH). **IR** (KBr): 3321, 1745, 1662, 1531cm$^{-1}$. **$^1$H NMR** (200 MHz, $CDCl_3$): δ 7.43-7.17 [5m, 5H,

2 Aib NH, 3 Ala NH], 7.36 [s, 5H, Z fenile], 6.67 [s, 1H, Aib NH], 5.72-5.71 [d, 1H, Ala NH], 5.25-5.05 [q, 2H, Z $CH_2$], 4.63-4.56 [m, 1H, Alaα-CH], 4.42-4.35 [m, 1H, Alaα-CH], 4.04-3.94 [m, 2H, 2 Alaα-CH], 3.66 [s, 3H, -OMe $CH_3$], 1.59-1.16 [m, 30H, 3 Aib 2 β-$CH_3$, 4 Alaβ-$CH_3$].

**Z-Aib-L-Ala-Aib-L-Ala-Aib-L-Ala-Aib-L-Ala-OMe**

This product was obtained from 0.3 g of Z-Aib-OH (1.2 mmol) and H-L-Ala-Aib-L-Ala-Aib-L-Ala-Aib-L-Ala-OMe (1.2 mmol; obtained *via* catalytic hydrogenation as seen previously). The activation was accomplished with HOAt/EDC coupling reactant in dry DCM. The product was directly purified on silica gel chromatographic column (90:10 $CHCl_3$:EtOH) without aqueous work-up and then precipitated from EtOAc/PE as a white solid. Yield 95%. M.p.: 143-146°C. $Rf_1$: 0.35; $Rf_2$: 0.75; $Rf_3$: 0.10. $[\alpha]_D^{20}$: -77.4° (c[g·mL$^{-1}$] =0.2, MeOH). IR (KBr): 3321, 1742, 1660, 1530cm$^{-1}$. $^1$H NMR (200 MHz, $CDCl_3$): δ 7.51-7.13 [7m, 7H, 3 Aib NH, 4 Ala NH], 7.36 [s, 5H, Z fenile], 6.38 [s, 1H, Aib NH], 5.22-5.02 [q, 2H, Z $CH_2$], 4.65-4.50 [m, 1H, Ala α-CH], 4.44-4.33 [m, 1H, Ala α-CH], 4.05-3.73 [m, 2H, 2 Ala α-CH], 3.65 [s, 3H, -OMe $CH_3$], 1.58-1.25 [m, 36H, 4 Aib 2 β-$CH_3$, 4 Ala β-$CH_3$].

**Z-L-Ala-Aib-L-Ala-Aib-L-Ala-Aib-L-Ala-Aib-L-Ala-OMe**

This product was obtained from 0.2 g of Z-L-Ala-OH (0.8 mmol) and H-L-Ala-Aib-L-Ala-Aib-L-Ala-Aib-L-Ala-OMe (0.8 mmol; obtained *via* catalytic hydrogenation as seen previously). The activation was accomplished with HOAt/EDC coupling reactant in dry DCM. The product was directly purified on silica gel chromatographic column (90:10 $CHCl_3$:EtOH) without aqueous work-up and then precipitated from EtOAc/PE as a white solid. Yield 71%. **M.p.**: 103-106°C. **$Rf_1$**: 0.35; **$Rf_2$**: 0.75; **$Rf_3$**: 0.10. **$[\alpha]_D^{20}$**: -26.8° (c[g·mL$^{-1}$] =0.9, MeOH). **IR** (KBr): 3321, 1744, 1662, 1531cm$^{-1}$. **$^1$H NMR** (200 MHz, $CDCl_3$): δ 7.75-7.34 [8m, 8H, 4 Aib NH, 4 Ala NH], 7.35 [s, 5H, Z fenile], 6.86 [s, 1H, Ala NH], 5.24-5.06 [q, 2H, Z $CH_2$], 4.62-4.32 [2m, 2H, 2 Ala α-CH], 4.06-4.90 [m, 3H, 3 Ala α-CH], 3.66 [s, 3H, -OMe $CH_3$], 1.90-1.29 [m, 39H, 4 Aib 2 β-$CH_3$, 5 Ala β-$CH_3$].

**Synthesis of Ac- Series**

Each Z- derivatives have been converted in part to its Ac- analogue. The general synthetic procedure is further described synthetically for Ac-(Aib-L-Ala)$_4$-OMe.

50 mg of Z-(Aib-L-Ala)$_4$-OMe (0.7 mmol) were solved into 5 mL of MeOH in a 50 mL round bottom flask. Under stirring, $N_2$ was flushed for 15'. Then, 10mg of Pd/C (10%) was added and $H_2$ flushed instead of $N_2$. The reaction was followed for 20' at r.t.. The catalyzer was filtered off on celite and the MeOH removed under reduced pressure till complete dryness. Then, the residue was taken in 5 mL dry DCM and 1 mL of $Ac_2O$ straight added to solution. The reaction was followed on TLC plate for 10'. Then the solvent was removed under vacuum, taking at least 4 times with acetonitrile. Then, distilled water (5 mL) was added to residue and the so-obtained solution was finally lyophilized. The product has been purified on silica gel column ($CHCl_3$:EtOH 99:1). Yield 90%. **ESI-MS** (m/z)= 699.4 [M+H$^+$], 721.4 [M+Na$^+$]. **IR** (KBr):3317, 1743, 1656, 1534 cm$^{-1}$.**$^1$H NMR** (200 MHz, $CDCl_3$): δ7.59-7.32 (m, 8H, 8 NH), 4.54-4.47 (t, 1H, Ala α-CH), 4.32-4.25 (t, 1H, Ala α-CH), 4.05-3.96 (m, 2H, 2 Ala α-CH), 3.68 (s, 3H, s, 3H, -OMe $CH_3$), 2.04 (s, 3H, Ac $CH_3$), 1.56-1.42 (m, 36H, 4 Aib 2 β-$CH_3$, 4 Ala β-$CH_3$).

REFERENCES


1) Santagada V.,Caliendo G., *Peptidi e Peptidomimetici. Progettazione, Sintesi e Caratterizzazione, Applicazioni di Nuove Strategie Sintetiche (Chimica Combinatoriale, Microonde)*, **2003**. Padova, Piccin Ed.. Piccin Nuova Libraria S.p.A.
2) a) Bock J.E., Gavenois J.,Kritzer J.A., *ACS Chemical Biology*, **2012**, in press ; b) Chen Y., Mant C.T., *et al.*, *The Journal of Biological Chemistry*, **2005**, 13 (1), 12316-12329 ; c) Cowell S.M., Lee Y.S., Cain J.P.,Hruby V.J., *Current Medicinal Chemistry*, **2004**, 11, 2785-2789 ; d) Hanessian S., McNaughton-Smith G., Lombart H.-G.,Lubell W.D., *Tetrahedron*, **1997**, 53 (38), 12789-12854 ; e) Hruby V.J., Li G., Haskell-Luevano C.,Shenderovich M., *Biopolymers*, **1997**, 43 (3), 219-266 ; f) Meyer F.-M., Collins J.C., *et al.*, *Journal of Organic Chemistry*, **2012**, 77 (3099-3114) ; g) Tiwari R.K.,Parang K., *Current Pharmaceutical Design*, **2012**, 18, 2852-2866 ; h) Wang B., Gangwar S., *et al.*, *Journal of Organic Chemistry*, **1997**, 62, 1363-1367 ; i) Wender P.A., Mitchell D.J., *et al.*, *PNAS*, **2000**, 97 (24), 13003-13008
3) a) Bellanda M., Mammi S., *et al.*, *Chemistry - A European Journal*, **2007**, 13 (407-416) ; b) Crisma M., Bisson W., *et al.*, *Biopolymers*, **2002**, 64 (5), 236-245 ; c) Karle I.L.,Balaram P., *Biochemistry*, **1990**, 29 (6747-6756) ; d) Kaul R.,Balaram P., *Bioorganic & Medicinal Chemistry*, **1999**, 7, 105-117 ; e) Moretto A., Formaggio F., *et al.*, *Biopolymers (Pept Sci)*, **2008**, 90 (4), 567-574 ; f) Polese A., Formaggio F., *et al.*, *Chemistry - A European Journal*, **1996**, 2, 1104-1111 ; g) Toniolo C., Crisma M., Formaggio F.,Peggion C., *Biopolymers (Pept Sci)*, **2001**, 60 (6), 396-419
4) Benedetti E., Bavoso A., *et al.*, *Journal of American Chemical Society*, **1982**, 104, 2437-2444
5) a) Pavone V., Benedetti E., *et al.*, *Journal of Biomolecular Structure & Dynamics*, **1990**, 7, 1321-1331 ; b) Toniolo C.,Benedetti E., *Trends in Biochemical Sciences*, **1991**, 16, 350-353
6) Benedetti E., Blasio B.D., *et al.*, *Journal of the Chemical Society, Perkin Transactions*, **1990**, 2, 1829-1837
7) Otoda K., Kitagawa Y., Kimura S.,Imanishi Y., *Biopolymers*, **1993**, 33, 1337-1345
8) Formaggio F., Crisma M., Toniolo C.,Kamphuis J., *Biopolymers*, **1996**, 38, 301-304
9) a) Kennedy D.F., Crisma M., Toniolo C.,Chapman D., *Biochemistry*, **1991**, 30, 6541-6548 ; b) Vijayakumar E.K.S.,Balaram P., *Tetrahedron*, **1983**, 39, 2725-2731
10) Martin D.,Hauthal G., *Dimethyl Sulphoxide*, **1975**. Wokingam, UK, Van Nostrand-Reinhold
11) Arikuma Y., Nakayama H., Morita T.,Kimura S., *Langmuir*, **2011**, 27, 1530-1535
12) Toniolo C., Formaggio F., *et al.*, *Tetrahedron: Asymmetry*, **1994**, 5, 507-510
13) Mayr W., Oekonomopulos R.,Jung G., *Biopolymers*, **1979**, 18, 425-450
14) Formaggio F., Crisma M., *et al.*, *Chemistry - A European Journal*, **2000**, 6 (4), 4498-4504
15) a) Kitagawa K., Morita T.,Kimura S., *Angewandte Chemie International Edition*, **2005**, 44, 6330-6333 ; b) Okamoto S., Morita T.,Kimura S., *Langmuir*, **2009**, 25,

3297-3304 ; c) Otoda K., Kimura S.,Imanishi Y., *Biochimica et Biophysica Acta*, **1993**, 1150, 1-8 ; d) Takeda K., Morita T.,Kimura S., *Journal of Physical Chemistry B*, **2008**, 112, 12840-12850

16) Carpino L.A., *Journal of American Chemical Society*, **1993**, 115, 4397-4398
17) a) Goodman M., Verdini A.S., *et al.*, *PNAS*, **1969**, 64, 444-450 ; b) Holzwarth G.,Doty P., *Journal of American Chemical Society*, **1965**, 87 (218-228)
18) a) Formaggio F., Peggion C., *et al.*, *Chirality*, **2004**, 16, 388-397 ; b) Manning M.C.,Woody R.W., *Biopolymers*, **1991**, 31, 569-586
19) Moretto A., Crisma M., *et al.*, *Biopolymers (Pept Sci)*, **2007**, 88, 233-238
20) Oekonomopulos R.,Jung G., *Biopolymers*, **1980**, 19, 203-214
21) Toniolo C., Bonora G.M.,Mutter M., *Journal of American Chemical Society*, **1979**, 101, 450-454
22) Millhauser G.L., *Biochemistry*, **1995**, 34, 3873-3877
23) Shamala N., Nagaraj R.,Balaram P., *Journal of the Chemical Society, Chemical Communications*, **1978**, (996-997)
24) Toniolo C., Bonora G.M., *et al.*, *Macromolecules*, **1985**, 18, 895-902
25) Krieger D.T., *Science*, **1983**, 222, 975-985
26) Crisma M., Saviano M., *et al.*, *Journal of American Chemical Society*, **2007**, 129, 15471-15473
27) Tanaka M., Demizu Y., Doi M.,Suemune H., *Angewandte Chemie International Edition*, **2004**, 43, 5360-5363
28) Jung G., Bosch R., *et al.*, *Biopolymers*, **1938**, 22, 241-246
29) a) Arikuma Y., Nakayama H., Morita T.,Kimura S., *Angewandte Chemie International Edition*, **2010**, 49, 1800-1804 ; b) Ishikawa T., Morita T.,Kimura S., *Journal of Peptide Science*, **2008**, 14, 192-202 ; c) Kai M., Takeda K., Morita T.,Kimura S., *Journal of Peptide Science*, **2008**, 14 (192-202) ; d) Nakayama H., Morita T.,Kimura S., *Journal of Physical Chemistry C*, **2010**, 114, 4669-4674 ; e) Vijayakumar E.K.S.,Balaram P., *Biopolymers*, **1983**, 22 (2133-2140)

# II

## Role of amino acid chirality and helical conformation in inducing plasmonicCD bands of peptide-capped gold nanoparticles

### INTRODUCTION

Peptide-functionalized gold nanoparticles constitute quite appealing supramolecular systems for their ability to mimic properties of natural proteins. Indeed, by confining on the surface of a cluster of gold atoms several copies of a peptide, a nanosystem that resembles a protein in size (a few nanometers), shape (globular), and possibly, function, may be obtained. Peptide-functionalized gold nanoparticles have been used, inter alia, in catalysis, selective protein recognition, drug delivery, and gene transfection.[1] Whenever a protein is considered, chirality is a peculiar property of the biopolymer, both because of the presence of the chiral amino acids and, when present, of the helical conformation of the sequence. Accordingly, a mimetic system of a protein must take into account in its features this relevant property. In spite of this, little attention has been paid so far to the chiral properties of peptide-functionalized gold nanoparticles considering the whole supramolecular system (gold core and peptide passivating monolayer) and not just the easily-addressable peptide units. A number of interesting papers have been reported in the last several years after the first observation by Whetten of optical activity of glutathione (a tripeptide)-passivated gold nanoparticles.[2] It is now well accepted that chirality in such nanosystems may derive from: a) the chiral arrangement of the metal cluster of the gold core; b) the binding of the thiolates on the gold surface to form chirally arranged staples (an unusual bridged binding motif involving gold and sulfur); and c) the chirality of the surrounding monolayer of passivating organic molecules. Among the chiral biomolecules reported so far for nanocluster passivation are DNA,[3] peptide nanotubes,[4]cysteine,[5,6] glutathione,[7] and peptides.[8]

We have recently demonstrated that peptide sequences rich in $C^{\alpha}$-tetra substituted α-amino acids are endowed of the peculiar property to stabilize the metallic cluster of gold (and other noble metals as well) nanoparticles in very polar solvents.[9] This was attributed to the strong propensity of these sequences to fold into rather robust $3_{10}$- or α-helix conformations. Critical parameters, like main-chain length and type of solvent used, have been fairly assessed for helix formation of these peptides in solution.[10,11] However, nothing is known concerning their folding behavior when bound to the

surface of a gold nanoparticle. Furthermore, no study is available on the role of the individual amino acids and secondary structure of the sequence in inducing chiroptical properties to the passivated nanoparticles. This paper specifically addresses these points.We have already reported on the helical folding properties in water of a series of N-terminally acetylated, C-terminally methoxylatedoligopeptides, characterized by a sequence with alternating Aib (α-amino *iso*butyric acid) and L-Ala residues, from the dimer to the nonamer.[11] We found that the critical main-chain length for $3_{10}$- and α-helix formation in aqueous solution, although not to a full extent, is six residues. These structurally robust sequences constituted the bases for our investigation.

## RESULTS AND DISCUSSION

The Z-derivated peptide oligomers[11] were modified by thiol-functionalization at the N-terminus for passivation of the gold nanoclusters. The seven peptides with Aib/L-Ala alternating residues and N-mercaptopropionyl (mpr-) N-termination (**2**-**8**, see **Figure 1**) were synthesized by conventional solution protocols. Even sequences are characterized by an Aib amino acid at the N-terminus while odd ones are characterized by a L-Ala amino acid because our optimized synthetic protocol uses L-Ala as C-terminus starting peptide.

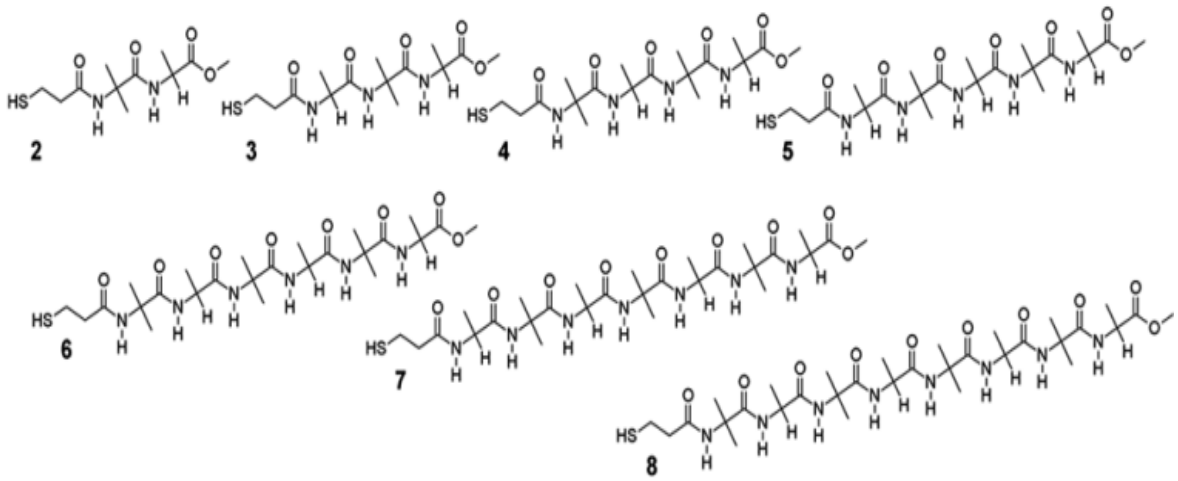


***Fig. 1.***Chemical structure for: **2**, m*pr*-Aib-Ala-OMe; **3**, m*pr*-Ala-Aib-Ala-OMe; **4**, m*pr*-(Aib-Ala)$_2$-OMe; **5**, m*pr*-Ala-(Aib-Ala)$_2$-OMe; **6**, m*pr*-(Aib-Ala)$_3$-OMe; **7**, m*pr*-Ala-(Aib-Ala)$_3$-OMe; **8**, m*pr*-(Aib-Ala)$_4$-OMe.

All the seven peptides were chemically characterized in full and, because of their good solubility in water, we were able to record their ECD spectra in the far-UV region in this solvent at neutral pH. In spite of the presence of potentially interfering chromophores (the N-terminal mercapto-propionamide and the C-terminal methyl ester)[12–14] the spectra didn't show marked modification of the dichroic signature. This resembles that found for the parent oligomers devoid of the thiolated unit. **Figure 2A** shows the ECD spectra of all oligomers. Noteworthy, there is an increase in folding propensity and associated chiroptical properties in the series, but such a trend is not linear due to two contrasting effects at play as the sequence elongates. In fact, on one side all even-number oligomers should exhibit a significantly higher helicity than that of their immediately lower (odd) oligomer, not only by virtue of their slightly longer main chain but also because the newly incorporated residue is the strongly helicogenic Aib.[15–

[17] On the other side, the chiral L-Ala added to form each odd oligomer, although remarkably less helicogenic than Aib, should contribute to the observed ellipticity much more than the achiral Aib. The data show, in line with our previous results that, in the sequential series **2-8**, a helical conformation starts to form with the hexamer while a complete helix is observed only with the octamer.

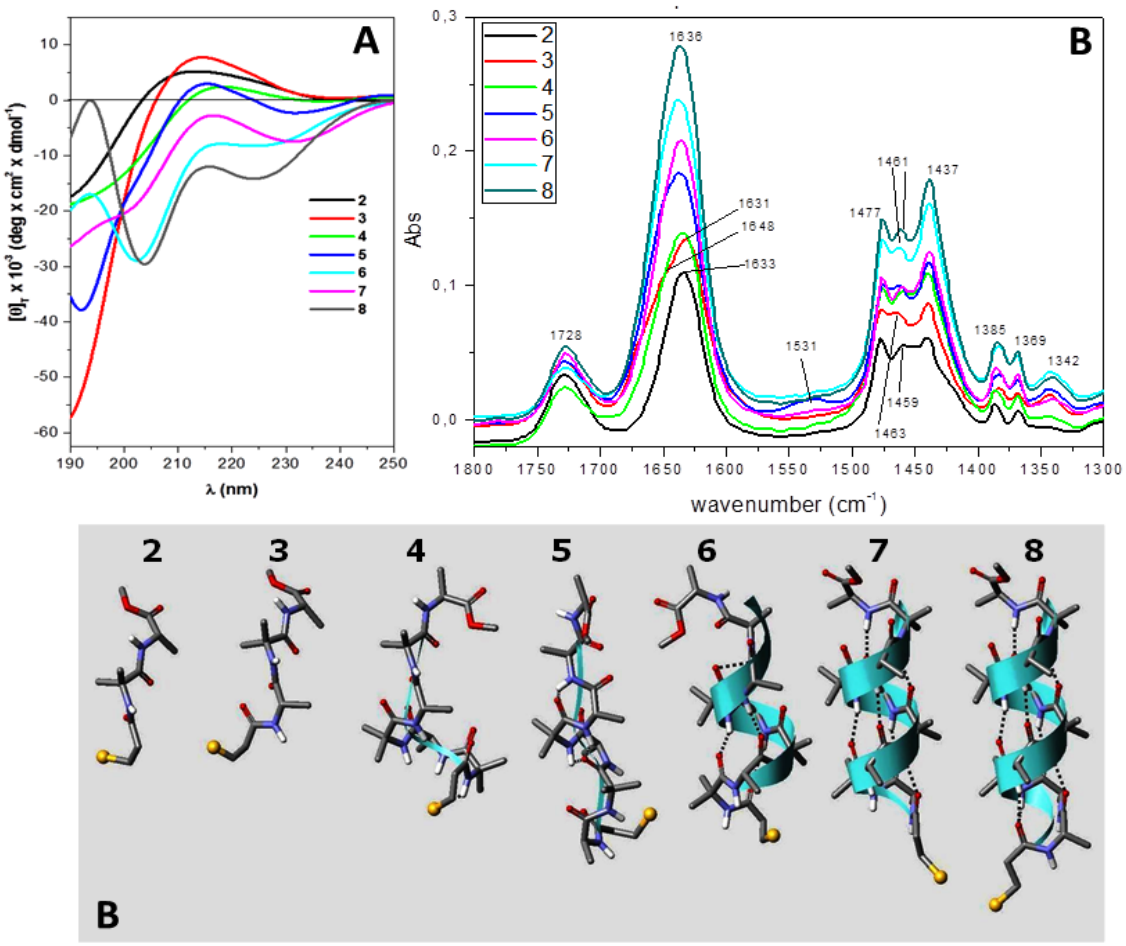


***Fig. 2*** **A**: Far-UV ECD spectra of **2-8** series recorded in water at 20°C. Concentration 1 mM. **B**: FTIR absorption spectra of **2-8** series recorded in *deuterated* water at 20°C. Concentration 10 mM. **C**: proposed folding process for the **2-8** series.

The analysis of the ellipticity ratios (R) between the negative 222 nm (peptide n → π* transition, Cotton effect) and that near 205 nm allows the discrimination between the $3_{10}$- and α-helix structure.[18] It is well accepted that a value of 0.15-0.35 for R is considered diagnostic for a $3_{10}$-helix, while a value close to the unity is typical of a α-helix. In our case R is ca. 0.3 for **8** supporting the assignment of a $3_{10}$-helix conformation. Information obtained from ECD experiments were confirmed by FTIR absorption spectra in the C=O stretching region, which were recorded for the sequential

series 2-8 in *deuterated* water (**Figure 2B**). The ester C=O band is located at 1728 $cm^{-1}$, while the amide I C=O band spans from 1633 (**2**) to 1638 (**8**) $cm^{-1}$ (amide II band is located in the 1460 $cm^{-1}$ region). The peptide chain elongation results into an increasing molar absorption in going from peptide 2 to 8, as the result of the larger number of chromophores in the longer peptides. The concomitant shift of the absorption maxima to slightly higher wavenumbers confirms the formation of consecutive C=O···H-N intramolecular H-bonds of the β-turn type, that finally results in a stabilized helical structure from the hexamer to the octamer. The overall folding process is reported in **Figure 2C**.These oligopeptides where then used as passivating agents for the synthesis of the gold nanoparticles AuNp**2-8**. The nanoparticles were prepared by one phase $NaBH_4$ reduction of $HAuCl_4$ in water/methanol and in the presence of a two-fold molar excess of the peptides. After purification *via* gel filtration, the nanoparticles were characterized by TEM and TGA analysis, as previously reported,[9a] to obtain the relevant characterization data summarized in **Table 1**. Inspection of **Table 1** shows that diameters of the obtained nanoparticles are fairly constant in the 2.0-2.4 nm range.

***Tab. 1*** Chemical structures data for all peptide-capped AuNp**2-8** reported in this work.

| Entry | Core *d* (nm) | Au atoms forAuNp[b] | Pep. chain for AuNp[c] | Footprint ($nm^2$) |
|---|---|---|---|---|
| AuNp**2** | 2.0 | 247 | 126 | 0.10 |
| AuNp**3** | 2.2 | 329 | 138 | 0.11 |
| AuNp**4** | 2.3 | 376 | 119 | 0.14 |
| AuNp**5** | 2.0 | 247 | 55 | 0.23 |
| AuNp**6** | 2.3 | 376 | 54 | 0.31 |
| AuNp**7** | 2.4 | 427 | 33 | 0.45 |
| AuNp**8** | 2.4 | 427 | 27 | 0.68 |

[a] *d* = diameter. Calculated by averaging the size of at least 200 nanoparticles;[b] Calculated assuming a spherical model.

On the contrary, there is a huge decrease in the number of peptides necessary to fully passivate the gold cluster surface as the sequence elongates. In fact with AuNp**8** the number of peptides reduces to ca. one fifth with respect to that required for shorter peptides. This implies a larger surface coverage exerted by each peptide (footprint increases from ca. 0.1 $nm^2$ to 0.2 $nm^2$ and eventually to ca. 0.7 $nm^2$). Footprint values obtained for AuNp**1**-**3** are similar to those reported for gold nanoparticles passivated by alkylthiols or poly(Aib) short peptides, and indicate a dense packing of the coating molecules on the particles surface. On the other hand, footprints observed for AuNp**8** are similar to the ones we previously reports for gold nanoparticles coated with helical

peptides.[8] This quite interesting behavior of the peptides when bound to the gold nanocluster will be discussed in detail below. **Figure 3A** reporting the results of the ECD analysis of AuNp**2**-**8** evidences the different behavior observed with respect to the peptides in solutions. In fact, AuNp**2**, **4**, **6** display a Cotton effect below 200 nm with concomitant weak positive dichroism at 215-220 nm suggesting an un-ordered conformation. On the other hand, AuNp**3** and **5** have a negative band at ca. 235 nm providing evidence of β-sheet formation. As in solution, the formation of a significant amount of helical conformation requires at least a 6mer sequence.

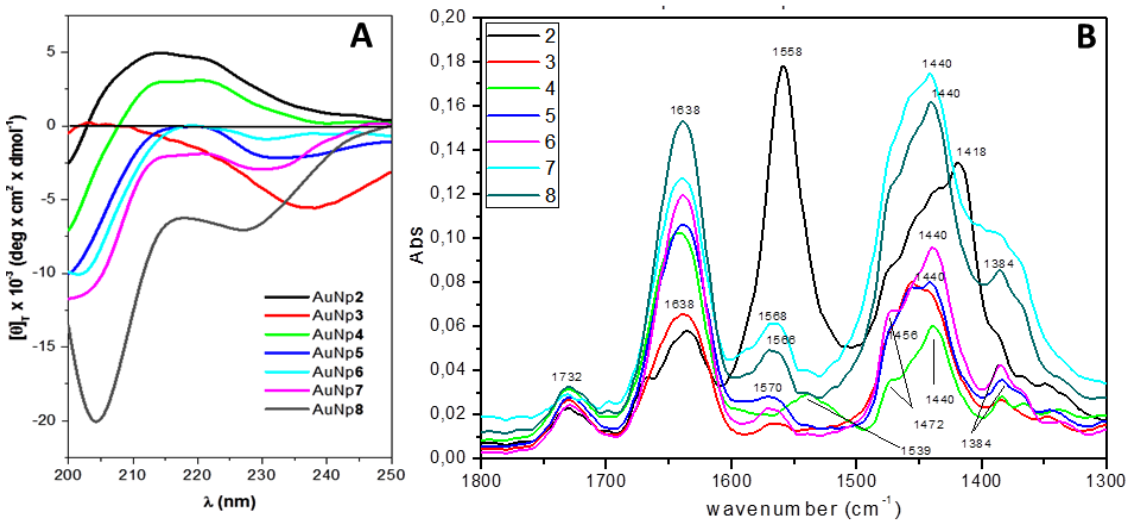


***Fig. 3*** **A**: Far-UV ECD spectra of **2**-**8** AuNpsseries recorded in water at 20°C. Concentration 1 mM. **B**: FTIR absorption spectra of **2**-**8** AuNpsseries recorded in $D_2O$ at 20°C.

However, when compared to the spectra of the free, unbound peptides reported in **Figure 2A**, the ones of the AuNps indicate that the helical content is decreased for identical sequences when bound to the nanocluster surface. The spectra of **Figure 3A** and the structural information they provide suggest also a plausible explanation for the observation we have made above concerning the number of peptides required for the passivation of the gold cluster. Peptides **2**-**4** are likely un-ordered. They may form weak intermolecular H-bonds or may interact with the gold surface. On the contrary peptides **6**-**8** are more ordered as they start developing a helical conformation (that of a $3_{10}$-helix for **8**). They are hence involved in the formation of intramolecular H-bonds. Because of the lack of an helical conformation, shorter sequences may be more tightly packed on the surface as compared to the longer ones. A simple calculation reveals that a $3_{10}$-helix displays an (circular) axial backbone footprint close to 0.55 $nm^2$ [considering a *d* (side chain)$_i$→(side chain)$_{i+1}$, of *ca.* 8.3 Å], while that of an extended conformation

(elliptical) is close to 0.12 $nm^2$ (considering two *section*, $C=O_i \rightarrow C=O_{i+1}$, of *ca*. 3.8 Å and *d* $(\text{side chain})_i \rightarrow (\text{side chain})_{i+1}$, of *ca*. 4.3 Å).This is fully consistent with the data of **Table 1**. FTIR absorption spectra in the C=O stretching region were recorded as well for the sequential series AuNp**2-8** in *deuterated* water (**Figure 3B**). Although the overall spectra profiles are similar to the above discussed **2-8** ligands series, one additional bandlocated at 1558 $cm^{-1}$, exceptionally intense for AuNp**2** (1558 $cm^{-1}$)**,** emerged. Recently, Hamm and co-workers reported an FTIR surface enhancement effect on the amide group when conjugated to AuNps.[19] We might attributed this band to a gold-amide interaction that take place extremely only for the shortest peptide ligand (**2**). Apart to this peculiar behavior, the peptide chain elongation results again into an increasing molar absorption from peptide-capped nanoparticles **2-8**. The UV-Vis spectra of AuNp**2-8** in neutral water solution (**Figure 4A**) are fully consistent with their size as they show only a very weak, if any, plasmon resonance band above 500 nm.

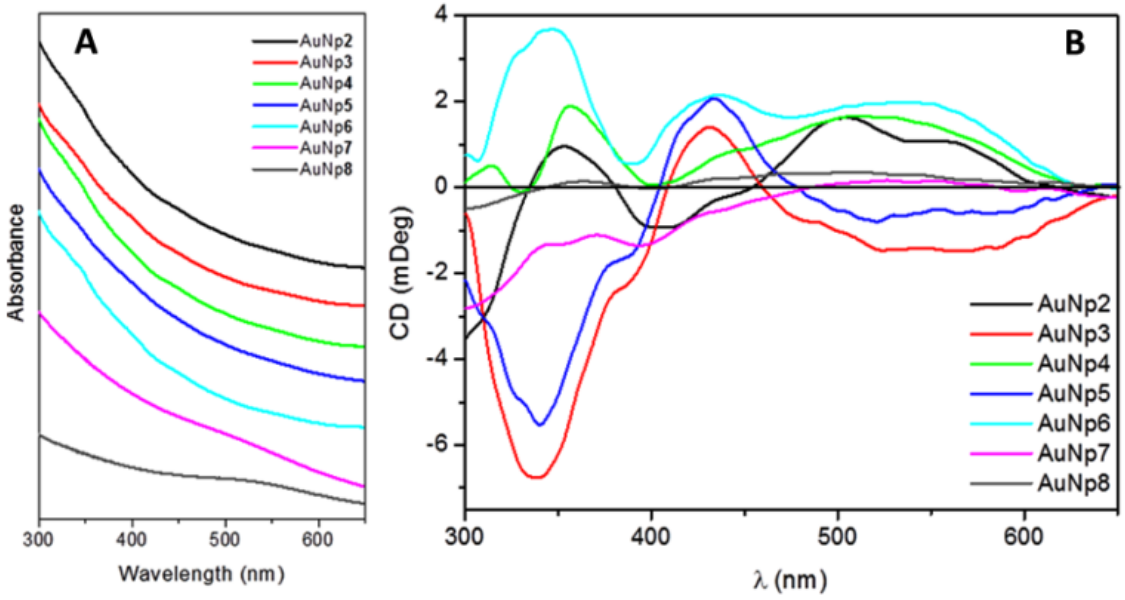


***Figure 4.***UV-Vis spectra (**A**) and ECD spectra (**B**) of the AuNps(2-8) series synthesized in this work. Solvent: water.

It is known that this band becomes relevant only for gold nanoparticles larger than 3 nm. In addition, all the absorption spectra exhibit little resolved fine structure below 400 nm, similar to that we have reported for Aib-based short peptide AuNps, but not as well resolved as those reported for smaller (0.7-1.3 nm) gold particles passivated by L-glutathione, penicillamine and *N*-isobutyryl-L-cysteine. Remarkably, the ECD spectra of AuNp**5-8** in the 300-650 nm region (**Figure 4B**) reveal quite interesting patterns. In fact, dicroic bands are observed also in this region. The behavior of these bands with the

elongation of the peptides sequence is intriguing. First of all, the intensity of the bands is larger for shorter sequences than for longer ones. As a matter of fact the spectrum of AuNp**8**, i.e. of the most helical peptide is almost flat. Second, the spectra show a peculiar pattern related to the presence of an achiral amino acid (Aib) or a chiral one (L-Ala) close to the gold surface. Dichroic bands are roughly inverted for the two series of peptides (AuNp**2**, AuNp**4**, AuNp**6** and AuNp**3**, AuNp**5** and AuNp**7**). The best comparison can be done for AuNp**2** and AuNp**3** that show the strongest signals. The ECD spectrum of AuNp**2** (for which Aib is the amino acid close to the surface)presents two positive bands located at 505 and 560 nm and, in the 300-450 nm region, a set of alternating, intense bands. The spectrum of AuNp**3** (for which L-Ala is the amino acid close to the surface) shows, on the contrary, a large negative band located at 550 nm in addition to a positive band at 440 nm and a strong negative one at 340 nm. Thus the odd and even peptide sequences behave like pseudo enantiomers in their ECD spectrum. This alternating pattern continues along the series although the intensity of the bands progressively decreases as the ordered structure of the sequences increases. Interestingly enough, a 1.8 nm-diameter nanoparticles coated with peptide **4** and prepared by a different synthetic procedure (thiol exchange on nanoparticles coated with secondary amines) revealed the same chiroptical properties. The similarity of these patterns with those recently reported by Bürgi and co-workers for the two enantiomers of $Au_{40}(SCH_2CH_2Ph)_{24}$ is striking and could suggest that, depending on the Aib-Ala order in the peptide sequence (likely the amino acid that is closest to the Au surface), one of the two possible nanoparticles is preferentially formed.[15] Although with the present data it is not possible to provide a clear explanation for this behavior a number of observations can be made. First, the formation of a helical conformation kills ellipticity as shown in **Figure 4**. This means that intramolecular H-bonding prevents a critical interaction for the formation of stereogenic units. Second, at least two independent chiral sources appear to contribute to the observed chiroptical signal. One could be related to the formation of chiral staples (of the type $(RSAu)_nSR$ with n=1 or 2), the second to the chiral α carbon of L-Ala when it is the closest amino acid to the gold surface.In both case, as aforementioned, the stereogenic selection could be associated *i*) with inter-peptide H-bonds formation (similar to a β-sheet) or *ii*) with a very week but relevant coordination of a nitrogen or oxygen of an amide bond toone of the gold atoms. Of course, both could operate at the same time to provide a three-point contact, a key concept in stereo-selection, as reported for the interaction of cysteine on a Au (110)

surface. This suggestion is supported by the observation of β-sheet-like bands in the ECD spectra only for the particles coated with peptides **3** and **5** and not in the case of those coated with **2** and **4**. Additional evidence for different inter-ligand interactions depending on the amino acid positions in the chain is provided by FTIR second order derivative deconvolution of the absorption spectra signals (**Figure 5**).

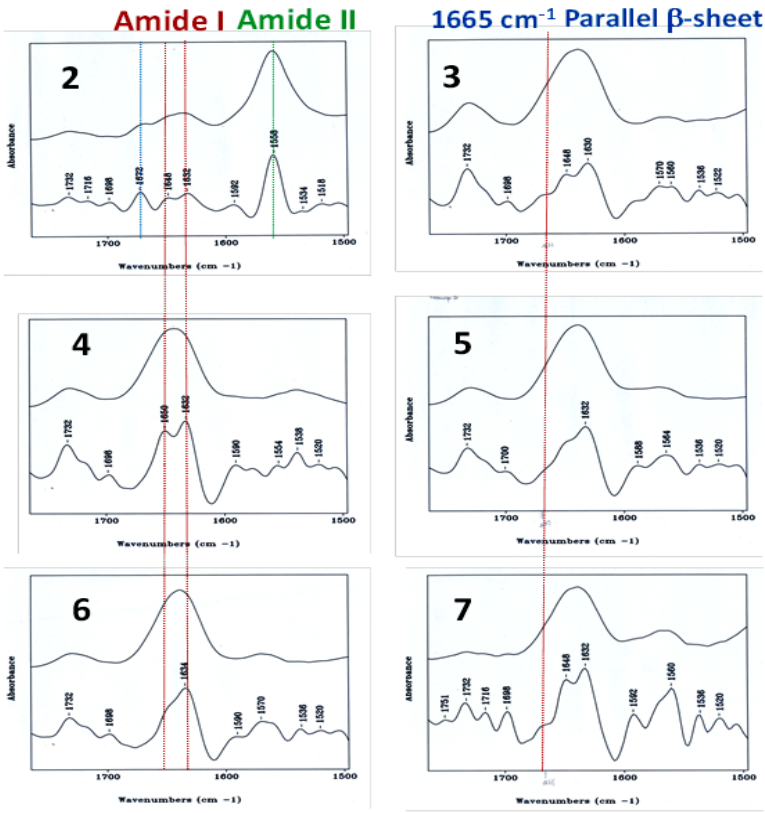


***Fig.5*** FTIR absorption spectra second order derivative deconvolution of **2-8** AuNps series recorded in *deuterated* water at 20°C.

All the nanoparticles have very broad amide I bands, likely corresponding to the overlap of different band arising for different secondary structures. However, second order derivative deconvolution of the signals evidences a relevant difference between odd and even peptide coated nanoparticles. In fact, the latter (AuNp**2**, **4** and **6**) show only two bands at 1630 and 1645 $cm^{-1}$ respectively, which could arise from random and turn structures; on the other hand, nanoparticles coated with odd peptides **3**, **5** and **7** display also shoulder at 1665 $cm^{-1}$ not observed in the related free peptides. The presence of an IR absorption band at this wavenumber has been recently attributed to the formation of anti-parallel β-sheet structures. Next, we decide to investigate the ECD behavior at different temperatures (**Figure 6**).

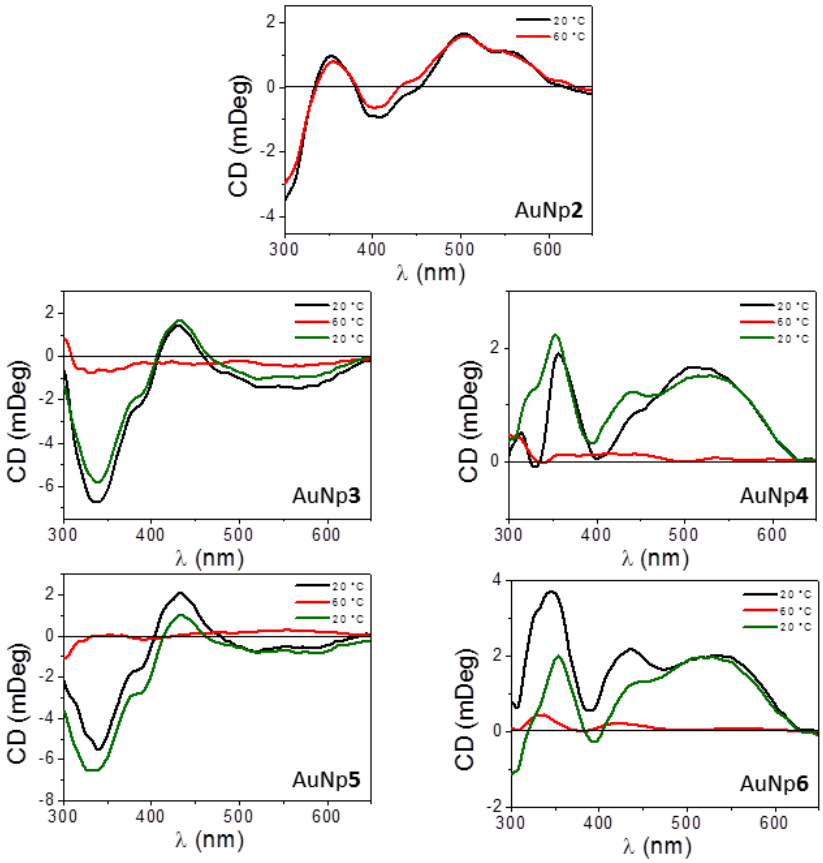


***Fig.6*** ECD spectra of the AuNps(**2**-**6**) recorded at different temperatures. Solvent: water.

In the case of AuNp**2** the ECD spectra recorded at 20 and 60 °C did not display any significant difference. For the AuNp**3**-**6** series the ECD spectra were run at 20, 60 and again at 20 °C. Surprising enough, at 60 °C the ECD signals in the Vis region were suppressed for all the series members. After a cooling time aim to restore the initial 20 °C condition, the ECD signals were reestablished at almost the original intensities. This is to our knowledge the first example of a temperature dependent ECD-memory effect on gold nanoparticles. From all of the above experimental data we might propose an hypothetical folding process of peptides**2**-**8** when conjugated to AuNp (**Figure 7**).

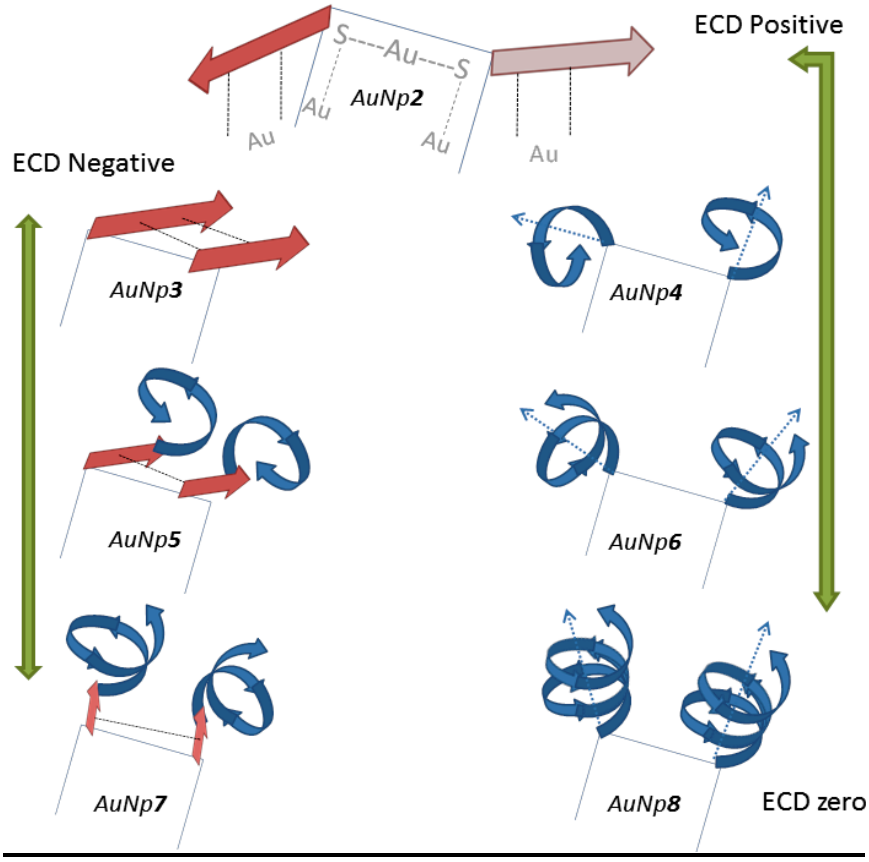


***Fig. 7*** Hypothetical folding process for the peptide-conjugated AuNps series discussed in this work.

By assuming an AuNp staple model, in the odd AuNp**3**, AuNp**5** and AuNp**7** the first Ala (the closest amino acid respect to the gold surface) is able, at least in part, to drive a parallel β-sheet type intermolecular H-bonds thus to generate a preferred *sin-conformation* between paired peptides anchored on the matching staple. Alongside the backbone elongation the parallel β-sheet motif is still conserved (in part) on the N-terminus, although the rest of the amino acid sequence is able to fold in a pronounced β-turn type motif along the remained backbone. In case of AuNp**4**, AuNp**6** andAuNp**8** thefirst Aib close to the gold surface act as β-sheet breaker and as a β-turn promoter. Along with the backbone elongation the β-turn motif turn out to be the main folding motif, thus to generate an extended helical structure for the longest peptides. This peculiarity should drive, for steric reason, the peptide ligands in an *anti-conformation* respect to the matching staple. In the case of AuNp**2** we might assume an *anti-conformation* orientation arising from a strong gold-amide interaction and Aib (close to gold surfice) sterical repulsion. Anyway, we cannot exclude for all the AuNps families members theoccurrence of of weak amide-Au surface interaction whichseems be the responsible of the above mentioned ECD memory effect.

## CONCLUSIONS

In conclusion, our studies established the occurrance of chiroptical properties in peptide-coated 2 nm diameter gold nanoparticles. These properties were detected for the first time in nanoparticles of such a size showing moderately strong ECD signals in the range of 300-650 nm, corresponding to the gold nanoparticle's quantized electronic structure. The peptides, although their only chiral amino acid is L-Ala, behave like pseudo enantiomers according to the number of amino acids in the sequence (odd or even) or, more likely, in accordance with the type of amino acid closest to the gold surface (Aib or L-Ala). Such a behavior appears to be strongly influenced by the secondary structure assumed by the peptides whenpassivating the nanoparticles and vanishes when the sequence is long enough to assume a $3_{10}$-helix conformation.

## EXPERIMENTAL SECTION

GENERAL METHODS

**FTIR:** The KBr spectra were recorded on a Perkin-Elmer 580 B equipped with an IR data station Perkin-Elmer 3600. For spectra in $D_2O$ a Perkin-Elmer 1720X was employed. The instrument operates in FT and is interfaced to a IBM PS/2 50 Z computer. 50μm $CaF_2$ pathway cells have been employed. For each spectrum have been collected 50 scans ($4cm^{-1}$ resolution) under nitrogen.

**UV-Vis Absorption:** The electronic absorption spectra were recorded using a Shimadzu model UV-2501 PC spectrophotometer. A 1 cm path length quartz cell was used.

**CD:** The ECD measurements have been collected on a J-715 Jascospectropolarimeter, with quartz cells Hellma (0.02cm pathway length). Values are reported in total molar ellipticy (deg x $cm^2$ x $dmol^{-1}$) :

$$[\Theta]_T = (MW \times \Theta)/(l \times c) = 3300 \times \Delta\varepsilon = 3300 \times (\varepsilon_L - \varepsilon_R)$$

$\Theta$ = observed ellipticy

MW = molecular weight

l = pathway length (cm)

c = concentration in gr/l

$\Delta\varepsilon = \varepsilon_L - \varepsilon_R$ = difference between left- and right-handed component of estinction coefficients of polarized light

**TEM:** Samples were analyzed on a Jeol 300PX instrument. Samples were prepared before used, by 100 times dilution of a 2mg/ml MeOH solution of AuNp-**3**, AgNp-**3**, or PtNp-**3**. A glow discharged carbon coated grid was floated on a small drop of gel solution and excess was removed by #50 hardened Whatman filter paper.

**TGA:** TGA measurements have been collected by solid state on a Platinum-HT pan, heating the sample from 100°C to 900°C under nitrogen atmosphere, therefore treating from 900°C to 1000°C under oxygen at the same scanning rate.

SYNTHESIS AND CHARACTERIZATION

**Trt-S-$CH_2$-$CH_2$-CO-Aib-L-Ala-OMe**

Triphenylmethyl (Trt)-S-$(CH_2)_2$-COOH (0.65 g, 1.18 mmol) was dissolved in anhydrous $CH_2Cl_2$ and kept at 0°C. Then, HOAt (0.25 g, 1.85 mmol), EDC·HCl (0.36 g, 1.85 mmol), H-Aib-L-Ala-OMe (obtained by catalytic hydrogenation of the corresponding N-protected Z-Aib-L-Ala-OMe (Z, benzyloxycarbonyl) in methanol solution (0.5g, 1.55 mmol)( and TEA (0.52 mL, 3.78 mmol) were added to the solution. After stirring the solution at room temperature for 24 hours, $CH_2Cl_2$ was evaporated under reduced pressure. The oily residue was dissolved in EtOAc and washed with 10% $KHSO_4$, $H_2O$, 5% $NaHCO_3$, and H2O, dried over anhydrous $Na_2SO_4$, and evaporated to dryness under reduced pressure. The crude product was purified by flash chromatography. The product was crystallized from EtOAc/petroleum ether.**Yield** 87%.**IR** (KBr): 3329, 3272, 3056, 2983, 2936, 1754, 1744, 1657 $cm^{-1}$. **$^1$H NMR** (200 MHz, $CDCl_3$): δ 7.45-7.17 [m, 15H, Trt aromatic rings], 6.90-6.86 [d, 1H, Ala NH], 5.72 [s, 1H, AibNH], 4.53-4.46 [dt, 1H, Alaα-CH], 3.69 [s, 3H, -$CH_3$], 2.60-2.49 [m, 2H, -$CH_2$-], 2.04-1.94 [m, 2H, -$CH_2$-], 1.36-1.32 [d, 6H, Aibβ-$CH_3$], 1.24-1.21 [d, 3H, Alaβ-$CH_3$].

**Trt-S-$CH_2$-$CH_2$-CO-L-Ala-Aib-L-Ala-OMe**

Triphenylmethyl (Trt)-S-$(CH_2)_2$-COOH (0.56 g, 1.6 mmol) was dissolved in anhydrous $CH_2Cl_2$ and kept at 0 °C. Then, HOAt (0.22 g, 1.6 mmol), EDC•HCl (0.33 g, 1.7 mmol), H-L-Ala-Aib-L-Ala-OMe (obtained by catalytic hydrogenation of the corresponding N-protected Z-L-Ala-Aib-L-Ala-OMe (Z, benzyloxycarbonyl) in methanol solution (0.5 g, 1.3 mmol)) and triethylamine TEA (0.45 mL, 3.50 mmol) were added to the solution. After stirring the solution at room temperature for 24 hours, $CH_2Cl_2$ was evaporated under reduced pressure. The oily residue was dissolved in EtOAc and washed with 10% $KHSO_4$, $H_2O$, 5% $NaHCO_3$, and $H_2O$, dried over anhydrous Na2SO4, and evaporated to dryness under reduced pressure. The crude product was purified by flash chromatography. The product was crystallized from EtOAc/petroleum ether.**Yield** 93%.**IR** (KBr): 3310, 3056, 2983, 2936, 1742, 1653, 1535 $cm^{-1}$.**$^1$H NMR** (200 MHz, $CDCl_3$): δ 7.40-7.17 [m, 15H, Trt aromatic rings], 6.95-6.91 [d, 1H, Ala NH], 6.52 [s, 1H, AibNH], 5.75-5.72 [d, 1H, Ala NH], 4.53-4.46 [dt,

1H, Alaα-CH], 4.27-4.10 [m, 1H, Alaα-CH], 3.71 [s, 3H, OMe$CH_3$], 2.56-2.51 [m, 2H, -$CH_2$-], 2.49-1.95 [m, 2H, -$CH_2$-], 1.58-1.21 [m, 12H, Aibβ-$CH_3$, 2Ala β-$CH_3$].

**Trt-S-$CH_2$-$CH_2$-CO-Aib-L-Ala-Aib-L-Ala-OMe**

Triphenylmethyl (Trt)-S-$(CH_2)_2$-COOH (0.42 g, 1.2 mmol) was dissolved in anhydrous $CH_2Cl_2$ and kept at 0 °C. Then, HOAt (0.17 g, 1.2 mmol), EDC·HCl (0.23 g, 1.2 mmol), H-Aib-L-Ala-Aib-L-Ala-OMe (obtained by catalytic hydrogenation of the corresponding N-protected Z-Aib-L-Ala-Aib-L-Ala-OMe (Z, benzyloxycarbonyl) in methanol solution (0.6 g, 1.1 mmol)) and triethylamine TEA (0.33 mL,2.4 mmol) were added to the solution. After stirring the solution at room temperature for 24 hours, $CH_2Cl_2$ was evaporated under reduced pressure. The oily residue was dissolved in EtOAc and washed with 10% $KHSO_4$, $H_2O$, 5% $NaHCO_3$, and $H_2O$, dried over anhydrous $Na_2SO_4$, and evaporated to dryness under reduced pressure. The crude product was purified by flash chromatography. The product was crystallized from EtOAc/petroleum ether.**Yield** 83%. **IR** (KBr): 3312, 3056, 2984, 2936, 2871, 1743, 1657, 1534 $cm^{-1}$.**$^1$H NMR** (200 MHz, $CDCl_3$): δ 7.42-7.24 [m, 15H, Trt aromatic rings], 7.21 [d, 1H, Ala NH] 7.13 [s, 1H, Aib NH], 6.69-6.67 [d, 1H, Ala NH], 6.58 [s, 1H, AibNH], 4.55-4.48 [m, 1H, Alaα-CH], 4.10-4.00 [m, 1H, Alaα-CH], 3.70 [s, 3H, OMe$CH_3$], 2.80-2.75 [m, 2H, -$CH_2$-], 2.55-2.49 [m, 2H, -$CH_2$-], 1.58-1.17 [m, 18H, 2Aib β-$CH_3$, 2Ala β-$CH_3$].

**Trt-S-$CH_2$-$CH_2$-CO-L-Ala-Aib-L-Ala-Aib-L-Ala-OMe**

Triphenylmethyl (Trt)-S-$(CH_2)_2$-COOH (0.21 g, 0.6 mmol) was dissolved in anhydrous $CH_2Cl_2$ and kept at 0 °C. Then, HOAt (0.08 g, 0.6 mmol), EDC·HCl (0.12 g, 0.6 mmol), H-L-Ala-Aib-L-Ala-Aib-L-Ala-OMe (obtained by catalytic hydrogenation of the corresponding N-protected Z-L-Ala-Aib-L-Ala-Aib-L-Ala-OMe (Z, benzyloxycarbonyl) in methanol solution (0.6 g, 1.1 mmol)) and triethylamine TEA (0.17mL,1.2 mmol) were added to the solution. After stirring the solution at room temperature for 24 hours, $CH_2Cl_2$ was evaporated under reduced pressure. The oily residue was dissolved in EtOAc and washed with 10% $KHSO_4$, $H_2O$, 5% $NaHCO_3$, and $H_2O$, dried over anhydrous $Na_2SO_4$, and evaporated to dryness under reduced pressure. The crude product was purified by flash chromatography. The product was crystallized from EtOAc/petroleum ether.**Yield** 80%. **IR** (KBr): 3352, 3330, 3310, 3053, 3029, 2984, 2937, 1741, 1715, 1669, 1533 $cm^{-1}$.**$^1$H NMR** (200 MHz, $CDCl_3$): δ 7.42-7.08 [m,

18H, Trt aromatic rings, Aib+2Ala NH], 6.45 [s, 1H, Aib NH], 6.02 [d, 1H, Ala NH], 4.58-4.47 [m, 1H, Alaα-CH], 4.38-4.27 [m, 1H, Alaα-CH], 4.14-4.10 [m, 1H, Alaα-CH] 3.63 [s, 3H, OMe$CH_3$], 2.87-2.77 [m, 2H, -$CH_2$-], 2.45-2.11 [2m, 2H, -$CH_2$-], 1.62-1.24 [m, 21H, 2Aib β-$CH_3$, 3Ala β-$CH_3$].

**Trt-S-$CH_2$-$CH_2$-CO-Aib-L-Ala-Aib-L-Ala-Aib-L-Ala-OMe**

Triphenylmethyl (Trt)-S-$(CH_2)_2$-COOH (0.32 g, 0.7 mmol) was dissolved in anhydrous $CH_2Cl_2$ and kept at 0 °C. Then, HOAt (0.17 g, 0.7 mmol), EDC·HCl (0.25 g, 0.7 mmol), H-Aib-L-Ala-Aib-L-Ala-Aib-L-Ala-OMe (obtained by catalytic hydrogenation of the corresponding N-protected Z-Aib-L-Ala-Aib-L-Ala-Aib-L-Ala-OMe (Z, benzyloxycarbonyl) in methanol solution (0.5 g, 0.6 mmol)) and triethylamine TEA (0.38 mL, 1.4 mmol) were added to the solution. After stirring the solution at room temperature for 24 hours, $CH_2Cl_2$ was evaporated under reduced pressure. The oily residue was dissolved in EtOAc and washed with 10% $KHSO_4$, $H_2O$, 5% $NaHCO_3$, and $H_2O$, dried over anhydrous $Na_2SO_4$, and evaporated to dryness under reduced pressure. The crude product was purified by flash chromatography. The product was crystallized from EtOAc/petroleum ether.**Yield** 75%. **IR** (KBr): 3341, 3056, 2984, 2935, 2873, 1745, 1857, 1533 $cm^{-1}$.**$^1$H NMR** (200 MHz, $CDCl_3$): δ 7.22-7.19 [m, 18H, Trt aromatic rings, Aib+2Ala NH], 6.99-6.91 [d, 1H, Ala NH], 6.71 [d, 1H, Ala NH], 5.70 [s, 1H, Aib NH], 4.65-4.57 [m, 1H, Alaα-CH], 4.38-4.35 [m, 1H, Alaα-CH], 4.10-3.90 [m, 1H, Alaα-CH] 3.66 [s, 3H,OMe$CH_3$], 3.01-2.90 [m, 2H, -$CH_2$-], 2.50-2.05 [2m, 2H, -$CH_2$-], 1.62-1.24 [m, 27H, 3Aib β-$CH_3$, 3Ala β-$CH_3$].

**Trt-S-$CH_2$-$CH_2$-CO-L-Ala-Aib-L-Ala-Aib-L-Ala-Aib-L-Ala-OMe**

Triphenylmethyl (Trt)-S-$(CH_2)_2$-COOH (0.32 g, 0.7 mmol) was dissolved in anhydrous $CH_2Cl_2$ and kept at 0 °C. Then, HOAt (0.17 g, 0.7 mmol), EDC·HCl (0.25 g, 0.7 mmol), H-Aib-L-Ala-Aib-L-Ala-Aib-L-Ala-OMe (obtained by catalytic hydrogenation of the corresponding N-protected Z-Aib-L-Ala-Aib-L-Ala-Aib-L-Ala-OMe (Z, benzyloxycarbonyl) in methanol solution (0.4 g, 0.6 mmol)) and triethylamine TEA (0.38 mL, 1.4 mmol) were added to the solution. After stirring the solution at room temperature for 24 hours, $CH_2Cl_2$ was evaporated under reduced pressure. The oily residue was dissolved in EtOAc and washed with 10% $KHSO_4$, $H_2O$, 5% $NaHCO_3$, and $H_2O$, dried over anhydrous $Na_2SO_4$, and evaporated to dryness under reduced pressure. The crude product was purified by flash chromatography. The product was crystallized

from EtOAc/petroleum ether.**Yield** 75%. **IR** (KBr): 3337, 3060, 3031, 2932, 2912, 2647, 2568, 1703, 1662, 1533 $cm^{-1}$.**$^1$H NMR** (200 MHz, $CDCl_3$): δ 7.41-7.27 [m, 21H, Trt aromatic rings, 3Aib+3Ala NH], 6.25 [s, 1H, Aib NH], 4.56-4.49 [m, 1H, Alaα-CH], 4.36-4.29 [m, 1H, Alaα-CH], 4.10-3.90 [m, 1H, Alaα-CH] 3.66 [s, 3H, $OMeCH_3$], 3.01-2.90 [m, 2H, -$CH_2$-], 2.50-2.05 [2m, 2H, -$CH_2$-], 1.62-1.24 [m, 27H, 3Aib β-$CH_3$, 3Ala β-$CH_3$].

**General synthesis and purification of gold nanoparticles peptide conjugate**

Trt-S-$(CH_2)_2$-CO-derivated ofthe peptide and $HAuCl_4$ (0.3 eq.) were combined in 10 ml of a 1:1 methanol/water solvent mixture. The resulting solution was allowed to stand for 1 h under stirring. Then, $NaBH_4$ (10 eq.) in water were rapidly added and the solution was stirred at room temperature for additional 10 minutes. The solvent was removed under reduced pressure and the residue solved in water. The so-obtained solution was straight charged in a gel-filtration column. The Nps were obtained by liophylization.

REFERENCES


1) a) Boisselier E.,Astruc D., *Chemical Society Review*, **2009**, 38, 1759-1782 ; b) Daniel M.-C.,Astruc D., *Chemical Reviews*, **2004**, 104, 294-346 ; c) O'Neal D.P., Hirsch L.R., *et al.*, *Cancer Letters*, **2004**, 209, 171-176
2) a) Whetten R.L., Khoury J.T. *et al.*, Advanced Materials, **1996**, 8 (5), 428-433; b) Alvarez J.T., Khoury T. *et al*., Journal of Physical Chemistry B, **1997**, 101, 3706-3712
3) Shemer G., Kruchevski O., *et al.*, *Journal of American Chemical Society*, **2006**, 128, 11006-11007
4) George J.,Thomas G., *Journal of American Chemical Society*, **2010**, 132, 2502-2503
5) a) Shukla N., Bartel M.,Gellman A., *Journal of American Chemical Society*, **2010**, 132, 8575-8580 ;b) Rezanka P., Koktan J.,Kral V., *Colloids Surf.*, **374**, 374, 77-83
6) Schaaff T.G.,Whetten R.L., *Journal of Physical Chemistry B*, **2000**, 104, 2630-2641
7) Slocik J.M., Govorov A.O.,Naik R.R., *Nano Letters*, **2011**, 11, 701-705
8) a) Rio-Echevarria I.M., Tavano R., *et al.*, *Journal of American Chemical Society*, **2011**, 133, 8-11 ;b) Schade M., Moretto A., *et al.*, *Nano Letters*, **2010**, 10, 3057-3061
9) a) Otoda K., Kitagawa Y., Kimura S.,Imanishi Y., *Biopolymers*, **1993**, 33, 1337-1345 ;b) Longo E., Moretto A., Formaggio F.,Toniolo C., *Chirality*, **2011**, 23, 756-760
10) Jadzinsky P.D., Calero G., *et al.*, *Science*, **2007**, 318, 430-433
11) a) Holzwarth G.,Doty P., *Journal of American Chemical Society*, **1965**, 87, 218-228 ;b) Toniolo C., Formaggio F.,Woody R.W., *Electronic circular dichroism of peptides*, Comprehensive chiroptical spectroscopy, **2011**. Hoboken, NJ, Wiley
12) a) Karle I.L.,Balaram P., *Biochemistry*, **1990**, 29 (29), 6747-6756 ;b) Benedetti E., Blasio B.D., *et al.*, *Biopolymers*, **1992**, 32, 453-456 ;c) Toniolo C., Crisma M., Formaggio F.,Peggion C., *Biopolymers (Pept. Sci.)*, **2001**, 60, 396
13) a) Manning M.C.,Woody R.W., *Biopolymers*, **1991**, 31, 569-586 ;b) Toniolo C., Polese A., *et al.*, *Journal of American Chemical Society*, **1996**, 118, 2744-2745 ;c) Formaggio F., Crisma M., *et al.*, *Chemistry -An European Journal*, **2000**, 6 (24), 4498-4504 ;d) Toniolo C., Formaggio F., *et al.*, *Biopolymers*, **2004**, 75, 32-45 ;e) Formaggio F., Peggion C., *et al.*, *Chirality*, **2004**, 16, 388-397
14) Fabris L., Antonello S., *et al.*, *Journal of American Chemical Society*, **2006**, 128, 326-336
15) a) Yao H., Miki K., *et al.*, *Journal of American Chemical Society*, 127, 15536-15543 ;b) Gautier C.,Bürgi T., *Journal of American Chemical Society*, **2006**, 128, 11079-11087
16) a) Ferri D.,Bürgi T., *Journal of American Chemical Society*, **2001**, 123, 12074-12084 ;b) Ferri D., Bürgi T.,Bailaker A., *Chemical Communication*, 2001, 1172-1173 ;c) Bieri M.,Bürgi T., *Journal of Physical Chemistry B*, **2005**, 109, 10243-10250 ;d) Bieri M.,Bürgi T., *Chemical Physical Chemistry*, **2006**, 7, 514-523
17) Humblot V., Haq S., *et al.*, *Journal of American Chemical Society*, **2002**, 124 (3), 503-510
18) Hofer W.A., Humblot V.,R.Raval, *Surface Science*, 554, 141-149

19) Donaldson P.M.,P.Hamm, *Angewandte Chemie International Edition*, **2013**, 52, (2), 634-638

# III

## Hydrophobic Aib/Ala peptides solubilize in water through formation of supramolecular assemblies

## INTRODUCTION

Our interest in self-assembly arose from the rationalization of the evidence for water solubility property of a peptides series containing alternating Ala and Aib (α-aminoisobutyric acid).[1] During the solution syntheses of peptides containing alternating Ala and Aib (α-aminoisobutyric acid) stretches, we observed unusually low yields. After a careful inspection of all synthetic steps, we discovered that much of the product was lost in the purification procedures as, unexpectedly, these peptides are soluble in water.[1,2] To the best of our knowledge, this is the first example of a class of N- and C-terminal protected, hydrophobic peptides able to dissolve in water. This finding is even more surprising in view of the absence of any residue having a charged (*e.g.*Lys, Asp) or a polar (*e.g.* Ser, Thr) side chain. The explanation of such a behavior is not straightforward. Therefore, we started a series of experiments aimed at explaining the observed hydrosolubility. The preliminary results of our efforts, reported in this work,focus on the undecapeptide Z-(L-Ala)$_3$-(Aib-L-Ala)$_4$-OMe,[2] where Z is benzyloxycarbonyl and OMe is methoxy.

Interestingly, these Ala/Aib peptides maintain in water[2] the same helical conformations they display in organic solvents.[3-7] Thus, one cannot ascribe their solubility in water to a conformational change, according to which, for instance, the polar peptide moieties would be exposed to the solvent and not any longer engaged in intramolecular H-bonds. A different mechanism has definitely to be involved. In a $3_{10}$- or α-helical peptide two or three, respectively, amide carbonyls at the C-terminus are not part of the intramolecular H-bonding network. The same situation applies to the first two or three amide NHs at the N-terminus. Taking into account these observations, we hypothesized that aggregates of helical peptides would form, in which the N- and/or C-terminal segments are located on the external surface, in contact with water molecules, whereas the hydrophobic sections the peptides are embedded in the aggregate.

## RESULTS AND DISCUSSION

### PEPTIDE CONFORMATION

The ECD spectra in water of Z-(L-Ala)$_3$-(Aib-L-Ala)$_4$-OMe and its C-terminal free analog Z-(L-Ala)$_3$-(Aib-L-Ala)$_4$-OH are reported in **Figure 1**. Although slightly diverging, the two spectra are indicative of α-helical structures, as the ratios of the ellipticities between the two negative Cotton effects at about 222 nm and 205 nm are 0.74 for Z-(L-Ala)$_3$-(Aib-L-Ala)$_4$-OMe and 0.91 for Z-(L-Ala)$_3$-(Aib-L-Ala)$_4$-OH.[8,9]

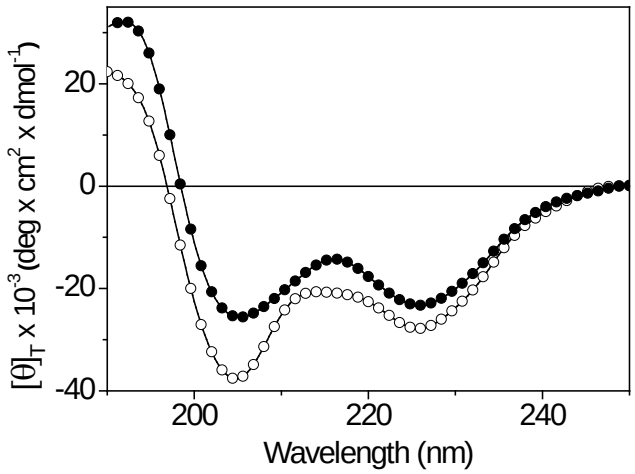


***Fig. 1*** Far-UV ECD spectra of Z-(L-Ala)$_3$-(Aib-L-Ala)$_4$-OMe (o) and Z-(L-Ala)$_3$-(Aib-L-Ala)$_4$-OH (●) in water at 20 °C. Peptide concentration: 1 mM.

To get a closer look into conformational features possibly responsible for the water solubility of our Ala/Aib peptides, we tried to grow single crystals of Z-(L-Ala)$_3$-(Aib-L-Ala)$_4$-OMe. Our attempts were successful only for its closely related analog Z-(L-Ala)$_3$-(Aib-L-Ala)$_4$-OH. Its molecular conformation, as determined by single-crystal X-ray diffraction, is illustrated in **Figure 2**.

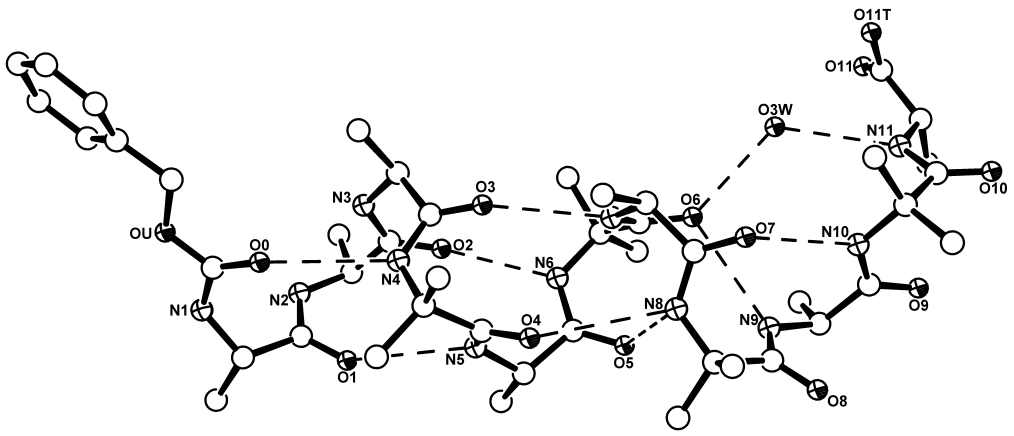


***Fig. 2*** X-ray diffraction structure of Z-(Ala)$_3$-(Aib-L-Ala)$_4$-OH crystallized from 2-propanol solution. Only one of the three co-crystallized water molecules in shown. The intramolecular H-bonds are represented by dashed lines.

Relevant torsion angles are reported in **Table 1**, while intra- and intermolecular H-bond parameters are listed in **Table 2**.

***Tab. 1*** Selected torsion angles [°] for Z-(L-Ala)$_3$-(Aib-L-Ala)$_4$-OH trihydrate.

| | | | |
|---|---|---|---|
| C02-C01-C07-OU | 148.6(3) | CA5-C5-N6-CA6 | 177.27(19) |
| C06-C01-C07-OU | -32.1(5) | C5-N6-CA6-C6 | -55.5(3) |
| C01-C07-OU-C0 | 171.1(3) | N6-CA6-C6-N7 | -45.0(3) |
| C07-OU-C0-N1 | -174.5(3) | CA6-C6-N7-CA7 | -176.1(2) |
| OU-C0-N1-CA1 | -172.4(2) | C6-N7-CA7-C7 | -61.0(3) |
| C0-N1-CA1-C1 | -64.7(3) | N7-CA7-C7-N8 | -41.0(3) |
| N1-CA1-C1-N2 | -38.8(3) | CA7-C7-N8-CA8 | -175.7(2) |
| CA1-C1-N2-CA2 | -179.2(2) | C7-N8-CA8-C8 | -60.8(3) |
| C1-N2-CA2-C2 | -67.9(3) | N8-CA8-C8-N9 | -24.4(3) |
| N2-CA2-C2-N3 | -42.2(4) | CA8-C8-N9-CA9 | 179.5(3) |
| CA2-C2-N3-CA3 | 179.4(2) | C8-N9-CA9-C9 | -72.6(4) |
| C2-N3-CA3-C3 | -61.1(3) | N9-CA9-C9-N10 | -19.3(4) |
| N3-CA3-C3-N4 | -44.8(3) | CA9-C9-N10-CA10 | 177.9(3) |
| CA3-C3-N4-CA4 | -179.0(2) | C9-N10-CA10-C10 | 53.4(4) |
| C3-N4-CA4-C4 | -54.1(3) | N10-CA10-C10-N11 | 52.2(4) |
| N4-CA4-C4-N5 | -48.5(3) | CA10-C10-N11-CA11 | -175.5(3) |
| CA4-C4-N5-CA5 | -176.0(2) | C10-N11-CA11-C11 | -151.6(3) |
| C4-N5-CA5-C5 | -70.7(3) | N11-CA11-C11-O11T | 50.0(3) |
| N5-CA5-C5-N6 | -43.3(3) | | |

***Tab. 2*** Hydrogen bonds for Z-(L-Ala)$_3$-(Aib-L-Ala)$_4$-OH trihydrate [Å and °].

| D-H...A | d(D-H) | d(H...A) | d(D...A) | <(DHA) |
|---|---|---|---|---|
| N4-H04...O01 | 0.86 | 2.28 | 3.118(3) | 164.7 |
| N5-H05...O1 | 0.86 | 2.44 | 3.260(3) | 159.8 |
| N6-H06...O2 | 0.86 | 2.03 | 2.876(3) | 169.7 |
| N7-H07...O3 | 0.86 | 2.09 | 2.918(2) | 160.9 |
| N8-H08...O4 | 0.86 | 2.52 | 3.289(3) | 149.7 |
| N8-H08...O5 | 0.86 | 2.62 | 3.156(3) | 121.9 |
| N9-H09...O6 | 0.86 | 2.42 | 3.163(3) | 145.3 |
| N10-H010...O7 | 0.86 | 2.21 | 3.026(3) | 157.7 |
| N11-H011...O3W | 0.86 | 2.03 | 2.863(3) | 161.2 |
| O3W-H3WA...O6 | 0.83 | 1.99 | 2.780(3) | 159.8 |
| O11T-H11T...O9#1 | 0.82 | 1.83 | 2.634(3) | 166.0 |
| N1-H01...O10#2 | 0.86 | 2.23 | 3.052(3) | 159.9 |
| N2-H02...O1W#2 | 0.86 | 2.17 | 3.011(3) | 167.2 |
| N3-H03...O2W#2 | 0.86 | 2.29 | 3.043(3) | 146.1 |
| O1W-H1WA...O10 | 0.80 | 1.98 | 2.767(3) | 167.6 |
| O1W-H1WB...O11#3 | 0.88 | 2.01 | 2.833(4) | 154.9 |
| O2W-H2WA...O1#4 | 0.85 | 2.24 | 3.006(4) | 149.0 |
| O2W-H2WB...O1W101 | 0.86 | 2.05 | 2.857(4) | 156.6 |
| O3W-H3WB...O8#1 | 0.90 | 2.05 | 2.930(4) | 165.3 |

Symmetry transformations used to generate equivalent atoms:
#1 x,y+1,z; #2 x-1/2,y+1/2,z-1; #3 -x+5/2,y-1/2,-z+2; #4 x+1/2,y+1/2,z+1

The conformation adopted by the undecapeptide is right-handed α-helical for most of its length. Indeed, starting from the N-terminus, five consecutive, N-H···O=C intramolecularly H-bonded $C_{13}$ structures (α-turns) are observed (**Table 3**).[10] The H-bond donors are the NH groups of residues 4 to 8, and the acceptors the Z-urethane carbonyl oxygen O0 and the carbonyls of residues 1 to 4, respectively. The average values of the backbone torsion angles for residues 1-7 are $\phi$ = -62.1°, $\psi$ = -43.4°, very close to those obtained from a statistical analysis of high resolution crystal structures of α-helical peptides ($\phi$ = -63°, $\psi$ = -42°).[11] The N8-H group, in addition to being H-bonded to O4 in a $C_{13}$ structure, is also H-bonded to O5, thus forming a $C_{10}$ structure (β-turn) as well. [12] In this three-center H-bond arrangement, the N8-H···O4 interaction is rather elongated and distorted (Table 3).[13,14] Then, the backbone folding continues as $3_{10}$-helical, in that two consecutive $C_{10}$ structures are found, the H-bond donors of which are the N9-H and N10-H groups, and the acceptors the carbonyl oxygens of residues 6 and 7, respectively. The first of these two latter $C_{10}$ structure is of type-III whereas the second is close to type-I, as the backbone torsion angles of Ala(9), which occupies its *i*+1 corner position, lie in the "bridge" region of the $\phi$,$\psi$ space (**Table 2**).[12,15] The following Aib(10) residue adopts torsion angles belonging to the left-handed

helical region of the conformational map. As a result of the screw sense inversion of Aib(10) relative to the preceding residues, the N11-H moiety, that would have been a donor to O8 if the backbone had continued a helical path, is located outside the helix now. The N11-H group is H-bonded to the cocrystallized water molecule O3W which, in turn, is H-bonded as the donor to the O6 carbonyl oxygen, thus forming a water-mediated Schellman motif.[18] The occurrence of such helix C-capping motif in peptides carrying an Aib residue at the penultimate position has been crystallographically documented in a number of cases,[16] including a few examples in which the $i$+5 $\rightarrow i$ N-H$\cdots$O=C intramolecular H-bond ($C_{16}$ structure) is mediated by the insertion of a cocrystallized solvent (methanol) molecule.[17,18] The C-terminal Ala(11) residue, with $\phi,\psi$ = -151.6(3)°, 50.0(3)°, adopts a *quasi*-extended conformation.

The largely $\alpha$-helical folding of Z-(L-Ala)$_3$-(Aib-L-Ala)$_4$-OH, described above, is closely mirrored by the structures of two peptides of comparable length based on alternating Aib-L-Ala residues. Specifically, in the structure of the dodecapeptide *p*BrBz-(Aib-L-Ala)$_6$-OMe a $C_{10}$ structure at the N-terminus is encompassed within a $C_{13}$ structure that is followed by seven additional $C_{13}$ structures. Then, a $C_{10}$ and a $C_{16}$ structure constitute the Schellman motif that acts as the C-cap of the $\alpha$-helix, with screw-sense inversion at the level of the penultimate Aib(11) residue.[19] Similarly, both the dihydrate[19] and the *bis*-DMSO solvate[20] of the decapeptide *p*BrBz-(Aib-L-Ala)$_5$-OMe display five consecutive $C_{13}$ structures, followed by two $C_{10}$ structures and a $C_{16}$ structure, thus terminating again with a Schellman motif. It is worth noting that the corresponding backbone torsion angles of the four ($i$+1 ÷ $i$+4) residues encompassed within the H-bonded $C_{16}$ structure are identical (within 6°) in the three (Aib-Ala)$_n$ structures, whereas in our undecapeptide much larger deviations (19° ÷ 31°) are observed for both $\phi,\psi$ values of residue $i$+3 and the $\psi$ value of the screw-sense inverting residue $i$+4, in all probability to allow the replacement of the direct $i$+5 $\rightarrow$ $i$ N-H $\cdots$ O=C intramolecular H-bond by the water-mediated $C_{16}$ structure. In the packing mode, the N1-H group is H-bonded to the O10 carbonyl oxygen of a (-1/2+x, ½+y, -1+z) symmetry related molecule, while the N2-H group is connected to the same acceptor through the insertion of the O1W water molecule. O1W is also H-bonded, as the acceptor, to O2W which, in turn, is H-bonded to the N3-H group. These either direct or water-mediated interaction link peptide molecules, head to tail, along the *abc* direction.

In addition, one direct and one water-mediated H-bonds laterally connect peptide molecules along the *b* direction. Specifically, the C-terminal (carboxylic) O11T-H group is H-bonded to the O9 carbonyl oxygen of a (x, 1+y, z) molecule, and the O3W water molecule (inserted between the N11-H and the O6 carbonyl in the Schellman motif) is H-bonded to O8 (symmetry: x, 1+y, z). The remaining H-bonding donor capability of O1W is satisfied by a (5/2-x, -1/2+y, 2-z) symmetry equivalent of O11, thus indirectly connecting molecules along the *ac* direction, whereas O2W donates a H-bond to O1 (symmetry equivalence: ½+x, ½+y, 1+z).

MORPHOLOGY OF THE AGGREGATE PEPTIDES IN WATER

To assess the presence of molecular aggregates, DLS is a fast and reliable technique. According to our measurements (data not shown), all water-soluble Aib/Ala peptides previously investigated do form in water large aggregates [above to the critical aggregate concentration (CAC) of 15 mM], with average dimensions of which range from 20 to 100 nm.[1,2] In this preliminary report we decided to focus on Z-(L-Ala)$_3$-(Aib-L-Ala)$_4$-OMe in view of its relevant size and applications.[2] DLS measurements of this peptide in water solution (**Figure 3**) clearly indicate the presence of large aggregates, of up to 100 nm hydrodynamic radius. These measurements, repeated several times on newly prepared peptide solutions, were completely reproducible. Interestingly, when our undecapeptide was dissolved in methanol, the DLS analysis detected structures about ten times smaller (2-10 nm in hydrodynamic radius), consistent with the presence of isolated peptide molecules and small aggregates. It is worth reminding here that the N-to-C length of an α-helical peptide of 11 residues does not exceed 2 nm. Therefore, these data clearly indicate that large, self-assembled, peptide bodies do form in water.

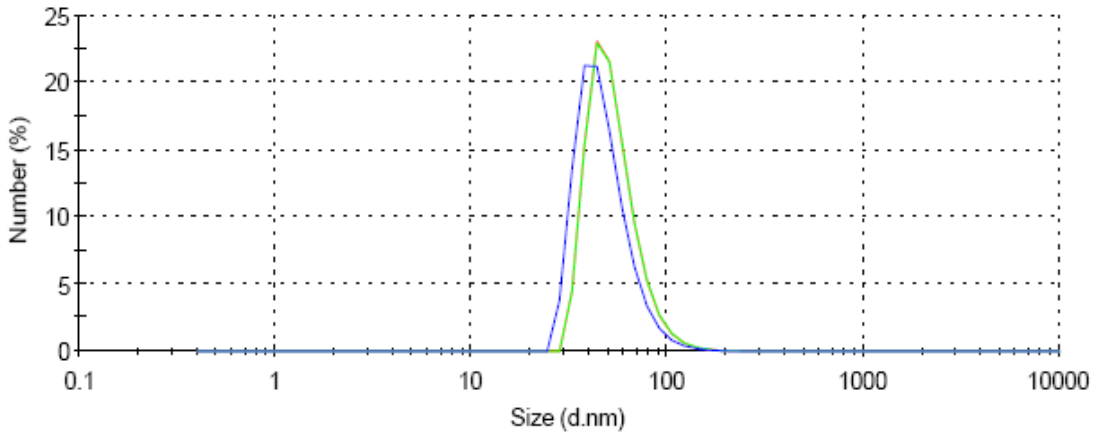


***Fig. 3*** DLS patterns of a 15mM Z-$(Ala)_3$-$(Aib\text{-}L\text{-}Ala)_4$-OMe in water

To further evaluate the size and shape of our aggregates, aqueous solutions of Z-$(L\text{-}Ala)_3$-$(Aib\text{-}L\text{-}Ala)_4$-OMe were investigated also by means of the TEM technique with uranyl acetate as staining agent. Spherical assemblies were observed (**Figure 4**), comparable in size to those revealed by DLS (**Figure 3**). Smaller spherical aggregates (about 10 nm) are also present (**Figure 4A**). They possibly represent the initial steps of a pathway leading to the larger aggregates.

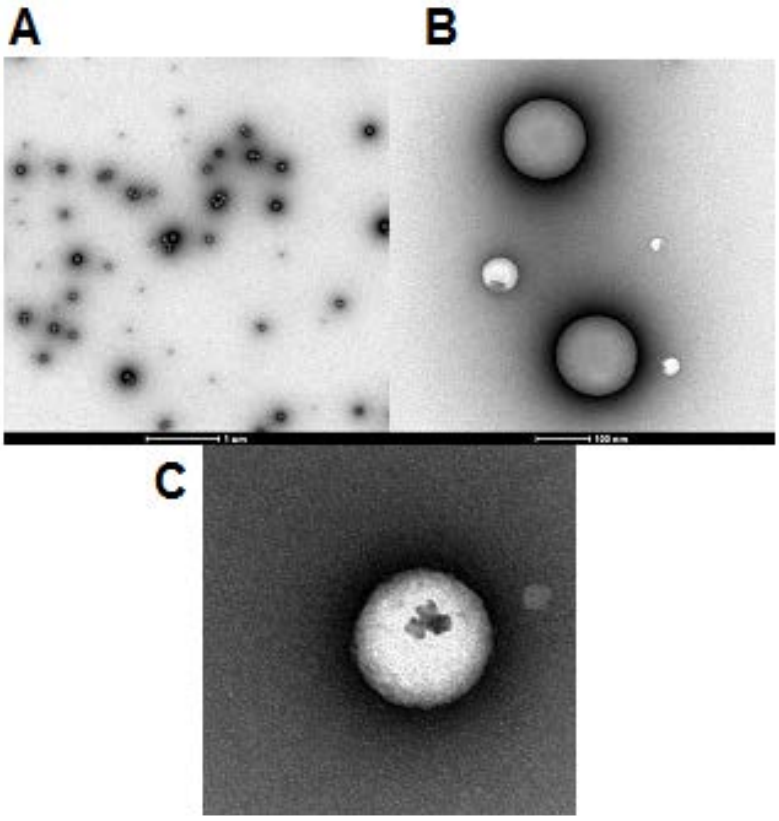


***Fig. 4*** TEM images of Z-$(Ala)_3$-$(Aib\text{-}L\text{-}Ala)_4$-OMe from an aqueous solution. The sample was stained negatively with uranylacetate. The scale bars represent 1000 (**A**),100 (**B**) and 50 (**C**) nm, respectively

The AFM analysis of the same peptide sample, deposited on a mica substrate, confirms the size (about 100 nm, **Figure 5A**) and, most importantly, the spherical nature (**Figure 5B**) of these peptide aggregates.

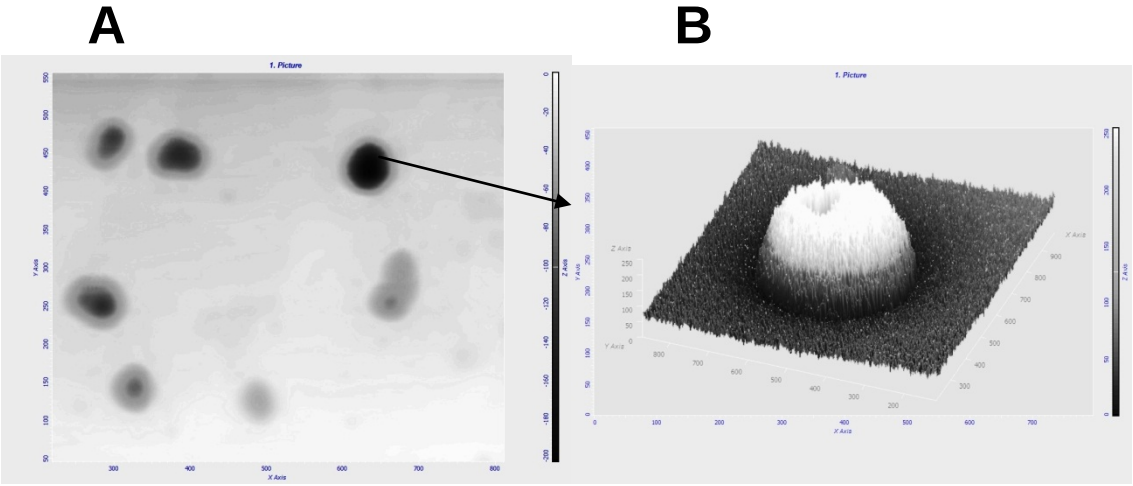


***Fig. 5*** AFM images of the Z-$(Ala)_3$-$(Aib\text{-}L\text{-}Ala)_4$-OMe aggregates formed in aqueous solution. The *x* axis of panel **A**spansabout 0.6μm. In panel **B** the 3D-structure of an aggregate is reported.

The CAC was investigated by TEM. A set of different solution of Z-$(Ala)_3$-$(Aib\text{-}L\text{-}Ala)_4$-OMe at concentration of 5, 10, 15 and 20 mM in were submitted to TEM analysis and the results are shown in **Figure 6**. From the TEM results that is clearly visible only from concentrations above 15 mM.

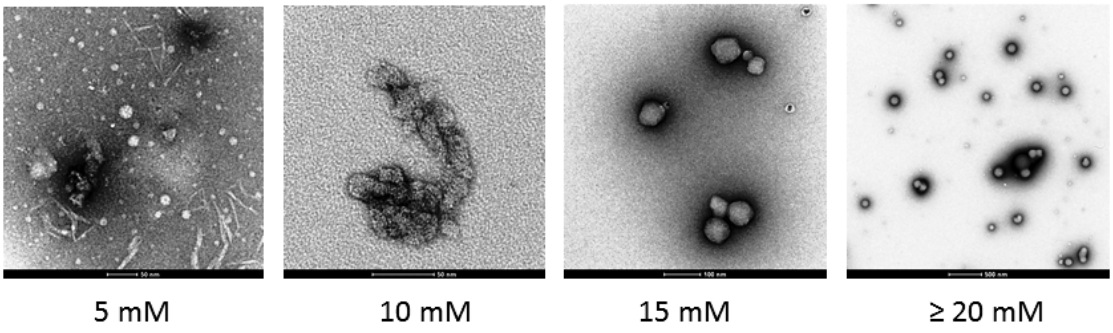


***Fig. 6*** TEM images of Z-$(Ala)_3$-$(Aib\text{-}L\text{-}Ala)_4$-OMe at different concentrations from an aqueous solution. The sample was stained negatively with uranyl acetate.

One possible explanation for the origin of the spherical microstructure from Z-$(Ala)_3$-$(Aib\text{-}L\text{-}Ala)_4$-OMe in water solution is depicted in **Figure 7**. We assume that above the CAC the single monomers (**Fig. 7/1**) could “dimerized” (**Fig. 7/2**) as consequence of the

π-π stacking (non-covalent) interactions generate from the Z-group in aqueous media. These interaction could be extended to several dimers that induced self-assembly to generate fibrillar type network (**Fig. 7/3**). These fibrillar network are able to generate spherical aggregate to minimize the overall solvation energy.

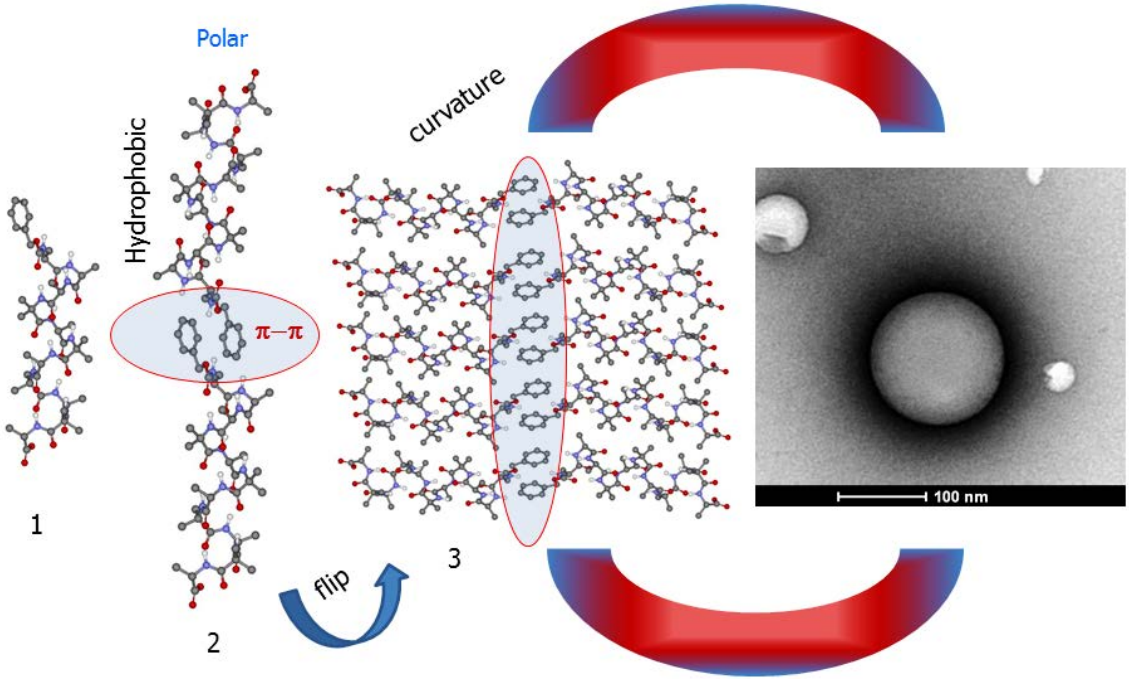


***Fig. 7*** Proposed mechanism of spherical micro-aggregate formation from Z-$(Ala)_3$-$(Aib\text{-}L\text{-}Ala)_4$-OMe in water solution.

**Encapsulation experiments**

We also checked the ability of the Z-$(Ala)_3$-$(Aib\text{-}L\text{-}Ala)_4$-OMe aggregates to encapsulate other molecules. As guest, we chose the water soluble, peptide-coated Au nanoparticles AuNps11,[2] characterized by an average diameter of 6 nm (2 nm the Au core, 2+2 nm the helical peptide capping layer). A dark, red colored, water solution of AuNps11 was added to a clear and colorless water solution of Z-$(Ala)_3$-$(Aib\text{-}L\text{-}Ala)_4$-OMe. To remove the free, not encapsulated, AuNps11the mixture was applied to a size-exclusion Superdex 75 preparative column (3000-70000 Dalton, GE Healthcare Life Sciences). At the expected retention time, one major peak was observed, isolated and subsequently analyzed by means of DLS and TEM. Interestingly, the solution corresponding to this peak was colored, which indicates the presence of AuNps11. DLS

analysis of this fraction revealed the presence of aggregates with hydrodynamic radius of about 100 nm (**Figure 8A**). As a control,the same technique gave an one order of magnitude smaller size for AuNps11 alone (**Figure 8B**).

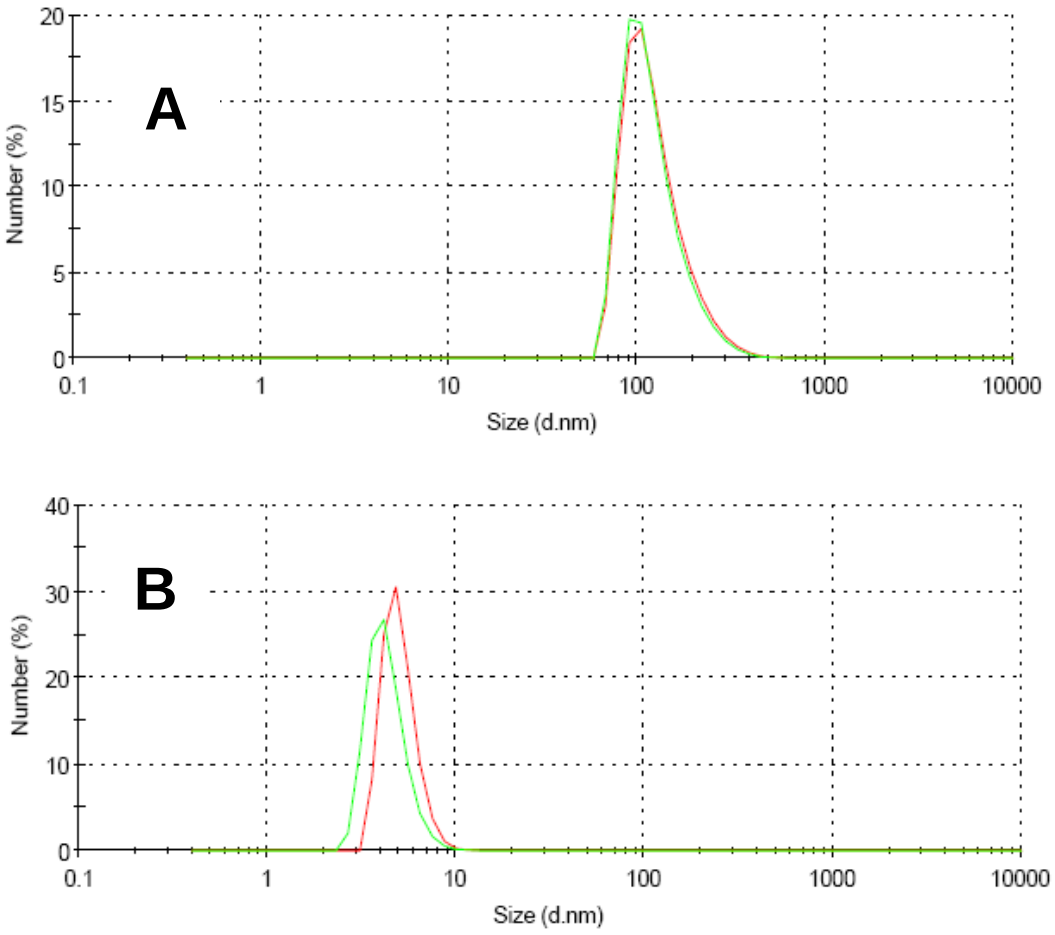


***Fig. 8*** DLS patterns for Z-$(Ala)_3$-$(Aib\text{-}L\text{-}Ala)_4$-OMe/AuNps11 aggregates (**A**) and AuNps11 alone (**B**) in water.

The TEM images of the same samples (**Figure 9**) are in agreement with the DLS analysis (**Figure 8**). In these TEM experiments,the uranyl acetate staining was not needed, as the Au atoms of the encapsulated AuNps11 allowed an easy detection. **Figure 9A** shows a TEM image of the Z-$(Ala)_3$-$(Aib\text{-}L\text{-}Ala)_4$-OMe/AuNps11 mixture, before the size-exclusion chromatography separation. It is quite clear that several AuNps11 have been incorporated into our undecapeptide aggregates, thus permitting their detection. The size (about 100 nm) of the two large bodies of **Figure 9A** is in agreement with the values obtained from the DLS measurements (**Figure 8A**). On the

other hand, the numerous small dark spots, enlarged in the inset of **Figure 9A**, are ascribed to free, not encapsulated AuNps11, as their size (2 nm) matches that of the AuNps11 metal core. After size-exclusion chromatography, the small spots of free AuNps11 disappear (**Figure 9B**) as clearly seen in the expansion (**Figure 9C**). Under these conditions, only the large peptide aggregates, with the AuNps11 encapsulated, are observed.

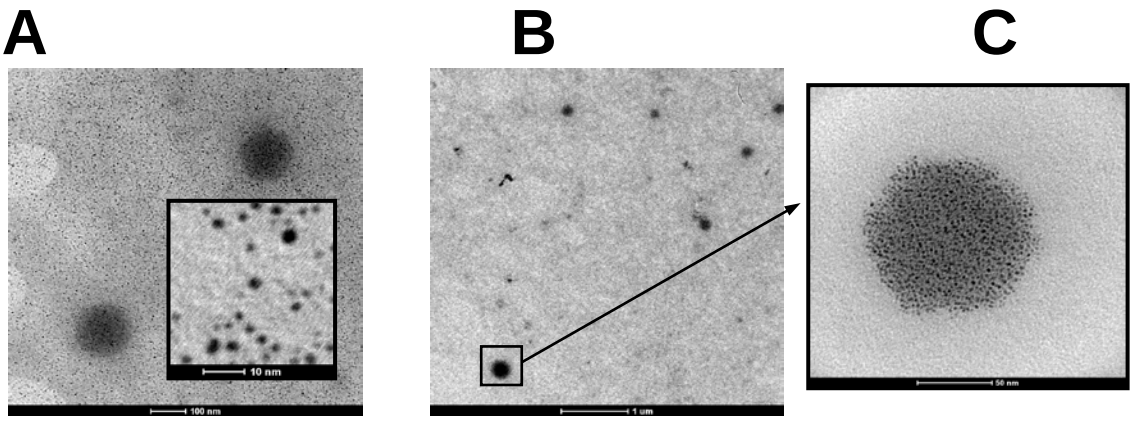


***Fig. 9*** TEM images fromaqueous solutions containing Z-$(Ala)_3$-$(Aib\text{-}L\text{-}Ala)_4$-OMe and AuNps11 before (**A**) with the inset of smaller spots (free AuNps11) and after (**B** and **C**) size-exclusion chromatography. No staining with uranyl acetate was performed. Thescale bars represent 100 (**A**), 10 (**A**, inset), 1000(**B**) and 50 (**C**) nm.

**Aggregate constituents**

Given for granted the formation in water of large, spherical, self-assembled aggregates for Z-$(L\text{-}Ala)_3$-$(Aib\text{-}L\text{-}Ala)_4$-OMe,[2] and related shorter peptides,[1] the main question to be answered is what these aggregates are made of: only peptides or peptides and solvent (water)? Micelles and vesicles are two well known spherical assemblies occurring in Nature. For their formation, amphiphilic molecules are required. Our Aib/Ala peptides do not possess charges or highly polar groups, with the exception of amide N-H and C=O groups not intramolecularly H-bonded at the N- and C-terminus, respectively. Interestingly, in the undecapeptide crystal structure discussed above, the Shellman motif allows the occurrence of four free carbonyl oxygens, rather than three as found in a regular α-helix. In addition, the Shellman motif induces a kink on the peptide helix. These two features might be relevant for the formation of the supramolecular, self-assembled structures observed by TEM and DLS, although at the present stage of our

studies we cannot formulate a precise model. In any case, micellar aggregates of Z-(L-Ala)$_3$-(Aib-L-Ala)$_4$-OMe would have a diameter not larger than 5 nm, *i.e.* approximately twice the length of the peptide helix (about 2 nm). Conversely, the aggregates observed by DLS and TEM possess a diameter about ten times larger. Then, the likely formation of vesicles should be taken into account. In this event, our aggregates could contain water in the inner part. To assess this possibility, we are planning the incorporation of appropriate spectroscopic probes into our self-assembled aggregates. [21,22]

## CONCLUSIONS

Recent reviews comprehensively explored the up-to-date research on peptide-amphiphiles (amphiphilic peptides that can give supra-molecular aggregates in solution).[23,24] In a review, Hamley includes the PA in two groups: (i) designed purely peptidic systems with amphiphilic properties arising from sequences of hydrophobic and hydrophilic (charged) residues, and (ii) peptides modified by attachment of hydrophobic lipid chains these are termed peptide amphiphiles (PAs). Peptides are intriguingly useful precursors for self-assembled structure design even due to the high number of exploitable amino acid building blocks. This free-energy driven mechanism of aggregation organizes molecules in a high ordered structure at multiple lenght scale. The tuning of self-assembly can also be ruled by controlling several environment parameters such as pH,[25,26] solvent,[27,28] metal ions,[29] and temperature.[30] Peptides have been recognized as very useful building blocks for self-assembly nano-structures. Their ability to fold into a specific secondary structure provides an unique platform for the design of molecular nano-structure. Furthermore, the secondary structure in peptides is strongly controlled by the amino-acid content, even in conjugation with tailored higlhy hydrophilic sub-units.[27]

The main contribution of this work consists in the discovery that a series of Aib/Ala peptides, lacking any charge or polar group, dissolve in water through the formation of self-assembled bodies. These aggregates are larger than a typical micelle, although it is not clear yet if they form vesicles or a different type of supramolecular structure. Our contention, supported by X-ray diffraction data, is that a hydrophilic side (the N- and/or the C-terminus and/or a face of the helix) of the peptide has to be located on the outer layer of these aggregates. Additional syntheses and experiments are

currently in progress in our laboratory to understand the chemical composition of these large, spherical structures. We are confident that our efforts will add a new tool to the number of possible applications envisaged for peptide self-assembled aggregates.[21,23,24,31-33]

## EXPERIMENTAL SECTION

GENERAL METHODS

**SYNTHESIS:** The undecapeptide Z-(L-Ala)$_3$-(Aib-L-Ala)$_4$-OMe, its C-unprotected analogue (free COOH) and the Au nanoparticle (AuNp11) used for the encapsulation experiments were prepared by solution procedures as previously reported.[1,2] AuNp11 is an Au nanoparticle coated with the same peptide segment, -(L-Ala)$_3$-(Aib-L-Ala)$_4$-, responsible for the formation in water of the large aggregates described in this work.

**TLC**: The products and intermediates have been checked on TLC plate with the following eluant systems:

| | |
|---|---|
| $CHCl_3$/EtOH 9:1 | $Rf_1$ |
| 1-Butanol/AcOH/$H_2O$ 3:1:1 | $Rf_2$ |
| toluene/EtOH 7:1 | $Rf_3$ |

**CD:** The ECD spectra were obtained on a Jasco (Tokyo, Japan) model J-715 spectropolarimeter. Cylindrical fused quartz cells (Hellma, Müllheim, Germany) of 0.1 mm path length were employed. The data are expressed in terms of $[\theta]_T$, the total molar ellipticity (deg x cm$^2$ x dmol$^{-1}$). The solvent used was MilliQ (Millipore Corporation, Billerica, MA) pH 7 water.

**DLS:** Dynamic Light Scattering (DLS) measurements were performed with a Malvern Zetasizer NanoS instrument equipped with a thermostated cell holder and Ar laser operating at 633 nm. Hydrodynamic particle diameters were obtained from cumulant or distribution fit of the autocorrelation functions collected at 178° scattering angle. Size measurements were performed at 25° C in water.

**TEM:** The samples, prepared immediately before use by dilution of the peptide aggregates solution (100 times) with water and vortex, analyzed on a Jeol 300PX instrument. A glow discharged carbon coated grid was floated on a small drop of gel solution and excess was removed by #50 hardened Whatman filter paper. The grid was then floated on 2% uranyl acetate solution for 10 seconds, and the excess was removed by #50 hardened Whatman filter paper.

**AFM:** AFM images were taken using a Park Autoprobe CP instrument operating in contact mode in air. Samples were prepared immediately before analysis, by dilution of the peptide aggregates solution with water and vortex. The topographies were acquired under environment conditions. The scan rate was 1.0 Hz and the force set point was the lowest to improve resolution at the same time minimizing damage to the samples. Surface morphological investigations were performed on as-prepared samples (ca. 2×2 $cm^2$) obtained by drop casting the aggregate solutions at different concentrations on mica substrate.

**X-RAYS DIFFRACTION:** Single crystals of Z-(L-Ala)$_3$-(Aib-L-Ala)$_4$-OH were grown by slow evaporation from a 2-propanol solution. X-ray diffraction data were collected with an Agilent Technologies Gemini E four-circle kappa diffractometer equipped with a 92 mm EOS CCD detector, using graphite monochromated Cu Kα radiation (λ = 1.54178 Å). Data collection and reduction were performed with the CrysAlisPro software (version 1.171.35.11, Agilent Technologies). A semi-empirical absorption correction based on the multi-scan technique using spherical harmonics, implemented in SCALE3 ABSPACK scaling algorithm, was applied. The measurements were accomplished by Dr. Marco Crisma, CNR-ICB, Padova.

The structure was solved by direct methods of the SIR 2002 program.[34] The asymmetric unit is composed of one peptide molecule and three cocrystallized water molecules. Refinement was carried out by full-matrix least-squares procedures on $F^2$, using all data, by application of the SHELXL-97 program,[35] with all non-H-atoms anisotropic. H-atoms of the peptide molecule were calculated at idealized positions and refined using a riding model. The positions of the H-atoms of the cocrystallized water molecules were recovered from a difference Fourier map and they were not refined. Relevant crystal data and structure refinement parameters are listed in **Table 3**. CCDC 908157contains the supplementary crystallographic data for this paper. These data can be obtained from The Cambridge Crystallographic Data Centre via www.ccdc.cam.ac.uk/data_request/cif

***Tab. 3*** Crystal data and structure refinement for Z-(L-Ala)$_3$-(Aib-L-Ala)$_4$-OH trihydrate

| | |
|---|---|
| Empirical formula | C45 H77 N11 O17 |
| Formula weight | 1044.18 |
| Temperature | 293(2) K |
| Wavelength | 1.54178 Å |
| Crystal system | Monoclinic |
| Space group | C2 |
| Unit cell dimensions | $a$ = 33.2617(13) Å α= 90°<br>$b$ = 8.4156(2) Å β= 124.813(6)°<br>$c$ = 24.4073(10) Å γ = 90° |
| Volume | 5609.2(3) Å$^3$ |
| $Z$ | 4 |
| Density (calculated) | 1.236 Mg/m$^3$ |
| Absorption coefficient | 0.796 mm$^{-1}$ |
| $F$(000) | 2240 |
| Crystal size | 0.50 × 0.28 × 0.04 mm$^3$ |
| Theta range for data collection | 2.68 to 61.02°. |
| Index ranges | -37 ≤ h ≤ 37, -9 ≤ k ≤ 8, -27 ≤ l ≤ 27 |
| Reflections collected | 22711 |
| Independent reflections | 7604 [R(int) = 0.0342] |
| Completeness to theta = 61.02° | 99.4 % |
| Absorption correction | Semi-empirical from equivalents |
| Max. and min. transmission | 1.00000 and 0.60880 |
| Refinement method | Full-matrix least-squares on $F^2$ |
| Data / restraints / parameters | 7604 / 1 / 658 |
| Goodness-of-fit on $F^2$ | 0.993 |
| Final $R$ indices [I>2sigma(I)] | $R_1$ = 0.0413, $wR_2$ = 0.1057 |
| $R$ indices (all data) | $R_1$ = 0.0465, $wR_2$ = 0.1102 |
| Absolute structure parameter | -0.12(17) |
| Largest diff. peak and hole | 0.166 and -0.159 e.Å$^{-3}$ |

SYNTHESIS AND CHARACTERIZATION

The synthesis of shorter intermediates refer to Chapter 1.[1] Here below are reported the sytheses of the intermediate 10-mer and the 11-mer as they were prepared.

**Z-L-Ala-L-Ala-Aib-L-Ala-Aib-L-Ala-Aib-L-Ala-Aib-L-Ala-OMe**

This compound was prepared from Z-L-Ala-OH (0.16 g, $7.0 \cdot 10^{-4}$ moli) and H-L-Ala-Aib-L-Ala-Aib-L-Ala-Aib-L-Ala-Aib-L-Ala-OMe ($5.8 \cdot 10^{-4}$ mol; obtained *via* cathalytic hydrogenation in MeOH of the Z-derivative) as previously described for Z-L-Ala-Aib-L-Ala-Aib-L-Ala-Aib-L-Ala-Aib-L-Ala-OMe. The product precipitated from EtOAc/PE. Yield 98%. **m.p.:** 159-163°**C**. **$Rf_1$:** 0.25; **$Rf_2$:** 0.75; **$Rf_3$:** 0.10. **$[\alpha]_D^{20}$**: -36.7° (c[$gmL^{-1}$] =0.6, MeOH). **IR** (KBr): 3320, 1743, 1661, 1531 $cm^{-1}$. **$^1$H NMR** (200 MHz, $CDCl_3$): δ 7.79-7.18 (9m, 9H, 4 Aib NH, 5 Ala NH), 7.36 (s, 5H, Z fenile), 6.97 (d, 1H, Ala NH), 5.13 (s, 2H, Z $CH_2$), 4.56-4.29 (2m, 2H, 2 Ala α-CH), 4.01-3.99 (m, 4H, 4 Ala α-CH), 3.67 (s, 3H, -OMe $CH_3$), 1.61-1.20 (m, 42H, 4 Aib 2 β-$CH_3$, 6 Ala β-$CH_3$).

**Z-L-Ala-L-Ala-L-Ala-Aib-L-Ala-Aib-L-Ala-Aib-L-Ala-Aib-L-Ala-OMe**

This compound was prepared from Z-L-Ala-OH ($8.8 \cdot 10^{-2}$ g, $3.4 \cdot 10^{-4}$ mol) and H- L-Ala-L-Ala-Aib-L-Ala-Aib-L-Ala-Aib-L-Ala-Aib-L-Ala-OMe ($3.3 \cdot 10^{-4}$ mol; obtained *via* cathalytic hydrogenation in MeOH of the Z-derivative) as previously described for Z-L-Ala-Aib-L-Ala-Aib-L-Ala-Aib-L-Ala-Aib-L-Ala-OMe. The product precipitated from EtOAc/PE. Yield 70%. **m.p.:** 134-138°**C**. **$Rf_1$:** 0.15; **$Rf_2$:** 0.75; **$Rf_3$:** 0.10. **$[\alpha]_D^{20}$**: -10.1° (c($gmL^{-1}$) =0.4, MeOH). **IR** (KBr) 3230, 1740, 1662, 1531 $cm^{-1}$. **$^1$H NMR** (200 MHz, $CDCl_3$): δ 8.10-7.20 (10m, 10H, 4 Aib NH, 6 Ala NH), 7.36 (s, 5H, Z fenile), 7.16 (d, 1H, Ala NH), 5.18 (s, 2H, Z $CH_2$), 4.54-4.26 (2m, 4H, 4 Ala α-CH), 4.10-3.95 (m, 5H, 5 Ala α-CH), 3.68 (s, 3H, -OMe $CH_3$), 1.61-1.20 (m, 45H, 4 Aib 2 β-$CH_3$, 7 Ala β–$CH_3$).

REFERENCES


(1) Longo, E.; Moretto, A.; Formaggio, F.; Toniolo, C. *Chirality* **2011**, *23*, 756.
(2) Rio-Echevarria, I. M.; Tavano, R.; Causin, V.; Papini, E.; Mancin, F.; Moretto, A. *Journal of American Chemical Society* **2011**, *133*, 8.
(3) Arikuma, Y.; Nakayama, H.; Morita, T.; Kimura, S. *Angewandte Chemie Inernational Edition* **2010**, *49*, 1800.
(4) Arikuma, Y.; Nakayama, H.; Morita, T.; Kimura, S. *Langmuir* **2011**, *27*, 1530.
(5) Kennedy, D. F.; Crisma, M.; Toniolo, C.; Chapman, D. *Biochemistry* **1991**, *30*, 6541.
(6) Otoda, K.; Kimura, S.; Imanishi, Y. *Biochimica & Biophysica Acta* **1993**, 1.
(7) Vijayakumar, E. K. S.; Balaram, P. *Biopolymers* **1983**, *22*, 2133.
(8) Manning, M. C.; Woody, R. W. *Biopolymers* **1991**, *31*, 569.
(9) Toniolo, C.; Polese, A.; Formaggio, F.; Crisma, M.; Kamphuis, J. *Journal of American Chemical Society* **1996**, *118*, 2744.
(10) Toniolo, C. *CRC Critical Review in Biochemistry* **1980**, *9*.
(11) Crisma, M.; Formaggio, F.; Moretto, A.; Toniolo, C. *Biopolymers (Peptide Science)* **2006**, *84*, 3.
(12) Venkatachalam, C. M. *Biopolymers* **1968**, *6*, 1425.
(13) Taylor, R.; Kennard, O.; Versichel, W. *Journal of American Chemical Society* **1984**, *106*, 244.
(14) Görbitz, C. H. *Acta Crystallographica* **1989**, *B45*, 390.
(15) Zimmerman, S. S.; Pottle, M. S.; Némethy, G.; Scheraga, H. A. *Macromolecules* **1977**, *10*, 1.
(16) Datta, S.; Shamala, N.; Banerjee, A.; Pramanik, A.; Bhattacharja, S. *Journal of American Chemical Society* **1997**, *119*, 9246.
(17) Karle, I. L.; Banerjee, A.; Bhattacharjva, S.; Balaram, P. *Biopolymers* **1996**, *38*, 515.
(18) Banerjee, A.; Raghothama, S. R.; Karle, I. L.; Balaram, P. *Biopolymers* **1996**, *39*, 279.
(19) Benedetti, E.; Blasio, B. D.; Pavone, V.; Pedone, C.; Santini, A.; Bavoso, A.; Toniolo, C.; Crisma, M.; Sartore, L. *Journal of Chemical Society, Perkin Trans.* **1990**, *2*, 1829.
(20) DiBlasio, B.; Pavone, V.; Saviano, M.; Fattorusso, R.; Pedone, C.; Benedetti, E.; Crisma, M.; Toniolo, C. *Pept. Res.* **1994**, *7*, 55.
(21) Tanisaka, H.; Kizaka-Kondoh, S.; Makino, A.; Tanaka, S.; Hiraoka, M.; Kimura, S. *Bioconjugated Chemistry* **2008**, *19*, 109.
(22) Tovar, J. D.; Claussen, R. C.; Stupp, S. I. *Journal of American Chemical Society* **2005**, *127*, 7337.
(23) Cui, H.; Webber, M. J.; Stupp, S. I. *Biopolymers (Peptide Science)* **2009**, *94*.
(24) Hamley, I. W. *Soft Matter* **2011**, *7*, 4122.
(25) Jin, Y.; Xu, X.-D.; Chen, C.-S.; Cheng, S.-X.; Zhang, X.-Z.; Zhuo, R.-X. *Macromolecular Rapid Communications* **2008**, *29*, 1726.
(26) Shera, J. N.; Sun, X. S. *Biomacromolecules* **2009**, *10*, 2446.
(27) James, J.; Mandal, B. *Journal of Colloid and Interface Science* **2011**, *360*, 600.
(28) Kimura, S.; Kim, D.-H.; Sugiyama, J.; Imanishi, Y. *Langmuir* **1999**, *15*, 4461.
(29) Dublin, S. N.; Conticello, V. P. *Journal of American Chemical Society* **2008**, *130*, 49.
(30) Dreher, M. R.; Simnick, A. J.; Fischer, K.; Smith, R. J.; Patel, A.; Schmidt, M.; Chilkoti, A. *Journal of American Chemical Society* **2008**, *130*, 687.
(31) Zhang, S. *Biotechnology* **2003**, *21*, 1171.
(32) Colombo, G.; Soto, S.; Gatiz, E. *Trends Biotechnology* **2007**, *25*, 211.
(33) Zhao, X.; Pan, F.; Lu, J. R. *Progress in Natural Science* **2008**, *18*, 653.
(34) Burla, M. C.; Camalli, M.; Carrozzini, B.; Cascarano, G. L.; Giacovazzo, C.; Polidori, G.; Spagna, R. *Journal of Applied Crystallography* **2003**, *36*, 1103.
(35) Sheldrick, G. M. *Acta Crystallographica* **2008**, *64*, 112.

# IV

## Bis-azobenzene photoswitchable, prochiral, $C^{\alpha}$-tetrasubstituted α-amino acids for nanomaterial applications

### INTRODUCTION

Great interest is currently devoted to molecular or supramolecular entities that have access to two or more forms, the interconversion of which can be triggered by an external stimulus.[1] Several switching systems have been reported which are based on photochromic behaviour, resulting in optical control of chirality, fluorescence, intersystem crossing, electrochemically and photochemically induced changes in liquid crystals, thin films and membranes.[2] The design of molecular compounds that exhibit photoinduced magnetization and magnetic transitions is one of the main challenges in the field of materials science because of their possible application to future optical memory and switching devices.[3] Hence, the construction of a new class of optically switchable magnetic compounds that exhibit both large magnetization changes and ferromagnetic order even at room temperature is nowadays an issue of great potential.[3a-c, 4] Particularly interesting are photoactive molecules formed on the surface of gold, silver, and platinum nanoparticles. Due to the high surface-to-volume ratio, the concentration of photoactive compounds compared to the number of gold atoms allows for standard characterization techniques such, as UV/Vis or FTIR absorption spectroscopy, to be employed to detect photochromic switching.[3b] Azobenzenes were among the first photochromic switches used and are still subject of extensive investigation.[5] Their *cis*- and *trans* (hereafter termed **c** and **t**)-isomers have a different spatial arrangement of the aromatic moieties, and consequently show significantly different physical and chemical properties, including dipole moments. We are currently expanding this field by developing a novel family of $C^{\alpha}$-tetrasubstituted α-amino acids, characterized by two azobenzene moieties covalently linked to their α-carbon atom, to be exploited as photo-responsive building-blocks able to drive conformational and other stereochemical changes even if conjugated with other molecules. These compounds are based on the symmetrical di[4-(phenylazo)benzyl]glycine (*p*Dazbg), and its 3-(phenylazo)benzyl analogue (*m*Dazbg).

## RESULTS AND DISCUSSION

As a first step, we synthesized the two $C^{\alpha}$-tetrasubstituted α-amino ethylesters, $H_2$-*p*Dazbg-OEt (**1**) and $H_2$-*m*Dazbg-OEt (**2**), as illustrated for the former compound in Scheme 1 (for synthetic details, see experimental section). The key step (iv), the double alkylation of ethyl isocyanoacetate with (*E*)-1-[4-(bromomethyl)phenyl]-2-phenyldiazene, was performed in excellent yield and the product was easily isolated. Next, treatment of the ethyl 2-isocyano derivative with concentrated HCl in ethanol gave **1** as the ammonium salt, which, in turn, by acidic hydrolysis, quantitatively afforded the related *p*Dazbg free $C^{\alpha}$-tetrasubstituted α-amino acid. The synthesis of (**2**) was performed in a similar way, starting from 3-aminobenzoic acid and nitrosobenzene (for synthetic details, see SI). By slow evaporation of a $CH_2Cl_2$/TFA (trifluoroacetic acid) solution of **1** we were able to grow single crystals, suitable for X-ray diffraction analysis (**Figure 1**). The backbone of the α-amino ethyl ester adopts an extended conformation [N1-C1A-C1-OT ($\psi_T$) torsion angle -179.8(3)°], which allows the presence of an intra-residue H-bond ($C_5$ form) between the N1-H1B group and the O1 carbonyl oxygen.

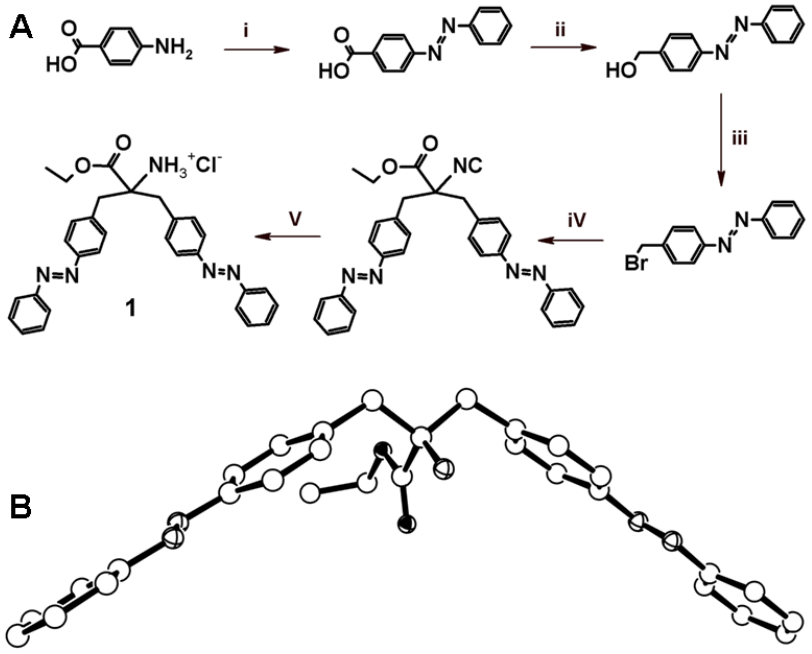


***Fig. 1*** A) Synthesis of **1**. Reagents and conditions: (i) AcOH, nitosobenzene, rt, 24 h, 80 %; (ii) THF, $LiAlH_4$, rt, 24 h, 93%; (iii) triphenylphosphine, *N*-bromosuccinimide, $CH_2Cl_2$, rt, 12 h, 91%; (iv) ethyl isocyanoacetate, tetrabutylammonium bisulfate, $K_2CO_3$, 50 ºC, 24 h, 96%; (v) HCl, EtOH, rt, 2 h, 100 %. B) X-ray diffraction structure of the "albatross-like" compound **1**.

The occurrence of the fully-extended conformation has been crystallographically documented for other $C^{\alpha,\alpha}$-symmetrically disubstituted glycines, including Dbg, in simple derivatives and peptides.[6] The $\chi$1 torsion angles about the C1A–C1B1 (*pro-S* side-chain) and C1A–C1B2 (*pro-R* side chain) bonds are in the $g^+$ [62.9(3)°] and the $g^-$ [-62.7(3)°] disposition, respectively. The two azobenze mojetis are in that conformation. The two side chain extend essentially flat, the angle between normals to the benzyl and phenyl ring being 10.3° and 2.6° for the *pro-S* and the *pro-R* chain, respectively. Interestingly, the distance between the carbon atoms, terminal to the two side chains, is 20.29 Å. In the second part of our study, we investigated the switch properties induced by light on the two thiol-containing compounds [trityl (Trt)-protected mercaptopropionic acid] Trt-S-$(CH_2)_2$-CO-*p*Dazbg-OH (**3**) (**Figure 2**) and Trt-S-$(CH_2)_2$-CO-*m*Dazbg-OH (**4**) (for synthetic details, see SI). We choose this thiol for subsequent studies that take advantage of these compounds as capping layer for metallic nanoparticles. These compounds were characterized by UV-Vis spectroscopy, NMR and reverse-phase HPLC. We found that both **3** and **4** undergo multiple, reversible isomerizations (**Figure 2**) in a variety of solvents by irradiation with Vis light (450 nm to **t**) or UV light (350 nm to **c**). However, when both compounds are dispersed in a paraffin medium, their photoswitch processes are blocked. Interestingly, using HPLC and NMR, we were also able to detect an intermediate state in the interconversion pathway (in which only one of the two azobenzene undergoes isomerization), namely the racemate of the **t**/**c** and **t**/**c** conformations (**Figure 2**). Specifically, two 0.1 mM solutions in MeOH (as well in several different solvents, data not shown) one containing **3** and the other **4** were separately irradiated under multiple cycles at two different wavelengths, 350 and 450 nm. Under Uv irradiation at 350 nm, we observed in both samples that the strong absorption maximum at 356 nm, typical for the *trans* form of azobenzene moieties, rapidly decreases in intensity, while the weak absorption band at 450 nm concomitantly increases (**figure 2 II**). The opposite phenomenon takes place when the samples were subsequently illuminated with visible light.

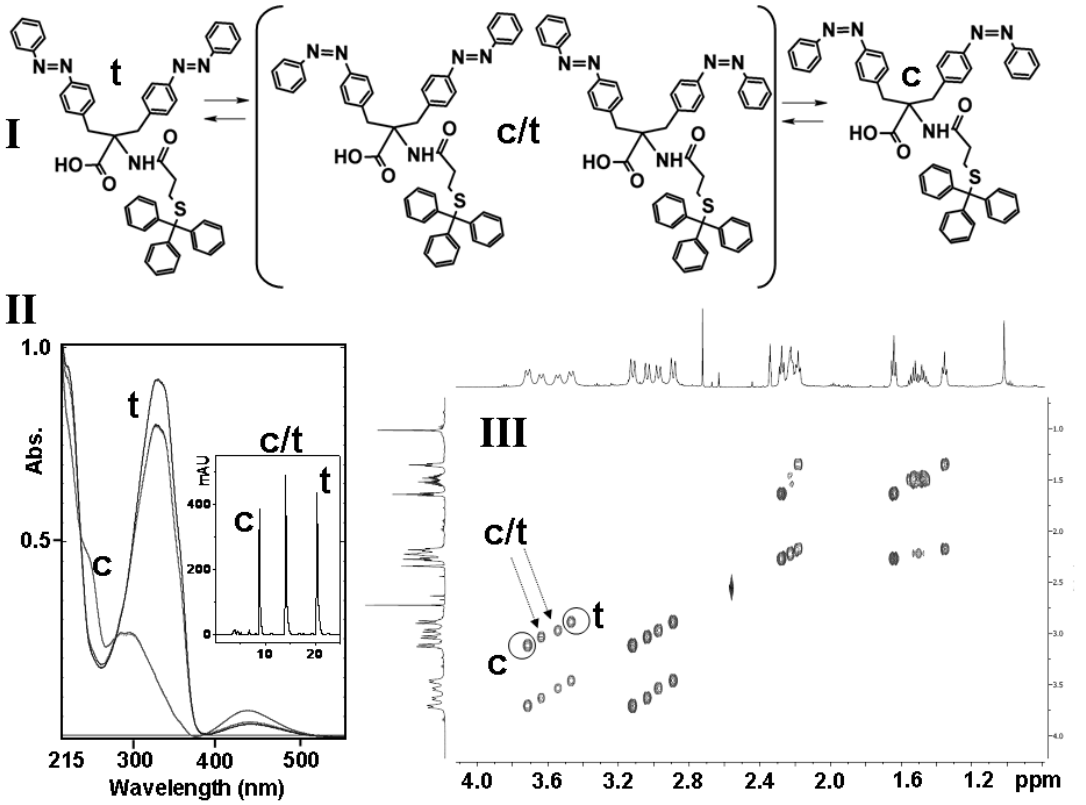


***Fig.2.*** (I) Mechanism of light driven isomerization for **3** (same mechanism, not shown for **4**). (II) Uv-vis absorption spectra of the multiple, reversible, **c**/**t** isomerization of **3**, in a 0.1 mM in MeOH solution, and (inset) HPLC profile of the 2-min irradiated (at 350 nm) solution. (III) The 2D-NMR spectrum run after 2-min irradiation at 350 nm (HPLC profiles B), shows the concomitant presences of three isomeric species.

As detected by HPLC, the conversion from the **t** form to the **c** form and *vice versa*, goes through an intermediate (**Figure 2 II, inset**). We associate this intermediate to the isomerization of only one of the two azobenzene side chains. As a consequence of this limited photoswitch, the $C^{\alpha}$-atom becomes chiral, and therefore a mixture of two enantiomers is generated. To confirm our hypothesis of "mono" isomerization, we carried out (DQF) COSY NMR experiments on the all-**t** compound, its all- **c** isomer, and on a 1:1:1 mixture of all-**t**, **t**/**c**, and **c**/**t** isomers genarated by 2-min irradiation with UV light. In this latter case (**Figure 2 III**), the NMR spectrum provides clear evidence for the occurrence of three independent species in a photo-stationary equilibrium. This phenomenon was further, albeit indirectly, demonstrated by investigating the photoisomerization of the chiral dipeptide containing one bis-azobenzeneresidue (*p*Dazbg) coupled with H-L-Leu-OMe, namely H-*p*Dazbg-L-Leu-OMe (**5**). In this case, due to the presence of L-Leu, the intermediate species generated upon isomerization of

a single azobenzene unit are diastereomers, H-(*R*)-*p*azoDbg-L-Leu-OMe and H-(*S*)-*p*azoDbg-L-Leu-OMe (**Figure 3**), and should therefore be distinguishable in the HPLC and NMR experiments.

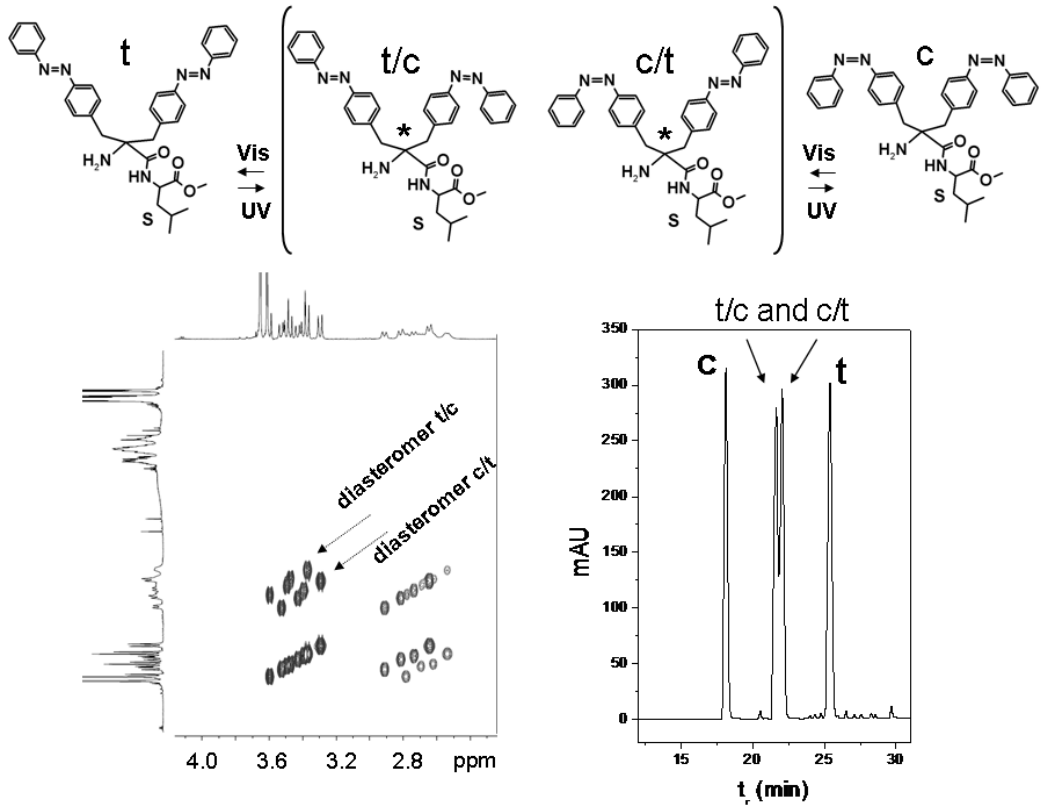


***Fig. 3*** (I) Mechanism of light-driven isomerization for **5**. (II) The 2D-NMR spectrum run after 3-min of irradiation at 350 nm (HPLC profile shown in the inst) highlights the concomitant presence of four isomeric species.

A solution of compound **5** in MeOH in the all-*t* conformation was prepared and the isomerization process under irradiation with UV light was followed by HPLC (**Figure 3 II**). Beside the two peaks corresponding to the all-*t* and all-*c* forms, two additional peaks of similar intensity were detected and assigned to the diastereomeric dipeptides exhibiting each azobenzene group of the *p*azoDbg residue in a different isomeric state, that is, the *t*/*c* and *c*/*t* species in Figure 3 I. This "mono" isomerization step was also analyzed by DQF-COSY experiments on a ≈ 1:1:1:1 mixture of all four isomers (Figure 3 II). This study demonstrated that the remote L-Leu stereocenter affects all of the diastereotopic -CβH2- protons, which resulted in a further splitting of the DQF COSY cross-peak patterns as compared to those in **Figure 2 III**. Indeed, these experiments provide evidence for the presence of four independent species in a photo-stationary equilibrium.

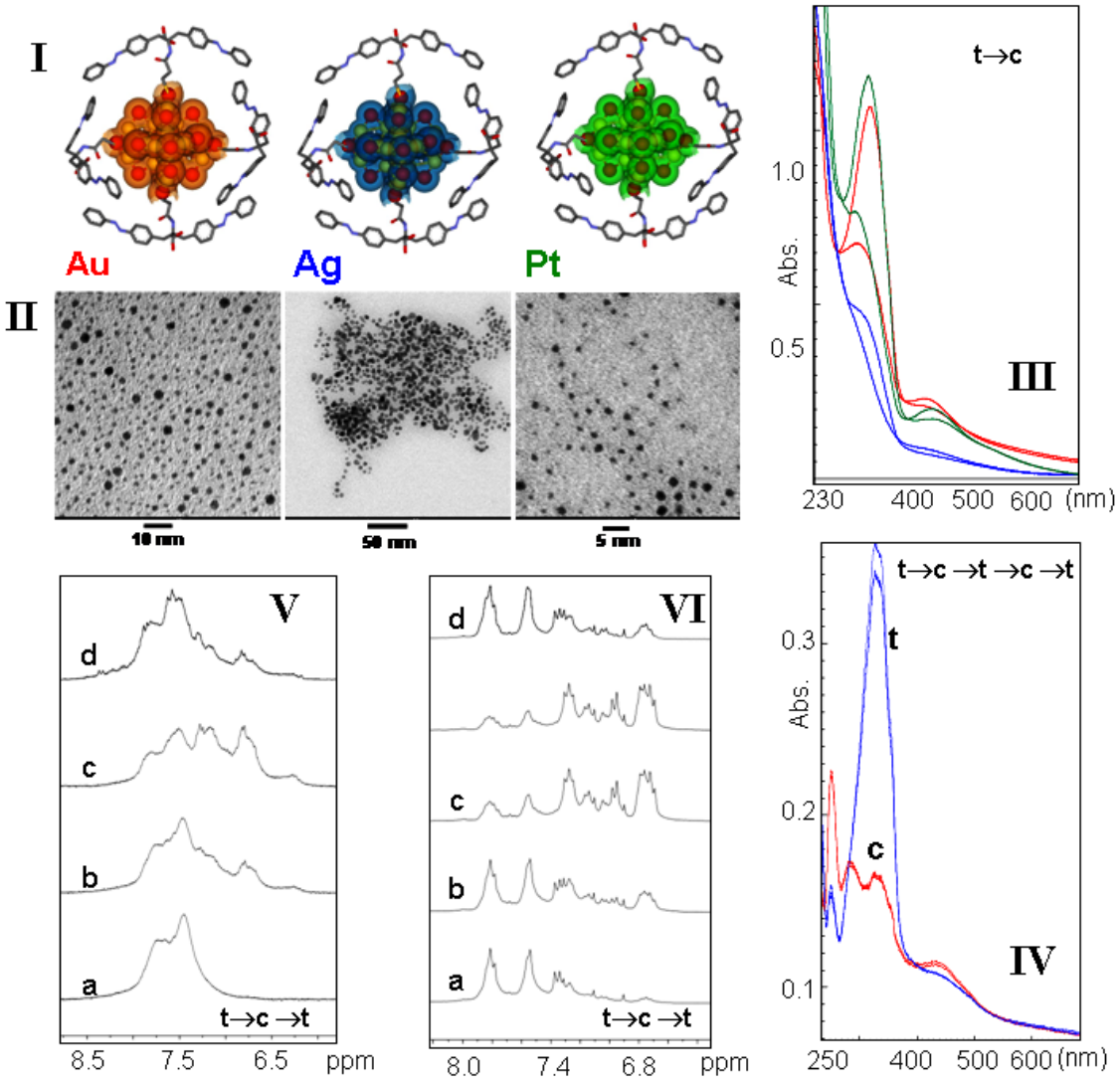


***Fig.4*** Light-driven isomerization of the **3**-conjugated metal nanoparticles. (I) Representations of AuNp-**3** (left), AgNp-**3** (center) and PtNp-**3** (right). (II) Representative TEM micrographs. (III) UV-Vis absorption spectra of the *c*↔*t* isomerization of Ag, Au, Pt nanoparticles capped with **3** in MeOH. Colors of the curves match those of the corresponding nanoparticle-conjugates in part (I). (IV) UV-Vis absorption spectra for the *c*↔*t* isomerization of AuNp-**3** in a paraffin medium (solid state). (V) 1H-NMR spectra of AuNp-**3** run after different times of irradiation: (a) 0 min, all-*t*; (b) 6-min irradiation at 350 nm; (c) 10-min irradiation at 350 nm, all-*c*; and (d) 20-min irradiation at 450 nm. (VI) 1H-NMR spectra of PtNp-**3** run after different times of irradiation: (a) 0 min, all-*t*; (b) 6-min irradiation at 350 nm; (c) 10-min irradiation at 350 nm, all-*c*; and (d) 20-min irradiation at 450 nm.

The behavior of different metal nanoparticles conjugated with **3** was next investigated. Au, Ag and Pt nanoparticles (**Figure 4 I**) were prepared by chemical reduction (with $NaBH_4$) of $HAuCl_4$, $AgNO_3$ and $H_2PtCl_6$, respectively, in a CHCl3/methanol/water mixture in the presence of **3**.[8] According to our TEM analysis (**Figure 4 II**) spherical Ag, Au and Pt nanoparticles (1.5–4 nm diameter) were obtained. Formation of the **3**-conjugated nanoparticles was confirmed by the UV-Vis absorption spectra, where weak

(due to the small nanoparticle size and the large absorption coefficient of the azobenzene moieties) metal-dependent plasmonic bands were observed. The photoswitch behavior of the conjugates was initially investigated by UV-Vis spectroscopy in solution (**Figure 4 III**), which allowed us to follow the reversible isomerization process. Then, the Au nanoparticles (AuNp-**3**) were examined in the solid state (dispersed in a paraffin medium; **Figure 4 IV**), where the photoinduced molecular switch was clearly seen over several cycles of irradiation. For the AuNp-**3** and Pt nanoparticles (PtNp-**3**) the *c*↔*t* isomerization was also studied by NMR (**Figures 4V** and **4 VI**) and HPLC (**Figure 5**).

In the NMR experiments, part of the complex envelope of broad peaks, corresponding to the aromatic protons of both metallic nanoparticles, showed a significant upfield shift during the irradiation process at 350 nm. The irradiation was stopped after 10 min, when the NMR spectra did not change anymore. Then, the NMR tube was irradiated with Vis light for 20 min. At this point, the new NMR signals were almost superimposable to those in the initial spectra recorded before UV irradiation. Monitoring the isomerization process by HPLC (**Figura 5**), it was found that the peak corresponding to the all-*t* form of AuNp-**3** (and PtNp-**3** as well) changed its retention time under UV irradiation.

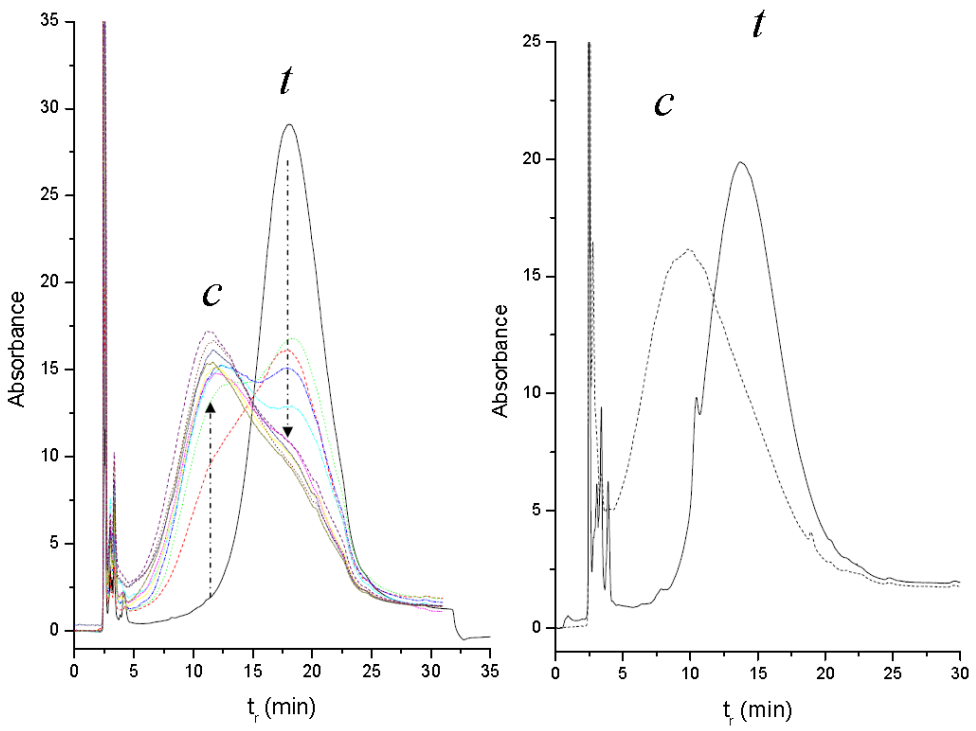


***Fig. 5*** HPLC profiles for AuNP-**3** (left: function of time exposure at 350nm) and PtNp-**3** (right), for the light-driven *trans* to *cis* isomerization process.

As recently reported by Einaga and co-workers,[3a-c] azobenzene passivated gold nanoparticles show a "controlled" ferromagnetism.[9] They demonstrated that this property can be selectively modulated by alternating photoillumination with UV and Vis light (that is, by exploiting *c*↔*t* isomerization) in the solid state. Based on this result, we investigated the magnetic susceptibility χ of AuNp-**3** by solution-state NMR at room temperature.[10] The method is based on the fact that the resonance frequency for a given nucleus depends, among other factors, upon the volume susceptibility of the medium. We used *tert*-butanol as the inert indicator compound and $CD_3OH$ as the solvent, and focused our attention on AuNp-**3**. This conjugate was subjected to sequential irradiation at 350 nm (5 time points), 450 nm (3 time points) and again 350 nm (3 time points). The resulting chemical shifts for the *tert*-butanol $CH_3$ protons (inner and outer NMR tubes) are reported in **Figure 5**. The modulation of χ as a consequence of irradiation is proportional to the relative difference (in Hz) between the two signals. It is clear from the graph that the behavior of χ is strongly correlated to the isomerization of **3** (as a grafted ligand). In detail, starting from the all-*t* conformation for AuNp-**3**, upon irradiation at 350 nm the value of χ increased to a maximum corresponding to the all-*c* conformation (this value did not change under prolonged photoillumination). Then, upon irradiation at 450 nm, the χ value reversibly decreased, down to almost its initial value. This behavior was reproducible for several switches (2 cycles are shown in **Figure 6**) between the UV and Vis irradiation wavelengths.

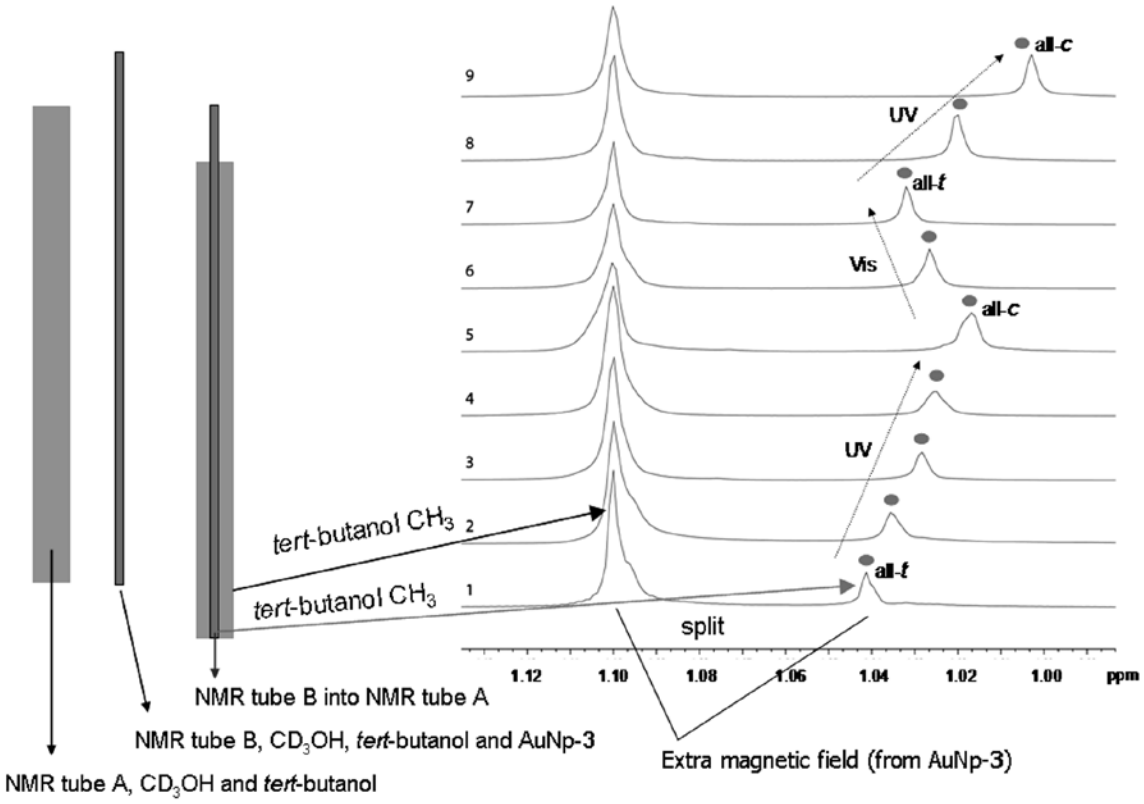


***Fig. 6*** Modulation of the magnetic susceptibility of AuNp-**3**. Outer compartment (tube A): 4% *tert*-butanol in CD3OH. Inner compartment (tube B): 4% *tert*-butanol and 2.5 mg/ml AuNp-**3** in CD3OH (the resonance signals of CD3OH are not shown). Spectrum 1, all-*t* conformation for AuNp-**3**. From spectrum 2 to spectrum 5, four different periods of irradiation with UV light. Spectra 6 and 7 were recorded after two different times of irradiation with Vis light. Spectra 8 and 9 were recorded after two different times of irradiation with UV light.

## EXPERIMENTAL SECTION

GENERAL METHODS

**NMR:** 1H spectra were recorded at room temperature on a Bruker AV-400 (400 MHz) or a Bruker AC-300 (300 MHz) instrument using the partially deuterated solvent or TMS as internal references. The multiplicity of a signal is indicated as: s - singlet, d - doublet, t - triplet, q - quartet, m - multiplet (br stands for broad). Chemical shifts (δ) are expressed in ppm and coupling constants (*J*) in Hertz.

**FT-IR:** FT-IR spectra were recorded with a Perkin-Elmer 1720X or a Nicolet Avatar 360 FTIR spectrophotometer; ν max is given for the main absorption bands.

**Mass Spectrometry:** High-resolution mass spectra were obtained by electrospray ionization (ESI) on a Perseptive Biosystem Mariner ESI-TOF or a Bruker Microtof-Q spectrometer.

**HPLC:** The HPLC measurements were performed using an Agilent 1200 series apparatus, equipped with a UV detector at variable wavelengths. For compounds **3**, **4**, and **5** HPLC conditions: Phenomenex C18 (100 Å) (stationary phase), 10–70% B, 25 min, 1 ml/min (eluents: A = water/acetonitrile 9/1, 0.05% TFA; B = water/acetonitrile 1/9, 0.05% TFA). For compounds AuNp-**3** and PtNp-**3** HPLC conditions: Phenomenex Onyx Monolithic C18 (stationary phase), 15–75% B, 25 min, 1 ml/min. (eluents: A = water/isopropanol 9/1, 0.1% TFA; B = water/isopropanol 1/9, 0.1% TFA).

**UV-Vis Absorption:** The electronic absorption spectra were recorded using a Shimadzu model UV-2501 PC spectrophotometer. A 1 cm path length quartz cell was used.

**TEM:** Samples were analyzed on a Jeol 300PX instrument. Samples were prepared before used, by 100 times dilution of a 2mg/ml MeOH solution of AuNp-**3**, AgNp-**3**, or PtNp-**3**. A glow discharged carbon coated grid was floated on a small drop of gel solution and excess was removed by #50 hardened Whatman filter paper.

**X-RAY DIFFRACTION:** X-ray diffraction data were collected with an Oxford Diffraction Gemini E four-circle kappa diffractometer equipped with a 92 mm EOS CCD detector, using graphite monochromated Cu Kα radiation (λ = 1.54178 Å). The sample to detector distance was 50 mm. A total of 1344 frames were collected by 1.0° omega oscillation with exposure times of 1.5, 4, or 70 s, depending on the theta values, in the 4.11°–68.46° theta range. Data collection and reduction were performed with the CrysAlisPro software (version 1.171.33.52; Oxford Diffraction). A semi-empirical

absorption correction based on the multi-scan technique using spherical harmonics, implemented in SCALE3 ABSPACK scaling algorithm, was applied. The structure was solved by ab initio procedures of the SIR 2002 program,[11] and refined by full matrix least squares on F2, using all data, by application of the SHELXL 97 program,[12]with all non-H atoms anisotropic. All phenyl rings were constrained to the idealized geometry. The positions of the H-atoms of the N-terminal free amino group were estimated by performing a rotational search of the electron density in the expected cone on the N atom and were not refined. All of the remaining H-atoms were calculated at idealized positions and refined using a riding model. Relevant crystallographic data and diffraction parameters are reported in Table 2. CCDC 832775 contains the supplementary crystallographic data for this paper. These data can be obtained from The Cambridge Crystallographic Data Centre via www.ccdc.cam.ac.uk/data_request/cif

SYNTHESIS AND CHARACTERIZATION

All reagents from commercial suppliers were used without further purification. Thin-layer chromatography (TLC) was performed on Macherey-Nagel Polygram syl G/UV precoated silica gel polyester plates. The products were visualized by exposure to UV light (254 nm), iodine vapour or submersion in ninhydrin or cerium molybdate stain [aqueous solution of phosphomolybdic acid (2%), $CeSO_4 \cdot 4H_2O$ (1%) and $H_2SO_4$ (6%)]. Column chromatography was performed using Macherey-Nagel 60Å silica gel.

**SYNTHESIS OF H-*pazo*Dbg-OEt (1)**

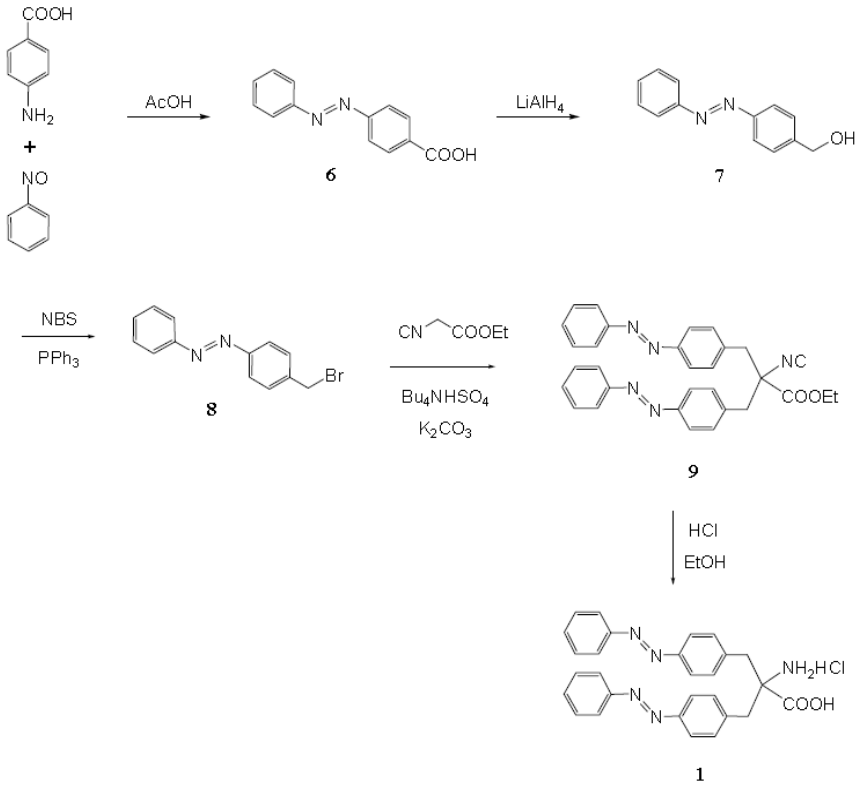


***p*-(Phenylazo)benzoic acid (6)**

A solution of nitrosobenzene (2.00 g, 18.69 mmol) in glacial acetic acid (20 mL) was added to a suspension of *p*-aminobenzoic acid (3.07 g, 22.43 mmol) in glacial acetic acid (15 mL) and the mixture was stirred at room temperature for 24 h. The solvent was evaporated to dryness and the residue was suspended in water and lyophilized. Recrystallization from ethyl acetate afforded pure **6** as an orange solid (3.37 g, 14.91 mmol, 80% yield). **M.p.** 247 ºC. **IR (KBr)** ν 3200–2300, 1678, 1429, 1289 $cm^{-1}$. **$^1$H NMR (DMSO-*d*6, 400 MHz) δ** 7.56–7.65 (m, 3H); 7.88–7.99 (m, 4H); 8.10–8.17 (m,

2H); 13.13 (brs, 1H). **HRMS (ESI)** $C_{13}H_9N_2O_2$ [M–H]–: calcd. 225.0670, found 225.0661.

***p*-(Phenylazo)benzyl alcohol (7)**

A solution of **6** (3.05 g, 13.50 mmol) in anhydrous THF (60 mL) was added in small portions to a suspension of $LiAlH_4$ (616mg, 16.20 mmol) in anhydrous THF (40 mL) kept at 0 ºC under an argon atmosphere. The reaction mixture was allowed to warm to room temperature and stirred for 24 h. The system was then cooled to 0 ºC and water (0.6 mL) was added slowly, followed by 10% aqueous NaOH (1.2 mL) and additional water (2 mL). The salts were eliminated by filtration through Celite and the resulting solution was dried over $MgSO_4$. The crude product obtained by evaporation of the solvent was chromatographed (eluent: hexanes/ethyl acetate 6/4) to give pure **7** as an orange solid (2.65 g, 12.52 mmol, 93% yield). **M.p.** 142 ºC. **IR (KBr) ν** 3303, 1441, 1023 $cm^{-1}$. **$^1$H NMR ($CDCl_3$, 400 MHz) δ** 1.85 (brs, 1H); 4.78 (s, 2H); 7.44–7.55 (m, 5H); 7.90–7.94 (m, 4H). **HRMS (ESI)** $C_{13}H_{13}N_2O$ [M+H]+: calcd. 213.1022, found 213.1017.

***p*-(Phenylazo)benzyl bromide (8)**

To a solution of **7** (2.63 g, 12.40 mmol) in anhydrous THF (60 mL) kept at 0 ºC, triphenylphosphine (4.87 g, 18.60 mmol) and *N*-bromosuccinimide (3.31 g, 18.60 mmol) were added in small alternate portions and the reaction system was stirred at room temperature overnight. The insoluble material was eliminated by filtration through a small pad of silica gel and washed thoroughly with THF. The filtrates were evaporated and the residue obtained was purified by column cromatography (eluent: hexanes/ethyl acetate 8/2) to afford pure **8** as an orange solid (3.11 g, 11.32 mmol, 91% yield). **M.p.** 121 ºC. **IR (KBr) ν** 1577, 1482, 1438, 687 $cm^{-1}$. **$^1$H NMR ($CDCl_3$, 400 MHz) δ** 4.56 (s, 2H); 7.48–7.56 (m, 5H); 7.88–7.94 (m, 4H). **HRMS (ESI)** $C_{13}H_{12}BrN_2$ [M+H]+: calcd. 275.0178, found 275.0168.

**Ethyl bis[*p*-(phenylazo)benzyl]isocyanoacetate (9)**

A solution of ethyl isocyanoacetate (600 mg, 5.31 mmol) in acetonitrile (70 mL) was treated with finely powdered $K_2CO_3$ (4.40 g, 31.86 mmol), tetrabutylammonium bisulfate (541 mg, 1.59 mmol) and **8** (3.65 g, 13.27 mmol). The resulting heterogeneous mixture was heated at 50 ºC with vigorous stirring for 24 h. The solvent was evaporated to dryness and the residue was partitioned between dichloromethane (80 mL) and water (60 mL). The aqueous layer was discarded and the organic phase was dried and filtered. Removal of the solvent followed by column cromatography (eluent: hexanes/ethyl

acetate 8/2) afforded pure **9** as an orange solid (2.55 g, 5.09 mmol, 96% yield). **M.p.** 157 ºC. **IR (KBr) ν** 2133, 1728, 1439, 1238, 1107 $cm^{-1}$. **$^1$H NMR ($CDCl_3$, 400 MHz) δ** 1.09 (t, 3H, *J* = 7.1 Hz); 3.19 (d, 2H, *J* = 13.5 Hz); 3.48 (d, 2H, *J* = 13.5 Hz); 4.10 (q, 2H, *J* = 7.1 Hz); 7.44–7.55 (m, 10H); 7.88–7.95 (m, 8H). **HRMS (ESI)** $C_{31}H_{28}N_5O_2$ [M+H]+: calcd. 502.2238, found 502.2222.

**Ethyl bis[*p*-(phenylazo)benzyl]glycinate (H-*p*azoDbg-OEt, 1)**

Concentrated HCl (8 mL) was added dropwise to a suspension of **9** (2.40 g, 4.80 mmol) in ethanol (80 mL) kept at 0 ºC and the reaction mixture was stirred at room temperature for 2 h. The solvent was evaporated and the residue was taken up in water and lyophilized to afford **1** as a solid (2.53 g, 4.80 mmol, 100% yield). **M.p.** 120 ºC. **IR (KBr) ν** 3434, 1740, 1444, 1220, 1108 $cm^{-1}$. **$^1$H NMR (DMSO-*d*6, 400 MHz) δ** 1.27 (t, 3H, *J* = 7.1 Hz); 3.40 (d, 2H, *J* = 13.9 Hz); 3.48 (d, 2H, *J* = 13.9 Hz); 4.26 (q, 2H, *J* = 7.1 Hz); 7.52–7.64 (m, 10H); 7.85–7.91 (m, 8H); 8.80 (brs, 3H). **HRMS (ESI)** $C_{30}H_{30}N_5O_2$ [M+H]+: calcd. 492.2394, found 492.2391.

**SYNTHESIS OF H-*m*azoDbg-OEt (2)**

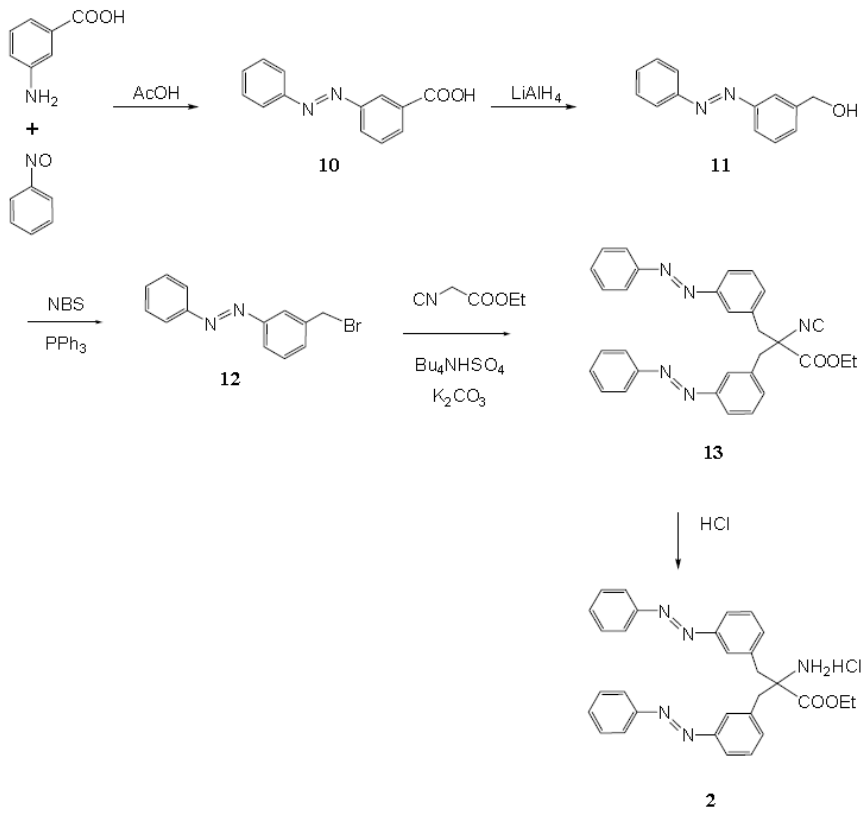

***m*-(Phenylazo)benzoic acid (10)**

A solution of nitrosobenzene (4.00 g, 37.38 mmol) in glacial acetic acid (45 mL) was added to a suspension of *m*aminobenzoic acid (6.15 g, 44.86 mmol) in glacial acetic acid (30 mL) and the mixture was stirred at room temperature for 48h. The solvent was evaporated to dryness and the residue was suspended in water and lyophilized. Recrystallization from ethyl acetate afforded pure **10** as a brown solid (6.33 g, 28.01 mmol, 75% yield). **M.p.** 168 ºC. **IR (KBr) ν** 3300–2100, 1681, 1419, 1311 $cm^{-1}$. **$^1$H NMR ($CDCl_3$, 400 MHz) δ** 7.48–7.58 (m, 3H); 7.62–7.68 (m, 1H); 7.94–8.00 (m, 2H); 8.15–8.26 (m, 2H); 8.67 (m, 1H). **HRMS (ESI)** C13H9N2O2 [M–H]–: calcd. 225.0670, found 225.0666.

***m*-(Phenylazo)benzyl alcohol (11)**

A solution of **10** (2.96 g, 13.11 mmol) in anhydrous THF (60 mL) was added in small portions to a suspension of LiAlH4 (598mg, 15.73 mmol) in anhydrous THF (40 mL) kept at 0 ºC under an argon atmosphere. The reaction mixture was allowed to warm to room temperature and then heated at 40 ºC for 72 h. The system was cooled to 0 ºC and water (0.6 mL) was added slowly, followed by 10% aqueous NaOH (1.2 mL) and additional water (2 mL). The salts were eliminated by filtration through Celite and the resulting solution was dried over $MgSO_4$. The crude product obtained by evaporation of the solvent was chromatographed (eluent: hexanes/ethyl acetate 8/2) to give pure **11** as an orange solid (1.75 g, 8.25 mmol, 63% yield). **M.p.** 45 ºC. **IR (KBr) ν** 3356, 1446, 1087 $cm^{-1}$. **$^1$H NMR (CDCl3, 400 MHz) δ** 1.77–1.93 (m, 1H); 4.70–4.75 (m, 2H); 7.37–7.49 (m, 5H); 7.76–7.88 (m, 4H). **HRMS (ESI)** $C_{13}H_{12}N_2NaO$ [M+Na]+: calcd. 235.0842, found 235.0840.

***m*-(Phenylazo)benzyl bromide (12)**

To a solution of **11** (1.74 g, 8.20 mmol) in anhydrous THF (60 mL) kept at 0 ºC, triphenylphosphine (3.22 g, 12.30 mmol) and *N*-bromosuccinimide (2.19 g, 12.30 mmol) were added in small alternate portions and the reaction system was stirred at 45 ºC overnight. The insoluble material was eliminated by filtration through a small pad of silica gel and washed thoroughly with THF. The filtrates were evaporated and the residue obtained was purified by column cromatography (eluent: hexanes/ethyl acetate 9/1) to afford pure **12** as an orange solid (2.02 g, 7.33 mmol, 89% yield). **M.p.** 39 ºC. **IR (KBr) ν** 1630, 1460, 1441, 690 $cm^{-1}$. **$^1$H NMR (CDCl3, 400 MHz) δ** 4.59 (s, 2H); 7.47–7.56 (m, 5H); 7.85–7.96 (m, 4H). **HRMS (ESI)** $C_{13}H_{12}BrN_2$ [M+H]+: calcd. 275.0178, found 275.0178.

**Ethyl bis[*m*-(phenylazo)benzyl]isocyanoacetate (13)**

A solution of ethyl isocyanoacetate (300 mg, 2.65 mmol) in acetonitrile (50 ml) was treated with finely powdered $K_2CO_3$ (2.19 g, 15.90 mmol), tetrabutylammonium bisulfate (270 mg, 0.80 mmol), and **12** (1.53 g, 5.57 mmol). The resulting heterogeneous mixture was heated at 50 ºC with vigorous stirring for 48 h. The solvent was evaporated to dryness and the residue was partitioned between dichloromethane (60 mL) and water (40 mL). The aqueous layer was discarded and the organic phase was dried and filtered. Removal of the solvent followed by column chromatography (eluent: hexanes/ethyl acetate 8/2) afforded pure **13** as an orange solid (1.16 g, 2.31 mmol, 87% yield). **M.p.** 80 ºC. **IR (KBr) ν** 2134, 1752, 1445, 1195, 1089 $cm^{-1}$. **$^1$H NMR (CDCl3, 400 MHz) δ** 1.10 (t, 3H, *J* = 7.1 Hz ); 3.23 (d, 2H, *J* = 13.6 Hz); 3.53 (d, 2H, *J* = 13.6 Hz); 4.11 (q, 2H, *J* = 7.1 Hz); 7.42–7.55 (m, 10H); 7.81–7.92 (m, 8H). **HRMS (ESI)** $C_{31}H_{28}N_5O_2$ [M+H]+: calcd. 502.2238, found 502.2237.

**Ethyl bis[*m*-(phenylazo)benzyl]glycinate (H-*m*azoDbg-OEt, 2)**

Concentrated HCl (4 mL) was added dropwise to a suspension of **13** (1.12 g, 2.24 mmol) in ethanol (40 mL) kept at 0 ºC and the reaction mixture was stirred at room temperature for 2 h. The solvent was evaporated and the residue was taken up in water and lyophilized to afford **2** as a solid (1.18 g, 2.24 mmol, 100% yield). **M.p**. 100 ºC. **IR (KBr) ν** 3451, 1744, 1447, 1094 $cm^{-1}$. **$^1$H NMR (DMSO-*d*6, 400 MHz) δ** 1.30 (t, 3H, *J* = 7.1 Hz); 3.43 (d, 2H, *J* = 14.0 Hz); 3.52 (d, 2H, *J* = 14.0 Hz); 4.26 (q, 2H, *J*= 7.1 Hz); 7.50–7.64 (m, 10H); 7.82–7.90 (m, 8H); 8.80 (brs, 3H). **HRMS (ESI)** $C_{30}H_{30}N_5O_2$ [M+H]+: calcd. 492.2394, found 492.2398.

**SYNTHESIS OF Trt-S-(CH2)2-CO-*p*azoDbg-OH** (**3**)

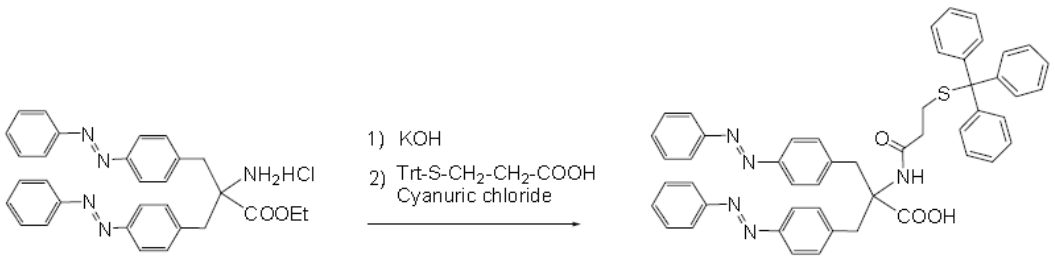


**1** **3**

A 2N solution of KOH in ethanol (2 mL) and water (1 mL) were added to a suspension of **1** (639mg, 1.21 mmol) in ethanol (30 mL) and the reaction mixture was stirred at 40 ºC for 48 h. The solvent was evaporated and the residue was suspended in water (30 mL), neutralized with 2N HCl and extracted with dichloromethane (3 × 20 mL). The combined organic layers were dried over MgSO4 and filtered. The yellow solid (400 mg, 0.86 mmol) isolated by evaporation of the solvent was dissolved in dry DMF (5 mL). *N*,*N*-Diisopropylethylamine (300 µl, 1.72 mmol) was added and the solution obtained was kept for the next step. Separately, S-(Trityl)-3-mercaptopropionic acid (440 mg, 1.30 mmol) and cyanuric chloride (380 mg, 2.01 mmol) were dissolved in dry dichloromethane (15 ml) at 0 oC. Pyridine (101 µl, 1.3 mmol) was added dropwise to this solution at room temperature and the resulting suspension was vigorously stirred for 30 min. Then, the DMF solution previously prepared from **1** was slowly added to this suspension and the mixture was stirred at room temperature for 48 h. After removal of the solvent, the residue was dissolved in ethyl acetate and washed successively with 10% $KHSO_4$, water, 5% $NaHCO_3$, 0.5N HCl and water, dried over Na2SO4, and evaporated to dryness. Purification by column chromatography (eluent: chloroform/ethanol 95/5) afforded pure **3** (430 mg, 0.54 mmol, 63% yield). **M.p.** 220 °C. **IR (KBr): ν** 3341, 1674, 1665, 1521, 1442 $cm^{-}1$. **$^{1}$H NMR (CDCl3, 300 MHz) δ** 1.85 (t, 2H, *J* = 8.6 Hz); 2.59 (t, 2H, *J* = 8.6 Hz); 3.33 (d, 2H, *J* = 15.9 Hz); 4.10 (d, 2H, *J* = 15.9 Hz); 5.95 (s, 1H); 7.17–7.29 (m, 10H); 7.40–7.47 (m, 15H); 7.72–7.88 (m, 8H). **HRMS (ESI)** $C_{50}H_{44}N_5O_3S$ [M+H]+: calcd. 794.3086, found 794.3078.

**SYNTHESIS OF Trt-S-(CH2)2-CO-*m*azoDbg-OH (4)**

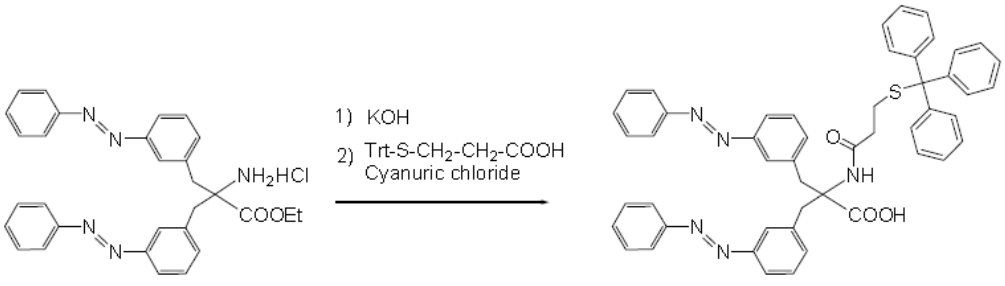


**2** **4**

**Trt-S-(CH2)2-CO-*m*azoDbg-OH (4)**

A 2N solution of KOH in ethanol (1 mL) and water (1mL) were added to a solution of **2** (294 mg, 0.56 mmol) in ethanol (20 mL) and the reaction mixture was stirred at 40 ºC

for 48 h. The solvent was evaporated and the residue was suspended in water (30 mL), neutralized with 2N HCl and extracted with dichloromethane (3 × 15 mL). The combined organic layers were dried over $MgSO_4$ and filtered. The yellow solid (260 mg, 0.39 mmol) isolated by evaporation of the solvent was dissolved in dry DMF (5 mL). *N*,*N*-Diisopropylethylamine (140 μl, 0.8 mmol) was added and the solution obtained was kept for the next step. Separately, S-(Trityl)-3-mercaptopropionic acid (200 mg, 5.78 mmol) and cyanuric chloride (171 mg, 0.92 mmol) were dissolved in dry dichloromethane (10 ml) at 0 oC. Pyridine (44 μl, 5.78 mmol) was added dropwise to this solution at room temperature and the resulting suspension was vigorously stirred for 30 min. Then, the DMF solution previously prepared from **2** was slowly added to this suspension and the mixture was stirred at room temperature for 4 days. After removal of the solvent, the residue was dissolved in ethyl acetate and washed successively with 10% $KHSO_4$, water, 5% $NaHCO_3$, 0.5N HCl and water, dried over Na2SO4, and evaporated to dryness. Purification by column chromatography (eluent: chloroform/ethanol 95/5) afforded pure **4** (177 mg, 0.22 mmol, 57% yield). **M.p.** 180 °C. **IR (KBr): ν** 3335, 1672, 1661, 1526, 1444 $cm^{-1}$. **$^1$H NMR ($CDCl_3$, 600 MHz) δ** 1.79 (t, 2H, *J* = 9.0 Hz); 2.15 (t, 2H, *J* = 9.0 Hz); 3.33 (d, 2H, *J* = 12.0 Hz); 3.58 (d, 2H, *J* = 12.0 Hz); 6.99 (s, 1H); 7.16–7.33 (m, 19H); 7.52–7.65 (m, 10H); 7.80–7.83 (m, 4H). **HRMS (ESI)** $C_{50}H_{44}N_5O_3S$ [M+H]+: calcd. 794.3086, found 794.3076.

**SYNTHESIS OF H-*pazo*Dbg-L-Leu-OMe (5)**

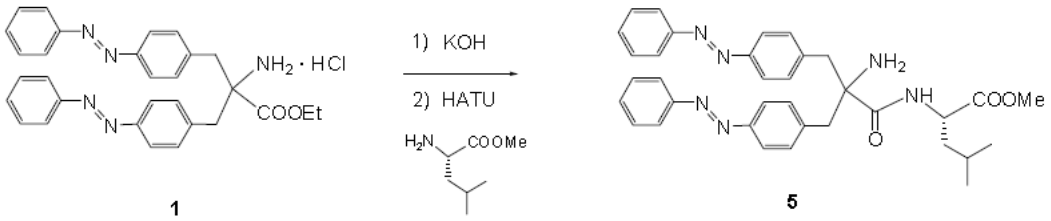


1 5

A 2N solution of KOH in ethanol (2 mL) and water (1 mL) were added to a suspension of **1** (483 mg, 0.92 mmol) in ethanol (30 mL) and the reaction mixture was stirred at 40 ºC for 48 h. The solvent was evaporated and the residue was suspended in water (30 mL), neutralized with 2N HCl and extracted with dichloromethane (3 × 20 mL). The combined organic layers were dried over MgSO4 and filtered. After evaporation of the solvent, the solid obtained (300 mg, 0.65 mmol) was dissolved in dry DMF (5 mL) at 0 oC and HATU (230 mg, 0.61 mmol), HOAt (82 mg, 0.61 mmol) and *N*,*N*-

diisopropylethylamine (250 µl, 1.30 mmol) were added. Then, a solution of H-L-Leu-OMe hydrochloride (550 mg, 3.25 mmol) and *N*,*N*-diisopropylethylamine (610 µl, 3.3 mmol) in dry DMF (10 mL) was slowly added and the mixture was stirred at room temperature for 24 h. After removal of the solvent, the oily residue was dissolved in ethyl acetate and washed successively with 10% KHSO4, water, 5% $NaHCO_3$, 0.5N HCl and water, dried over $Na_2SO_4$, and evaporated to dryness. Purification by column chromatography (eluent: chloroform/methanol 95/5) afforded pure **5** (351 mg, 0.59 mmol, 91% yield). **M.p.** 138 °C. **IR (KBr) ν** 3387, 1729, 1672, 1663, 1522, 1441 $cm^{-1}$. **$^1$H NMR ($CDCl_3$, 300 MHz) δ** 0.76 (d, 3H, *J* = 7.8 Hz); 0.83 (d, 3H, *J* = 7.5 Hz); 1.20–1.46 (m, 3H); 2.79 (d, 1H, *J* = 15.9 Hz); 2.92 (d, 1H, *J* = 15.9 Hz); 3.53 (d, 1H, *J* = 15.9 Hz); 3.60 (d, 1H, *J* = 15.9
Hz) overlapped with 3.61 (s, 3H); 4.44–4.50 (m, 1H); 7.33–7.54 (m, 11H); 7.81–7.92 (m, 8H). **HRMS (ESI)** $C_{35}H_{39}N_6O_3$ [M+H]+: calcd. 591.3005, found 591.2997.

**SYNTHESIS AND PURIFICATION OF AuNp-3, PtNp-3, AgNp-3**

**AuNp-3**

Trt-S-(CH2)2-CO-*p*azoDbg-OH (**3**) (150 mg, 0.19 mmol) was treated with a 1/1 TFA/dichloromethane solution containing 1% triisopropylsilane for 10 min to eliminate the trityl protecting group. The solvent was evaporated and the residue was dissolved in a 1/1/1 chloroform/methanol/water mixture (10 mL). $HAuCl_4 \cdot 3H_2O$ (24 mg, 0.063 mmol) was added and the resulting solution was allowed to stand for 1 h under stirring. Then, 10 equivalents of $NaBH_4$ (1.65 mL of a 600 mM solution in water) were added and the solution was stirred at room temperature for additional 6 h. The product was precipitated by adding an excess of acetonitrile, pelleted for 8 min at top speed in a centrifuge, resuspended in a 7/3 diethyl ether/ethanol mixture, pelleted again, and dried overnight at room temperature. **IR (KBr) ν** 3336, 1665, 1445 $cm^{-1}$.

**PtNp-3**

Trt-S-(CH2)2-CO-*p*azoDbg-OH (**3**) (150 mg, 0.19 mmol) was treated with a 1/1 TFA/dichloromethane solution containing 1% triisopropylsilane for 10 min to eliminate the trityl protecting group. The solvent was evaporated and the residue was dissolved in a 1/1/1 chloroform/methanol/water mixture (10 mL). $H_2PtCl_6 \cdot 6H_2O$ (36 mg, 0.063 mmol) was added and the resulting solution was allowed to stand for 1 h under stirring.

Then, 10 equivalents of $NaBH_4$ (2.2 mL of a 300 mM solution in water) were added and the suspension was stirred at room temperature for additional 6 h. The product was precipitated by adding an excess of acetonitrile, pelleted for 8 min at top speed in a centrifuge, resuspended in a 7/3 diethyl ether/ethanol mixture, pelleted again, and dried overnight at room temperature. **IR (KBr) ν** 3339, 1668, 1441 $cm^{-1}$.

**AgNp-3**

Trt-S-(CH2)2-CO-*p*azoDbg-OH (**3**) (150 mg, 0.19 mmol) was treated with a 1/1 TFA/dichloromethane solution containing 1% triisopropylsilane for 10 min to eliminate the trityl protecting group. The solvent was evaporated and the residue was dissolved in a 1/1/1 chloroform/methanol/water mixture (10 mL). $AgNO_3$ (12 mg, 0.063 mmol) was added and the resulting solution was allowed to stand for 1 h under stirring. Then, 10 equivalents of $NaBH_4$ (2.2 mL of a 300 mM solution in water) were added and the suspension was stirred at room temperature for additional 6 h. The product was precipitated by adding an excess of acetonitrile, pelleted for 8 min at top speed in a centrifuge, resuspended in a 7/3 diethyl ether/ethanol mixture, pelleted again, and dried overnight at room temperature. **IR (KBr) ν** 3329, 1664, 1449 $cm^{-1}$.

X-RAY DIFFRACTION ANALYSIS OF H-*p*azoDbg-OEt (1)

Orange crystals in the shape of thin rods were grown by slow evaporation from a mixture of dichloromethane and methanol. X-ray diffraction data were collected with an Oxford Diffraction Gemini E four-circle kappa diffractometer equipped with a 92 mm EOS CCD detector, using graphite monochromated Cu Kα radiation (λ = 1.54178 Å). The sample to detector distance was 50 mm. A total of 1344 frames were collected by 1.0° omega oscillation with exposure times of 1.5, 4, or 70 s, depending on the theta values, in the 4.11°–68.46° theta range. Data collection and reduction were performed with the CrysAlisPro software (version 1.171.33.52; Oxford Diffraction). A semi-empirical absorption correction based on the multi-scan technique using spherical harmonics, implemented in SCALE3 ABSPACK scaling algorithm, was applied. The structure was solved by ab initio procedures of the SIR 2002 program,[11] and refined by full matrix least squares on F2, using all data, by application of the SHELXL 97 program,[12]with all non-H atoms anisotropic. All phenyl rings were constrained to the idealized geometry. The positions of the H-atoms of the N-terminal free amino group were estimated by performing a rotational search of the electron density in the expected

cone on the N atom and were not refined. All of the remaining H-atoms were calculated at idealized positions and refined using a riding model. Relevant crystallographic data and diffraction parameters are reported in Table 2. CCDC 832775 contains the supplementary crystallographic data for this paper. These data can be obtained from The Cambridge Crystallographic Data Centre via www.ccdc.cam.ac.uk/data_request/cif

| | | |
|---|---|---|
| Identification code | mc162f | |
| Empirical formula | $C_{30}\ H_{29}\ N_5\ O_2$ | |
| Formula weight | 491.58 | |
| Temperature | 293(2) K | |
| Wavelength | 1.54178 Å | |
| Crystal system | Monoclinic | |
| Space group | C2/c | |
| Unit cell dimensions | a = 45.954(6) Å | α= 90°. |
| | b = 5.8410(3) Å | β= 111.695(12)°. |
| | c = 21.615(2) Å | γ = 90°. |
| Volume | 5390.9(9) $Å^3$ | |
| Z | 8 | |
| Density (calculated) | 1.211 $Mg/m^3$ | |
| Absorption coefficient | 0.622 $mm^{-1}$ | |
| F(000) | 2080 | |
| Crystal size | 0.40 x 0.07 x 0.07 $mm^3$ | |
| Theta range for data collection | 4.11 to 68.46°. | |
| Index ranges | $-52 \le h \le 50, -4 \le k \le 6, -25 \le l \le 25$ | |
| Reflections collected | 11412 | |
| Independent reflections | 4671 [R(int) = 0.0371] | |
| Completeness to theta = 68.46° | 94.7 % | |
| Absorption correction | Semi-empirical from equivalents | |
| Max. and min. transmission | 0.9578 and 0.7891 | |
| Refinement method | Full-matrix least-squares on $F^2$ | |
| Data / restraints / parameters | 4671 / 0 / 286 | |
| Goodness-of-fit on $F^2$ | 0.939 | |
| Final R indices [I>2sigma(I)] | $R_1$ = 0.0662, $wR_2$ = 0.1914 | |
| R indices (all data) | $R_1$ = 0.1061, $wR_2$ = 0.2204 | |
| Largest diff. peak and hole | 0.515 and -0.201 $e.Å^{-3}$ | |

***Tab. 2*** Crystal data and structure refinement for H-*p*azoDbg-OEt (**1**).

REFERENCES


1) a) *Molecular Switches* (Ed: B. Feringa), Wiley-VCH, Weinheim, Germany, **2003**; b) Key E.R., Leigh D.A., Zerbetto F., *Angew. Chem. Int. Ed.* **2007**, *46*, 72-191; c) Andréasson J., Pischel U., *Chem. Soc. Rev.* **2010**, *39*, 174-188; d) de Silva A.P., Vance T.P., West M.E.S., Wright G.D., *Org. Biomol. Chem.* **2008**, *6*, 2468-2481; e) Balzani V., Credi A., Venturi M., *Chem. Soc. Rev.* **2009**, *38*, 1542-1550; f) de Silva A.P., Gunaratne H.Q.N., Gunnlaugsson T., Huxley A.J.M., McCoy C.P., Rademacher J.T., Rice T.E., *Chem. Soc. Rev.* **1997**, *97*, 1515-1566; g) Balzani V., Credi A., Raymo F., Stoddart J.F., *Angew. Chem. Int. Ed.* **2000**, *39*, 3348-3391.

2) a) Liu Z.E., Hashimoto K., Fujishima A., *Nature* **1990**, *347*, 658-660; b) Zahan S., Canary J.W., *Angew. Chem. Int. Ed.* **1998**, *37*, 305-307; c) Huck N.P.M., Jager W.F., de Lange B., Feringa B., *Science* **1996**, *273*, 1686-1688; d) Nolan E.M., Lippard S.J., *Acc. Chem. Res.* **2009**, *42*, 193-203; e) Takashima Y., Martínez V., Furukawa S., Kondo M., Shimomura S., Uehara H., Nakahama M., Sugimoto K., Kitagawa S., *Nat. Commun.* **2011**, 2:168, DOI:10.1038/ncomms1170; f) Yu H.F., Ikeda T., *Adv. Mater.* **2011**, *23*, 2149-2180; g) Cheetham A.K., Rao C.N.R., Feller R.K., *Chem. Commun.* **2006**, 4780-4795; h) Cheetham R.M., Bramble J.P., McMillan D.G.G., Krzeminski L., Han X., Johnson B.R.G., Bushby R.J., Olmsted P.D., Jeuken L.J.C., Marritt S.J., Butt J.N., Evans S.D., *J. Am. Chem. Soc.* **2011**, *133*, 6521-6524.

3) a) Suda M., Kameyama N., Suzuki M., Kawamura N., Einaga Y., *Angew. Chem. Int. Ed.* **2008**, *47*, 160-163; b) Klajn R., Stoddart J.F., Grzybowsky B.A., *Chem. Soc. Rev.* **2010**, *39*, 2203-2237; c) Ikegami A., Suda M., Watanabe T., Einaga Y., *Angew. Chem. Int. Ed.* **2010**, *49*, 372-374.

4) Klajn R., *Pure Appl. Chem.* **2010**, *82*, 2247-2279.

5) a) Schrader T.E., Cordes T., Schreier W.J., Koller F.O., Dong S.-L., Moroder L., Zinth W., *J. Phys. Chem. B* **2011**, *115*, 5219-5226; (b) Beharry A.A., Wong L., Tropepe V., Woolley G.A., *Angew. Chem. Int. Ed.* **2011**, *50*, 1325-1327; (c) Backus E.H.G., Bloem R., Donaldson P.M., Ihalainen J.A., Pfister R., Paoli B., Caflish A., Hamm P., *J. Phys. Chem. B* **2010**, *114*, 3735-3740; (d) Yu Z., Hecht S., *Angew.Chem. Int. Ed.* **2011**, *50*, 1640-1643; (e) Böckmann M., Doltsinis N.L., Marx D., *Angew. Chem. Int. Ed.* **2010**, *49*, 3382-3384; (f) Bonardi F., London G., Nouwen N., Feringa B.L., Driessen A.J.M., *Angew. Chem. Int. Ed.* **2010**, *49*, 7234-7238; (g) Martin S., Haiss W., Higgins S.J., Nichols R.J., *Nanolett.* **2010**, *10*, 2019-2023; (h) Osono N., Kajitani T., Fukushima T., Ito K., Sasaki S., Takata M., Aida T., *Science* **2010**, *330*, 808-811; (i) Venkataramani S., Jana U., Dommaschk M., Sönnichsen F.D., Tuczek F., Herges R., *Science* **2011**, *331*, 445-448; (j) Hashim P.K., Thomas R., Tamaoki N., *Chem. Eur. J.* **2011**, *17*, 7304-7312.

6) (a) Crisma M., Valle G., Bonora G.M., Toniolo C., Lelj F., Barone V., Fraternali F., Hardy P.M., Maia H.L.S., *Biopolymers* **1991**, *31*, 637-641; (b) Benedetti E., Di Blasio B., Pavone V., Pedone C., Toniolo C., Crisma M., *Biopolymers* **1992**, *32*, 453-456; (c) Crisma M., Formaggio F., Moretto A., Toniolo C., *Biopolymers (Pept. Sci)* **2006**, *84*, 3-12.

7) It is worth noting that the -$C^{\beta}H_2$- protons in the all-*c* and all-*t* isomers are an example of chemically non-equivalent protons occurring in a *non-chiral* molecule. For reference see e.g. M. H. Levitt, *Spin Dynamics. Basics of Nuclear Magnetic Resonance*, Wiley, Chichester, 1st edit., **2001**, p. 229.

8) Rio-Echevarria I.M., Tavano R., Causin V., Papini E., Mancin F., Moretto A., *J. Am. Chem. Soc.* **2011**, *133*, 8-11.
9) Ishii H., Sugiyama K., Ito E., Seki K., *Adv. Mater*. **1999**, *11*, 605-625.
10) a) Evans D.F., *J. Chem. Soc.* **1959**, 2003-2005; b) Löliger J., Scheffold R., *J. Chem. Educ.* **1972**, *49*, 646-647.
11) Burla M.C., Camalli M., Carrozzini B., Cascarano G.L., Giacovazzo C., Polidori G., Spagna R., *J. Appl. Crystallogr.*, **2003**, *36*, 1103.
12) Sheldrick G.M., *Acta Crystallogr. A* **2008**, *64*, 112-122.

# V

## Synthesis of peptides containing 4-amino-1,2-dithiolane-4-carboxylic acid (Adt) residues

### INTRODUCTION

Self-assembly has become one of the most useful strategy in the bottom-up fabrication technologies due to the easiness by which highly ordered thin films of organic material over layers and surfaces can be built. This kind of supra-molecular aggregation is exploited for biological and spectroscopic investigations, nano-engineering, sensing, bio-materials and electro-chemical applications.[1] In particular, peptide self-assembled monolayers are of current interest to study physicochemical properties of modified metal (*e.g.* Au) surfaces.[1e,2] The possibility to produce peptide SAMs over gold surface opens the road to the development of new nano-electronic devices for (i) monitoring the interaction between peptide or proteins layer and substrates, (ii) electron transfer occurring through a peptide chains and (iii) photocurrent generation.[1d,3]Thiol-gold linkage is by far the most extensively employed self-assembly method to get an ordered monolayers of organic molecules over gold surfaces.[4]The functionalization of C- or N-terminus of peptides with thiol linkers has been utilized, as well by side-chains (as cysteine or methionine). Among the several linkers toward gold, dithiolane (disulfur bridge) have been exploited for its ability to give a bidentate ligation.[5] Lipoic acid is an example of this kind of linkage. The presence of a carboxyl moiety allows also for the functionalization of molecules, as peptide chains, for binding over gold by means of the S-S dithiolane bridge.

At the beginning of the ‘70s a family of new dithiolane containing cyclic structures was firstly synthesized. The *4-amino-1,2-dithiolane-4-carboxylic acid* (herein called Adt, see **Figure 1**) was firstly synthesized as building block for organic synthesis.[6] In the last years Adt has also been discovered in natural compounds (Kottamides A-E; the structure of E is reported in **Figure 2**) produced by the New Zealand ascidian *Pycnoclavella kottae*.[7] More recently, Prof. Lucente group prepared Adt-containing derivatives and other constructs, as for example a complex with iron that found application in catalytic hydrogenation.[8]

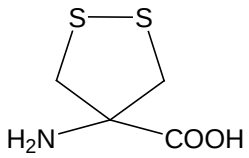


***Fig.1*** 4-amino-1,2-dithiolane-4-carboxylic acid (Adt) residue. Information on the synthesis in the experimental section.

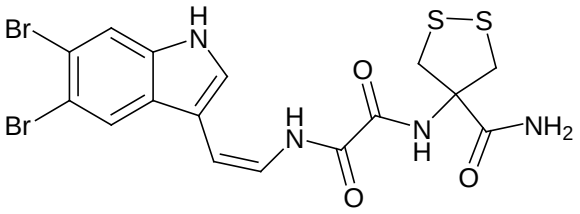


***Fig.2*** Kottamide E: a natural product containing Adt, found in the New Zealand ascidian *Pycnoclavellakottae*.

Belonging to the class of $C^{\alpha}$-tetrasubstituted amino acids whose prototype is the α-amino *iso*butiric acid (Aib), Adt shows a tendency to stabilize helical structures even in medium length or short peptides. The Thorpe-Ingold effect promotes β-turn conformations, experimentally found in some tri-peptides. From the conformational point of view, Adt showed the same behavior of its analogue $Ac_5c$.[8b,8d,8e,9] Moreover, beside such conformational property, the presence of a dithiolane S-S on the $C^{\alpha}$ side chain ring makes this moiety an extremely interesting candidate for functionalization of gold surfaces. Nevertheless, the short separation of the S-S linker from the peptide backbone allows to design much closer SAM layers to the metal surface as compared to the use of lipoic acid as linker. On the other hands, the bidentate ligation should permit an higher SAM rigidity in comparison with flexible linkers such as Cysteine (**Figure 3**).

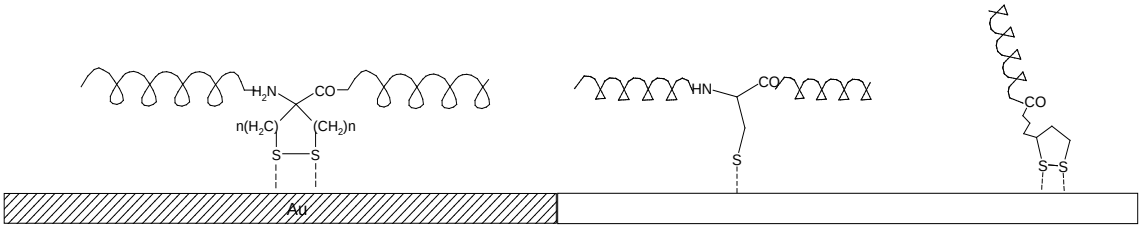


***Figure 3.*** Comparison between differen linkage models. Adt linkage (on the left) should be more rigid than cysteine one (in the middle) and permit a closer placing of peptides than lipoic acid linkage (on the right).

In any case, the possibility to introduce a linker such as Adt on the selected rigid peptide, could provide a differently packed SAM. In fact, the electron transfer (ET) phenomena involving the peptide helices has been already studied and the geometry of the SAM is not uninfluent over the ET mechanism.[10] Usually, the applications of peptide scaffold ET studies involve peptides structure able to link peptide helices in a one-site binding fashion. A parallel disposition of the peptide to a surface is therefore quite uncommon and might open new possibilities for the study of ET phenomena

mediated by peptides.[11] Thus, we designed and synthetized a series of constrained Adt-containing helical peptides based on Ala or alternating Ala-Aibhost functionalizedwith one or more Adt moieties. All of these family members were functionalized with a specific probe that finds application in electro-chemistry techniques. As probes we selected Pyrene acetic acid (PyrAc) and the Ferrocene carboxylic acid (Fc), on virtue of their well-known optical and redox properties.[1e,12] The choice of both peptide length and position of the Adt moiety was guided by our knowledge about conformationsof $C^{\alpha}$-tetrasubstituted containing peptides. In particular, sequences alternating $C^{\alpha}$-tetrasubstituted and $C^{\alpha}$-trisubstituted amino acids are known to promote $3_{10}$-helical structures till the number of residues in lower that 7, otherwise longer sequences promote α-helix structure.[13] So, as we wanted to ensure a distance of two turns between the Adt residues we hypothesized a sequence containing 10 residues, with Adt located at positions 1 and 8. Otherwise, we also designed an esapeptidethat would adopt a $3_{10}$-helical structure as shown by ESR measurements on TOAC (an analogue of Aib with a nitroxide moiety) containing peptides.[14]

Finally we selected:

1) **Y**-**Adt**-Ala-Aib-Gly-Aib-Ala-Aib-**Adt**-Ala-Aib-OMe (α-helix),
2) **Y**-**Adt**-Ala-Aib-**Adt**-Ala-Aib-OMe ($3_{10}$ helix)
3) **Y**-**Adt**-Ala-Ala-**Adt**-Ala-Ala-OMe (an analogue of the former).

**Y** corresponding to**PyrAc** or **Fc** respectively

We decided to synthetize, for comparison, a peptide containing only one Adt in the sequence, by replacing the position 1 with an Aib residue (see **Figure 4** in Results and Discussion).

Noteworthy, the opportunity to obtain more rigid scaffolds and more ordered SAM is a challenge in the research field of ET processes.[1e] Ferrocenederivated mono-layers show many intriguing properties: Fc undergoes to fast reversible electron transfer, is easily functionalized and is stable in non-oxidizing environments and evidences showed that the charge of the complex and oxidation state of the Iron atom do not affect the peptide conformation. Moreover, its insertion into peptide systems does not modify substantially the structure, because it is lipophilic and small sized. For these reasons, Ferrocene is widely exploited as a redox tag for the characterization of nucleic acids, proteins, and peptides.[12d] Nevertheless, it is still not well-know how peptide back-bone

can contribute in the ET process, and different main mechanisms are supposed.[1c,3b,10a,10c,15] Within 2nm, the process would take place through an electron tunneling mechanism (superexchange) through the peptides bon. Otherwise, above 2nm, two mechanisms are supposed: *i*) the hydrogen bonds act as a short-cut for the tunneling process, or *ii*) an hopping mechanism take place involving each single amide bond. Otherwise, for the most current theories, both these mechanisms could contribute to the overall ET process. Therefore, a short distance of redox tag (under 2nm) that is ensured by a parallel linkage of peptide scaffold to gold can improve the knowledge on these ET processes.[11a,15a,15b,15f]

Beside Ferrocene, also Pyrene has been taken into account, due to its propensity to promote photo-current generation phonomena.[8e,11b,15f] In the presence of an electron donor in solution (for example, triethanolamine) the irradiation of the Pyrene label (and even seen for Ferrocene) induces the generation of a catodic current detectable with the gold electrodes. This could be viewed as example of self-assembly device able to convert light to photo-generated current.

## RESULTS AND DISCUSSION

### Synthesis

This part of the project describes the synthesis of Adt containing peptides. **Figure 4** reports the chemical structure of the final products.

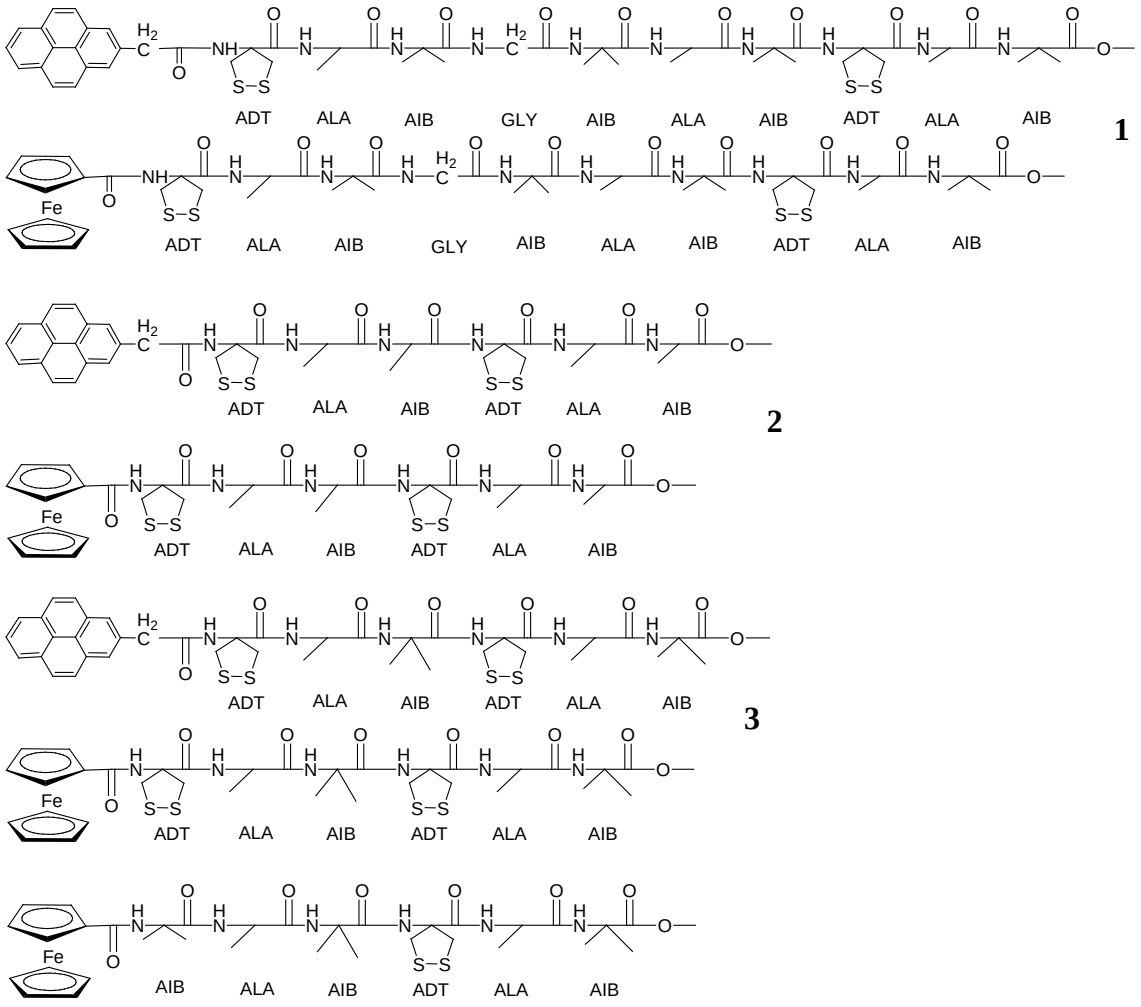


***Fig. 4*** Peptide chemical structures for: 10mers (**1**), esamers -Ala-Aib- (**2**), esamers -Ala-Ala- (**3**) and an esamer containing only one Adt residue.

The syntheses of the peptides have been accomplished in the Laboratories the prof. François Couty at the Versailles Saint-Quentin-en-Yvelines (France), in collaboration Dr. Karen Wright (CNRS, University of Versailles Saint-Quentin-en-Yvelines). Adt has been also synthesized as it is not commercially available (see **Figure 5** for synthetic pathway).[8e]

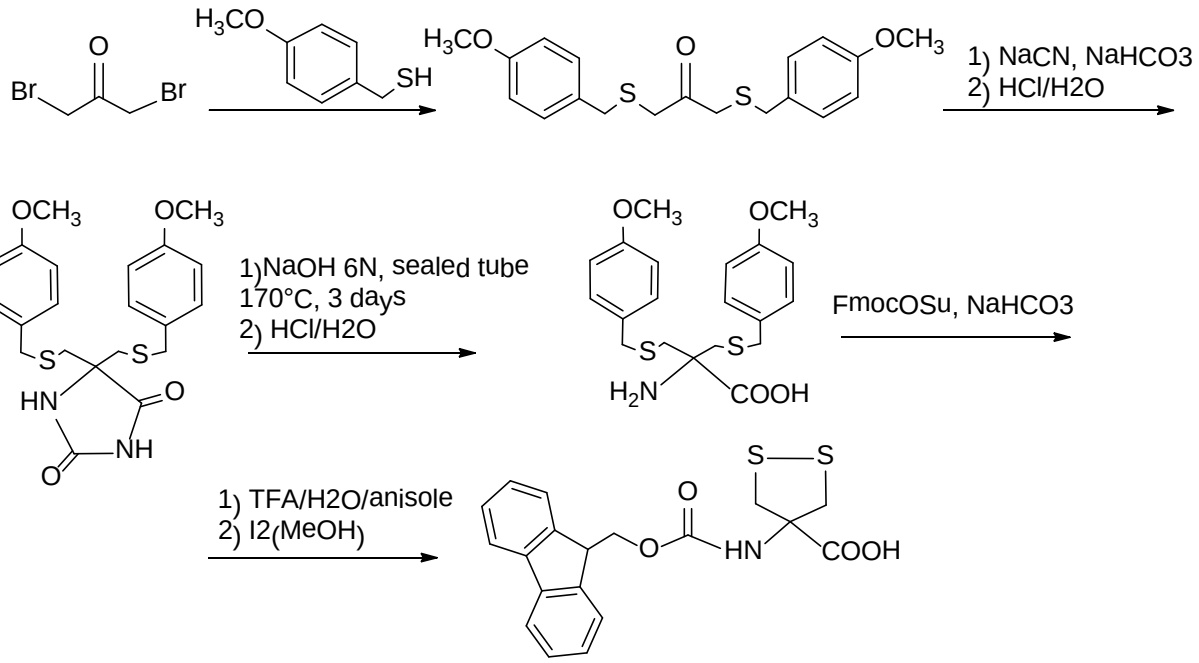


***Fig. 5*** Synthetic protocol for Fmoc-Adt-OH .

The syntheses of the peptides were performed *via* a step-by-step approach with classical methodologies in solution. As aforementioned in the introduction, for the (**1**) 10-mers we considered to insert Adt at positions 1 and 8 (two helical turns apart in an α-helix) wanting the dithiolated side-chains to stay on the same side of the helical structure. In fact, 3,6 residue *per* turn are needed for an α-helix. The choice of a distance of two turns was dictated by the willingness to exploit the length of the 10mers to ensure a higher rigidity in respect with the surface. Therefore, to get the two dithiolated side chains on the same side of the tri-dimensional structure six residues are need to be located between two Adt residues. Regarding (**2**) and (**3**) (6mers) the Adt should be located at positions 1 and 4, exactly at the distance of one turn of a $3_{10}$ helical structure. In this case, the number of residue *per* turn is 3,2. Therefore in order to achieve a tri-dimensional structure pointing two Adt on the same side, two residues are need to be located between two Adt.

Regarding the synthetic pathway, a series of different methods of –COOH activation and different protection group for N-terminus have been employed. In particular, Fmoc-protection has been exploited for Adt residue whereas Boc chemistry has been widely used for the others (Aib, Ala and Gly). By consideration that the global yield over 10mers synthesis would not have been high (due to the low reactivity of coupling over

Adt and the high amount of tetra-substitute amino acids in the sequence), we decided to modify the synthetic protocol for the 10mer in a segment-condensation fashion. To ensure a free racemization process the positions 4 and 5 in the 10mers should not be occupied by an alanine. For this reason we projected to insert an achiral glycine, in order to avoid possible racemization occurring during the further segment condensation (both Aib and Gly are achiral indeed). Thus, the 4mer Boc-Ala-Aib-Gly-Aib-OH has been coupled to H-Ala-Aib-**Adt**-Ala-Aib-OMe in order to achieve the Boc-protected 9mer precursor. In order to increase the overall yield of the probe-labelled derivatives, PyrAcAdtOH and FcAdtOH were prepared aside and successively conjugated to 9mer precursor BocAlaAibGlyAibAlaAibAdtAlaAibOMe. This strategy was preferred in order to reduce the number of coupling steps. For the same reason, a single coupling on the intermediate H-Ala-Aib-**Adt**-Ala-Aib-OMe with each labelled Adt and Aib derivative yielded the (**2**) group of final products (-[AdtAlaAib]$_2$-OMe and -AibAlaAibAdtAlaAibOMe). Noteworthy, the very low reactivity of coupling over Adt residue imposed another strategy in respect to usual activation with common coupling reagents (HATU or OXYMA/EDC), especially for the reaction between $^4$Aib and $^3$Adt in which an activation *via* acyl fluoride was preferred. Each intermediate has been purified, isolated and characterized (FTIR, $^1$H NMR, $^{13}$C NMR and mass spectra). The synthetic scheme of the for Fc-10mer and Fc-(AdtAlaAla)$_2$OMe are reported in **Figure 6** as example.

***Fig. 6*** Synthetic procedure for Fc-10mer

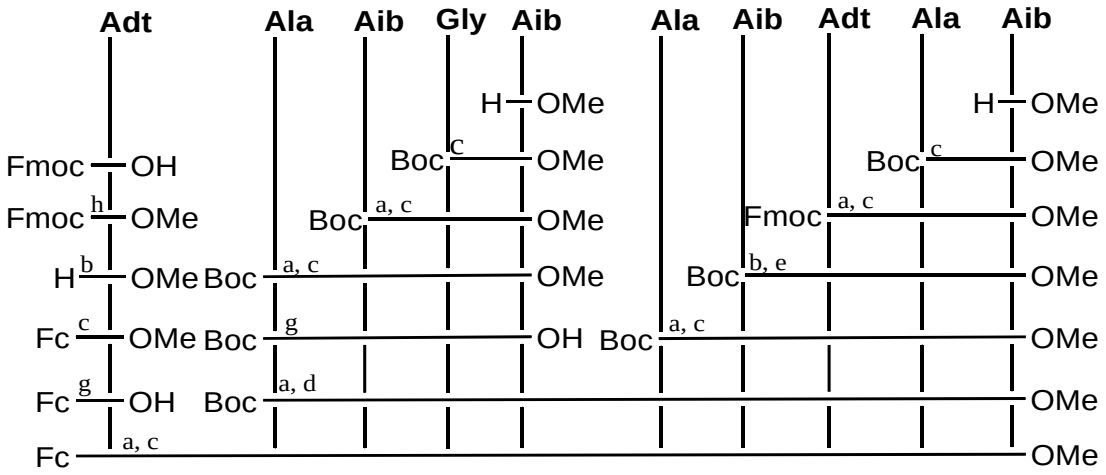


a) deprotection with TFA/DCM 1:1 b) deprotection with DEA/DCM 30%
c) coupling via OXYMA/EDC d) coupling via HATU
e) coupling via fluoride derivative (prepared with cyanuric fluoride, then 1 week)
f) coupling via oxazolone (prepared with EDC then 1 week in MeCN at reflux)
g) saponification wih NaOH(aq.)/MeOH h) esterification with $SOCl_2$ in MeOH

## Conformational characterization

FTIR

The FTIR spectra in $CDCl_3$ of each final product have been recoded. Spectra were collected on a Perkin-Elmer 580 B with a IR data station Perkin-Elmer 3600. Data are resumed in **Table 1**.

***Table 1*** FTIR signals of the final products. All spectra were recorded at $CDCl_3$, $10^{-3}$M concentration. Underlined values refer to strong peak.

| ***Compound*** | ***IR frequencies ($cm^{-1}$)*** |
|---|---|
| $Fc(AdtAlaAla)_2OMe$ | 3693, 3605, 3431, 3332, 2987, 2927, 1736, **1665**, 1535 |
| $Fc(AdtAlaAib)_2OMe$ | 3699, 3609, 3431, 3325, 2987, 2931, 1734, **1670**, 1524 |
| FcAibAlaAibAdtAlaAibOMe | 3691, 3607, 3431, 3327, 2989, 2934, 1734, **1668**, 1524 |
| FcAdtAlaAibGlyAibAlaAibAdtAlaAibOMe | 3691, 3605, 3319, 2987, 2927, 2855, 1724, **1654**, 1534 |
| $PyrAc(AdtAlaAla)_2OMe$ | 3690, 3613, 3424, 3331, 2989, 2929, 1734, **1668**, 1523 |
| $PyrAc(AdtAlaAib)_2OMe$ | 3691, 3612, 3423, 3333, 2989, 2929, 1734, **1670**, 1524 |
| PyrAcAdtAlaAibGlyAibAlaAibAdtAlaAibOMe | 3689, 3607, 3423, 3321, 2989, 2927, 1734, **1658**, 1534 |

The bands of N-H stretching lay between 3200-3500$cm^{-1}$ (amide A): the N-H groups which are involved in H-bonds below 3400$cm^{-1}$ and N-H groups not involved in H-bonds pattern and more exposed to solvent above 3400$cm^{-1}$. The carbonyl is also involved in vibrational modes that gives contributions between 1800 and 1500$cm^{-1}$ (~1700$cm^{-1}$ ester, ~1660$cm^{-1}$ amide I, ~1500$cm^{-1}$ amide II). For an helix conformation, the amide I signal lays between 1650-1665$cm^{-1}$. From Table 1, the wavenumbers for 6mers and 10mers are located in the range of 1650 and 1668 $cm^{-1}$. As reported in the literature, values below 1660 $cm^{-1}$are indicative of an $\alpha$-helix prevalent conformation, whereas above 1660 $cm^{-1}$is an indication of a prevalent $3_{10}$ helix.[16] The experimental amide I data for both the 10mers mode are located at 1650-1660$cm^{-1}$, whereas all the 6mers show a concordance between 1665 and 1670$cm^{-1}$. These parameters are in good agreement with those expected ($\alpha$ helix and $3_{10}$ respectively). More investigations are required anyway for assessing the actual conformation in solution, especially by NMR. Comparing the FTIR spectra in the amide A region, acquired at $10^{-3}$ M and $10^{-4}$ M concentrations in $CDCl_3$ solution, we can conclude that the H-bonded N-Hs are all intramolecularly bound as no dilution effect is observed (as it would be in the case of aggregation).

2D NMR

*Brief description of the utilized techniques*

The high potential of the 2D NMR is due to the spread of signals from a mono-dimensional to a bi-dimensional spectrum, that reduces the overlaps between peaks. The experiments employed during this Thesis were COSY,[17] TOCSY,[18] NOESY,[19] and ROESY.[20] COSY (COrrelation Spectroscopy) permits to evaluate scalar correlations between three bond distant protons. The experiment reveals the direct spin-spin couplings. COSY experiment is primarily used in order to obtain structural information via spin-spin connectivity. TOCSY (Total Correlation Spectroscopy) permits to evaluate spin correlations along a so called "spin system": in a tri-substituted amino acid as, for istance, Leucine, magnetization is transferred and detected through each α–β–γ–δ proton, mutually at a three bonds distance, and each proton couples with each other of the same system. This technique allows to recognize the tri-substitute amino acids in a sequence and assess their chemical shifts. NOESY (Nuclear Overhauser Effect Spectroscopy) allows to evaluate dipolar correlations between the protons through the space. Still NOESY is dependent on the size of the molecule another technique is applied in some cases. ROESY (Rotating-frame nuclear Overhauser Effect Spectroscopy) permits to get the same information of NOESY and is useful for systems for which NOE effects are zero.

*Secondary structure determination*

To assess the 3D structure of a molecule in solution by means of a NMR experiment we firstly need to assess the chemical shifts in the 1D spectrum to the proton resonances. In this case, COSY and TOCSY are very useful to distinguish each residue from each other, because the correlation between proton is present only inside the same residue. If the sequence is known, as in this case, these techniques allow to assess chemical shifts (except if two or more identical residues are present). However these experiments do not give any information on the sequence. In fact, in order to define the qorder of residue in the sequence and determinate the conformation in solution another experiment is needed. NOE effect is dependent on the dipolar interaction between protons and give information on the proximity of protons in space. Therefore, NOESY spectra is utilized for assessing the conformation. Typical cross-peaks can be recognized for helix structures.[21]

**PyrAc(AdtAlaAib)$_2$OMe**

In table 2 are reported the chemical shifts evaluated for this compounds in $CD_3CN$ with 30% $CD_3Cl$ at 298K. COSY, TOCSY and NOESY experiments have been employed.

.

| | **NH** | **$^{\alpha}$H** | **$^{\beta}$H** | **Others** |
|---|---|---|---|---|
| Pyr-$CH_2$- | | | | $CH_2$ 4.38-4.53 (dd)<br>aromat. 8.39-8.03 |
| Adt[1] | 7.93 | | 3.36-4.13<br>3.54-3.30 | |
| Ala[2] | 7.55 | 3.84 | 1.25 | |
| Aib[3] | 7.00 | | 0.81-0.51 | |
| Adt[4] | 7.16 | | 3.84-3.40 | |
| Ala[5] | 7.62 | 4.11 | 1.33 | |
| Aib[6] | 7.10 | | 1.34 | |
| -$OCH_3$ | | | | 3.58 |

***Tab. 2*** Chemical shifts for PyrAc(AdtAlaAib)$_2$OMe

TOCSY and COSY cross-peaks were useful to assess the resonance of Alanine protons (see TOCSY spectrum in the interest region in Experimental section, **Figure 20**). The assessment of NHs chemical shifts to their own residue has been achieved by analysis of the NOESY spectrum in NH→NH coupling region (**Figure 21** in the Experimental Section). All the spectra have been recorded in $CD_3CN$ with a 30% $CDCl_3$ at 298 K. The presence of all the expected cross-peaks for $NH_i \rightarrow NH_{i+1}$ couplings in NOESY spectrum is a proof for the presence of an helix structure.[21] In order to determinate the contributions of $3_{10}$-helix and α-helix of it, the most indicating zone in the NOESY spectrum is the so-called "finger print" region. This section of the spectrum includes all the cross-couplings between α-CH or β-$CH_2$ (usually below 5ppm) and NHs (see Figure 22 in Experimental Section). In our case, the presence of only two tri-substituted amino acids imposes necessaritly to check also the region of coupling of NH with β-$CH_3$ (Ala and Aib $CH_3$ - see Figure 23 in Experimental Section).

The presence of the correlations Adt[1]$CH_2$→Adt[4]NH, Ala[2]CH→Ala[5]NH (**Fig. 20**) and Aib[3]$CH_3$→Aib[6]NH (**Fig. 21**) of the type $CH_i \rightarrow NH_{i+3}$ is an evidence of an helical folding.[21] The preference for the $3_{10}$-helix versus an α-helix arrangement is usually assessed on observing the presence of $i \rightarrow i+2$ or $i \rightarrow i+4$ cross-peaks. An high number of the formers in the spectra (Adt[1]$CH_2$→Aib[3]NH, Ala[2]CH→Adt[4]NH, Aib[3]$CH_3$→Ala[5]NH, Adt[4]$CH_2$→Aib[6]NH) is a confirm that the peptide adopts a prevalent $3_{10}$-helix conformation, in agreement with the expectations for this sequence.[14]

Nevertheless, the cross peak $Ala^2CH \rightarrow Aib^6NH$ is an hint of the presence of a mixed conformation $3_{10}/\alpha$.

**Fc(AdtAlaAib)$_2$OMe**

In **Table 3** are reported the chemical shifts evaluated for this compounds in $CD_3CN$ with 30% $CD_3Cl$ at 298K. COSY, TOCSY and ROESY experiments have been employed (TOCSY spectra in the regions of interest for assessing $Ala^2$ and $Ala^5$ chemical shifts is reported in the Experimental Section, **Figure 24**).

| | **NH** | **$^{\alpha}$H** | **$^{\beta}$H** | **Others** |
|---|---|---|---|---|
| Fc- | | | | Cp rings: 4.89-4.84-4.78-4.48-4.42-4.30-2.29 |
| $Adt^1$ | 7.20 | | 3.59-3.72<br>3.60-3.98 | |
| $Ala^2$ | 7.59 | 4.00 | 1.34 | |
| $Aib^3$ | 7.63 | | 1.54 | |
| $Adt^4$ | 7.55 | | 4.01-3.62<br>3.27-3.79 | |
| $Ala^5$ | 7.77 | 4.16 | 1.38 | |
| $Aib^6$ | 7.25 | | 1.47 | |
| $-OCH_3$ | | | | 3.62 |

***Tab. 3*** Chemical shifts for Fc $(AdtAlaAib)_2OMe$

The assessment of NHs chemical shifts has been achieved by analysis of the ROESY spectrum in $NH_i \rightarrow NH_{i+1}$ coupling region (**Figure 25** in experimental section). All the spectra have been collected in $CD_3CN$ with a 30% $CDCl_3$. In Table 4 all the cross-peaks found in ROESY spectrum are reported. The presence of most of the expected cross-peaks for $NH_i \rightarrow NH_{i+1}$ couplings in ROESY spectrum is a proof for the presence of an helix structure.[21] Actually, the croo-peak between Aib3NH and Ala2NH has not been found due, probably, to the overlap of diagonal signals.

In order to determinate the contributions of $3_{10}$-helix and $\alpha$-helix of it, the most indicating zone in the ROESY spectrum is the so-called "finger print" region. This section of the spectrum includes all the cross-couplings between $\alpha$-CH or $\beta$-$CH_2$ (usually below 5ppm) and NHs. In our case, the presence of only two tri-substituted amino acids imposes necessaritly to check also the region of coupling of NH with $\beta$-$CH_3$ (Ala and Aib $CH_3$). The two spectra are reported below in Experimental Section in **Figure 26** and **27** respectively. In these two last regions only one useful cross-peak is

present in order to assess the conformation. $Adt^1$ $CH_2$ resonace at 3.66ppm couples with $Aib^3$ NH. So, this could be a confirm for the presence of a $3_{10}$-helix prevalent structure.

UV-Vis, ECD AND FLUORESCENCE

The presence in the final products of the chromophores (PyrAc and Fc) makes these compounds suitable to be investigated in the nearUV-Vis range. No intrinsic dichroism effects should be expected for Pyrene acetic acid and Ferrocene carboxylic acid, indeed. However, we recoded for both the PyrAc and the Fc labeled peptides the ECD spectra above 250nm. In fact, the presence of a chiral element could induce some chiroptical effect to these functional groups. The most useful region for assessing the peptide conformations (from 200 to 250nm) is hardly investigable because of an overlapping with the UV absorption bands of the chromophores. So, only the spectra in the Vis region have been recorded. The ECD spectra for PyrAc10OMe overlapped to PyrAc6OMe (left) and Fc10OMe overlapped to Fc6OMe (right) are reported in **Figure 13** and compared to UV-Vis absorption spectra in the same region. The ECD spectra of each final product have been recorded in $CDCl_3$ ($10^{-4}$ M solutions). As results, dichroic effects are present in the range of absorption for both the chromophores. In this region (above 250nm) the peptides cannot give any contribution to the spectra. So the dichroism signals appearing in the spectra could only come from the achiral chromophores and is due to the bound chiral peptide chain that induce a rigid chiral environment for the bound label.

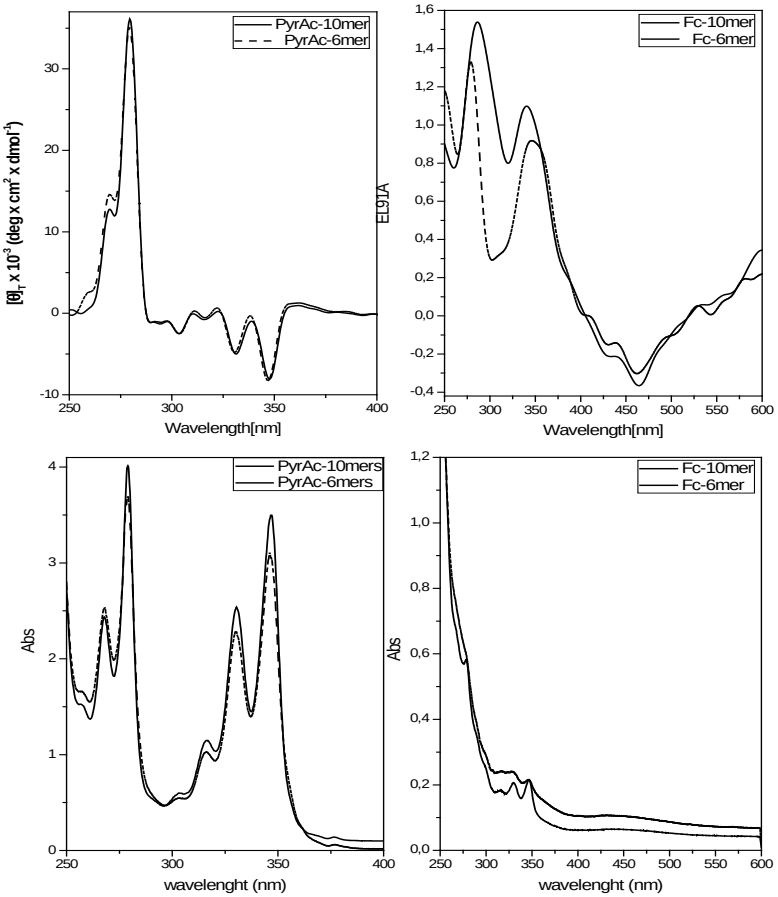


***Fig. 13*** EDC (**above**) and related UV-Vis absorption spectra (**below**) of **PyrAc-10mer** (dashed line) overlapped on **PyrAc-6mer (2)** (straight line) (**left**) and **Fc(AdtAlaAib)$_2$OMe** (**right**). All the spectra have been recorded for $10^{-4}$M solutions in $CDCl_3$, with a 1cm cell length. ECD specra are normalized respect the concentration. Absorption spectra are reported as Abs vs wavelength.

For comparison, the ECD spectra were recorded at the same conditions (solvent and concentration) for a sequence that do not possess any definite secondary structure in solution. To this aim, we decided to synthesize the Pyr and Fc derivatives of the dipeptide Boc-Ile-Leu-OMe (**Figure 14**).

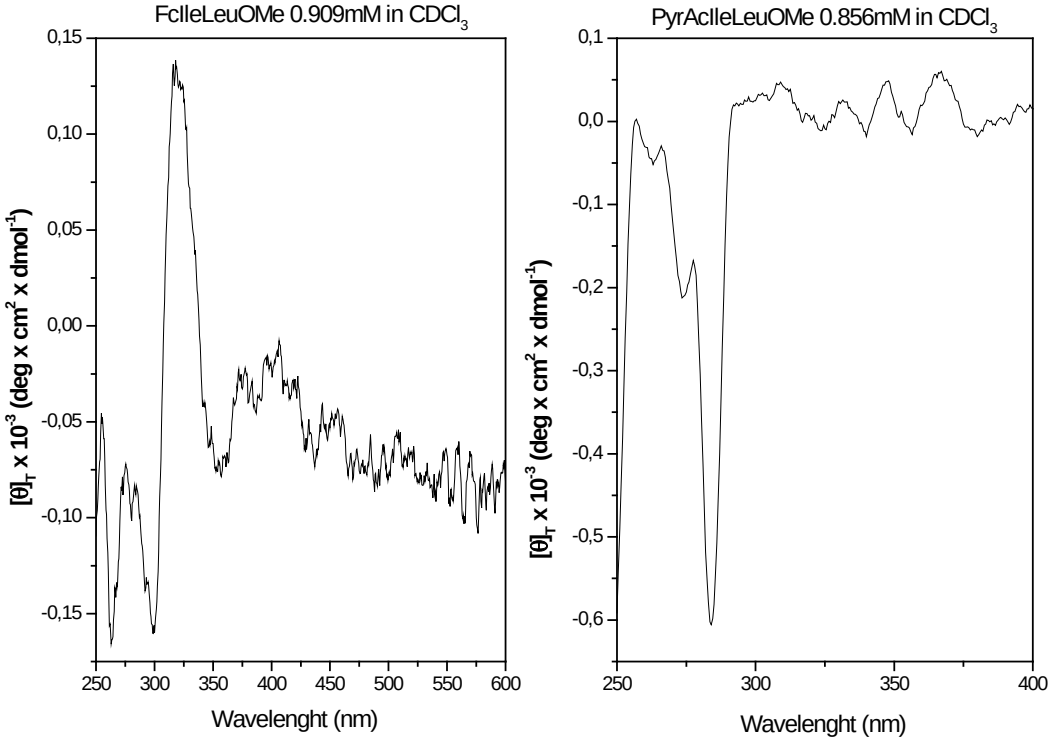


***Figure 14.*** EDC of **FcIleLeuOMe** (**above**) and **PyrAcIleLeuOMe** (below). All the spectra have been recorded for ~$10^{-4}$ M solutions in $CDCl_3$, with a 1cm cell length. ECD specra are normalized respect the concentration.

It is worth to note that: *i*) the profile of the ECD signals for this sequence in the region under investigation is definitively different from formers and *ii*) the intensity is extremely lower for dipeptides (one hundred times smaller for Pyrene derivative). Even though the content of chiral amino acids between -$(AdtAlaAib)_2$OMe and -IleLeuOMe is the same, the chiral effect on chromophores is different out of any doubt. Moreover, the intrinsic chiral contribution coming from the first residue bound to the chromophore is zero for Adt, being achiral, whereas Ile is intrinsically chiral. So, the chiral effect should be due to the different conformation of the two different sequences, instead of coming from the proximity of the nearest amino acid or from the simple sum of effects of single chiral contribution of each amino acid. In fact, this would not explain the change in sign of the ellipticity for the two different spectra.

The comparison between 10-mers and 6-mers shows small differences, in particular a different ratio of the two main bands at 290 and 340 nm for ferrocene containing peptides, whereas both the shape and the form of the spectrum of Fc-Ile-Leu-OMe is rather weaker and does not show any appreciable chiral effect under 300nm. Noteworthy, for PyrAc-Ile-Leu-OMe the band at 290 nm is even opposite to which of longer ones. This effect seems to be related only to the different conformations of the peptides in solution. However, many examples are reported in literature about exciton splitting due to excimer couple formation (inducing exciton splitting) that could induce a dichroic effect for Pyrene.[22] In order to better investigate whether any contribution could have come from such a mechanism, the fluorescence spectra for PyrAc10mer and for PyrAcIleLeuOMe have been recordedin $CDCl_3$.[23] The spectra are reported in **Figure 15**.

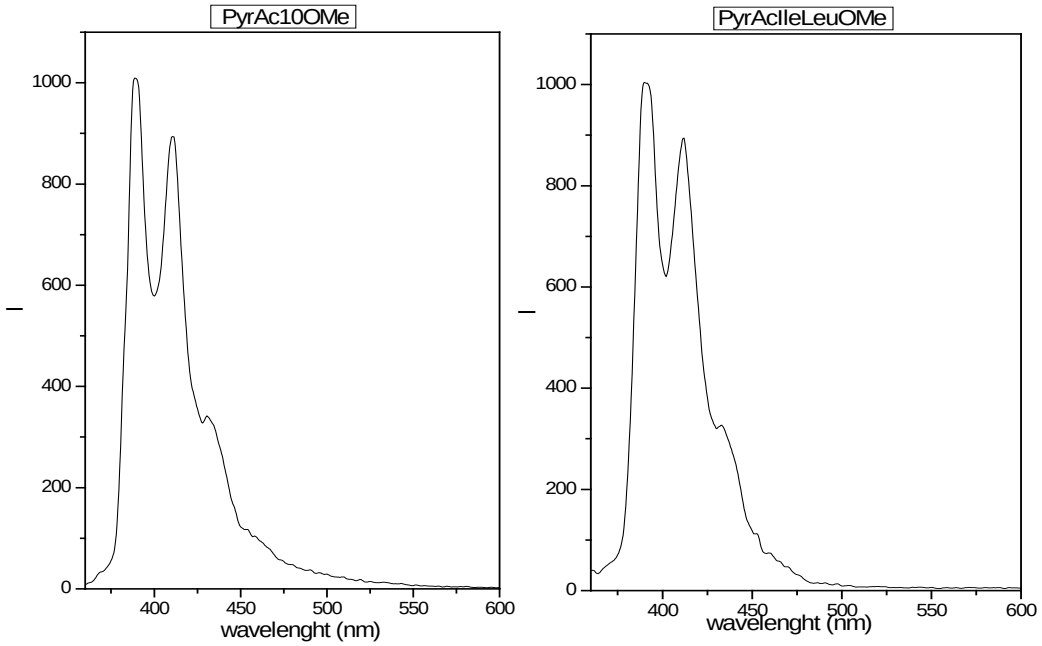


***Fig. 15*** fluorescence spectra in $CDCl_3$ for PyrAc10OMe and PyrAcIleLeuOMe. λex=345 nm, recorded Δλem=355-600 nm

The emission bands in the spectra are due only to the fluorescence of the monomer. For excimer the emission band would appear as a broad and more intense band between 470-550 nm, and is clearly absent in the shown spectra. Therefore, it is possible to state that the chiral effect cannot get any contribution from such a mechanism and is due only to the presence of the peptide bound to the pyrene. Whether or not the Pyrene is sensitive to the whole conformational constained sequence or to the first turn angle will be explained by further investigations.

ELECTROCHEMICAL CHARACTERIZATIONS

The electrochemical experiments have been carried out on modified Adt-peptide gold-electrodes (SAMs). The experiments and data elaboration were accomplished by prof. Venanzi's research group at the University of Tor-Vergata, Roma. The reported results are only briefly summarized here.

*Preliminary coating test on Fmoc intermediates*

Cyclic voltammetry measurements of the discharge of $[Fe(CN)_6]^{3-}$ on a bare gold electrode and in presence of peptides coating have been compared each other.[3e] To optimize the coating through by a Adt dithiolane bridge to Au surfaces it was performed a series of preliminary binding experiments. Panel **A** in **Figure 16** shows that the tripeptide FmocAdtAlaAlaOMe does bind to an Au-coated electrode of teflon. Indeed, the cyclic voltammetry of the bare Au electrode (red line) is markedly reduced in intensity when the peptide links to the electrode (blu line). Interestingly, when the intermediate 6mer Fmoc(AdtAlaAla)$_2$OMe was used, the electrode surface (Au-coated teflon electrode) was covered much more efficiently (higher reduction of intensity, panel **B**) and evaluated coverage is $3{,}1\cdot10^{-14}$mol/cm$^2$. This event supports the contention that the two Adt residues may act cooperatively. Finally, when using a flat Au surface (panel **C**) even the tripeptide (containing only one Adt residue) binds to the electrode surface very efficiently.

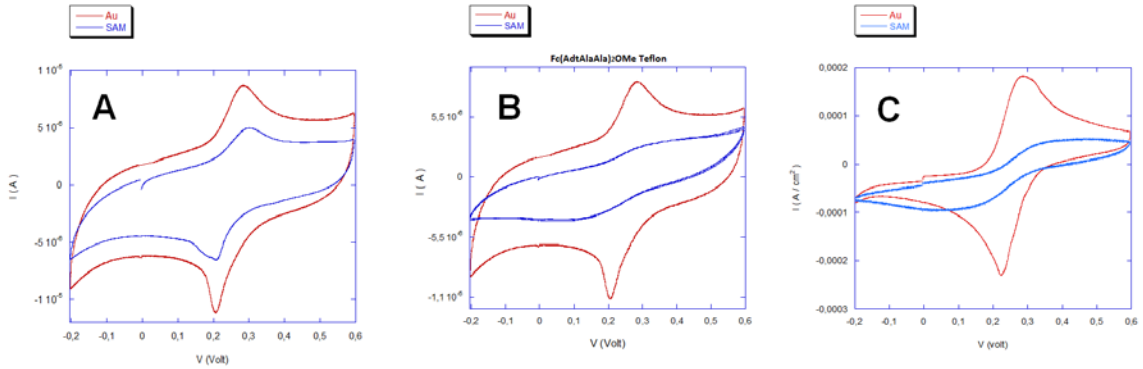


***Fig.16*** Cyclic voltammetry on bare gold electrodes (**red lines**). Comparison between FmocAdtAlaAlaOMe (**A, blue line**) and Fmoc(AdtAlaAla)$_2$OMe (**B**, **blue line**)

***Cyclic Voltammetry on Fc(AdtAlaAib)$_2$OMe***

The sample has been prepared by solving the Fc containing-compound in a suitable amount of chloroform. A concentration of 0.5mM and 0.05mM have been tested. The

concentrations have been determined by means of the absorption of Ferrocene chromophore in the SAM at 450nm (ε=400) where no overlap with other absorption take place. A gold thin plate (A=0,505cm$^2$) was treated with piranha solution ($H_2SO_4$ 96%, $H_2O_2$ 30% 2:1 v/v) for 15 minutes, washed twice with bidistilled water, dried over Argon then left into the sample solution for 18 hours.

In **Figure 17** (left and centre) a comparison between the CV of $K_3[Fe(CN)_6]$ ($E_{ox}$=0.27 mV, $E_{red}$=0.4 mV) for the bare electrode and the coated one respectively is reported. Besides, in **Figure 17** (right) the CV for Ferrocene-coating SAM is reported (0.1M $NaClO_4$ in acetonytrile).

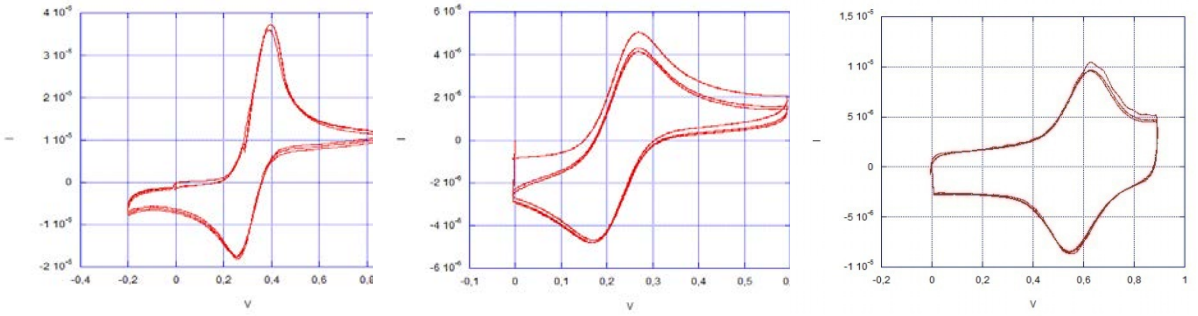

***Fig. 17*** Left: Fe(III) CV of bare gold electrode in $K_3[Fe(CN)_6]$/KCl solution; centre: Fe(III) CV of coated electrode in $K_3[Fe(CN)_6]$/KCl solution; right: CV of ferrocene SAM (supporting electrolyte: 0.1M $NaClO_4$/MeCN). Scan rate: 300mV/s.

From the comparison between **Figure 17/left** and **17/centre** is possible to say the the presence of the coating SAM doesn't inhibite completelly the reduction of Fe(III) complex, that indicate a low degree of SAM packaging. In **Figure 17/right** the CV curves for Ferrocene redox process are reported. The evaluated E° in is 0.56 mV and this value is due to the linkage *via* amide bond to the peptide (0.55 mV for Ferrocene carboxylic acid).[24] The ΔE is close to 0 mV in our case, indicating a good reversibility at this scan rate. Moreover, this evidence indicate also that there are not contributions from ET processes mediated by Ferrocene diffusion onto the gold surface.[25] The peaks are also broader and weaker than bare electrode CV. This effect has been associated to a rigid coating of the SAM. An analysis of CV curves depending on scan rate (**Figure 28/left** in Experimental Section) indicates that the ΔE between reduction and oxidation peaks are linearly dependent on scan rate (**Figure 28/right** in Experimental Section). This also is a confirm of the formation of the SAM. In fact, a free Ferrocene in solution should have displayed a square root dependence of ΔE on the scan rate instead of linear

one. Moreover, the evauated concentration of peptide on the surface is $3.128 \cdot 10^{-11}$ $mol \cdot cm^{-2}$. By assuming the maximun packaging available, a theoretical number of $2.17 \cdot 10^{-10}$ $mol \cdot cm^{-2}$ was proposed.[1e] The former value has been evaluated for the most packed helical peptide SAM (tilt angle=0°). So, the quite small surface coverage evaluated for Fc-6mer could be due to the 180° packaging on the surface (parallel disposition) induced by the two binding Adt in sequence.

***Photocurrent generation***

A photo-current generation experiment was carried out. The result suggests that Ferrocene induces the generation of wavelenght-dependent current (**Figure 18**). In Experimental Section the experiment set up is explained.

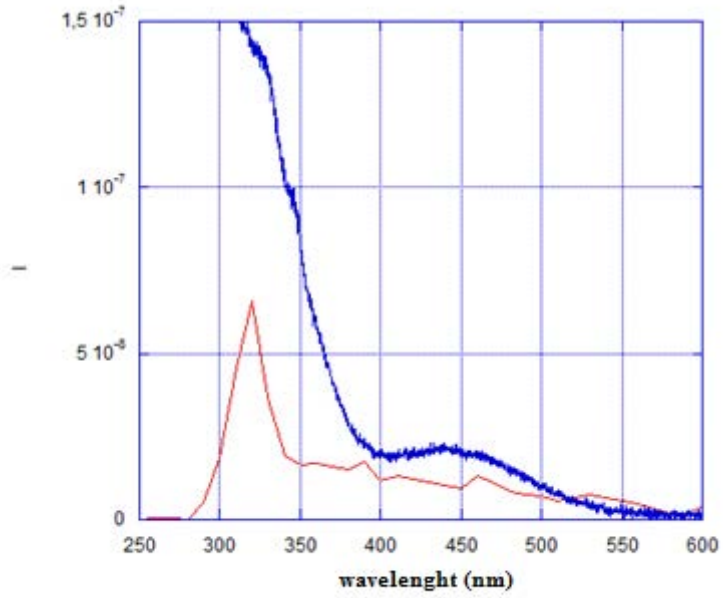


***Fig. 18*** Comparison of the UV-Vis absortion spectrum for Ferrocene in the 600-250nm range (blue) and the intensity of photo-generated current for $Fc(AdtAibAla)_2OMe$ on gold surface.

The process is stronger in the wavelenght region of higher absortpion of Ferrocene. Noteworthy, the higher current intensity peak between 300 and 350 nm is due to the photo-current generated by the gold electrode itself.

X-RAYS ANALYSIS

Single crystal of Adt-containing pentapeptide Boc-L-Ala-Aib-Adt-L-Ala-Aib-OMe were obtained from slow evaporation of a MeOH solution. The molecular structure was determined by X-ray diffraction analysis (structure solved by Dr. Marco Crisma, CNR-ICB, Padova). The pentapeptide is folded into a right-handed $3_{10}$-helix, stabilized by three intramolecular H-bonds, as expected for a short, Aib-containing peptides (**Figure 19**).

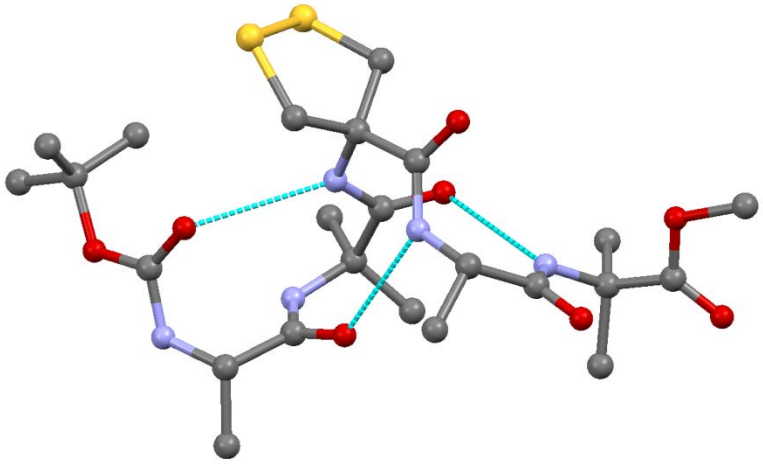

***Figure 19.*** X-rays structure for BocAlaAibAdtAlaAibOMe. Crystals obtained by precipitation from MeOH solution

As seen for the longer and more stabilized PyrAc(AdtAlaAib)$_2$OMe by analysis of NOESY cross-peaks, this result is in agreement with the supposed conformation.

## CONCLUSIONS

A series of Ferrocene and Pyrene labelled helical peptides containing one or more 4-amino-1,2-dithiolane-4-carboxylic acid (Adt) residues have been synthetized and fully chemically characterized. Such peptides have been designed to be employed in the formation of SAMs over gold surface (by means of linkage with the dithiolaneAdt side chains) for electrochemical applications. A detailed conformational study on a hexamers series and electrochemical characterization have been performed. In particular, 2D NMR experiment indicated a prevalent $3_{10}$ conformation, even if hints of the incoming α-structure have been detected. In fact, for longer peptides α-structure is known to be more stable in Ala/Aib containing peptides.[26] X-rays structure was resolved for a 5-mer intermediate, evidencing a $3_{10}$ helix conformation at that length stage. Therefore, electrochemical investigation on a Ferrocene containing 6-mer have been performed. In particular, the redox properties of the Ferrocene has been sampled by CV experiments on SAM. As result, the analises of the result suggets that the Adt residues in the sequence impose a parallel displacement (respect to the peptide axle) of the peptides over the gold, leading to a lower coverage of the surface in respect to a perpendicular displacement. Therefore, preliminary experiments aimed to generate photo-current have been investigated for the Ferrocene containing peptide. These last results indicated that these peptides are suitable to be good candidatefor thelight-current conversion process.

## EXPERIMENTAL SECTION

GENERAL METHODS

**SYNTHESIS:** The sntheses were accomplished in the Laboratories of prof. François Couty in Versailles (France). In solution methodology has been employed for all the intermediates and amino acids derivatives.

**NMR:** $^{1}H$ spectra were recorded at room temperature on a Bruker AV-400 (400 MHz) and a Bruker AV-3400 (300 MHz) instruments using deuterated solvents (chloroform, pyridine, DMSO or acetonytrile) with or without TMS. In absence of TMS, residual peaks of solvents have been used as reference for assessing chemical shifts. The multiplicity of a signal is indicated as: s - singlet, d - doublet, t - triplet, q - quartet, m - multiplet. Chemical shifts (δ) are expressed in ppm.

**FT-IR:** The KBr spectra were recorded on a Perkin-Elmer 580 B equipped with an IR data station Perkin-Elmer 3600. For spectra in $CDCl_3$ (98.8% Fluka), a Perkin-Elmer 1720X was emploeyd. The instrument operates in FT and is interfaced to a IBM PS/2 50 Z computer. 0.1 and 1cm $CaF_2$ pathway cells have been employed. For each spectrum have been collected 50 scans ($4cm^{-1}$ resolution) under nitrogen.

**Mass Spectrometry:** High-resolution mass spectra were obtained by electrospray ionization (ESI) on a Perseptive Biosystem Mariner ESI-TOF or a Bruker Microtof-Q spectrometer.

**HPLC:** The HPLC measurements were performed using an Agilent 1200 series apparatus, equipped with a UV detector at variable wavelengths. For compounds **3**, **4**, and **5** HPLC conditions: Phenomenex C18 (100 Å) (stationary phase), 40–70% B, 30 min.

**UV-Vis Absorption:** The electronic absorption spectra were recorded using a Shimadzu model UV-2501 PC spectrophotometer. A 1 cm path length quartz cell was used.

**CD:** The ECD measurements have been collected on a J-715 Jasco spectropolarimeter, with quartz cells Hellma (0.02cm pathway length). Values are reported in total molar ellipticy (deg x $cm^2$ x $dmol^{-1}$) :

$$[\Theta]_T = (MW \times \Theta)/(l \times c) = 3300 \times \Delta\varepsilon = 3300 \times (\varepsilon_L - \varepsilon_R)$$

Θ = observed ellipticy

MW = molecular weight

l = pathway length (cm)

c = concentration in gr/l

$\Delta\varepsilon = \varepsilon_L - \varepsilon_R$ = difference between left- and right-handed component of estinction coefficients of polarized light

**Fluorescence:** Fluorescence measurements have been accomplished on a Perkin-Elmer MPF-66 apparatus at 20°C . $\lambda_{exc}$ 345 nm, $\Delta\lambda_{em}$ 355-600 nm.

**Electro-chemical methods:** Ciclic Voltammetry measurements have been accomplished on a Heka PG310 potenziostat, on a calomel reference electrode, a Pt counter-electrode and the gold substrate as work electrode. $NaClO_4$ 0.1M in MeCN (20ml) has been used as support electrolyte. For the photocurrent measurements a $NaSO_4$ 0.1M and triethanolamine (TEOA) 0.05M were prepared in bidistilled water (25mL). The experimental set consists in a Xenon lump (150W) and a mono-chromator of excitation (band with 15nm), whereas the current was measured with the same instrument utilized for CV. The Cyclic Voltammetry experiments have been accomplished in collaboration with prof. Venanzi group at the University of Roma-Tor Vergata.

For photo-current generation, the experiments were carried out in a fluorescence Hellma quartz cell (for ensuring uniform irradiation) using the same experimental design of CV measurements. Cathodic photocurrent was detected utilizing 0.05M methyl viologen ($C_{12}H_{14}Cl_2N_2$) as electron donor (for gold) and acceptor (by Ferrocene). The photocurrent measurements have been carried out with 45 seconds irradiation, followed by 45 seconds of darkness. The measurements were performed between 600 and 250nm.

**X-Rays:** X-ray diffraction data were collected with an Agilent Technologies Gemini E four-circle kappa diffractometer equipped with a 92 mm EOS CCD detector, using graphite monochromated Cu Kα radiation (λ = 1.54178 Å). Data collection and reduction were performed with the CrysAlisPro software (version 1.171.35.11, Agilent Technologies). A semi-empirical absorption correction based on the multi-scan technique using spherical harmonics, implemented in SCALE3 ABSPACK scaling algorithm, was applied. (structure solved by Dr. Marco Crisma, CNR-ICB, Padova).

SYNTHESIS AND CHARACTERIZATION

**SYNTHESIS of Fmoc-Adt-OH**

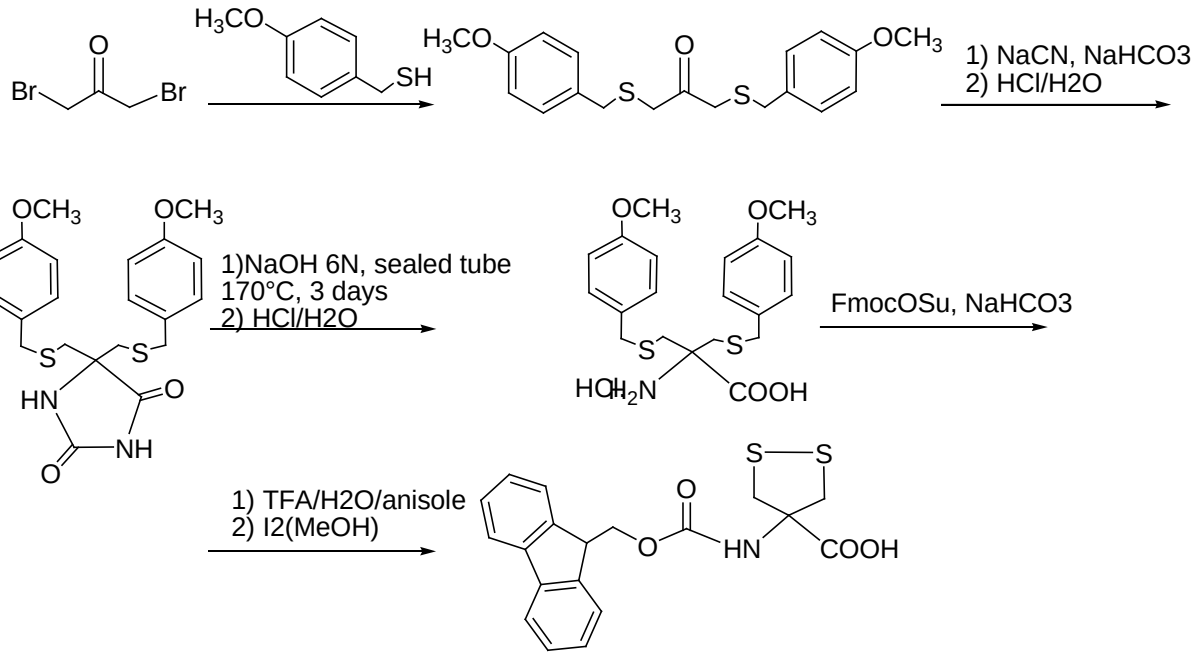


**1,3-bis(4-methoxybenzylthio)propan-2-one**

12.2 mL (44 mmol) of (4-methoxyphenyl)methanethiol were dissolved into 100 mL of NaOH (aq.) 1N under magnetic stirring into a 500mL flask. A 40 mL solution containing 9.46 g of 1,3-dibromopropan-2-one (43.84 mmol) in EtOH was added dropwise within an hour. The reaction procedeed overnight. The suspension so formed was filtered with a gooch. The liquid phase was evaporated and estracted with 200 mL of dicloromethane, and this one washed with 1/1 HCl 0.5M/brine. Organic phases were collected, dried over $MgSO_4$ and solvent removed at low pressure. A red oil was obtained (15 g). The product was purified with a chromatography on silica gel (eluant dichloromethane) obtaining 12.3g of pure product. Yield 77%. **NMR ($^{1}$H 300 MHz) δ ppm** 7.19-7.14 (d, 4H, *p*-MeOBn aromatic rings), 6.79-6.76 (d, 4H, *p*-MeOBn aromatic rings), 3.72 (s, 6H, -OMe $CH_3$), 3.57 (s, 4H, α-$CH_2$), 3.16 (s, 4H, Bn $CH_2$). **NMR ($^{13}$C 300 MHz) δ ppm** 200.0, 158.8, 130.4, 129.0, 113.9, 55.3, 37.4, 35.5. **FTIR (cm$^{-1}$)** 3080, 3035, 2994, 2953, 2933, 2908, 2835, 1679, 1605, 1580, 1507. **m.p.** 82-84°C.

**5,5-bis((4-methoxybenzylthio)methyl)imidazolidine-2,4-dione**

12 g of 1,3-bis(4-methoxybenzylthio) propan-2-one (33.2 mmol) were taken into a 1 L flask with a magnetic stirrer. Then 90 mL of EtOH and 60 mL of water were added. To this suspension 6.4 g of KCN and 13.1 g of $NH_4HCO_3$ were added. The reaction was heated at 75°C under reflux into a sealed reaction system for three days with an inflating balloon to avoid overpressures. The temperature was raised up to 90°C for 1 hour. Then the system was let cool down to room temperature. The solvent was evaporated at low pressure and the residue solved into EtOAc. The organic phase was washed several time with $NaHCO_3$(sat.) and brine. Then it was dried over $MgSO_4$. The product was obtained as a white solid by precipitation with EtOAc\PE. Yield 74%. **NMR ($^1$H 300 MHz $CD_3OD$) δ ppm** 7.13-7.10 (d, 4H, *p*-MeOBn aromatic rings), 6.75-6.72 (d, 4H, *p*-MeOBn aromatic rings), 3.66 (s, 6H, -OMe $CH_3$), 3.57 (s, 4H, β-$CH_2$), 2.68-2.55 (q, 4H, Bn $CH_2$). **FTIR (cm$^{-1}$)** 3387, 3252, 3076, 2917, 2831, 1752, 1728, 1699, 1613, 1503. **m.p.** 120-125°C.

**3-(4-methoxybenzylthio)-2-((4-methoxybenzylthio)methyl)-2-aminopropanoic acid hydrochloride**

10.5 g of 5,5-bis((4-methoxybenzylthio) methyl) imidazolidine-2,4-dione (25 mmol) were taken into 150 mL sealed glass reactor with a magnetic stirrer. Then 60 mL NaOH 2 N were added. The reaction was heated at 170°C for three days. The system was let cool down to room temperature. The moisture was put into a 500 mL flask diluting to 150 mL with water. The pH was lowered to 6 by carefully dropwise addition of HCl 2N, keeping the whole system into an ice bath and under continuos stirring. The suspension has so been filtered off on buchner and washed with cold ice and $Et_2O$. The product obtained, has so been dried under vacuum at low pressure and didn't need any other purification. Yield 96%.**NMR ($^1$H 300 MHz DMSO-$d_6$) δ ppm** 7.13-7.10 (d, 4H, *p*-MeOBn aromatic rings), 6.75-6.72 (d, 4H, *p*-MeOBn aromatic rings), 3.66 (s, 6H, -OMe $CH_3$), 2.82-2.48 (s, 4H, Bn $CH_2$), 2.33 (s, 4H, α-$CH_2$). **FTIR (cm$^{-1}$)** 2998, 2953, 2839, 2038, 1613, 1589, 1507. **m.p.** 195-200°C.

**3-(4-methoxybenzylthio)-2-((4-methoxybenzylthio)methyl)-2-(N-Fmoc)- amino propanoic acid**

10.6 g of 3-(4-methoxybenzylthio)-2-((4-methoxybenzylthio) methyl)-2- amino

propanoic acid hydrochloride (24 mmol) were taken into 1 L flask with a magnetic stirrer. The solid was suspended into 200 mL of water. Then the temperature was lowered to 0°C and 18 g (234 mmol) of $NaHCO_3$ were added along with 100 mL of acetone containing 11 g of Fmos-OSu (30.34 mmol). So, the temperature was increased to r.t. and the system has left reacting for four days. The acetone has so been evaporated and water solution estracted several time with small portion of $Et_2O$. The water solution was carefully acidified to pH 3 by means of HCl 2 N and estracted with EtOAc (5x100 mL). The product was washed with HCl 0.5N and brine, then the acetate was dried over $MgSO_4$. The product was precipitated from EtOAc\PE. Yield 90%.**NMR ($^1$H 300 MHz, MeOD) δ ppm** 7.66-7.25 (m, 8H, Fmoc aromatic rings), 7.16-6.76 (dm, 8H, 2 *p*MeO-Bz aromatic rings), 6.08 (s, 1H, NH), 4.53 (br, 2H, Fmoc $CH_2$), 3.73 (s, 6H, 2 *p*MeO-Bz $CH_3$), 3.47-2.91 (dd, 4H, β-$CH_2$). **FTIR (cm$^{-1}$)** 1719, 1607, 1503. **m.p.** 52-54°C.

**N-Fmoc-4-amino-1,2-dithiolane-4-carboxylic acid** [**Fmoc-Adt-OH**]

8 g of 3-(4-methoxybenzylthio)-2-((4-methoxybenzylthio) methyl)-2-(N-Fmoc)-amino propanoic acid (12.8 mmol) were taken into 500 L flask with a magnetic stirrer. The solid was solved into 80 mL of TFA\H2O\anisole 20\1\1. The solution was kept under stirring at 75°C for 2 hours. So, the temperature was lowered to room temperature and the TFA removed under vacuum. 400 mL of methanol were added to the residue and a solution 0.1M of $I_2$ in methanol was added dropwise under stirring till the colour was persistently dark yellow. The solution has so been decoloured with $Na_2S_2O_{3(conc)}$. The methanol was removed under vacuum, the residue diluted with water and estracted with EtOAc. Water phase was washed with EtOAc and organic phases dried over $MgSO_4$. The product was eluted on silica gel (dichloromethane\methanol 95\5). Yield 76%.**NMR ($^1$H 300 MHz, DMSO-d$_6$) δ ppm** 7.90-7.30 (m, 8H, Fmoc aromatic rings), 4.22 (s, 3H, OMe), 3.71-3.51 (dd, 4H, β-$CH_2$). **TOF MS ES+ [m/z]** M+H$^+$ 388. **FTIR (cm$^{-1}$)** 3351, 3050, 2942, 1684, 1591, 1510. **m.p.** 135-140°C.

**Synthesis of amino acids derivatives**

**Fmoc-Adt-OMe**

2g of Fmoc-Adt-OH (5.2mmol) were solved in 40mL of MeOH. The temperature was lowered to 0°C and 48 μL of $SOCl_2$ (5.2mmol) added to solution. Then, the reaction was heated at 65°C and left reacting overnight. The solvent and $SOCl_2$ were removed

under vacuum and the residue taken several time in toluene and $Et_2O$ and evaporated. The product was a white sticking solid and didn't need of further purification. Yield 93%.**NMR ($^1$H 300 MHz) δ ppm** 7.79-7.31 (m, 8H, Fmocarom.), 5.43 (s, 1H, AdtNH), 4.43 (m, 2H, Fmoc $CH_2$), 3.79 (s, 3H, -$OCH_3$), 3.65-3.36 (2d, 4H, Adtβ-$CH_2$). **NMR ($^{13}$C 300 MHz) δppm** 155.1, 143.6, 141.4, 127.8, 127.1, 125.0, 120.1, 71.2, 67.1, 47.4, 4è.1, 14.2**. TOF MS ES+ [m/z]** M+$H^+$ 402.08, M+$Na^+$ 424.07. **FTIR (cm$^{-1}$)** 3343, 3019, 2950, 1738, 1711, 1696, 1711, 1696, 1506. **m.p.** 65-70°C

**H-Adt-OMe**

1.92g of Fmoc-Adt-OMe(4.8mmol) were solved in 10mL of DCM/DEA 8/2 and left stirring for 2 hours. The solvent was removed at low pressure and product purified on silica gel (95/5 DCM/MeOH). The product was a sticky pale yellow solid. Yield 100%. **NMR ($^1$H 300 MHz) δ ppm** 3.79 (s, 3H, -$OCH_3$), 3.65-3.36 (2d, 4H, Adtβ-$CH_2$), 2.11 (br s, 2H, $NH_2$). **TOF MS ES+ [m/z]** M+$H^+$ 180.01, M+$Na^+$ 192

**Pyrene-$CH_2$-CO-Adt-OMe**

58mg of Pyrene acetic acid (0.22mmol) were solved into 5mL of dry DCM. To this solution, at 0°C, 28mg of DMAP (0.22mmol), 51 mg of EDC (0.24 mmol) and 30 μL of NMM (0.24mmol) were added. The solution was left stirring at 0°C until the complete solubilization of starting material. 40mg of H-Adt-OMe (0.22mmol) was added and left stirring at room temperature under Ar atmosphere overnight. The solvent was removed under vacuum, the residue taken into EtOAc and washed with HCl 5%, water, $NaHCO_{3(sat)}$ and brine. The organic phase was dried over $MgSO_4$. The product was purified on silica gel (DCM/EtOAc 95/5).Yield 50%.**NMR ($^1$H 300 MHz) δ ppm** 8.15-7.90 (m, 9H, arom.), 6.07 (s, 1H, AdtNH), 4.29 (s, 2H, pyrene-$CH_2$-CO-), 3.72 (s, 3H, OMe),3.53-3.16 (2d, 4H, Adtβ-$CH_2$). **NMR ($^{13}$C 300 MHz) δ ppm** 170.9, 169.9, 129.6, 128.4, 127.6, 127.4, 126.3, 125.6, 125.5, 125.2, 122.9, 70.7, 53.3, 46.9, 41.7. **TOF MS ES+ [m/z]** M+$H^+$ 421. **FTIR (cm$^{-1}$)** 3247, 3035, 2938, 1730, 1642, 1537. **m.p.** 181-185°C.

**Pyrene-$CH_2$-CO-Adt-OH**

90mg of Pyrene-$CH_2$-CO-Adt-OMe(0.21 mmol) were solved into 1 mL of MeOH. To this solution, 214 μL of a NaOH 2N solution in water (0.42 mmol) was added along with 2mL of THF for the solubility. The solution was left stirring at r.t. under Ar

atmosphere overnight. The solvent was removed under vacuum, the residue taken into 10mL HCl 2N and estracted with EtOAc. The organic phase was dried over $MgSO_4$ and then removed at low pressure. The product is a pale yellow solid. Yield 80%.**NMR ($^1$H 300MHz DMF-$d_7$) δ ppm** 8.59-8.15 (m, 9H, pyrene), 4.81 (s, 2H, pyrene-$CH_2$-CO), 3.77-3.35 (br m, 4H, Adt β-$CH_2$). **NMR ($^{13}$C 300MHz DMF-$d_7$) δ ppm** 206.1, 131.55, 131.16, 129.04, 127.74, 127.51, 127.15, 126.36, 126.33, 125.23, 125.98, 124.60, 48.92, 40.07, 20.57. **TOF MS ES+ [m/z]** $M+H^+$ 408. **FTIR (cm$^{-1}$)** 3346, 3256, 3039, 2921, 2851, 1715, 1634, 1507. No m.p. detectable: decomposition above210°C.

**Ferrocene-CO-Adt-OMe**

116 mg of ferrocene carboxylic acid (0.5 mmol) were solved in 5 mL of dry DCM, along with 62 mg of DMAP (0.5 mmol), 116mg of EDC (0.6 mmol) and 72μL of NMM. The solution has been left stirring ay 0°C for 20'. Then, 75mg of H-Adt-OMe(0.42 mmol) were added. The solution has been left stirring overnight. The solvent was removed under vacuum, the residue solved in EtOAc and washed with HCl 5%, water, $NaHCO_{3(sat)}$ and brine. The organic phase was dried over $MgSO_4$. The solvent was evaporated yielding the product as a red solid.Yield 70%.**NMR ($^1$H 300 MHz) δ ppm** 6.12 (s, 1H, NH), 4.78 (s, 2H, ferrocene), 4.46 (s, 2H, ferrocene), 4.36 (s, 5H, ferrocene), 3.74 (s, 3H, OMe), 3.63-3.40 (2d, 4H, Adtβ-$CH_2$). **NMR ($^{13}$C 300 MHz) δ ppm** 169.9**,** 71.3, 70.6, 53.5, 46.8. **TOF MS ES+ [m/z]** $M+H^+$ 392. **FTIR (cm$^{-1}$)** 3282, 2946, 2927, 1738, 1618, 1533. Decomposition over 185°C.

**Ferrocene-CO-Adt-OH**

55 mg of Ferrocene-CO-Adt-OMe(0.141mmol) were solved in 1mL of MeOH. To this solution, 0.141 μL of NaOH 2 N (in water) were added along with 2mL of MeCN for the solubility. The reaction proceeded overnight. The solvent was removed at low pressure and r.t., the residue taken in HCl 2N and estracted with DCM. The organic phase was dried over $MgSO_4$. The solvent was evaporated yielding the product as a red solid. Yield 99%.**NMR ($^1$H 300MHz DMF-$d_7$) δppm** 5.12 (s, 2H, ferrocene), 4.48 (s, 5H, ferrocene), 4.24 (s, 2H, ferrocene), 4.20-3.30 (br m, 6H, Adtβ-$CH_2$). **NMR ($^{13}$C 300MHz) δppm** 219.3, 202.8, 69.76, 50.85. **TOF MS ES+ [m/z]** $M+H^+$ 377. **FTIR (cm$^{-1}$)** 3378, 3351, 2923, 2848, 1730, 1626, 1499. Decomposition over 210°C.

**Ferrocene-CO-Aib-OMe**

206 mg of Ferrocene carboxylic acid (0.89 mmol) were solved in 5 mL of dry DCM, along with 130 mg of OXYMA (0.89 mmol), 206mg of EDC (1.07 mmol) and 155 μL of DIEA. The solution has been left stirring ay 0°C for 10'. The solvent was evaporated and the residue purified on silica gel (pure DCM) yielding 180 mg of Ferrocene-CO-OXYMA. Yield 57%. The product was straightly used for coupling with H-Aib-OMe. **NMR ($^{1}$H 300 MHz) δ ppm** 4.96 (s, 2H, ferrocene), 4.57 (s, 2H, ferrocene), 4.48-4.41 (q, 2H, OXYMA -$CH_2$-), 4.23 (s, 5H, ferrocene), 1.40-1.36 (t, 3H, OXYMA –$CH_3$). **TOF MS ES+ [m/z]** $M+H^+$ 355 **NMR ($^{13}$C 300MHz) δppm** 166.7, 166.1, 157.3, 130.4, 73.4, 70.9, 70.59, 65.0, 64.4, 14.1. **FTIR (cm$^{-1}$)** 2985, 1769, 1726, 1572,1256, 982. Decomposition over 105°C.

175 mg of Ferrocene-CO-OXYMA were taken in 5mL of MeCN, along with 156 mg of HCl·H-Aib-OMe (1.02 mmol) and 150μL of DIEA. The system was left reacting overnight heating at 50°C under stirring. The solvent was removed under vacuum, the residue solved in EtOAc and washed with HCl 5%, water, $NaHCO_{3(sat)}$ and brine. The organic phase was dried over $MgSO_4$. The solvent was evaporated yielding the product as a red solid.Yield 89% (over both the reactions).**NMR ($^{1}$H 300 MHz) δ ppm** 6.26 (s, 1H, NH), 4.71 (s, 2H, ferrocene), 4.38 (s, 2H, ferrocene), 4.29 (s, 5H, ferrocene), 3.78 (s, 3H, OMe), 1.63 (s, 6H, Aibβ-$CH_3$). **TOF MS ES+ [m/z]** $M+H^+$ 330, $M+Na^+$ 352. **FTIR (cm$^{-1}$)** 3355, 3301, 3085, 2985, 2946, 1742, 1618, 1533. Decomposition over 185°C.

**Ferrocene-CO-Aib-OH**

150 mg of Ferrocene-CO-Aib-OMe (0.456 mmol) were solved in 2.5 mL of MeOH. To this solution, 0.456 μL of NaOH 2 N (in water) were added along with 2 mL of MeCN for the solubility. The reaction proceeded overnight. The solvent was removed at low pressure and r.t., the residue taken in HCl 2 N and estracted with DCM. The organic phase was dried over $MgSO_4$. The solvent was evaporated yielding the product as a red solid. Yield 99%. **NMR ($^{1}$H 300MHz) δ ppm** 7.72 (s, 1H, NH), 4.77 (s, 2H, ferrocene), 4.36 (s, 2H, ferrocene), 4.25 (s, 5H, ferrocene), 1.51 (s, 6H, Aibβ-$CH_3$). **NMR ($^{13}$C 300 MHz) δ ppm** 69.8, 69.1, 67.9, 39.6, 39.3, 39.0, 38.7, 38.5, 24.3. **TOF MS ES+ [m/z]** $M+H^+$ 316. **FTIR (cm$^{-1}$)** 3328, 3098, 2986, 2927, 2851, 2553, 1711,

1624, 1513. Decomposition over 204°C.

**Synthesis of Adt containing peptide series**

**Boc-L-Ala-L-Ala-OMe**

0.75 g of Boc-L-Ala-OH (3.9 mmol) were added into a 250 mL flask with a magnetic stirrer. The solid was suspended into 5 mL of THF and the temperature lowered to 0°C. Then, 0.53 g of HOBt (3.9 mmol), 0.74g of EDC (4 mmol) and 0.9 mL of DIEA (5 mmol) were added. After 10', 0,66g of HCl·H-L-Ala-OMe (0.44 mmol) along with 0.9 mL of DIEA (5 mmol) were added to the solution and the temperature increased to room temperature. The reaction was followed via TLC. Then, the THF was removed under vacuum, the residue taken into EtOAc and washed with HCl 5%, water, $NaHCO_{3(sat)}$ and brine. The organic phase was dried over $MgSO_4$. The product precipitated from EtOAc\PE. Yield 84%.**NMR ($^1$H 300 MHz) δppm** 7.28 (d, 1H, Ala NH), 5.01 (d, 1H, Ala NH), 4.55 (m, 1H, Alaα–CH), 4,13 (m, 1H, Alaα–CH), 3.76 (s, 3H, OMe $CH_3$), 1.46 (s, 9H, Boc $C(CH_3)_3$), 1.43-1.36 (d, 6H, 2 Alaβ–$CH_3$). **FTIR (cm$^{-1}$)** 3313, 3255, 3081, 2981, 2934, 1734, 1676, 1649, 1553, 1518. **$[\alpha]_D^{25}$** -40.0. **m.p.** 106-110°C.

**Fmoc-Adt-L-Ala-L-Ala-OMe**

0.51 g of Boc-L-Ala-L-Ala-OH (1.84 mmol) were added into a 250 mL flask with a magnetic stirrer. The solid was solved into 10 mL of HCl\$Et_2O$ and stirred overnight. Then, the solvent was removed under vacuum. The solid was added to a cooled solution of 0.7g Fmoc-Adt-OH (1.84mmol), 0.71g of HATU (1.83mmol) and 0.81μL of DIEA (4mmol). 0.53 g of HOBt (3.9mmol), 0.74 g of EDC (4mmol) and 0.9 mL of DIEA (5mmol) were added. After 10', 0,66g of HCl·H-L-Ala-OMe (0.44 mmol) along with 0.9mL of DIEA (5 mmol) were added to the solution and the temperature increased to room temperature. The reaction was followed via TLC. Then, the THF was removed under vacuum, the residue taken into EtOAc and washed with HCl 5%, water, $NaHCO_{3(sat)}$ and brine. The organic phase was dried over $MgSO_4$. The product precipitated from EtOAc\PE. Yield 70%.**NMR ($^1$H 300 MHz) δ ppm** 7.78-7.26 (m, 8H, Fmoc aromatic ring), 6.99-6.06 (d, 1H, NH Ala), 6.85 (br d, 1H, NH Ala), 5.65 (s, 1H, NH Adt), 4.51-4.46 (m, 2H, Fmoc $CH_2$ + Alaα–CH) 4.23-4.21 (m, 1H, Ala NH), 3.72 (s, 3H, OMe $CH_3$), 3.72-3.35 (dm, 4H, Adt 2 β–$CH_2$), 1.38-1.36 (d, 6H, 2 Alaβ–$CH_3$).

**NMR ($^{13}$C 300 MHz) δ ppm** 173.0, 171.3, 168.9, 143.3, 141.3, 127.9, 127.1, 127.1, 124.8, 120.1, 71.69, 67.2, 52.4, 49.4, 48.2, 47.1, 38.8, 29.7, 17.8. **TOF MS ES+ [m/z]** $M+H^+$ 544, $M+Na^+$ 566. **FTIR ($cm^{-1}$)** 3641, 3571, 3390, 3332, 2938, 1703, 1661, 1626, 1506**.** $[\alpha]_D^{25}$ -3.6°. **m.p.** 115-120°C.

**Ac-Adt-L-Ala-L-Ala-OMe**

20 mg of Fmoc-Adt-L-Ala-L-Ala-OH (0.04mmol) were added into a 50mL flask with a magnetic stirrer. The solid was solved into 1mL of DEA\dichloromethane 2\8 and stirred for 4h. The solvent was removed under vacuum. The solid was taken in 1mL anhydrous $CH_3CN$ and 3.8 μL of $Ac_2O$ (40 μmol) were added under stirring. The reaction was followed by TLC. After 2h the solvent was removed under vacuum and the residue taken into EtOAc, washing with HCl 5%, water, $NaHCO_{3(sat)}$ and brine. The organic phase was dried over $MgSO_4$. The product was purified on silica gel column (dichloromethane\methanol 95\5). Yield 50%.**NMR ($^1$H 300 MHz) δppm** 7.11- 7.08 (d, 1H, Ala NH), 6.88-6.84 (d, 1H, Ala NH), 6.37 (s, 1H, Adt NH), 4.54, 4.44 (m, 2H, 2 Alaα–CH), 3.74 (s, 3H, OMe $CH_3$), 3.64-3.40 (m, 4H, Adt 2 β–$CH_2$), 2.10 (s, 3H, Ac $CH_3$), 1.44-1.40 (d, 6H, 2 Alaβ–$CH_3$). **TOF MS ES+ [m/z]** $M+H^+$ 364. **FTIR ($cm^{-1}$)** 3301, 2985, 2934, 1738, 1657, 1530. **m.p.** 80-85°C.

**Boc-L-Ala-Adt-L-Ala-L-Ala-OMe**

0.41 g of Fmoc-Adt-L-Ala-L-Ala-OH (0.76 mmol) were added into a 250mL flask with a magnetic stirrer. The solid was solved 5mL of DEA\dichloromethane 2\8 and stirred for 4h. The solvent was removed under vacuum. Then, 0.15 g Boc-L-Ala-OH (0.8 mmol), 0.14 g of HOBt (1 mmol), 0.20g of EDC (1mmol) and 0.36 mL of DIEA (2 mmol) were taken in dicloromethane at 0°C and this solution was added to the residue. The reaction was followed via TLC. DCM was removed under vacuum, the residue taken into EtOAc and washed with HCl 5%, water, $NaHCO_{3(sat)}$ and brine. The organic phase was dried over $MgSO_4$. The product was purified on silica gel column (dichloromethane\methanol 95\5). Yield 64%. **NMR ($^1$H 300 MHz) δ ppm** 7.76 (d, 1H, Ala NH), 7.32 (d, 1H, Ala NH), 6.85 (s, 1H, Adt NH), 5.23 (m, 1H, Ala NH), 4.6-4.4 (m, 2H, 2 Alaα–CH), 3.9 (m, 1H, Alaα–CH), 3.74 (s, 3H, OMe $CH_3$), 3.6-3.05 (dm, 4H, Adt 2 β–$CH_2$), 1.4-1.25 (m, 18H, *t*But $C(CH_3)_3$ + 3 Alaβ–$CH_3$). **NMR ($^{13}$C 300 MHz) δ ppm** 173.7, 173.1,171.8, 81.6, 70.9, 52.5, 52.3, 49.8, 48.1, 47.8, 46.0, 28.2,

17.7, 17.4. **TOF MS ES+ [m/z]** $M+H^+$ 493, $M+Na^+$ 515. **FTIR ($cm^{-1}$)** 3317, 3293, 2981, 2934,1738, 1661, 1645, 1518. **$[\alpha]_D^{25}$** -48.8°. **m.p.**110-115°C.

**Boc-L-Ala-L-Ala-Adt-L-Ala-L-Ala-OMe**

0.22 g of Boc-L-Ala-Adt-L-Ala-L-Ala-OH (0.45 mmol) were added into a 100 mL flask with a magnetic stirrer. The solid was solved into HCl\$Et_2O$ and stirred for 2h. The solvent was removed under vacuum. Then, 0.17 g Boc-L-Ala-OH (0.9 mmol), 0.13 g of OXYMA (0.9 mmol), 0.21 g of EDC (1 mmol) and 0.36 mL of DIEA (2 mmol) were taken in dicloromethane at 0°C and this solution was added to the residue. The reaction was followed via TLC. DCM was removed under vacuum, the residue taken into EtOAc and washed with HCl 5%, water, $NaHCO_{3(sat)}$ and brine. The organic phase was dried over $MgSO_4$. The product was purified on silica gel column (dichloromethane\methanol 95\5). Yield 70%.**NMR ($^1$H 300MHz) δppm** 7.76 (d, 1H, Ala NH), 7.32 (d, 1H, Ala NH), 6.85 (s, 1H, Adt NH), 5.23 (m, 1H, Ala NH), 4.6-4.4 (m, 2H, 2 Alaα–CH), 3.9 (m, 1H, Alaα–CH), 3.74 (s, 3H, OMe $CH_3$), 3.6-3.05 (dm, 4H, Adt 2 β–$CH_2$), 1.4-1.25 (m, 18H, *t*But $C(CH_3)_3$ + 3 Alaβ–$CH_3$). **NMR ($^{13}$C 300MHz) δppm** 174.3, 173.7, 173.1,171.8, 81.6, 70.9, 52.5, 52.3, 49.8, 48.1, 47.8, 46.0, 28.2, 17.7, 17.4. **TOF MS ES+ [m/z]** $M+H^+$ 493, $M+Na^+$ 515. **FTIR ($cm^{-1}$)** 3278, 2981, 2927, 2857, 1738, 1657, 1522**. $[\alpha]_D^{25}$** -20.0°. **m.p.** 95-100°C.

**Fmoc-Adt-L-Ala-L-Ala-Adt-L-Ala-L-Ala-OMe**

0.13 g of Boc-L-Ala-L-Ala-Adt-L-Ala-L-Ala-OH (0.23 mmol) were added into a 100 mL flask with a magnetic stirrer. The solid was solved into HCl\$Et_2O$ and stirred for 2h. The solvent was removed under vacuum. 0.27 g Fmoc-Adt-OH (0.8 mmol), 0.13 g of HATU (0.8 mmol) and 0.24 mL of DIEA (1.4 mmol) had been taken in dicloromethane at 0°C and this solution was added to the residue. The reaction was followed via TLC. After 2 days DCM was removed under vacuum, the residue taken into EtOAc and washed with HCl 5%, water, $NaHCO_{3(sat)}$ and brine. The organic phase was dried over $MgSO_4$. The product was purified on silica gel column (dichloromethane\methanol 95\5). Yield 53%.**NMR ($^1$H 300MHz) δppm** 7.82-7.28 (m, 12H, Fmoc aromatic rings + 3 Ala NH + Adt NH), 6.85 (br d, 1H, NH Ala), 5.1 (s, 1H, NH Adt), 4.53-4.07 (m, 6H, Fmoc $CH_2$ + Alaα–CH) 4.2-3.2 (dm, 4H, Adt 2 β–$CH_2$), 3.74 (s, 3H, OMe $CH_3$), 3.72-3.35 (dm, 4H, Adt 2 β–$CH_2$), 1.38-1.36 (m, 12H, 4 Ala 2 β–$CH_3$). **NMR ($^{13}$C 300MHz) δppm** 174.51, 174.46, 173.38, 172.82, 170.04, 156.82, 143.11, 141.37,

141.30, 128.0, 127.25, 127.16, 124.96, 124.67, 120.21, 71.75, 71.57, 67.53, 52.45, 52.31, 52.13, 50.20, 49.07, 48.31, 47.63, 47.44, 47.08, 17.27, 17.17, 16.65, 15.90. **TOF MS ES+ [m/z]** $M+H^+$ 833, $M+Na^+$ 855. **FTIR ($cm^{-1}$)** 3313, 2919, 2853, 1742, 1715, 1649, 1514**.** **$[\alpha]_D^{25}$** -83.3°. **m.p.**110-115°C.

**Pyrene-$CH_2$-CO-Adt-L-Ala-L-Ala-Adt-L-Ala-L-Ala-OMe**

15mg (0.18 mmol) of Fmoc-Adt-L-Ala-L-Ala-Adt-L-Ala-L-Ala-OMe were solved in 2mL of DCM/DEA 8/2. The solution has been left stirring for 2 hours. After that solvent was removed under vacuum, washing several times with $Et_2O$ till the complete remotion of DEA. The product was purified on silica gel chromatography (DCM to DCM/MeOH 8.5/1.5).Besides, 50mg of pyrene acetic acid (180 μmol) were taken in dry and redistilled DCM (0.5 mL) under Ar atmosphere, along with 10 μL of dry DMF to achieve the complete solubility. To this solution, 0.5mL of dry and redistilled DCM containing 17 μL of $(CO)_2Cl_2$ were added dropwise within 2', under Ar. After 1h, the solvent was removed under vacuum. The residue was solved in 1mL dry DCM, 100 μL of which straightly added to H-Adt-L-Ala-L-Ala-Adt-L-Ala-L-Ala-OMe solved in 2mL dry DCM along with 4 μL of DIEA. The solution has been left under stirring and Ar atmosphere for 3 days. The solvent was evaporated and the product directly purified on TLC preparative plate (9/1 DCM/MeOH). Yield 10%. **MS ES+ [m/z]** $M+H^+$ 853. **FT-IR ($cm^{-1}$)** 3302, 2957, 2921, 2848, 1733, 1646, 1530, 1453.

**Ferrocene-CO-Adt-L-Ala-L-Ala-Adt-L-Ala-L-Ala-OMe**

23 mg (41 μmol) of Boc-L-Ala-L-Ala-Adt-L-Ala-L-Ala-OMe were solved in 3 mL of DCM and 3 mL of $HCl_{(Et2O)}$ were added. The solution has been left stirring for overnight. After that solvent was removed under vacuum, washing several times with toluene and $Et_2O$. The pepdide so obtained was suspended in 3 mL of dry DCM with 14.8 mg of **11** (40 μmol), 14.7 mg of HATU (40 μmol) and 16 μL of DIEA. The solution has been left stirring for 7 days.The DMF was removed under vacuum and the product purified with TLC preparative plate (95/5 AcOEt/ pentane with 5% MeOH). Yield 70%.**NMR ($^1$H 300MHz, Pyridine-*d5*) δppm** 9.87 (s, 1H, NH), 8.78 (d, 1H, NH), 8.61-8.59 (d, 1H, NH), 8.45 (s, 1H, NH), 8.44-8.41 (d, 1H, NH), 8.19-8.17 (d, 1H, NH), 5.07-5.00 (m, 4H, 2H cyclopentadienyl ring + 2 Ala α-CH), 4.61 (s, 2H, cyclopentadienyl ring), 2.64-4.51 (m, 2H, 2 Adt β-$CH_2$), 4.51-4.45 (m, 2 Ala α-CH),

4.33 (m, 7H, 5H cyclopentadienyl ring + 2 Adt β-$CH_2$), 4.15-4.13 (m, 2H, 2 Adt β-$CH_2$), 3.93-3.78 (m, 2H, 2 Adt β-$CH_2$), 3.59 (s, 3H, -OMe -$CH_3$), 1.79-1.75 (6H, m, 2 Ala β-$CH_3$), 1.61-1.58 (m, 3H, Ala β-$CH_3$), 1.39-1.37 (m, 3H, Ala β-$CH_3$). **NMR ($^{13}$C 300MHz, Pyridine-*d5*) δppm**175.4, 175.3, 173.9, 173.6, 173.4, 173.1, 170.8, 75.5, 73.2, 73.0, 72.0, 70.6, 70.4, 69.0, 53.0, 52.3, 50.7, 50.1, 49.6, 49.2, 48.0, 18.2, 17.8, 16.9, 16.8, 1.2.**TOF MS ES+ [m/z]** $M+H^+$ 493, $M+Na^+$515. **FTIR (cm$^{-1}$)** 3313, 2919, 2853, 1742, 1715, 1649, 1514**.**

**Boc-L-Ala-Aib-OMe**

Into a 500mL round bottom flask were put 4g of HCl·H-Aib-OMe (26.14mmol), 6.6g of Boc-L-Ala-OH (39.21mmol), 5.57g of OXYMA (39.21mmol), 7.52g of EDC (39.21mmol) and 7.7mL DIEA (44.5mmol) in 100mL of dried dichloromethane at 0°C. The reaction was checked with TLC for 1 days. The solvent was removed, the residue taken into EtOAc and washed with HCl 5%, water, $NaHCO_{3(sat)}$ and brine. The organic phase was dried over $MgSO_4$ and solvent removed at low pressure. The product appeared as an uncolored oil. Yield 70%.**NMR ($^1$H 300MHz) δppm** 6.73 (s, 1H, Aib NH), 5.0-4.95 (d, 1H, Ala NH), 4.10-4.95 (m, 1H, Ala α–CH), 4,13 (m, 1H, Alaα–CH), 3.73 (s, 3H, OMe $CH_3$), 1.44 (s, 9H,), 1.43-1.30 (m, 15H, Boc $C(CH_3)_3$ + Alaβ–$CH_3$ + Aib 2 β–$CH_3$). **TOF MS ES+ [m/z]** $M+H^+$ 289.**$[\alpha]_D^{25}$** -29.5°

**Fmoc-Adt-L-Ala-Aib-OMe**

Into a 250 mL round bottom flask were put 4g of Boc-L-Ala-L-Ala-OMe (10 mmol) and solved it into 20 mL of $HCl_{(Et2O)}$. The reaction was followed on TLC and finished after 3h. The solid was dried under vacuum and taken several time with $Et_2O$. Separately, 3.5 g of Fmoc-Adt-OH (9.1mmol), 1.54 g of OXYMA (9.1mmol), 2.1 g of EDC (10.8 mmol) and 1.2 mL of DIEA (10.8 mmol) were taken together at 0°C in dichloromethane. This solution was left stirring for 10 minutes, then added to product of cleavage. The reaction was followed on TLC for five days, under stirring at room temperature The solvent was removed, the residue taken into EtOAc and washed with HCl 5%, water, $NaHCO_{3(sat)}$ and brine. The organic phase was dried over $MgSO_4$ and solvent removed at low pressure. The crude product (3.5 g) was purified on silica gel chromatography (dichloromethane\methanol 9:1). Yield 50%. **NMR ($^1$H 300 MHz) δ ppm** 7.55-7.11 (m, 8H, Fmoc aromatic rings + Ala NH), 6.46 (s, 1H, Aib NH), 5.56 (s, 1H, Adt NH), 4.54-4.37 (m, 2H, Fmoc $CH_2$ + Ala α-CH), 3.77 (s, 3H, OMe $CH_3$),

3.72-3.35 (dm, 4H, Adt 2 β-$CH_2$), 1.58-1.37 (m, 9H, Aibβ-$CH_3$ + Ala 2 β-$CH_3$). **TOF MS ES+ [m/z]**M+$Na^+$ 580. **FTIR ($cm^{-1}$)** 3328, 2996, 2946, 1746, 1726, 1645, 1507. **m.p.** 70-75°C.

**Boc-Aib-Adt-L-Ala-Aib-OMe**

Into a 250 mL round bottom flask were put 2.8 g of Fmoc-Adt-L-Ala-L-Ala-OMe (5.16 mmol) and solved it into 20 mL of DCM/DEA 8/2. The reaction was followed on TLC and finished after 2h. The solution was dried under vacuum and taken several time with toluene and $Et_2O$, achieving product as sticking solid. Product was purified on silica gel column (DCM 100%, then DCM/MeOH 8/2). Yield 100% (**A**). Separately, 1.12 g of Boc-Aib-OH (5.5 mmol) and 1.08 mL of cyanuric fluoride (11 mmol) were solved together into 1.08 mL of pyridine (10.8 mmol) at 0°C. The reaction was left stirring at -15°C for $1^h$, then an hour at r.t. The solvent was removed under vacuum and residue taken several times in toluene and re-evaporated. The residue was solved in DCM and washed with cooled water. DCM was evaporated. Residue was an pale yellow oil (**B**). **B** was taken in 10 mL of anhydrous DCM, 1.32 mL of NMM (12 mmol) added and the solution cooled at 0°C. Then, **A** was solved into 10mL of anhydrous DCM and added to **B**. The reaction was followed for $3^d$. The solvent was removed, the residue taken into EtOAc and washed with HCl 5%, water, $NaHCO_{3(sat)}$ and brine. The organic phase was dried over $MgSO_4$ and solvent removed at low pressure. The crude product (2 g) was purified on silica gel chromatography (EtOAc/pentane 1/9 with 1% of MeOH added). The product crystallized spontaneously. Yield 59%.**NMR ($^1$H 300 MHz) δ ppm** 7.98 (d, 1H, Ala NH), 7.26 (s, 1H, AibNH), 6.71 (s, 1H, AdtNH), 5.00 (s, 1H, AibNH), 4.48-4.40 (m, 1H, Alaα-CH), 3.68 (s, 3H, OMe $CH_3$), 1.54-1.45 (m, 24H, Boc $C(CH_3)_3$ + Alaβ-$CH_3$ + 2 Aib 2 β-$CH_3$).**FTIR ($cm^{-1}$)** 3317, 3293, 2981, 2934,1738, 1661, 1645, 1518. **$[\alpha]_D^{25}$** +58.0°. **m.p.** 85-90°C.

**Boc-L-Ala-Aib-Adt-L-Ala-Aib-OMe**

Into a 250 mL round bottom flask were put 0.74 g of Boc-Aib-Adt-L-Ala-Aib-OMe (1.4 mmol) and solved into 10mL DCM/TFA 9/1. The solution was stirred for 4 hours. The solvent was removed under reduced pressure and the residue taken several time in toluene and $HCl_{(Et2O)}$. Separately, 0.265 g of Boc-L-Ala-OH (1.4 mmol), 0.528 mg of HATU (1.39 mmol) and 0.73 mL DIEA (4.2 mmol) were solved together in 10mL of anhydrous THF at 0°C. This solution was directly added to peptide. The system was left

reacting for $3^d$ at r.t. The solvent was removed, residue taken in EtOAc and washed with HCl 5%, water, $NaHCO_{3(sat)}$ and brine. The organic phase was dried over $MgSO_4$ and solvent removed at low pressure. The product was purified on silica gel (2/1 pentane with 1% MeOH added). Yield 52%. **NMR ($^1$H 300 MHz) δ ppm** 7.97-7.93 (d, 1H, Ala NH), 7.67 (s, 1H, AibNH), 7.52 (s, 1H, Adt NH), 6.82 (s, 1H, Aib NH), 5.26 (d, 1H, Ala NH), 4.95-3.85 (m, 2H, 2 Alaα-CH), 1.60-1.30 (m, 27H, Boc $C(CH_3)_3$ + 2 Alaβ-$CH_3$ + 2 Aib 2 β-$CH_3$). **NMR ($^{13}$C 300 MHz) δ ppm** 175.1, 174.8, 173.5,169.1, 81.9, 71.7, 56.5, 52.3, 50.0, 48.5, 47.6, 28.3, 26.8, 25.4, 23.4, 16.9. **FTIR (cm$^{-1}$)** 3289, 2977, 2930, 1738, 1665, 1653, 1522**.** **$[\alpha]_D^{25}$** +56.4°. **m.p.** 109-113°C.

**Ferrocene-CO-Aib-L-Ala-Aib-Adt-L-Ala-Aib-OMe**

50 mg (84 μmol) of Boc-L-Ala-Aib-Adt-L-Ala-Aib-OMe were solved in 3 mL of DCM and 3 mL of $HCl_{(Et2O)}$ were added. The solution has been left stirring for overnight. After that solvent was removed under vacuum, washing several times with toluene and $Et_2O$. The pepdide so obtained was suspended in 3 mL of dry DCM at 0°C with 40mg of Ferrocene-CO-Aib-OH (128 μmol) and 50mg of HATU (128 μmol). To this solution 33μL of DIEA were added. The solution has been left stirring for 7 days at r.t.. The solvent was removed, the residue taken in $CHCl_3$ and washed with HCl 5%, water, $NaHCO_{3(sat)}$ and brine. The organic phase was dried over $MgSO_4$ and solvent removed at low pressure. The product was purified on silica gel (2/1 pentane with 1% MeOH added). Yield 70%. **NMR ($^1$H 300 MHz $CD_3CN$) δ ppm** 7.95 (s, 1H, NH), 7.91 (d, 1H, Ala NH), 7.81 (d, 1H, Ala NH), 7.61 (s, 1H, NH), 6.93 (s, 1H, NH), 4.84-4.81 (ds, 2H, 2H cyclopentadienyl ring), 4.45 (s, 2H, 3H cyclopentadienyl ring), 4.26 (s, 5H, cyclopentadienyl ring), 4.17 (m, 1H, Ala α-CH), 4.01-3.93 (m, 3H, Ala α-CH + Adt β-$CH_2$), 3.68-3.52 (m, 4H, 2 Adt β-$CH_2$), 3.61 (s, 3H, -OMe $CH_3$), 3.30-3.22 (m, 2H, Adt β-$CH_2$), 1.57-1.29 (m, 21H, 2 Ala β-$CH_3$ + 3 Aib 2 β-$CH_3$).**TOF MS ES+ [m/z]** M+H$^+$ 789, M+Na$^+$ 811. **FTIR (cm$^{-1}$)** 3337, 3288, 2988, 2924, 2850, 1730, 1651, 1527.

**Pyrene-$CH_2$-CO-Adt-L-Ala-Aib-Adt-L-Ala-Aib-OMe**

15 mg of Pyrene-$CH_2$-CO-Adt-OH (36.3μmol) were solved in 2mL of dry DCM at 0°C with 13.8 mg of HATU (36.3 μmol) and 20mg of HCl·H-Ala-Aib-Adt-L-Ala-Aib-OMe (36.3 μmol). To this solution 25μL of DIEA were added. The reaction proceeded at r.t. for 6 days. The solvent was removed, the residue was taken in $CHCl_3$ and washed with

HCl 0.5N, water, $NaHCO_{3(sat.)}$ and brine. The organic phase was dried over $MgSO_4$ and solvent removed at low pressure. The crude product was purified on silica gel (95/5 DCM/MeOH). Yield 80%. **NMR ($^1$H 300 MHz $CD_3CN$) δ ppm** 8.39-8.03 (m, 9H, Pyrene), 7.93 (s, 1H, $Adt^1$ NH), 7.62 (d, 1H, $Ala^5$ NH), 7.56 (d, 1H, $Ala^2$ NH), 7.16 (s, 1H, $Adt^4$ NH), 7.11 (s, 1H, $Aib^6$ NH), 7.01 (s, 1H, $Aib^3$ NH), 4.52-4.38 (dd, 2H, PyrAc $CH_2$), 4.11 (m, 1H, $Ala^5$ α-CH), 3.84 (m, 1H, $Ala^2$ α-CH), 4.11-3.13 (m, 8H, 2 Adt 2 β-$CH_2$), 3.58 (s, 3H, OMe $CH_3$), 1.43-1.25 (m, 12H, 2 Ala β-$CH_3$, $Aib^6$ 2 β-$CH_3$), 0.81-0.51 (2s, 6H, $Aib^3$ 2 β-$CH_3$).**TOF MS ES+ [m/z]** $M+H^+$ 881, $M+Na^+$ 903. **FTIR ($cm^{-1}$)** 3423, 3333, 2989, 1734, 1670, 1524. **$[\alpha]_D^{25}$** +136.9° (MeOH, c=0.3 $g \cdot mL^{-1}$).

**Ferrocene-CO-Adt-L-Ala-Aib-Adt-L-Ala-Aib-OMe**

14mg of **11** (36.3 μmol) were solved in 2mL of dry DCM at 0°C with 13.8mg of HATU (36.3 μmol) and 20mg of HCl·H-Ala-Aib-Adt-L-Ala-Aib-OMe (36.3 μmol). To this solution 25μL of DIEA were added. The reaction proceeded at r.t. for 6 days. The solvent was removed, the residue was taken in $CHCl_3$ and washed with HCl 0.5N, water, $NaHCO_{3(sat.)}$ and brine. The organic phase was dried over $MgSO_4$ and solvent removed at low pressure. The crude product was purified on silica gel (95/5 DCM/MeOH). Yield 80%. **NMR ($^1$H 300 MHz $CD_3CN$) δ ppm** 7.77 (d, 1H, $Ala^5$ NH), 7.64 (s, 1H, $Aib^3$ NH), 7.59 (d, 1H, $Ala^2$ NH), 7.55 (s, 1H, $Adt^4$ NH), 7.25 (s, 1H, $Aib^6$ NH), 7.20 (s, 1H, $Adt^1$ NH), 4.89-4.34 (m, 2H, 2H cyclopentadienyl ring), 4.30 (s, 5H, cyclopentadienyl ring), 4.16 (m, 1H, $Ala^5$ α-CH), 4.00 (m, 1H, $Ala^2$ α-CH), 4.01-3.28 (mm, 8H, 2 Adt 2 β-$CH_2$), 3.62 (s, 3H, -OMe $CH_3$), 1.54 (s, 6H, $Aib^3$ β-$CH_3$), 1.44 (s, 6H, $Aib^6$ β-$CH_3$), 1.38 (s, 3H, $Ala^2$ β-$CH_3$), 1.34 (s, 3H, $Ala^5$ β-$CH_3$). **TOF MS ES+ [m/z]** $M+H^+$ 851, $M+Na^+$ 873. **FTIR ($cm^{-1}$)** 3286, 3027, 2950, 2927, 2849, 2336, 1715, 1487, 1406.

**Boc-Gly-Aib-OMe**

In a 500 mL flask were melted together 2 g of Boc-Gly-OH (11.4 mmol), 1.62 g of HOBt (11.4 mmol), 2.6 g of EDC (13.7 mmol) and 6 mL of DIEA (68.4 mmol) in dry DCM at 0°C. The mixture has been left stirring for 20'. Then 3.5 g of HCl·H-Aib-OMe (22.8 mmol) were added. The solution reacted overnight at r.t. The solvent was removed at low pressure and the the residue was taken in EtOAc and washed with HCl 0.5N, water, $NaHCO_{3(sat.)}$ and brine. The organic phase was dried over $MgSO_4$ and solvent

removed at low pressure. The product was a white solid. Yield 99%. **NMR ($^1$H 300 MHz) δ ppm** 6.73 (s, 1H, Aib NH), 5.21-5.19 (m, 1H, Gly NH), 3.75-3.71 (d, 2H, Gly α-$CH_2$), 3.74 (s, 3H, OMe $CH_3$), 1.58 (s, 6H, Aib β-$CH_3$), 1.44 (s, 9H, Boc 3 $CH_3$). **FTIR (cm$^{-1}$)** 3340, 3274, 3042, 2996, 2977, 2934, 1715, 1661, 1530, 1449. **m.p.** 92-95°C.

**Boc-Aib-Gly-Aib-OMe**

2.9 g of Boc-Gly-Aib-OMe (10.5 mmol) were solved into 20 mL of a 8/2 DCM/TFA solution. After 3 hours the solvent was removed under vacuum and the residue taken several time in toluene, $Et_2O$, and $HCl_{(Et2O)}$ in order to remove TFA unreacted and exchange trifluoroacetic salt with more safe cloridric salt. In the meanwhile, 2.23 g of Boc-Aib-OH (10.5 mmol), 1.56 g of OXYMA (10.5 mmol), 2.1g of EDC (10.5 mmol) and 2.01 mL of NMM (21 mmol) were solved together at 0°C in dry DCM and left stirring for 20'. Then, this solution was added to peptide. The reaction proceeded overnight at r.t. under stirring. The solvent was removed under vacuum, the residue was taken in EtOAc and washed with HCl 0.5N, water, $NaHCO_{3(sat.)}$ and brine. The organic phase was dried over $MgSO_4$ and solvent removed at low pressure. The product was a white solid. Yield 70%. **NMR ($^1$H 300 MHz) δ ppm** 7.30 (s, 1H, AibNH), 6.89-6.86 (t, 1H, GlyNH), 4.96 (s, 1H, AibNH), 3.92-3.89 (d, 2H, Glyα-$CH_2$), 3.69 (s, 3H, OMe $CH_3$), 1.51-1.48 (s, 12H, 2 Aibβ-$CH_3$), 1.43 (s, 9H, Boc 3 $CH_3$). **FTIR (cm$^{-1}$)** 3359, 3301, 3282, 2992, 2946, 2328, 1738, 1692, 1653, 1533. **m.p.** 135-140°C.

**Boc-L-Ala-Aib-Gly-Aib-OMe**

2.4 g of Boc-Aib-Gly-Aib-OMe (6.7 mmol) were solved into 20mL of a 8/2 DCM/TFA solution. After 3 hours the solvent was removed under vacuum and the residue taken several time in toluene, $Et_2O$, and $HCl_{(Et2O)}$ in order to remove TFA unreacted and exchange trifluoroacetic salt with more safe cloridric salt. In the meanwhile, 1.50g of Boc-L-Ala-OH (8 mmol), 1.14 g of OXYMA (8 mmol), 1.53 g of EDC (8 mmol) and 1.83 mL of NMM (12 mmol) were solved together at 0°C in dry DCM and left stirring for 20'. Then, this solution was added to peptide along with 1.83 mL of NMM (12 mmol). The reaction proceeded overnight at r.t; under stirring. The solvent was removed under vacuum, the residue was taken in EtOAc and washed with HCl 0.5N, water, $NaHCO_{3(sat.)}$ and brine. The organic phase was dried over $MgSO_4$ and solvent removed at low pressure. The product was a white solid. Yield 87%. **NMR ($^1$H 300 MHz) δ ppm**

7.34 (m, 2H, 2 Aib NH), 6.73-6.69 (m, 1H, Gly NH), 5.17 (d, 1H, Ala NH), 3.97-3.85 (m, 3H, Ala α-CH + Gly α-$CH_2$), 3.69 (s, 3H, OMe $CH_3$), 1.51 (s, 12H, 2 Aib β-$CH_3$), 1.44 (s, 9H, Boc 3 $CH_3$), 1.37-1.34 (d, 3H, Ala β-$CH_3$). **TOF MS ES+ [m/z]** $M+H^+$ 431, $M+Na^+$ 453. **FTIR ($cm^{-1}$)** 3301, 3278, 2988, 2942, 1746, 1645, 1537, 1514**.** $[\alpha]_D^{25}$ -32.7°. **m.p.** 81-85°C.

**Boc-L-Ala-Aib-Gly-Aib-OH**

0.5 g (1.16 mmol) of Boc-Ala-Aib-Gly-Aib-OMe were solved in 10mL of a mixture 2/1 THF/MeOH and 1.16mL of $NaOH_{(aq.)}$ 2N was added. The solution has been stirring for 6 hours at room temperature. Then the solvent was removed under vacuum and the solution diluted in 20 mL HCl 2N and extracted with EtOAc. The organic phase was dried over $MgSO_4$ and solvent removed at low pressure. The product was a white crystalline powder. Yield 99%. **NMR ($^1$H 300 MHz) δ ppm** 7.60-7.50 (m, 2H, 2 Aib NH), 6.65 (s, 1H, Aib NH), 5.10-5.09 (d, 1H, Ala NH), 3.96-3.90 (m, 3H, Alaα-CH + Gly α-$CH_2$), 1.60-1.58 (m, 15H, Alaβ-$CH_3$ + 2 Aibβ-$CH_3$), 1.44 (s, 9H, Boc 3 $CH_3$), 1.37-1.34 (d, 3H, Alaβ-$CH_3$). **TOF MS ES+ [m/z]** $M+H^+$ 417, $M+Na^+$ 439. **FTIR ($cm^{-1}$)** 3268, 2986, 1738, 1682, 1654, 1611, 1558, 1531. $[\alpha]_D^{25}$ =-10°. **m.p.** 185-189°C.

**Boc-L-Ala-Aib-Gly-Aib-L-Ala-Aib-Adt-L-Ala-Aib-OMe**

150 mg of Boc-L-Ala-Aib-Adt-L-Ala-Aib-OMe (0.254 mmol) were solved in 2 mL of dry DCM and 5 mL of 1M $HCl_{(Et20)}$ were added. The reaction proceeded overnight. The solvent was removed and the residue washed several time with toluene and $Et_2O$. In the meanwhile, 90 mg of Boc-Ala-Aib-Gly-Aib-OH (0.217 mmol) were solved in 8 mL of dry DCM along with 83 mg of HATU (0.217 mmol) and 76 μL of DIEA (0.434 mmol). The reaction has been stirred at 0°C for 20'. Then, the chloridric salt of peptide previously made was added. The reaction has been left stirring at r.t. for 7 days. The solvent was removed, the the residue was taken in EtOAc and washed with HCl 0.5N, water, $NaHCO_{3(sat.)}$ and brine. The organic phase was dried over $MgSO_4$ and solvent removed at low pressure. The product was a white solid that didn't need further purification. Yield 70%. **NMR ($^1$H 300 MHz) δ ppm** 7.97-7.95 (m, 2H, Aib NH + Gly NH), 7.68 (d, 1H, NH), 7.47 (m, 2H, 2 NH), 7.35 (s, 1H, NH), 6.88 (s, 1H, NH), 5.51 (m, NH, Ala NH), 4.56 (m, 1H, Alaβ-CH), 3.95 (d, 2H, Glyα-$CH_2$), 3.90-3.75 (m, 2H, 2 Alaα-CH), 3.63 (s, 3H, OMe), 3.57-3.27 (2d, Adtβ-$CH_2$), 1.49-1.33 (m, 42H, Boc $CH_3$,

4 Aibβ-$CH_3$, 3 Alaβ-$CH_3$). **TOF MS ES+ [m/z]** $M+H^+$ 890, $M+Na^+$ 912. **FTIR ($cm^{-1}$)** 3289, 2973, 2930, 1734, 1653, 1518**.** **$[\alpha]_D^{25}$** +78.3°. **m.p.** 195-200°C.

**Pyrene-$CH_2$-CO-Adt-L-Ala-Aib-Gly-Aib-L-Ala-Aib-Adt-L-Ala-Aib-OMe**

15mg of Pyrene-$CH_2$-CO-Adt-OH (36.3 μmol) were solved in 2 mL of dry DCM at 0°C with 13.8 mg of HATU (36.5 μmol) and 30mg of HCl·H-Ala-Aib-Gly-Aib-L-Ala-Aib-Adt-L-Ala-Aib-OMe (36.3 μmol). To this solution 25 μL of DIEA were added. The reaction proceeded at r.t. for 6 days. The solvent was removed, the the residue was taken in $CHCl_3$ and washed with HCl 0.5N, water, $NaHCO_{3(sat.)}$ and brine. The organic phase was dried over $MgSO_4$ and solvent removed at low pressure. The crude product was purified on silica gel (95/5 DCM/MeOH). Yield 40%. **NMR ($^1$H 400 MHz, $CD_3CN$) δ ppm** 8.38-8.03 (m, 9H, Pyrene), 7.89 (d, 1H, $Adt^1$ NH), 7.76 (d, 1H, $Ala^9$ NH), 7.74 (s, 1H, $Aib^7$ NH), 7.68 (d, 1H, $Ala^2$ NH), 7.60 (s, 1H, $Aib^5$ NH), 7.57 (s, 1H, $Adt^8$ NH), 7.48 (d, 1H, $Ala^6$ NH), 7.40 (t, 1H, $Gly^4$ NH), 7.26 (s, 1H, $Aib^{10}$ NH), 6.79 (s, 1H, $Aib^3$ NH), 4.55-4.38 (dd, 2H, Pyrene-$CH_2$), 4.13 (m, 1H, $Ala^9$ α-CH), 4.00 (m, 1H, $Ala^2$ α-CH), 3.85 (m, 1H, $Ala^6$ α-CH), 3.92-3.16 (mm, 8H, 2 Adt 2 β-$CH_2$), 3.62 (s, 3H, -OMe $CH_3$), 3.59-3.53 (d, 2H, $Gly^4$ α-$CH_2$), 1.43 (s, 6H, $Aib^{10}$ 2 β-$CH_3$), 1.41 (s, 6H, $Aib^5$ 2 β-$CH_3$), 1.40 (s, 6H, $Aib^7$ 2 β-$CH_3$), 1.39 (s, 3H, $Ala^9$ β-$CH_3$), 1.33 (s, 3H, $Ala^6$ β-$CH_3$), 1.32 (s, 3H, $Ala^2$ β-$CH_3$), 0.59 (s, 6H, $Aib^3$ 2 β-$CH_3$). **TOF MS ES+ [m/z]** $M+H^+$ 1179, $M+Na^+$ 1201. **FTIR ($cm^{-1}$)** 2924, 2848, 1722, 1653, 1526. **$[\alpha]_D^{25}$** +143.8°.

**Ferrocene-CO-Adt-L-Ala-Aib-Gly-Aib-L-Ala-Aib-Adt-L-Ala-Aib-OMe**

14 mg of **11** (36.3 mol) were solved in 2mL of dry DCM at 0°C with 13.8 mg of HATU (36.5 μmol) and 30 mg of HCl·H-Ala-Aib-Gly-Aib-L-Ala-Aib-Adt-L-Ala-Aib-OMe. To this solution 25 μL of DIEA were added. The reaction proceeded at r.t. for 6 days. The solvent was removed, the the residue was taken in $CHCl_3$ and washed with HCl 0.5N, water, $NaHCO_{3(sat.)}$ and brine. The organic phase was dried over $MgSO_4$ and solvent removed at low pressure. The crude product was purified on silica gel (95/5 DCM/MeOH). Yield 45%. **$^1$H NMR (400 MHz, $CD_3CN$) δ** 7.87, 7.78, 7.64, 7.29, 7.16, 4.90, 4.80, 4.49, 4.30, 4.15, 4.14, 4.12, 4.10, 4.07, 4.06, 4.03, 3.99, 3.96, 3.94, 3.92, 3.71, 3.70, 3.67, 3.62, 3.52, 3.49, 3.48, 3.44, 3.30, 3.29, 3.23, 3.20, 1.53, 1.50, 1.48, 1.44, 1.36, 1.29. **TOF MS ES+ [m/z]** $M+H^+$ 1149, $M+Na^+$ 1171. **FTIR ($cm^{-1}$)** 3312, 2922, 2853, 1729, 1652, 1528.

2D NMR SPECTRA

**PyrAc(AdtAlaAib)$_2$OMe**

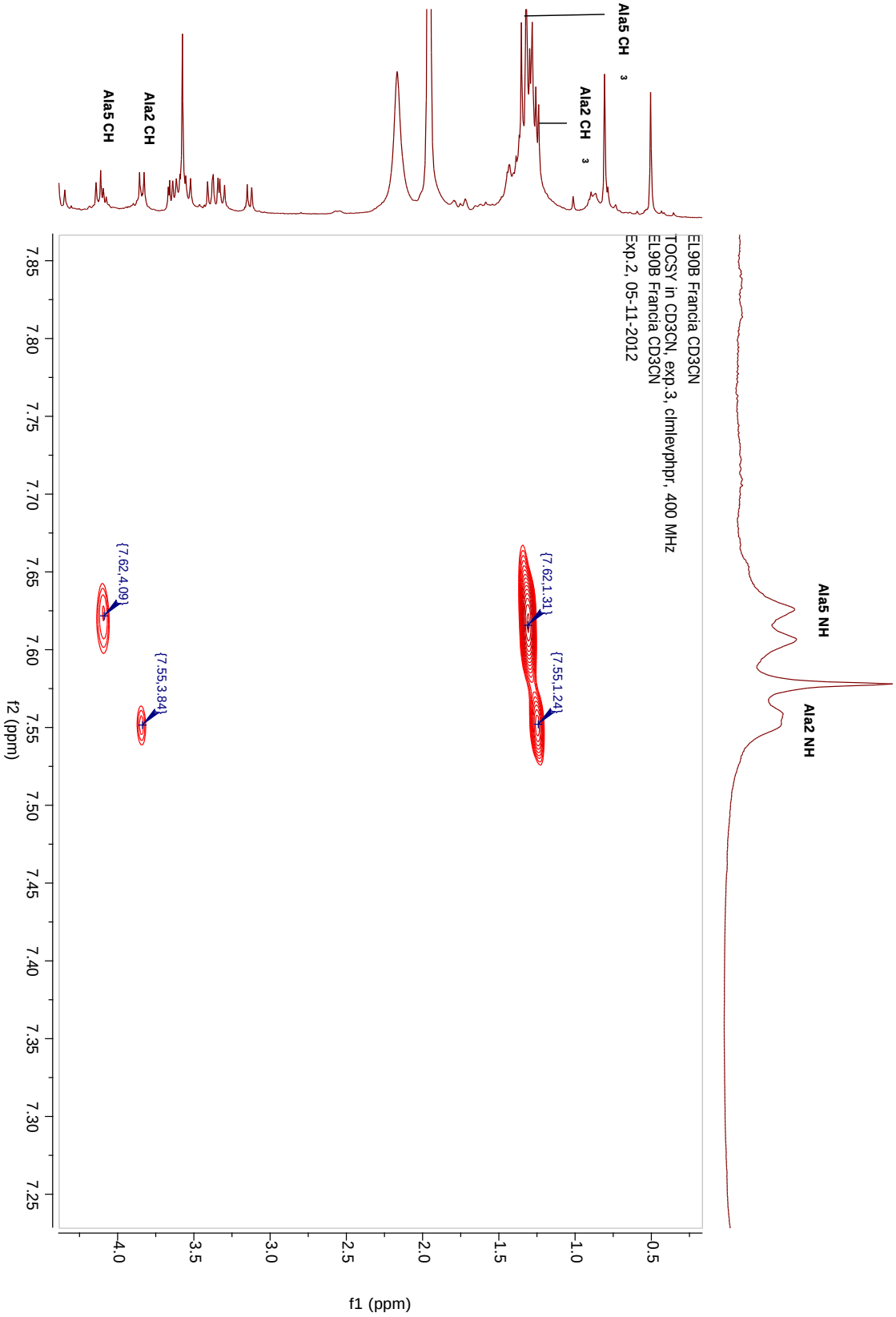


***Fig. 20*** TOCSY spectrum of PyrAc(AdtAlaAib)$_2$OMe in $NH_i \rightarrow CH_i$ and $NH_i \rightarrow CH_{3\ i}$ regions for PyrAc(AdtAlaAib)$_2$OMe . By means of these cross-couplings the two Ala spin systems have been assessed. Corrispondence in COSY spectrum (not shown).

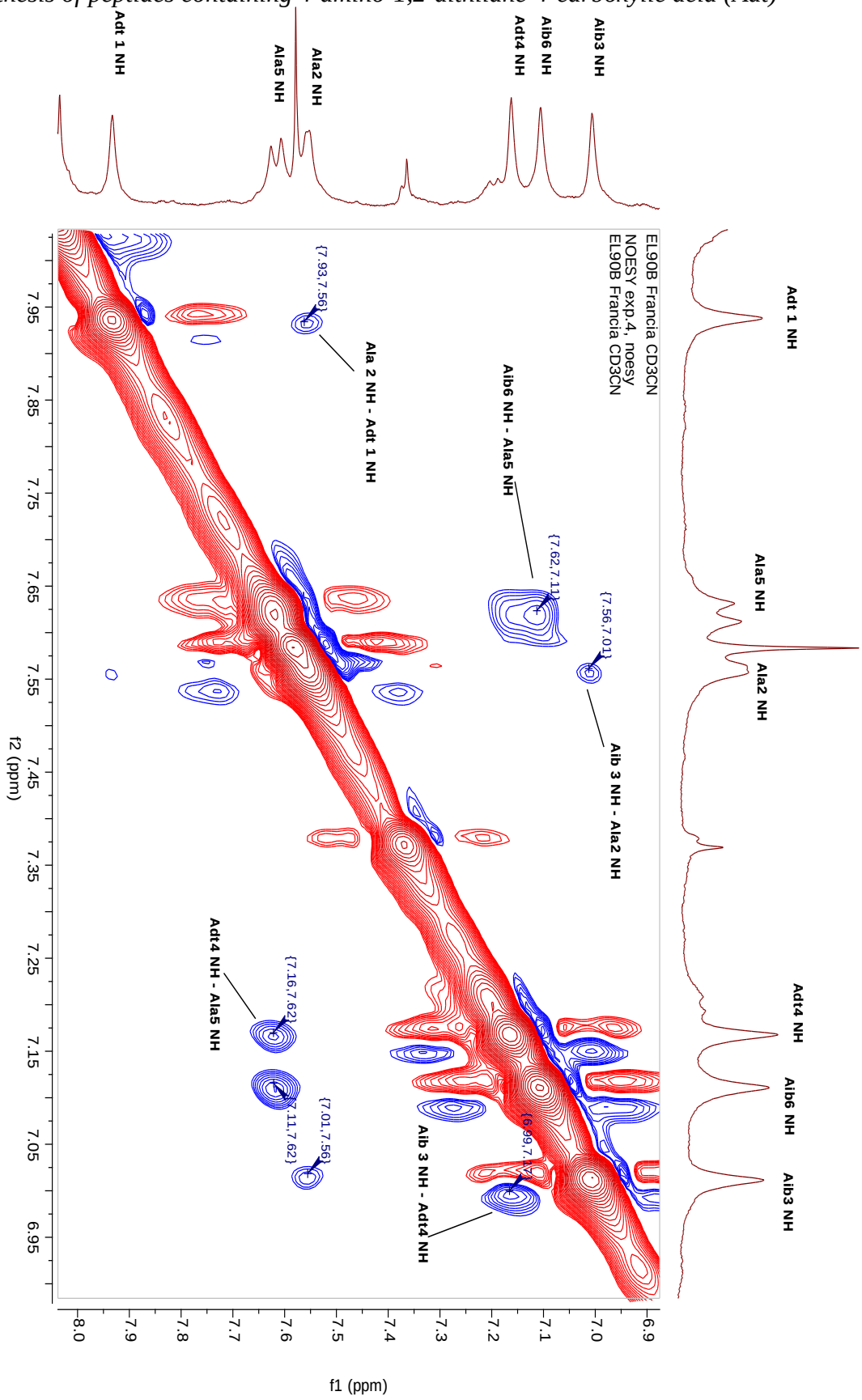


***Fig. 21*** Assessment of the $NH_i \rightarrow NH_{i+1}$ cross-couplings for $PyrAc(AdtAlaAib)_2OMe$.

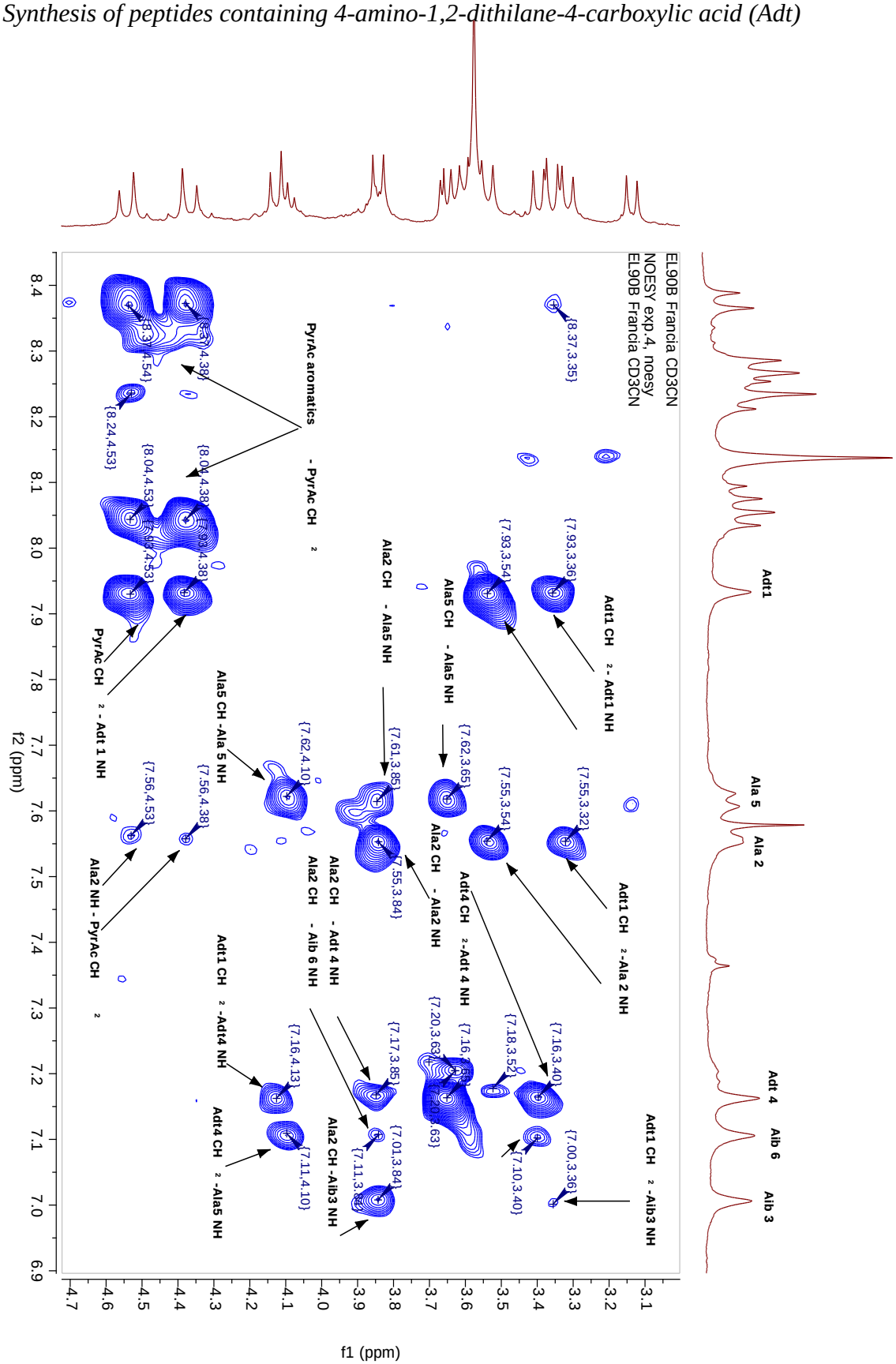


***Fig. 22*** Assessment of the $CH_i$ / $CH_{2\ i}$ $\rightarrow NH_{i+n}$ ***(n=0, 1, 2, 3, 4)*** cross-couplings in NOESY spectrum for PyrAc(AdtAlaAib)$_2$OMe.

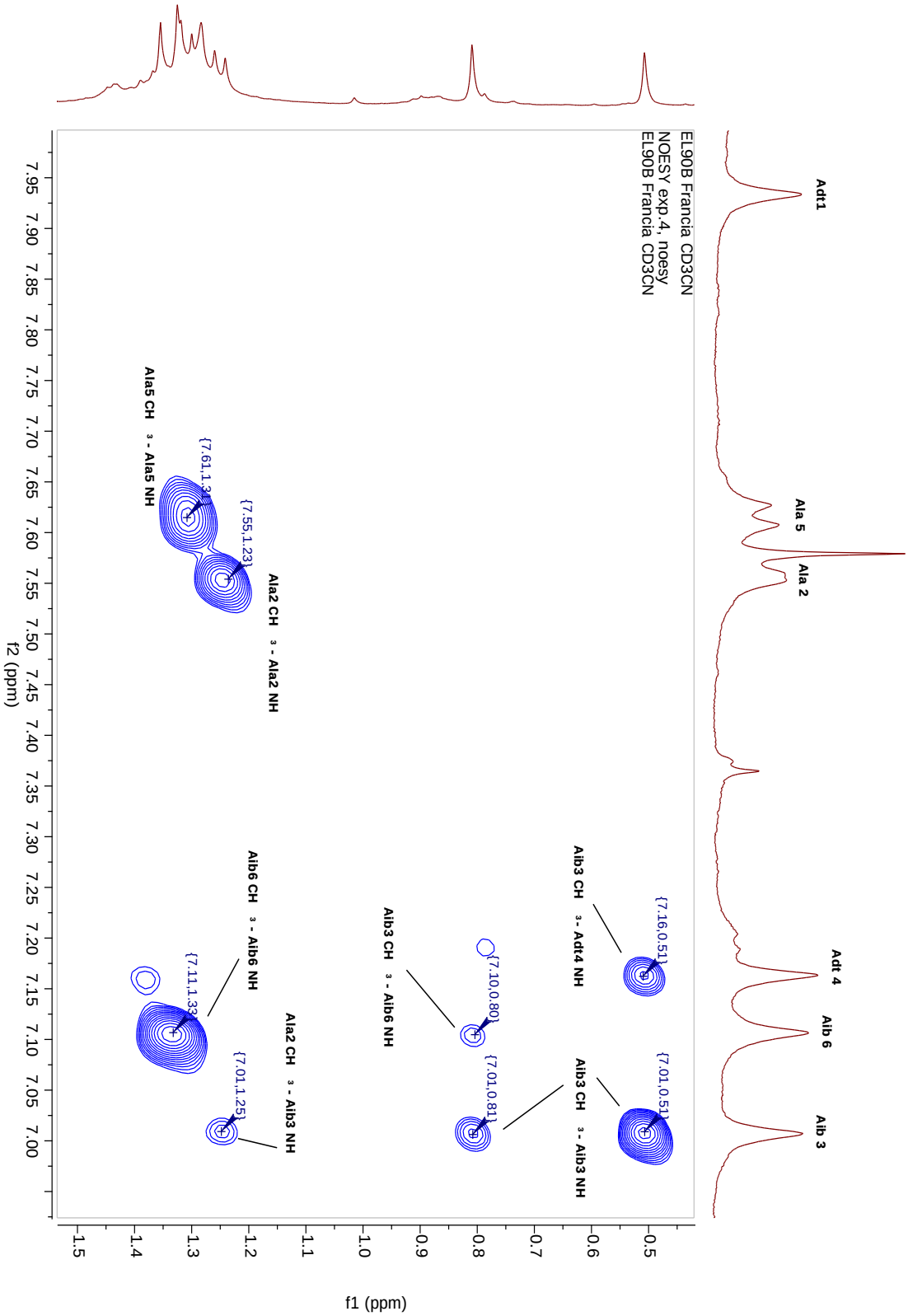


***Fig. 23*** Assessment of the $CH_{3\ i} \rightarrow NH_{i+n}$ ***(n=0, 1, 2, 3)*** cross-couplings in NOESY spectrum for PyrAc(AdtAlaAib)$_2$OMe.

**Fc(AdtAlaAib)$_2$OMe**

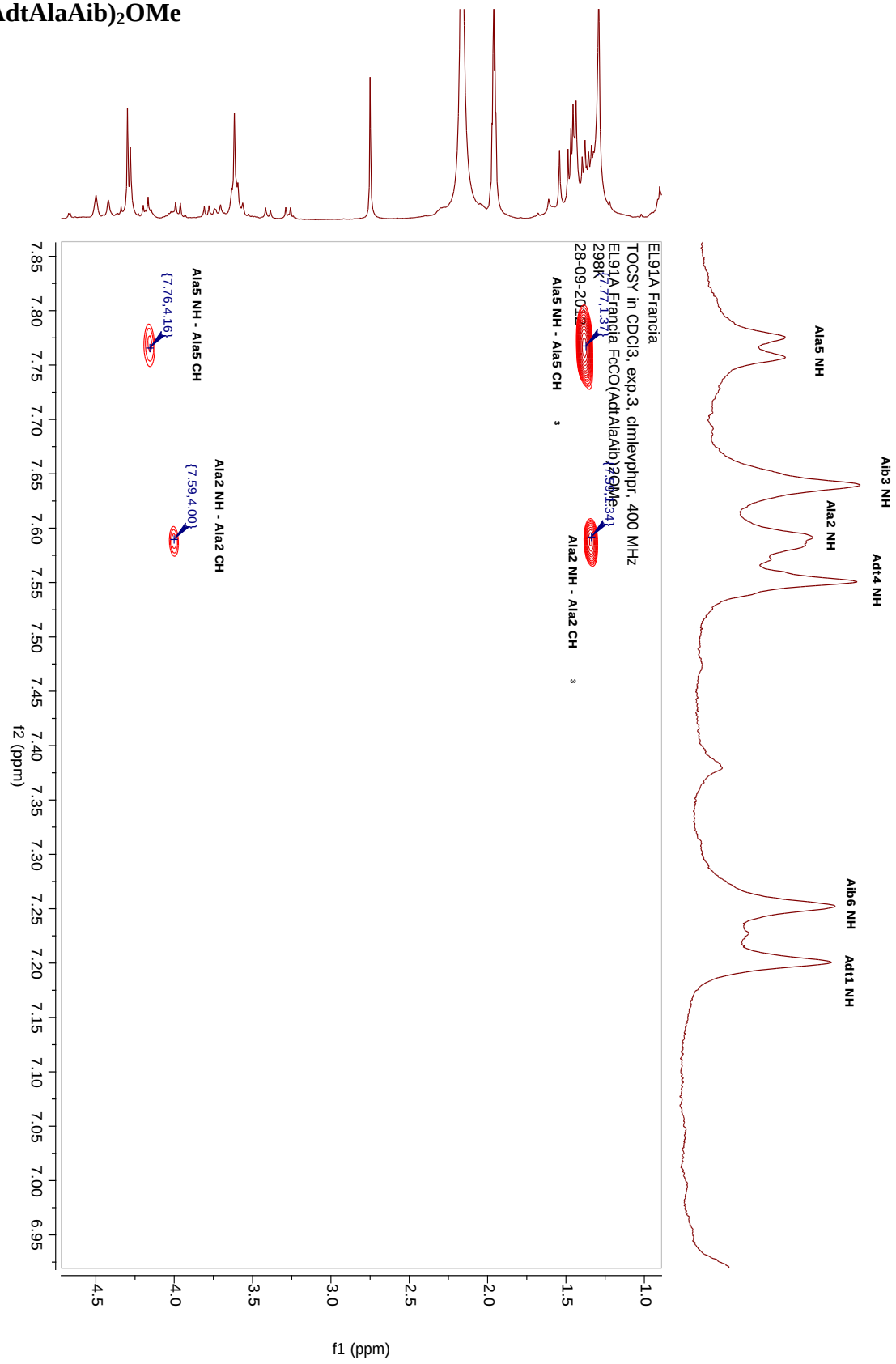


***Fig. 24*** TOCSY spectrum of Fc(AdtAlaAib)$_2$OMe in $NH_i \rightarrow CH_i$ and $NH_i \rightarrow CH_{3\ i}$ regions for Fc(AdtAlaAib)$_2$OMe . By means of these cross-couplings the two Ala spin systems have been assessed. Corrispondence in COSY spectrum (not shown).

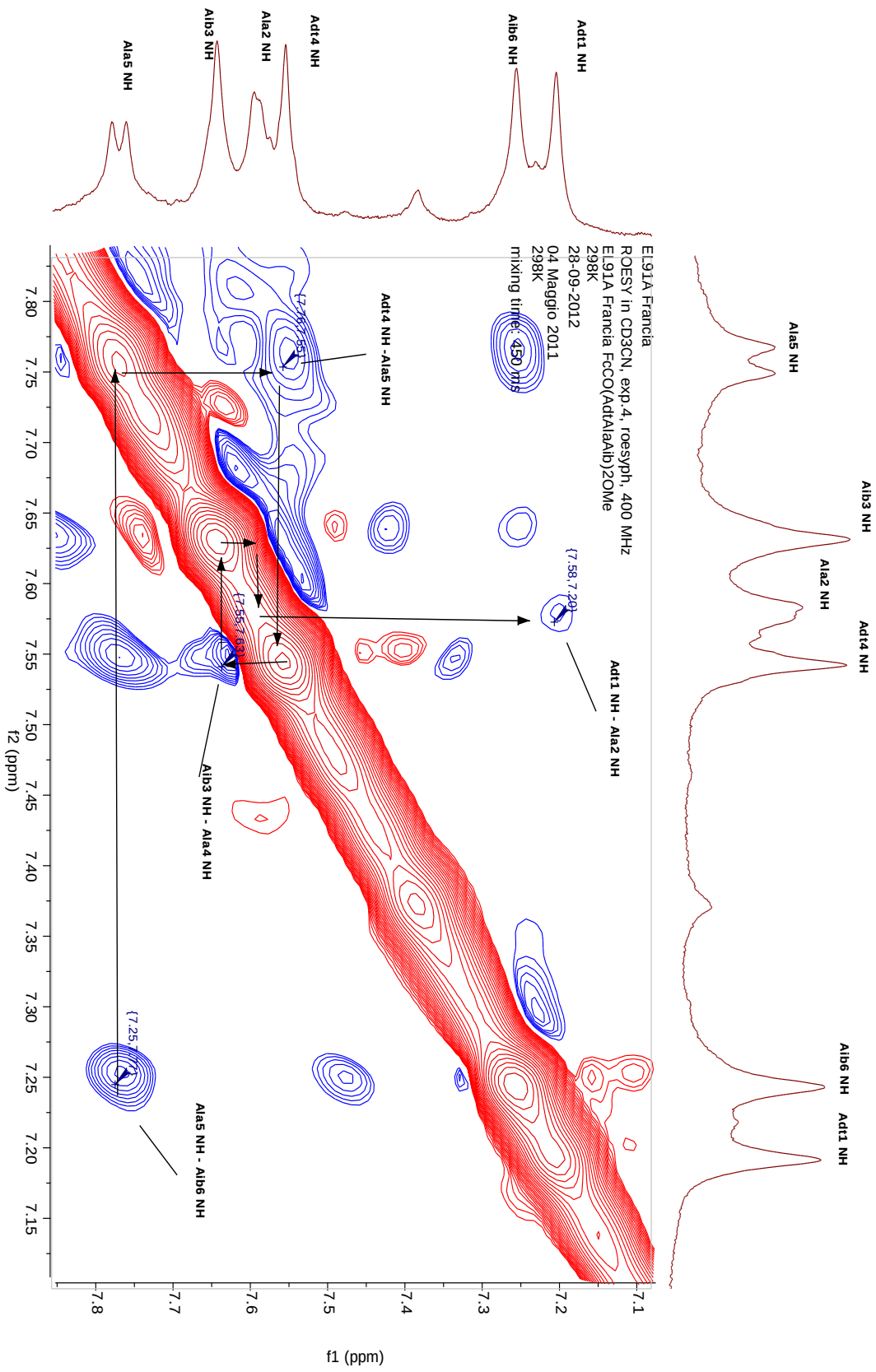


***Fig. 25*** Assessment of the $NH_i \rightarrow NH_{i+1}$ cross-couplings for $Fc(AdtAlaAib)_2OMe$ on ROESY spectrum. Probably the cross-peak of the coupling between Ala2 NH and Aib3 NH is hidden by diagonal peaks.

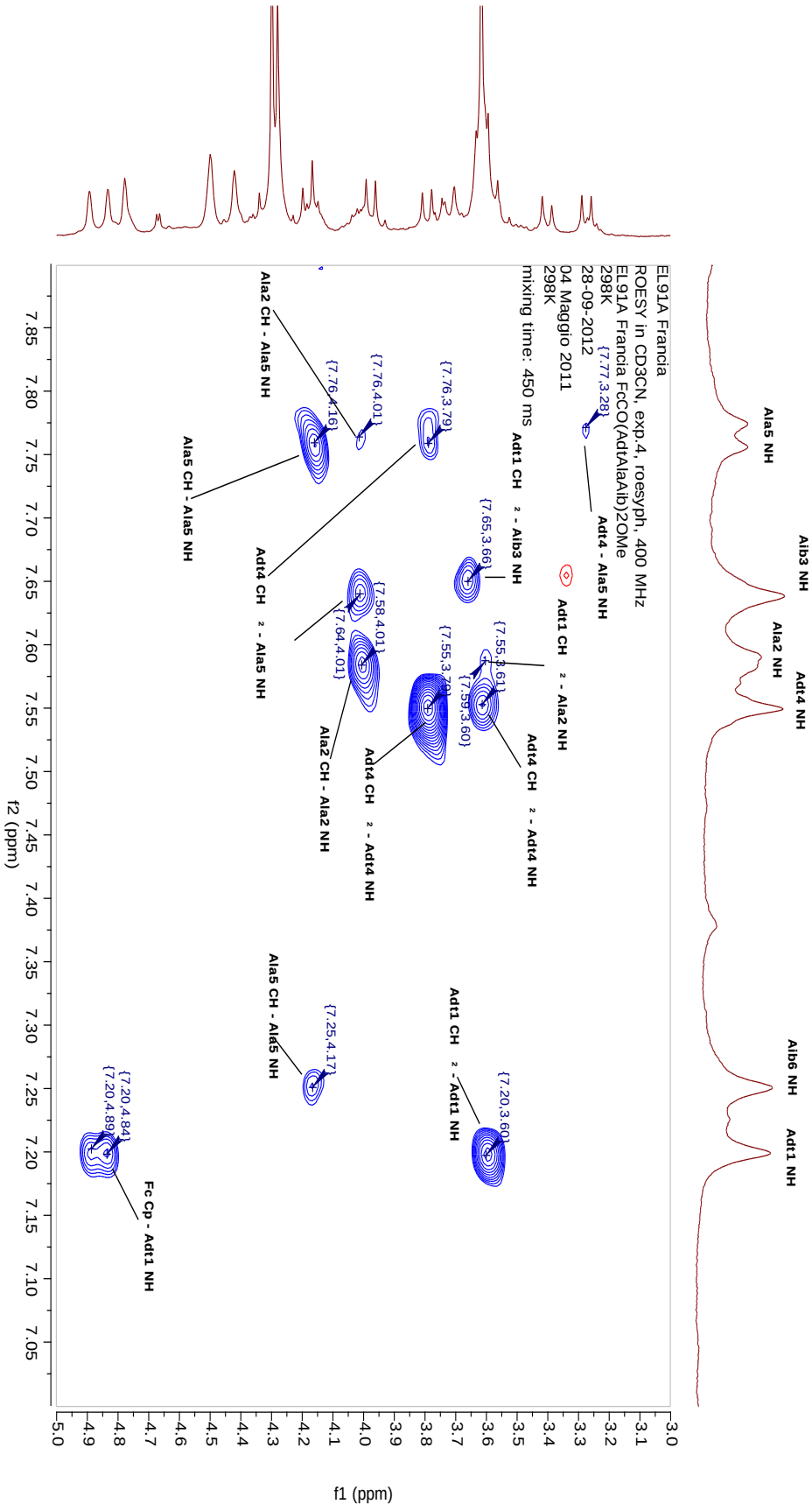


***Fig. 26*** Assessment of the $CH_i$ / $CH_{2\ i}$ $\rightarrow NH_{i+n}$ ***(n=0, 1, 2, 3, 4)*** cross-couplings in ROESY spectrum for $Fc(AdtAlaAib)_2OMe$.

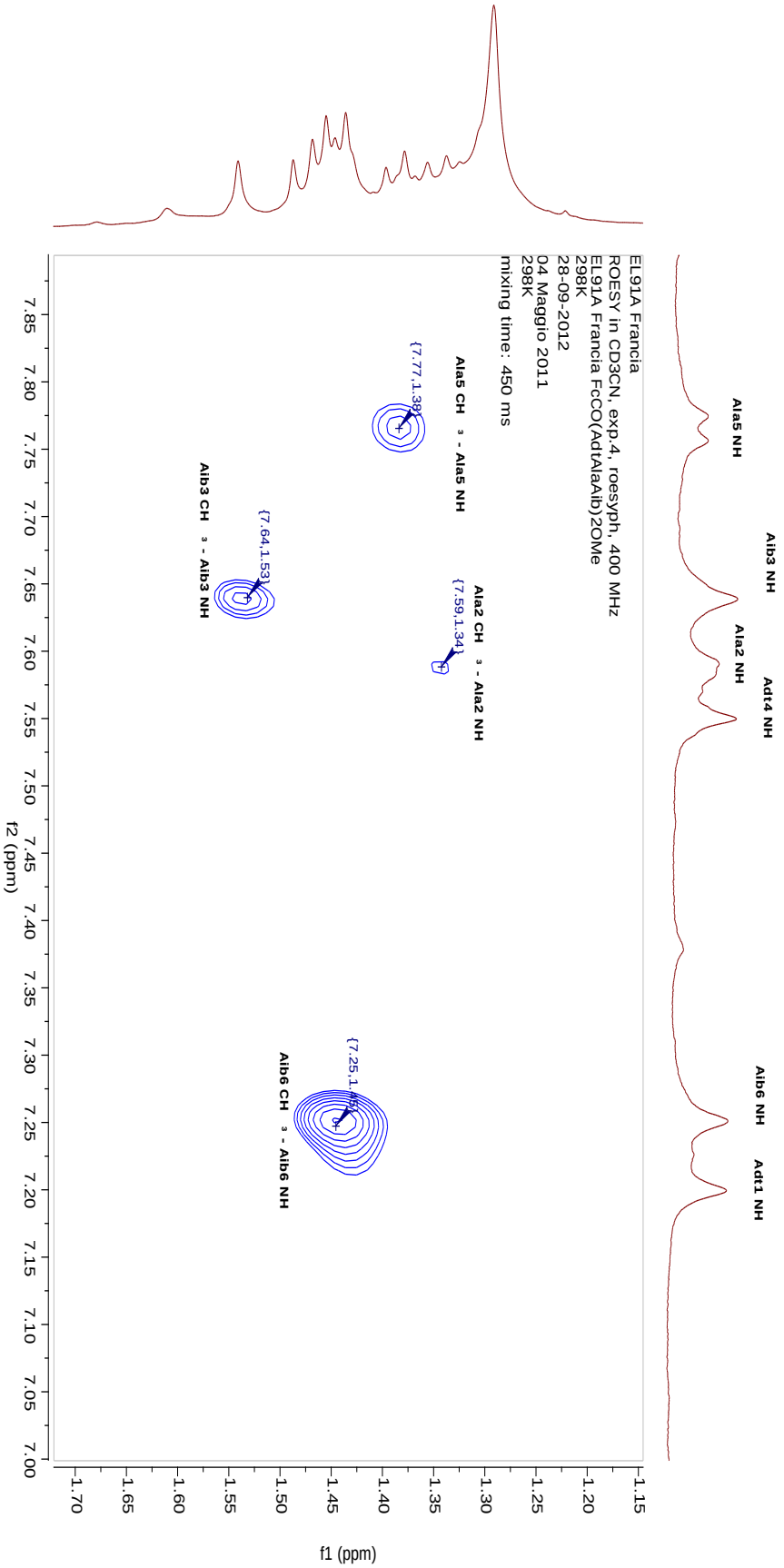


***Fig. 27*** Assessment of the $CH_{3\ i} \rightarrow NH_{i+n}$ ***(n=0, 1, 2, 3)*** cross-couplings in ROESY spectrum for $Fc(AdtAlaAib)_2OMe$.

ELECTROCHEMICAL AND RELATED MEASUREMENTS

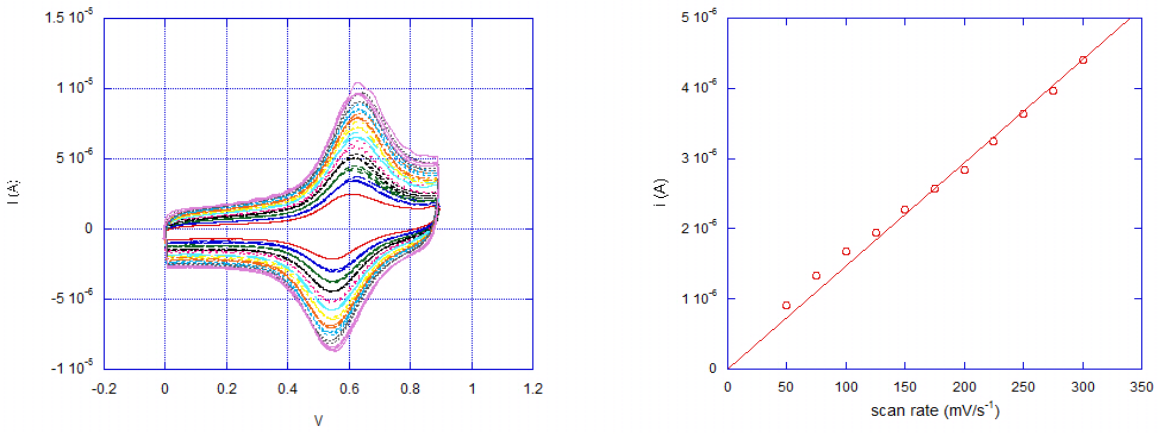


***Fig. 28*** Left: CV of the SAM at several scan rate: 50mV/s (red),75 (blue), 100 (green), 125 (black), 150 (fuchsia), 175 (teal), 200 (yellow), 225 (orange), 250 (pale blue), 275 (grey), 300 (purple); Right: dependence of ΔE on scan rate.

REFERENCES


1) a) Booth B.D., Vilt S.G., McCabe C.,Jennings G.K., *Langmuir*, **2009**, 25 (17), 9995-10001 ; b) Cheng H.,Hu Y., *Advances in Colloid and Interface Science*, **2012**, 171-172, 53-65 ; c) Eckermann A.L., Feld D.J., Shaw J.A.,Meade T.J., *Coordination Chemistry Reviews*, **2010**, 254, 1769-1802 ; d) Frasconi M., Mazzei F.,Ferri T., *Analytical and Bioanalytical Chemistry*, **2010**, 398 (4), 1545-1564 ; e) Gatto E., Porchetta A., *et al.*, *Langmuir*, **2012**, 28, 2817-2826 ; f) Jadhav S.A., *Journal of Material Chemistry*, **2012**, 22, 5894-5899 ; g) Klutse C.K., Mayer A., Wittkamper J.,Cullum B.M., *Journal of Nanotechnology*, **2012**, 2012, 1-10 ; h) Mandler D.,Kraus-Ophir S., *Journal of Solid State Electrochemistry*, **2011**, 15, 1535-1558 ; i) Mrksich M.,Whitesides G.M., *Annual Review of Biophysics and Biomolecular Structure*, **1996**, 25, 55-78 ; j) Whitesides G.M., Kriebel J.K.,Love J.C., *Progress in Surface Science Journal*, **2005**, 88 (1), 17-48 ; k) Zhang J., Chi Q., *et al.*, *FEBS letters*, **2012**, 586, 526-535
2) Gallardo I.F.,Webb L.J., *Langmuir*, **2012**, 28, 3510−3515
3) a) Pandey B., Demchenko A.V.,Stine K.J., *Microchimica Acta*, **2012**, 179, 71-81 ; b) Gatto E., Stella L., *et al.*, *Superlattices and Microstructures*, **2009**, 46, 34-39 ; c) Morita T.,Kimura S., *Journal of American Chemical Society*, **2003**, 125, 8732-8733
4) Vericat C., Vela M.E., *et al.*, *Chemical Society Review*, **2010**, 39, 1805-1834
5) Nuzzo R.G.,Allara D.L., *Journal of American Chemical Society*, **1983**, 105 (13), 4481-4483
6) a) Shen T.-Y.,Walford G.L., **1970,** U.S. ; b) Shen T.-Y.,Walford G.L., *Chemical Abstract*, **1971**, 75, 6336j
7) Appleton D.R.,Copp B.R., *Tetrahedron Letters*, **2003**, 44, 8963-8965
8) a) Apfel U.-P., Kowol C.R., *et al.*, *Journal of Inorganic Biochemistry*, **2009**, 103, 1236-1244 ; b) Aschi M., Lucente G., *et al.*, *Organic & Biomolecular Chemistry*, **2003**, 1980-1988 ; c) Morera E., Lucente G., *et al.*, *Bioorganic & Medicinal Chemistry*, **2002**, 10, 147-157 ; d) Morera E., Nalli M., *et al.*, *Journal of Peptide Science*, **2005**, 11, 104-112 ; e) Morera E., Nalli M., *et al.*, *Bioorganic & Medicinal Chemistry Letters*, **2000**, 10, 1585-1588
9) Toniolo C., Crisma M., Formaggio F.,Peggion C., *Biopolymers (Peptide Science)*, **2001**, 60, 396-419
10) a) Antonello S., Formaggio F., *et al.*, *Journal of American Chemical Society*, **2003**, 125, 2874-2875 ; b) Arikuma Y., Nakayama H., Morita T.,Kimura S., *Angewandte Chemie International Edition* **2010**, 49, 1800-1804 ; c) Cordes M.,Giese B., *Chemical Society Review*, **2009**, 38, 892-901
11) a) Garbuio L., Antonello S., *et al.*, *Journal of American Chemical Society*, **2012**, 134, 10628-10637 ; b) Long Y.-T., Abu-Irhayem E.,Kraatz H.B., *Chemistry- A European Journal*, **2005**, 11, 5186-5194 ; c) Wain A.J., Do H.N.L., *et al.*, *Journal of Physical Chemistry C*, **2008**, 112, 14513-14519
12) a) Driscoll P.F., Douglass E.F., *et al.*, *Langmuir*, **2008**, 24, 5140-5145 ; b) Lal B., Badshah A., *et al.*, *Applied Organometallic Chemistry*, **2011**, 25, 843-855 ; c) Mazur M.,Blanchard G.J., *Journal of Physical Chemistry B*, **2005**, 109, 4076-4083 ; d) Messina P., Hallais G., *et al.*, *Electrochimica Acta*, **2012**, 80, 180-186 ; e) Nakamura M., Saito N., *et al.*, *Chemistry Letters*, **2007**, 36 (5), 602-603
13) Karle I.L.,Balaram P., *Biochemistry*, **1990**, 29 (29), 6747-6755
14) Hanson P., Millhauser G., *et al.*, *Journal of American Chemical Society*, **1996**, 118, 7618-7625

15) a) Galoppini E.,Fox M.A., *Journal of American Chemical Society*, **1996**, 118, 2299-2300 ; b) Gao X., Tang S.,Zhou W., *Chemical Physics Letters*, **2007**, 445, 297-302 ; c) Mandal H.S.,Kraatz H.-B., *Chemical Physics*, **2006**, 326, 246-251 ; d) Polo F., Antonello S., *et al.*, *Journal of American Chemical Society*, **2005**, 127, 492-493 ; e) Stuchebrukhov A.A., *Theoretical Chemistry Accounts*, **2003**, 110, 291-306 ; f) Yasutomi S., Morita T., Imanishi Y.,Kimura S., *Science*, **2004**, 304, 1944

16) a) Bellamy M., *The Infra-Red Spectra of Complex Molecules*, **1956**. London, Methuen; b) Bonora G.M., Mapelli C., *et al.*, *International Journal of Biological Macromolecules*, **1984**, 6, 179 ; c) Kennedy D.F., Crisma M., Toniolo C.,Chapman D., *Biochemistry*, **1991**, 30, 6541-6548 ; d) Malon P., Bednarova L., *et al.*, *Chirality*, **2010**, 22, E47-E55 ; e) Palumbo M., DaRin S., Bonora G.M.,Toniolo C., *Macromolecular Chemistry*, **1976**, 177, 1477 ; f) Formaggio F.,Toniolo C., *Chirality*, **2010**, 22, E30-E39

17) a) Griesinger C., Otting G., Ernst R.R.,Wütrich K., *Journal of American Chemical Society*, **1988**, 110, 7870 ; b) Williams K.R.,King R.W., *Journal of Chemical Education*, **1990**, 67 (A125)

18) a) Braunschweiler L.,Ernst R.R., *Journal of Magnetic Resonance*, **1985**, 53, 521 ; b) Bazzo R., Boyd J., Campbell I.D.,Soffe N., *Journal of Magnetic Resonance*, **1987**, 73, 369

19) a) Bodenhausen G., Kogler H.,Ernst R.R., *Journal of Magnetic Resonance*, **1984**, 58, 370 ; b) Jeener J., Meier B.H., Bachman P.,Ernst R.R., *Journal of Chemical Physics*, **1988**, 69, 4546

20) a) Bothner-By A.A., Stephens R.L., *et al.*, *Journal of American Chemical Society*, **1984**, 106, 811 ; b) Bax D.,Davis D.G., *Journal of Magnetic Resonance*, **1985**, 63, 207

21) Wüthrich K., *NMR of Protein and Nucleic Acids*, **1986**. New York, Wiley

22) a) Kawamura S., Morita T.,Kimura S., *Science and Technology of Advanced Materials*, **2006**, 7, 544-551 ; b) Shoij O., Nakajima D.,Ohkawa M., *Macromolecules*, **2003**, 36, 4557-4566

23) a) Bains G.K., Kim S.H., Sorin E.J.,Narayanaswami V., *Biochemistry*, **2012**, 51, 6207-6219 ; b) Kalyanasundaram K.,Thomas J.K., *Journal of American Chemical Society*, **1977**, 99 (7), 2039-2044

24) Montalti M., Credi A., Prodi L.,Gandolfi M.T., *Handbook of Photochemistry*, **2006**. BOca RAton, USA, Taylor and Francis Group

25) Sharp M., Petersson M.,Edstrom K., *Journal of Electroanalytical Chemistry*, **1978**, 123-130

26) a) Benedetti E., Blasio B.D., *et al.*, *Journal of the Chemical Society, Perkin Transactions*, **1990**, 2, 1829-1837 ; b) Toniolo C., Crisma M., Formaggio F.,Peggion C., *Biopolymers (Pept Sci)*, **2001**, 60 (6), 396-419

# *CONCLUSIONS*

## *I*

The conformational preferences of a water-soluble peptide series made of a whole hydrophobic backbone, enclosing alternate-Aib-Ala- (2-mer to 9-mer) residues, have been investigated in water. The ECD measurements revealed at which stage of the peptide length the conformation switches from unfolded to $3_{10}$- and from $3_{10}$- to $\alpha$-helix (6-mer and 8-mer respectively). These results are in agreement with other reported examples for Aib containing peptides. However this is the first ECD characterization of a whole peptide series in water.

## *II*

A peptide-conjugated AuNp series was obtained from the corresponding peptide series of alternating Aib-Ala appropriately N-terminus functionalized. Conformational characterization of free peptides ligands and of the peptides bound to nanoparticles has been achieved. An ECD analysis on the optical and chiro-optical properties of the nanoparticles displayed a chiral plasmonic induction that take place from the peptides to the 2 nm sized metal core. The results show moderately strong ECD signals in the range of 300-650 nm, corresponding to the gold nanoparticle's quantized electronic structure. Even though their only chiral amino acid in the peptide sequences is L-Ala, the resulting peptide-conjugated AuNps behave like pseudo-diastereoisomeric species, according to the number of amino acids in the sequence (odd or even) and with the type of amino acid closest to the gold surface (Aib or L-Ala). Such chiro-optical property appears to be strongly influenced by the related peptide the secondary structure when conjugated to the nanoparticles and vanishes when the sequence is long enough to assume a $3_{10}$-helix conformation.

## *III*

The main contribution of this work consists in the discovery that a series of Aib/Ala peptides, lacking any charge or polar group, dissolve in water through the formation of self-assembled superstructures. These aggregates are larger than a typical micelle, although it is not clear yet if they form vesicles or a different type of supramolecular

structure. Our contention, supported by X-ray diffraction data, is that a hydrophilic side (the N- and/or the C-terminus and/or a face of the helix) of the peptide has to be located on the outer layer of these aggregates. Encapulation experiments have also been performed on such supra-molecular assemblies and peptide coated-AuNps. TEM images of the encapsulated nanoparticles demonstrate the ability of such large spheres (~100nm sized) to encapsulate smaller ones (AuNPs display a hydrodynamic radius of 610 nm). Further experiments will clarify the training force for the aggregation process and whether or not the peptide "vesicles" contain water inside.

## *IV*

We have reported the synthesis of two new $C^{\alpha}$-tetra substituted $\alpha$-amino acids, each characterized by the presence of two (phenylazo)benzyl moieties in the side chains. A detailed analysis of the optical properties revealed the formation of intermediate chiral species during the isomerization process driven by light. Moreover, diastereomeric species were unambiguously detected when the (phenylazo)benzyl-type amino acids were coupled with a chiral protein amino acid and irradiated with UV light. The light driven process worked also in solid state, by irradiating directly Au nanoparticles coated with the(phenylazo)benzyl-containing amino acid. The nanoparticles exhibited also a magnetic susceptibility dependence as function of the photo-irradiation process, that can be simply detected by $^{1}$H-NMR spectroscopy. Based on this behavior, these amino acids are of relevant potential for the development of a novel class of photo-switchable materials.

## *V*

A series of Ferrocene and Pyrene labeled helical peptides containing one or more 4-amino-1,2-dithiolane-4-carboxylic acid (Adt) residues have been synthetized and chemically characterized. Such peptides have been designed to be employed in the formation of SAMs over gold surface (by means of linkage with the dithiolane Adt side chains) for electrochemical applications. A detailed conformational study on a hexamers series and electrochemical characterization have been performed. The Adt residues in the sequence imposed a parallel displacement (respect to the peptide axle) of the peptides over the gold surface. Cyclic Voltammetry experiments were accomplished for testing the redox properties of the Ferrocene bound to peptide. Moreover, preliminary

experiments aimed to generate photo-current have been investigated for the Ferrocene containing peptide. These last results indicated that these peptides are suitable to be good candidate for the light-current conversion process.

RINGRAZIAMENTI

Vorrei ringraziare innanzitutto il mio supervisore Dott. Alessandro Moretto per avermi dato la possibilità di svolgere questo progetto di tesi. Il suo è stato un supporto prezioso al fine di giungere alla conclusione di questo progetto. In questi tre anni infatti ha sempre avuto validi suggerimenti e brillanti idee per qualunque problematica fosse sorta in merito al progetto. Lavorare affianco a ricercatori così dinamici e pieni di iniziativa è sicuramente uno sprono molto forte a fare sempre meglio il proprio lavoro.

Desidero quindi ringraziare la Scuola di Dottorato di Scienze Molecolari, che mi ha concesso di formarmi, in questi tre anni, assieme tanti altri amici e colleghi ed è sempre stata un supporto per il nostro lavoro e per la nostra formazione scientifica.

Per questo progetto inoltre vorrei ringraziare la Fondazione CARIPARO che ha finanziato questo e molti altri progetti di Dottorato in molte aree di ricerca nell'Università di Padova, anche in tempi economicamente difficili come quelli in cui ci troviamo.

Inoltre, un grazie per il supporto ricevuto da parte di molti che con me hanno collaborato e mi hanno aiutato in questi anni. Innanzi tutto, un grande ringraziamento va al prof. Fernando Formaggio che sempre è stato fonte di suggerimenti, consigli e sostegno, in particolar modo durante il mio periodo all'estero. Il suo supporto e la sua cordiale disponibilità sono stati molto preziosi. Vorrei poi ringraziare il dott. Marco Crisma, per l'aiuto con le strutture dei cristalli ed i consigli sulle proprietà IR dei peptidi. Il prof. Claudio Toniolo, per avermi concesso di lavorare nel suo gruppo, in cui sono cresciuto scientificamente fino ad ora e di cui ho condiviso la ricerca.

Vorrei poi ringraziare per il loro aiuto e per la grande disponibilità sempre dimostratami tutti i ricercatori ed assegnisti del gruppo. In special modo, la dott.ssa Cristina Peggion, la dott.ssa Barbara e la dott.ssa Marta De Zotti. La prof.ssa Marina Gobbo, per la gentilezza e disponibilità con cui mi ha accolto nel periodo trascorso nel suo laboratorio. Inoltre, un ringraziamento al dott. Renato Schiesari, per il supporto con gli spettri IR.

I want to thank Prof. François Couty that gave me the opportunity to work on my project in his laboratory. Moreover, I am grateful to him for his suggestions and supports with the synthesis of Adt-containing peptides. I want to thank also his collaborators, the Ph.D. students and PostDocs of his laboratory, for the kindness and

the help they gave me. In particular, I want to address a special thank to Dr Karen Wright, who always has been helping me with each problem concerning laboratory work and even with many bureaucratic problems. I didn't know I would have found so kind persons who helped me in any circumstace I had to face. I want to thank Bruno and Laurance for the help they gave me and the patience they always had with me during my stay in their laboratory (even for the patience they showed with my spoken French).

Senza meno, un grande grazie a tutti quanti, dottorandi e laureandi del gruppo che hanno condiviso con me alti e bassi del lavoro in laboratorio. In particolare, un grandissimo in bocca al lupo a Daniela e Andrea per il loro Dottorato. Un grazie anche a tutti i laureandi del gruppo, auguro loro un futuro lavorativo roseo anche in questo periodo nero. Spero che si siano trovati bene a lavorare con me tanto quanto io mi sono trovato bene a lavorare con tutti loro.

Un grande grazie a tutti coloro che mi sono stati vicini in questi anni. Ai miei genitori in particolare, ai quali devo tutto quello che sono. Il loro è stato un supporto morale e materiale sempre presente e costante ed un continuo incoraggiamento soprattutto di fronte alle difficoltà. Alla mia famiglia, che anche tra molte difficoltà e per quanto piccola, è sempre stata grande nell'aiutarmi e sostenermi nel difficile compito di cercare la mia strada nel mondo.

Un grande grazie anche a tutti gli amici, vicini e lontani. La vostra compagnia è stata la miglior medicina possibile per lo stress (inevitabile) di questi ultimi mesi.

Infine, un grazie enorme a te, Serena, che con pazienza e col sorriso hai saputo spesso cancellare le mie ansie e debolezze in quest'ultimo frenetico periodo. Grazie per essermi stata vicino nonostante anche tu sia in un periodo molto delicato. Ti voglio bene!!!